# Persistent Organic Pollutants in Fresh Water Ecosystems

Guest Editors: Fu-Liu Xu, Sven Erik Jorgensen, Yoshihisa Shimizu, and Eugen Silow

Persistent Organic Pollutants in Fresh Water Ecosystems

Persistent Organic Pollutants in Fresh Water Ecosystems

Guest Editors: Fu-Liu Xu, Sven Erik Jorgensen, Yoshihisa Shimizu, and Eugen Silow

Contents

Editorial
Persistent Organic Pollutants in Fresh Water Ecosystems

Fu-Liu Xu,[1] Sven Erik Jorgensen,[2] Yoshihisa Shimizu,[3] and Eugen Silow[4]

[1] *College of Urban and Environmental Sciences, Peking University, Beijing 100871, China*

[2] *Department of Environmental Chemistry, Institute of Analytical and Pharmaceutical Chemistry, Copenhagen University, 2100 Copenhagen Ø, Denmark*

[3] *Research Center for Environmental Quality Control, Kyoto University, Otsu, Kyoto 520-0811, Japan*

[4] *Institute of Biology, Irkutsk State University, Irkutsk 664003, Russia*

Correspondence should be addressed to Fu-Liu Xu; xufl@urban.pku.edu.cn

Persistent organic pollutants (POPs) are globally concerned pollutants due to their widespread occurrence, long-term persistence, strong resistance, long-range transportation, high bioaccumulation, and potentially significant impacts on human health and ecosystems. Some legacy POPs, such as hexachlorocyclohexanes (HCHs), dichlorodiphenyltrichloroethane (DDT), and polychlorinated biphenyls (PCBs), are still frequently detectable in the environment, although they have been banned or restricted for decades. For some emerging POPs, such as Polybrominated Diphenyl Ethers (PBDEs), Perfluorooctane Sulfonate (PFOS), and Polycyclic Aromatic Hydrocarbons (PAHs), their concentrations in the environment would be increased with social and economic development. Freshwater ecosystems play a pivotal role in supplying drinking water, fisheries, and recreation and in maintaining regional ecological balance and sustainable socioeconomic development, but the world's freshwater ecosystems are generally suffering from POPs pollution. Therefore, it is very meaningful to understand the environmental behaviors, processes, effects, and risks of POPs in freshwater ecosystems. This special issue would provide a window to show some study efforts in such fields.

9 papers selected form 17 submitted ones are published in the Special Issue on Persistent Organic Pollutants (POPs) in Fresh Water Ecosystems (POPFWEs). The studied contaminants covered legacy and emerging POPs including PAHs, organochlorine pesticides (OCPs) (especially HCHs and DDTs), and PBDEs. The studied media included the water, sediments, fishes, air, and soil. The contents covered the distributions in multimedia, source apportionment, transfer and transformation process, ecological and health risk assessment, and fate modeling. Except for one study in upland Irish headwater lake catchments, other studies were related to the Chinese lakes including Lake Chao, Lake Baiyangdian, Chinese reservoir (Guanting Reservoir), and the Chinese Tianjin coastal area. The air backward trajectories model, dynamic fugacity model, and species sensitivity distribution (SSD) model were developed and applied to the potential secondary source analysis, multi-media modeling, and ecological risk assessment, respectively.

Although some OCPs such as DDT, lindane, chlordane, mirex, aldrin, dieldrin, and endrin have been banned and their residual levels have gradually decreased since the 1980s, these OCPs could still be detected in various environmental and biological media. In this special issue, the OCPs in Lake Chaohu, the fifth largest lake and one of the most polluted lakes in China, were well studied. The residues, distributions, sources, and ecological risks of OCPs in the water and the simulation of the fate and seasonal variations of α-hexachlorocyclohexane (α-HCH) in Lake Chaohu were studied in "*Residues, distributions, sources, and ecological risks of OCPs in the water from Lake Chaohu, China*" and "*Simulation of the fate and seasonal variations of α-hexachlorocyclohexane in Lake Chaohu using a dynamic fugacity model,*" respectively. The levels, temporal-spatial variations, and sources of OCPs in ambient air of Lake Chaohu were investigated in "*Levels, temporal-spatial variations, and sources of organochlorine pesticides in ambient air of Lake Chaohu, China,*" since the air would serve as a very important source of OCPs in the water.

In China, the PAH emissions have been increasing greatly due to the increasing energy demand associated with rapid population growth and economic development and to the low efficiency of energy utilization. The threaten of PAHs pollution to ecosystem and human health has become more and more serious in China. In this special issue, there are three articles dealing with the PAHs in the aquatic ecosystems in the southern and northern China, the two of most PAHs-polluted regions in China. *"Distribution and bioconcentration of polycyclic aromatic hydrocarbons in surface water and fishes"* studied the spatial distribution and bioconcentration of PAHs in the water, suspended solids and fish collected from Pearl River Delta in the southern China, while *"Distributions, sources, and backward trajectories of atmospheric polycyclic aromatic hydrocarbons at Lake Small Baiyangdian, northern China"* investigated the distributions, sources and backward trajectories of PAHs at Lake Small Baiyangdian in the northern China. The levels, distribution and health risks of PAHs in four edible fish species from the freshwater in the northern China were presented in *"Levels, distribution, and health risks of polycyclic aromatic hydrocarbons in four freshwater edible fish species from the Beijing market"*. The findings are of great importance to understand the transport and fate of PAHs in aqueous systems, and the associated health risks through fish consumptions.

"Fate and transport of polycyclic aromatic hydrocarbons in upland Irish headwater lake catchments" presented the very important information on the fate and transport of PAHs in Upland Irish Headwater Lake catchments, since a few studies have evaluated the levels of PAHs within the Irish environment. Ireland, located on the western periphery of Europe and assumed to receive clean Atlantic air, has been used as an atmospheric reference for comparison to other Europe regions.

In view of the importance of catchments to contribute pollutants to aquatic ecosystems, two papers (*"Fate and transport of polycyclic aromatic hydrocarbons in upland Irish headwater lake catchments"* and *"HCHs and DDTs in soils around Guanting Reservoir in Beijing, China: spatial-temporal variation and countermeasures"*) dealing with the PAHs and OCPs in the lake/reservoir catchment were selected to be published.

The fresh water polluted by POPs would influence the seawater quality in coastal area. The sediments in the coastal area would record such effects. In view of this consideration, *"Concentration levels and ecological risks of persistent organic pollutants in the surface sediments of Tianjin coastal area, China"* that invested the concentration levels and ecological risks of PAHs, OCPs, and PBDEs in the surface sediments of Tianjin coastal area in the northern China was selected to be published in the POPFWE.

Fu-Liu Xu
Sven Erik Jorgensen
Yoshihisa Shimizu
Eugen Silow

Research Article

Concentration Levels and Ecological Risks of Persistent Organic Pollutants in the Surface Sediments of Tianjin Coastal Area, China

Xiaoxia Lu, Chaoqi Chen, Shu Zhang, Zhen Hou, and Junjun Yang

Ministry of Education Laboratory for Earth Surface Processes, College of Urban and Environmental Sciences, Peking University, Beijing 100871, China

Correspondence should be addressed to Xiaoxia Lu; luxx@urban.pku.edu.cn

Sediments were sampled from different surface water bodies in Tianjin coastal area, China, and persistent organic pollutants (POPs) including polycyclic aromatic hydrocarbons (PAHs), organochlorine pesticides (OCPs), polychlorinated biphenyls (PCBs), and polybrominated diphenyl ethers (PBDEs) were measured using GC/MS or GC/ECD. The purposes were to investigate the concentration levels of the POPs and to assess their ecological risks. The results showed that all the 16 priority PAHs were detected from the 10 sediments sampled with the total concentrations of the 16 PAHs ranging from 274.06 μg/kg to 2656.65 μg/kg, while the concentrations of the halogenated POPs were generally low except in the Dagu waste discharging river where the total concentrations of 24 OCPs, 35 PCBs, and 14 PBDEs were 3103.36 μg/kg, 87.31 μg/kg, and 13.88 μg/kg, respectively. In the studied sediments, PAHs exhibited risks to benthonic organisms; particularly the concentrations of naphthalene and/or acenaphthene exceeded their probable effect concentrations in several locations. In comparison, only in the Dagu waste discharging river, OCPs exhibited risks with the concentrations of heptachlor epoxide and lindane exceeding their probable effect concentrations. PCBs and PBDEs posed rare risks in the studied area.

1. Introduction

Persistent organic pollutants (POPs) are organic compounds resisting degradation through chemical, biological, and photolytic processes in the environment. They can bioaccumulate through food webs from the environment and pose a risk of causing harmful effects to the ecosystem and human health according to animal experiments and epidemiological studies [1]. Common POPs such as polycyclic aromatic hydrocarbons (PAHs), organochlorine pesticides (OCPs), polychlorinated biphenyls (PCBs), and polybrominated diphenyl ethers (PBDEs) are widely detected in the environment and the organisms [2–10]. Although there are a few natural sources of POPs, most are created by humans in industrial processes (details about the source analysis of PAHs are presented in the supplemental materials available at http://dx.doi.org/10.1155/2013/417435).

Tianjin is located in the west side of Bohai Bay and the center of the circular Bohai Belt. Depending on its rich natural resources and solid industrial base, Tianjin has become one of the most active and potential regions in economic development in China. Particularly, the development and opening up of the Tianjin coastal area has been fit into the National Eleven Five program and development strategy. However, with the development of economy and urbanization, Tianjin, especially the coastal area, faces increasing environmental problems that cause harm to the health of residents and the development of the city. Researches show that the surface soils in Tianjin coastal area have been widely polluted by PAHs, with the mean value of the total concentration of the 16 priority PAHs (ΣPAH_{16}) being 1148.10 ng/g [11]. In the sediments of the Dagu waste discharging river, the ΣPAH_{16} ranged from 370 ng/g to 5607 ng/g, and the total concentrations of 9 OCPs (ΣOCP_9) and 13 PBDEs ($\Sigma PBDE_{13}$) ranged from 325.3 ng/g to 1389.1 ng/g and 0.1 ng/g to 15.4 ng/g, respectively [12]. However, currently little is known about the concentration levels of POPs in other surface water bodies in the Tianjin coastal area.

Sediment-associated POPs are known to exhibit narcotic effects in benthic organisms, and they also have been

FIGURE 1: Plot of sediment sampling locations in Tianjin coastal area. b1: mouth of Hai River; b2: Dagu waste discharge river; b3: mouth of Dagu waste discharge river; b4: offshore river; b5: Du waste discharging river; b6: Bei waste discharging river; b7: offshore sea; b8: Yinghe reservoir; b9: mouth of yongding new river; b10: Beitang waste discharging river.

implicated in the development of tumors in bottom-feeding fish and in the induction malformation, loss of fertility, or immuno deficiency in many organisms [13]. POPs can enter the aquatic food webs and pose a risk to human health via consumption of seafood [14]. It has been reported that consumption of shellfish polluted by PAHs may cause lung cancer in humans [15]. Therefore, analyzing the ecological risk of POPs is crucial for protecting human health and marine environment security.

In this study, surface sediments were sampled from different surface water bodies in Tianjin coastal area. The concentrations of POPs including PAHs, OCPs, PCBs, and PBDEs were measured and sources of the POPs were analyzed. Based on the toxicity data of benthic organisms, the ecological risks of POPs were assessed. The purposes were to investigate the concentration levels of PAHs, OCPs, PCBs, and PBDEs in the surface sediments of Tianjin coastal area and to determine their ecological risks.

2. Materials and Methods

2.1. Sampling of the Sediments. In January 2009, surface sediments were sampled from 10 locations in Tianjin coastal area, as shown in Figure 1. The 10 locations were labeled b1 to b10. Among them, b1, b4, b7, and b9 were normal water bodies, b2, b3, b5, b6, and b10 were waste discharging rivers, and b8 was waste discharging lake. The waste discharging rivers and lake were artificial excavated canals and reservoir that were mainly used for discharging waste water from industry or municipality, while normal water bodies referred to natural water bodies. The locations of two major rivers, Hai River

and Dagu waste discharging river, were labeled in Figure 1. A grab dredging device was used to sample the surface sediments. The samples were collected in polyethylene bags with air being squeezed out and transported to the laboratory with ice. After arriving in the laboratory, the samples were stored in a −20°C freezer.

2.2. Analysis of Physiochemical Properties of the Sediments. Before analysis, the sediment samples were frozen dried and ground to pass through a 70 mesh metal sieve. Physicochemical properties including pH, available nitrogen (available-N), available phosphate (available-P), and total organic carbon (TOC) of the sediments were analyzed. For the pH, 5 g of each of the dried and sieved samples was thoroughly mixed with 25 mL distilled water and shaken for 3 h in a shaker; the turbid liquid was centrifuged at 5000 rpm for 10 min (g value 3773), then the supernatant was filtered through 0.45 μm filter membrane (cellulose acetate) and measured using a pH meter (METTLER DELTA320, Swiss). The available-N was measured using the alkaline hydrolysis diffusion method, and the available-P was measured using the sodium bicarbonate method [16]. The TOC was measured using the TOC analyzer (TOC-5000A, Shimadzu).

2.3. Analysis of Persistent Organic Pollutants in the Sediments. Microwave-assisted extraction was applied to extract the POPs from the dried and sieved sediments. For each sample, 5 g of the sediment and 50 ng of each of the surrogate

standards (naphthalene-d$_8$, acenaphthene-d$_{10}$, anthracene-d$_{10}$, chrysene-d$_{12}$, and perylene-d$_{12}$ for PAHs, 2,4,5,6-tetrachloro-m-xylene for OCPs, C^{13}-PCB-209 for PCBs, and C^{13}-PCB-141 for PBDEs) were added into a 55 mL extraction vessel of the Microwave Accelerated Reaction System (CEM MARS Xpress, USA) and extracted with 20 mL mixture of n-hexane and acetone (1 : 1, v/v) at 110°C and 1200 W for 20 min. The extract was evaporated to near dryness under reduced pressure at 35°C with a rotary evaporator. The cleanup of the extract was conducted using a multilayer chromatography column (30 cm × 10 mm i.d.). For measuring PAHs and OCPs, a two-layer column (from bottom to top, sequentially packed with aluminium oxide and silica gel) was used; the extract was successively eluted with 20 mL n-hexane and 70 mL dichloromethane. For measuring PCBs, and PBDEs, a five-layer column (from bottom to top, sequentially packed with aluminium oxide, neutral silica gel, alkaline silica gel, neutral silica gel, and acid silica gel) was used; the extract was eluted with 70 mL mixture of n-hexane and dichloromethane (1 : 1, v/v). The eluent was concentrated with the rotary evaporator and transferred to a 1.2 mL GC sample bottle. The final volume was adjusted to approximately 1 mL under a nitrogen stream. Then, 100 ng of each of the internal standards (2-fluoro-1,10-biphenyl and p-terphenyl-d$_{14}$ for PAHs, 4,4$'$-dichlorobiphenyl for OCPs, pentachloronitrobenzene for PCBs, and C^{13}-PCB-208 for PBDEs) was added to the GC bottle. Thereafter, the bottle was tightly sealed up with Teflon-lined butyl rubber septa and aluminum cap. The PAHs, OCPs, PCBs and PBDEs were, respectively, measured with GC/MS (Agilent GC6890/5973MSD, USA), GC/ECD (Agilent GC7890A, ^{63}Ni-ECD, USA), GC/MS/MS (Varian 320-MS, USA), and GC/NCI/MS (Agilent 7890A/5975C, USA). More details about the measurements can be seen in [17–19].

For quality analysis and quality control, reagent and procedure blanks were included in the measurements. Concentrations of the studied POPs in the blanks were below the detection limits, and recoveries of the objective compounds in the blanks spiked with the standards ranged from 60% to 128%. For all the sediment samples, the recoveries of the surrogates were 59% ∼ 94% for PAHs, 75% ∼ 102% for OCPs, 76% ∼ 103% for PCBs, and 57% ∼ 119% for PBDEs. Two replicates were analyzed for some samples and the relative deviation between the replicates was below 30% for the studied POPs.

The reagents acetone, n-hexane, and dichloromethane (analytical grade, Beijing Reagent, China) were purified by distillation before use. Silica gel (100–200 mesh, Qingdao Marine Chemical, China) was baked at 450°C for 4 h and activated at 130°C for 16 h prior to use. The surrogate standards, internal standards, and working standards (guarantee grade) were purchased from J&K Chemical, USA.

2.4. Ecological Risk Assessment of the POPs in the Sediments. Based on the toxicity data of the benthic organisms, the threshold and probable effect concentrations (TEC and PEC) derived from consensus-based sediment quality guidelines for the analytes were used to assess the ecological risks of PAHs, OCPs, and PCBs in the studied sediments [20, 21]. TEC values represent concentrations below which adverse effects to these organisms are not likely, whereas PEC values represent concentrations above which adverse effects are likely. At levels between the TEC and PEC benchmarks, incremental increases in toxicity of sediments have been noted [20]. Two hazard quotients, one representing the threshold effect concentration (TEC-HQ) and the other representing the probable effect concentration (PEC-HQ), were calculated as the ratio of the level of each POP in the sediments to either the TEC or PEC for that POP. When TEC-HQ values were less than 1, rare adverse ecological effects were expected. When TEC-HQ values were greater than 1 but PEC-HQ values were less than 1, adverse ecological effects were possible but less frequent than those observed at the PEC level. Finally, when PEC-HQ values were greater than 1, frequent adverse ecological effects were expected.

Based on the toxicity data of benthic organisms [22], the multiple-species no-observed-effect concentrations (MS NOEC) were derived to assess the ecological risks of PBDEs in the studied sediments [23]. The hazardous quotient (HQ) calculated as the ratio of the measured level to the MS NOEC was used to assess the ecological risk of each PBDE in the sediment. When HQ values were less than 1, rare adverse ecological effects were expected. When HQ values were greater than 1, frequent adverse ecological effects were expected.

3. Results and Discussion

3.1. Physicochemical Properties of the Sediments. Physicochemical properties of the 10 sediment samples were measured and shown in Table 1. Overall, the concentrations of available-N in the sediments collected from waste discharging rivers (b2, b3, b5, b6, b8, and b10) were greater than those collected from normal water bodies (b1, b4, b7, and b9), while no much difference between the normal water bodies and the waste discharging rivers was observed for the other parameters. The highest TOC value was detected in b1 (mouth of Hai River), followed by b3 (mouth of Dagu waste discharging river). The physicochemical properties may influence the behavior of POPs in the sediments.

3.2. Concentration Levels of POPs in the Sediments

3.2.1. Concentrations of PAHs in the Sediments. The 16 priority PAHs were all detected in the 10 sediment samples, as shown in Table 2. Overall, the concentration levels of PAHs in the river mouth (b1 and b3) were higher than those in the other locations, the levels of PAHs in the waste discharging rivers were higher than those in the normal water bodies, and the levels of low molecular weight (LMW, 2 ∼ 3 rings) PAHs were higher than those of high molecular weight (HMW, 4 ∼ 6 rings) PAHs. The ΣPAH$_{16}$ ranged from 274.06 μg/kg to 2656.64 μg/kg, with the mean value being 1198.51 μg/kg. The levels of PAHs in Tianjin coastal area were lower than

TABLE 1: Physicochemical properties of the sampled sediments.

Label	Location	pH	Available-N (mg/L)	Available-P (mg/L)	TOC (%)
b1	Mouth of Hai River	6.1	88.55	24.12	4.83
b2	Dagu waste discharge river	8.3	326.48	16.49	3.18
b3	Mouth of Dagu waste discharge river	7.1	104.34	19.11	4.69
b4	Offshore river	7.5	58.91	<0.10	2.65
b5	Du waste discharging river	8.1	104.72	30.97	1.47
b6	Bei waste discharging river	7.6	75.85	27.65	3.25
b7	Offshore sea	6.9	26.57	25.96	1.45
b8	Yinghe reservoir	7.0	41.97	6.26	1.78
b9	Mouth of Yongding new river	8.1	58.14	37.01	1.53
b10	Beitang waste discharging river	6.9	59.68	7.78	1.94

TABLE 2: Concentrations of PAHs in the sampled sediments (μg/kg).

PAH	b1	b2	b3	b4	b5	b6	b7	b8	b9	b10
Naphthalene	771.09	657.56	582.06	126.68	90.56	145.79	75.69	85.16	76.97	226.21
Acenaphthylene	41.77	15.16	24.72	10.66	4.19	7.83	4.08	42.83	3.91	13.99
Acenaphthene	344.24	77.51	51.62	51.00	22.86	33.48	33.98	21.09	27.04	358.71
Fluorene	245.17	79.40	129.82	208.65	27.88	81.69	40.79	37.79	28.04	255.55
Phenanthrene	289.16	103.49	312.03	54.23	37.76	215.01	56.15	83.57	31.26	134.74
Anthracene	52.72	15.59	60.03	10.54	4.86	41.23	9.69	29.46	6.08	27.11
Fluoranthene	6.72	68.19	256.16	93.34	32.67	275.56	55.69	326.82	32.44	2.41
Pyrene	239.06	55.64	272.13	77.43	24.52	220.19	46.16	194.15	27.22	78.34
Benzo(a)anthracene	71.86	7.18	42.41	15.08	3.66	75.73	3.35	34.37	3.04	30.47
Chrysene	77.46	17.62	117.84	13.90	7.22	171.90	12.73	84.18	7.56	36.50
Benzo(b)fluoranthene	194.85	16.85	83.22	25.53	15.83	106.85	21.32	84.79	13.95	86.15
Benzo(k)fluoranthene	42.01	0.02	52.08	16.11	9.91	66.88	13.34	53.07	8.73	20.19
Benzo(a)pyrene	90.40	6.72	105.78	6.29	3.82	136.30	7.44	30.10	4.27	36.76
Indeno(1,2,3-cd)pyrene	78.22	2.23	59.36	6.37	2.65	130.04	6.30	17.85	2.89	38.89
Dibenzo(a,h)anthracene	22.09	0.51	14.32	1.33	0.54	5.64	1.21	2.98	0.65	9.57
Benzo(ghi)perylene	89.83	2.71	52.93	4.84	2.72	94.66	4.97	11.19	0.01	1.28
$\sum \text{PAH}_{16}$	2656.64	1126.39	2216.51	721.98	291.63	1808.79	392.88	1139.40	274.06	1356.86

those in the Pearl River Delta and the Rizhao offshore area but higher than those in Xiamen Bay, Dalian Bay, and the mouth of Yangtze River as well its neighboring sea area in China [24–28].

It is generally believed that PAHs of different sources have different structures and compositions, and therefore characteristic ratios of some PAHs could be used to characterize the sources [29–31]. In this study, four ratios, that is, and fluoranthene to pyrene (FLA/PYR), pyrene to benzo(a)pyrene (PYR/BaP), indeno(1,2,3-cd)pyrene to the sum of indeno(1,2,3-cd)pyrene and benzo(ghi)perylene (IcdP/(IcdP+BghiP)), and fluoranthene to the sum of fluoranthene and pyrene (FLA/(FLA+PYR)), were calculated to analyze the sources of PAHs in Tianjin coastal area. The results showed that combustion of fossil fuels (such as coal and gasoline) was the major source of PAHs in the sediments, and in a few places there were inputs of petroleum products. These observations were in agreement with the results obtained in other studies [32, 33].

It was found that TOC was positively correlated with $\sum \text{PAH}_{16}$ ($R = 0.900$, $P = 0.000$) in this study, as shown in Figure 2. This further demonstrated that the sources of

PAHs were nonpoint. PAHs from the sources might enter the water bodies through atmospheric sedimentation, surface runoff, and so forth and accumulated in the sediments owing to the adsorption by the organic matters in the sediments. In addition, the sediments (particularly the polluted ones) were generally in anaerobic conditions under which the biodegradation of PAHs were slow. Therefore, there was good correlation between TOC and $\sum \text{PAH}_{16}$.

3.2.2. Concentration Levels of OCPs, PCBs, and PBDEs in the Sediments.
The concentrations of OCPs, PCBs, and PBDEs were generally low in the studied sediments except in the Dagu waste discharging river. Figures 3, 4, and 5 show the total concentrations of 24 OCPs (ΣOCP_{24}), 35 PCBs (ΣPCB_{35}), and 14 PBDEs (ΣPBDE_{14}) in the sediments of various locations. The OCPs data for b1 and b3 were missing due to sample damages. In the Dagu waste discharging river (b2), high concentrations for the halogenated POPs were observed, where hexachlorobenzene (HCB), α-benzene hexachloride (α-BHC) and β-benzene hexachloride (β-BHC) were the major OCPs with the concentrations being 1994.99 μg/kg,
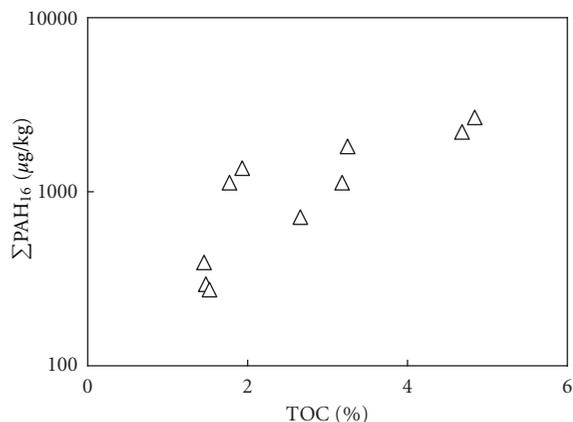
FIGURE 2: Relationship between TOC and total PAHs in the studied sediments.
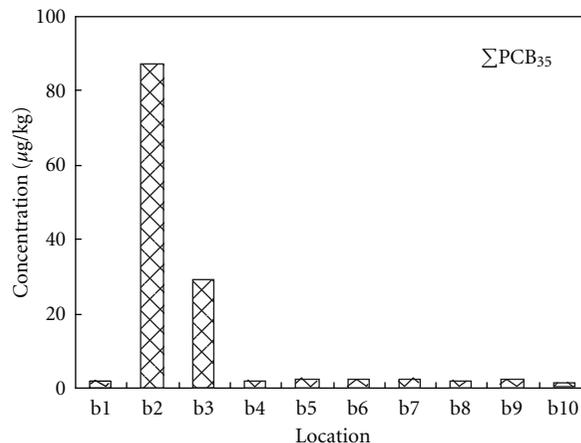
FIGURE 4: Concentrations of total PCBs in the studied sediments.
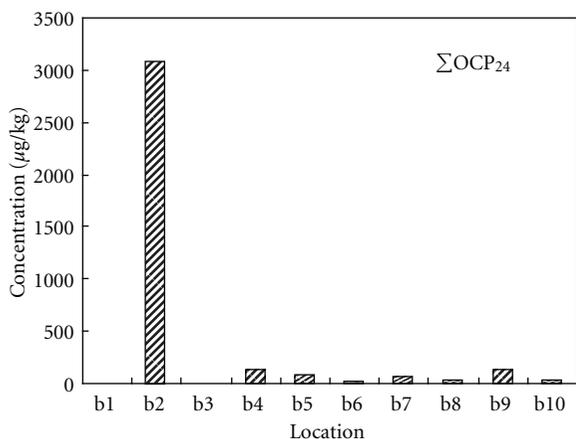
FIGURE 3: Concentrations of total OCPs in the studied sediments.
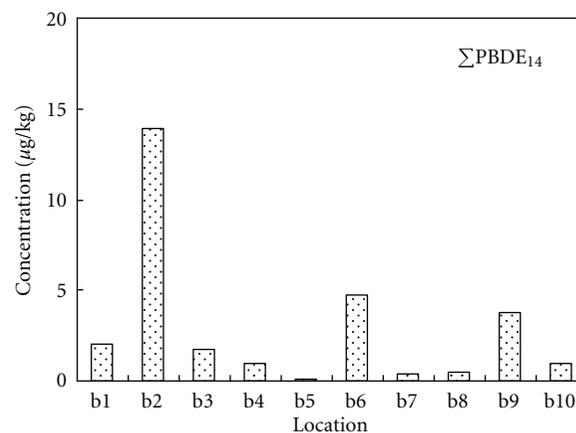
FIGURE 5: Concentrations of total PBDEs in the studied sediments.

337.27 μg/kg and 557.26 μg/kg, respectively, PCB-209, PCB-87, and PCB-70 were the major PCBs with the concentrations being 26.77 μg/kg, 32.30 μg/kg and 16.39 μg/kg, respectively, and BDE-209 was the major PBDE with the concentration being 12.97 μg/kg. The Dagu waste discharging river is a major waste discharging river in Tianjin, with daily discharge amount being over 800 thousand tons [34]. There are several chemical plants such as Tianjin chemical plant, Tianjin Dagu chemical plant located along the banks of the Dagu waste discharging river. These plants historically produced substantial OCPs like HCB, BHCs, and heptachlor epoxide. Wastes from the chemical plants may also contain PCBs and PBDEs that are used in the industry. In the mouth of the Dagu waste discharging river, the concentrations of PCBs and PBDEs were decreased, which were probably due to dilution by the sea water. Tables S1 to S3 in the supplemental materials show the individual concentrations of the OCPs, PCBs, and PBDEs in the studied sediments.

There was no significant correlation between TOC values and the concentrations of halogenated POPs in the sediment (R < 0.400, P > 0.300), indicating the sources of the halogenated POPs were of point. Compared to other coastal areas in China, the levels of OCPs in Tianjin were relatively high, exceeding the OCPs in the Pearl River Delta and its adjacent coastal areas of the South Sea, Yangtze River, the offshore of East Sea, and so forth [35–38]. The levels of PCBs and PBDEs were lower than most of the coastal areas in China [39–41].

3.3. Ecological Risks of the POPs in the Sediments.

The ecological risks of PAHs, OCPs, PCBs, and PBDEs in the studied sediments were assessed on basis of the toxicity data of benthic organisms. Relatively high risks were observed for PAHs, particularly LMW-PAHs. At each sampling location, at least one LMW-PAH had concentration over its TEC, and in several locations (b1, b2, b3, and b10), the concentrations of naphthalene and/or acenaphthene exceeded their PEC values, indicating adverse ecological effects to benthic organisms. Tables 3 and 4, respectively, show the TEC-HQ and PEC-HQ of PAHs in the studied sediments.

At six locations (b2, b5, b7, b8, b9, and b10), the concentrations of heptachlor epoxide exceeded the TEC value. In the Dagu waste discharging river (b2), the concentrations

TABLE 3: Threshold effect concentration hazard quotients (TEC-HQ) for PAHs[*].

PAH	TEC (μg/kg)	b1	b2	b3	b4	b5	b6	b7	b8	b9	b10
Naphthalene	176	**4.38**	**3.74**	**3.31**	0.72	0.51	0.83	0.43	0.48	0.44	**1.29**
Acenaphthylene	5.87	**7.12**	**2.58**	**4.21**	**1.82**	0.71	**1.33**	0.69	**7.30**	0.67	**2.38**
Acenaphthene	6.71	**51.30**	**11.55**	**7.69**	**7.60**	**3.41**	**4.99**	**5.06**	**3.14**	**4.03**	**53.46**
Fluorene	77.4	**3.17**	**1.03**	**1.68**	**2.70**	0.36	**1.06**	0.53	0.49	0.36	**3.30**
Phenanthrene	204	**1.42**	0.51	**1.53**	0.27	0.19	**1.05**	0.28	0.41	0.15	0.66
Anthracene	57.2	0.92	0.27	**1.05**	0.18	0.08	0.72	0.17	0.51	0.11	0.47
Fluoranthene	423	0.02	0.16	0.61	0.22	0.08	0.65	0.13	0.77	0.08	0.01
Pyrene	195	**1.23**	0.29	**1.40**	0.40	0.13	**1.13**	0.24	**1.00**	0.14	0.40
Benzo(a)anthracene	108	0.67	0.07	0.39	0.14	0.03	0.70	0.03	0.32	0.03	0.28
Chrysene	166	0.47	0.11	0.71	0.08	0.04	**1.04**	0.08	0.51	0.05	0.22
Benzo(b)fluoranthene	240	0.18	0.00	0.22	0.07	0.04	0.28	0.06	0.22	0.04	0.08
Benzo(k)fluoranthene	150	0.60	0.04	0.71	0.04	0.03	0.91	0.05	0.20	0.03	0.25
Benzo(a)pyrene	200	0.39	0.01	0.30	0.03	0.01	0.65	0.03	0.09	0.01	0.19
Indeno(1,2,3-cd)pyrene	33	0.67	0.02	0.43	0.04	0.02	0.17	0.04	0.09	0.02	0.29
Dibenzo(a,h)anthracene	170	0.53	0.02	0.31	0.03	0.02	0.56	0.03	0.07	0.00	0.01
$\sum$ PAH$_{16}$	1610	**1.65**	0.70	**1.38**	0.45	0.18	**1.12**	0.24	0.71	0.17	0.84

[*] Numbers in bold indicate TEC-HQ > 1.

TABLE 4: Possible effect concentration hazard quotients (PEC-HQ) for PAHs[*].

PAH	PEC (μg/kg)	b1	b2	b3	b4	b5	b6	b7	b8	b9	b10
Naphthalene	561	**1.37**	**1.17**	**1.04**	0.23	0.16	0.26	0.13	0.15	0.14	0.40
Acenaphthylene	128	0.33	0.12	0.19	0.08	0.03	0.06	0.03	0.33	0.03	0.11
Acenaphthene	88.9	**3.87**	0.87	0.58	0.57	0.26	0.38	0.38	0.24	0.30	**4.03**
Fluorene	536	0.46	0.15	0.24	0.39	0.05	0.15	0.08	0.07	0.05	0.48
Phenanthrene	1170	0.25	0.09	0.27	0.05	0.03	0.18	0.05	0.07	0.03	0.12
Anthracene	845	0.06	0.02	0.07	0.01	0.01	0.05	0.01	0.03	0.01	0.03
Fluoranthene	2230	0.00	0.03	0.11	0.04	0.01	0.12	0.02	0.15	0.01	0.00
Pyrene	1520	0.16	0.04	0.18	0.05	0.02	0.14	0.03	0.13	0.02	0.05
Benzo(a)anthracene	1050	0.07	0.01	0.04	0.01	0.00	0.07	0.00	0.03	0.00	0.03
Chrysene	1290	0.06	0.01	0.09	0.01	0.01	0.13	0.01	0.07	0.01	0.03
Benzo(b)fluoranthene	13400	0.00	0.00	0.00	0.00	0.00	0.00	0.00	0.00	0.00	0.00
Benzo(k)fluoranthene	1450	0.06	0.00	0.07	0.00	0.00	0.09	0.01	0.02	0.00	0.03
Benzo(a)pyrene	3200	0.02	0.00	0.02	0.00	0.00	0.04	0.00	0.01	0.00	0.01
Indeno(1,2,3-cd)pyrene	135	0.16	0.00	0.11	0.01	0.00	0.04	0.01	0.02	0.00	0.07
Dibenzo(a,h)anthracene	3200	0.03	0.00	0.02	0.00	0.00	0.03	0.00	0.00	0.00	0.00
$\sum$ PAH$_{16}$	22800	0.12	0.05	0.10	0.03	0.01	0.08	0.02	0.05	0.01	0.06

[*] Numbers in bold indicate PEC-HQ > 1.

of heptachlor epoxide and γ-BHC exceeded their PEC values (the PEC-HQ of γ-BHC was up to 7.49). In the other locations, there were rare risks for OCPs. For PCBs, slight risk was observed in the Dagu waste discharging river (b2) where the ΣPCB$_{35}$ exceeded the TEC but was far less than the PEC; no risk was observed in the other locations. As for PBDEs, all the HQ values were far less than 1 indicating no risk.

4. Conclusions

In the 10 sediments sampled from different surface water bodies in Tianjin coastal area, the 16 priority PAHs were all detected and the mean value of ΣPAH$_{16}$ was 1198.51 μg/kg.

The major source of PAHs was the combustion of fossil fuels, with inputs of petroleum products in a few places. The concentration levels of OCPs, PCBs, and PBDEs were generally low except in the Dagu waste discharging river where there were many chemical plants along the banks. The TOC in the sediments had good correlation with ΣPAH$_{16}$ but not with the halogenated POPs.

There were relatively high risks for PAHs in the studied sediments. At each sampling location, at least one LMW-PAH had concentration over its TEC, and in several locations, the concentrations of naphthalene and/or acenaphthene exceeded their PEC values. In the Dagu waste discharging river, relatively high risk for OCPs and slight risk for PCBs

were observed. In the other locations, the risks for the halogenated POPs were rare.

Acknowledgments

Conflict of Interests

The authors declare they have no conflict of interests.

References

[1] K. C. Jones and P. De Voogt, "Persistent organic pollutants (POPs): state of the science," *Environmental Pollution*, vol. 100, no. 1–3, pp. 209–221, 1998.

[2] J. Li, X. Shang, Z. Zhao, R. L. Tanguay, Q. Dong, and C. Huang, "Polycyclic aromatic hydrocarbons in water, sediment, soil, and plants of the Aojiang River waterway in Wenzhou, China," *Journal of Hazardous Materials*, vol. 173, no. 1–3, pp. 75–81, 2010.

[3] G. Ramdinea, D. Fichetb, M. Louisa et al., "Polycyclic aromatic hydrocarbons (PAHs) in surface sediment and oysters (*Crassostrea rhizophorae*) from mangrove of Guadeloupe: levels, bioavailability, and effects," *Ecotoxicology and Environmental Safety*, vol. 79, pp. 80–89, 2012.

[4] P. Baumard, H. Budzinski, P. Garrigues, J. C. Sorbe, T. Burgeot, and J. Bellocq, "Concentrations of PAHs (polycyclic aromatic hydrocarbons) in various marine organisms in relation to those in sediments and to trophic level," *Marine Pollution Bulletin*, vol. 36, no. 12, pp. 951–960, 1998.

[5] L. P. Chrysikou, P. G. Gemenetzis, and C. A. Samara, "Wintertime size distribution of polycyclic aromatic hydrocarbons (PAHs), polychlorinated biphenyls (PCBs) and organochlorine pesticides (OCPs) in the urban environment: street- versus rooftop-level measurements," *Atmospheric Environment*, vol. 43, no. 2, pp. 290–300, 2009.

[6] X. Li, Y. Gan, X. Yang, J. Zhou, J. Dai, and M. Xu, "Human health risk of organochlorine pesticides (OCPs) and polychlorinated biphenyls (PCBs) in edible fish from Huairou Reservoir and Gaobeidian Lake in Beijing, China," *Food Chemistry*, vol. 109, no. 2, pp. 348–354, 2008.

[7] Y. P. Liu, J. G. Li, Y. F. Zhao, S. Wen, F. F. Huang, and Y. N. Wu, "Polybrominated diphenyl ethers (PBDEs) and indicator polychlorinated biphenyls (PCBs) in marine fish from four areas of China," *Chemosphere*, vol. 83, no. 2, pp. 168–174, 2011.

[8] Q. Li, C. Yan, Z. Luo, and X. Zhang, "Occurrence and levels of polybrominated diphenyl ethers (PBDEs) in recent sediments and marine organisms from Xiamen offshore areas, China," *Marine Pollution Bulletin*, vol. 60, no. 3, pp. 464–469, 2010.

[9] J. Szlinder-Richert, I. Barska, Z. Usydus, and R. Grabic, "Polybrominated diphenyl ethers (PBDEs) in selected fish species from the southern Baltic Sea," *Chemosphere*, vol. 78, no. 6, pp. 695–700, 2010.

[10] E. F. Fitzgerald, B. A. Fletcher, E. Belanger, L. Tao, K. Kannan, and S. A. Hwang, "Fish consumption and concentrations of Polybrominated Diphenyl Ethers (PBDEs) in the serum of older residents of upper Hudson River communities," *Archives of Environmental and Occupational Health*, vol. 65, no. 4, pp. 183–190, 2010.

[11] J. Li, Y. L. Lü, W. T. Jiao et al., "Concentration and origin of polycyclic aromatic hydrocarbons in surface soil in the Industrial Area of Tianjin, China," *Acta Scientiae Circumstantiae*, vol. 28, no. 10, pp. 2111–2117, 2008.

[12] J. X. Lü, Y. W. Wang, Q. H. Zhang et al., "Contamination trends of polybrominated diphenyl ethers, organochlorine pesticides and heavy metals in the sediments of river mouth of Dagu waste discharging river in Tianjin," *Chinese Science Bulletin*, vol. 52, no. 3, pp. 277–282, 2007.

[13] A. X. Liu, Y. H. Lang, L. D. Xue, S. L. Liao, and H. Zhou, "Probabilistic ecological risk assessment and source apportionment of polycyclic aromatic hydrocarbons in surface sediments from yellow sea," *Bulletin of Environmental Contamination and Toxicology*, vol. 83, no. 5, pp. 681–687, 2009.

[14] S. Burreau, Y. Zebühr, D. Broman, and R. Ishaq, "Biomagnification of PBDEs and PCBs in food webs from the Baltic Sea and the northern Atlantic Ocean," *Science of the Total Environment*, vol. 366, no. 2-3, pp. 659–672, 2006.

[15] S. B. Gewurtz, R. Lazar, and G. D. Haffner, "Comparison of polycyclic aromatic hydrocarbon and polychlorinated biphenyl dynamics in benthic invertebrates of Lake Erie, USA," *Environmental Toxicology and Chemistry*, vol. 19, no. 12, pp. 2943–2950, 2000.

[16] Z. G. Li, Y. M. Luo, and Y. Teng, *Study Methods for Soil and Environmental Microorganisms*, Science Press, Beijing, China, 2008.

[17] S. Tao, W. Wang, W. Liu et al., "Polycyclic aromatic hydrocarbons and organochlorine pesticides in surface soils from the Qinghai-Tibetan plateau," *Journal of Environmental Monitoring*, vol. 13, no. 1, pp. 175–181, 2011.

[18] P. Zhou, K. F. Lin, X. Y. Zhou et al., "Distribution of polybrominated diphenyl ethers in the surface sediments of the Taihu Lake, China," *Chemosphere*, vol. 88, no. 11, pp. 1375–1382, 2012.

[19] G. H. Xing, Y. Yang, J. K. Yan Chan, S. Tao, and M. H. Wong, "Bioaccessibility of polychlorinated biphenyls in different foods using an in vitro digestion method," *Environmental Pollution*, vol. 156, no. 3, pp. 1218–1226, 2008.

[20] J. E. Weinstein, K. D. Crawford, T. R. Garner, and A. J. Flemming, "Screening-level ecological and human health risk assessment of polycyclic aromatic hydrocarbons in stormwater detention pond sediments of Coastal South Carolina, USA," *Journal of Hazardous Materials*, vol. 178, no. 1–3, pp. 906–916, 2010.

[21] D. D. MacDonald, C. G. Ingersoll, and T. A. Berger, "Development and evaluation of consensus-based sediment quality guidelines for freshwater ecosystems," *Archives of Environmental Contamination and Toxicology*, vol. 39, no. 1, pp. 20–31, 2000.

[22] Environment Canada, "Ecological Screening Assessment Report on Polybrominated Diphenyl Ethers (PBDEs)," 2006.

[23] Z. Z. Wang, W. J. Zhao, and X. F. Ma, "Ecological risk assessment of polybrominated diphenyl ether in the water environment of Zhujiang River mouth," *Environmental Protection*, vol. 36, no. 4, pp. 65–68, 2010.

[24] A. X. Liu, Y. H. Lang, L. D. Xue et al., "Ecological risk assessment of PAHs in the costal surface sediments from Yellow

Sea (rizhao city)," *Environmental Chemistry*, vol. 27, no. 6, pp. 805–809, 2008.

[25] X. J. Luo, S. J. Chen, B. X. Mai et al., "Source, transport and risk assessment of PAHs in surface sediments from Pearl River Delta," *Asian Journal of Ecotoxicology*, vol. 1, no. 1, pp. 17–24, 2006.

[26] B. Wang, Z. Y. Li, M. Z. Fu et al., "Distribution and ecological risk assessment of PAHs in surface sediments from the Yangtze Estuary and its adjacent areas," *Periodical of Ocean University of China*, vol. 37, supplemental, pp. 083–087, 2007.

[27] Q. Z. Li, G. X. Li, Z. X. Luo et al., "Pollution characteristics and ecological risk assessment of heavy metals and polycyclic aromatic hydrocarbons(PAHs) in sediment from Xiamen Bay," *Environmental Chemistry*, vol. 28, no. 6, pp. 869–875, 2009.

[28] L. Liu, J. H. Zhang, Y. Y. Hu et al., "Ecological risk assessment on polycyclic aromatic hydrocarbons in surface sediments of Dalian Bay," *Marine Environmental Science*, vol. 30, no. 4, pp. 477–480, 2011.

[29] M. A. Sicre, J. C. Marty, A. Saliot, X. Aparicio, J. Grimalt, and J. Albaiges, "Aliphatic and aromatic hydrocarbons in the mediterranean aerosol," *International Journal of Environmental Analytical Chemistry*, vol. 29, no. 1-2, pp. 73–94, 1987.

[30] X. L. Zhu, W. L. Liu, Y. Y. Lu et al., "Study on the characteristics of PAHs source profile of coal combustion," *Research of Environmental Sciences*, vol. 14, no. 5, pp. 4–8, 2001.

[31] M. B. Yunker, R. W. Macdonald, R. Vingarzan, R. H. Mitchell, D. Goyette, and S. Sylvestre, "PAHs in the Fraser River basin: a critical appraisal of PAH ratios as indicators of PAH source and composition," *Organic Geochemistry*, vol. 33, no. 4, pp. 489–515, 2002.

[32] X. M. Lin, W. X. Liu, J. L. Chen et al., "Distribution and ecological risk assessment of polycyclic aromatic hydrocarbons in surface sediments from Bohai Sea, China," *Acta Scientiae Circumstantiae*, vol. 25, no. 1, pp. 70–75, 2005.

[33] N. J. Hu, P. Huang, J. H. Liu et al., "Source apportionment of polycyclic aromatic hydrocarbons in surface sediments of the Bohai Sea, China," *Environmental Science and Pollution Research*. In press.

[34] Z. N. He, P. Hu, Y. Yu et al., "Distribution and source analysis of classic persistent organic pollutants in sediments from Dagu dainage canal, Tianjin, China," *Journal of Agro-Environment Science*, vol. 30, no. 10, pp. 2106–2112, 2011.

[35] Y. Q. Xing, F. Yin, H. Huang et al., "Residual of organochlorine pesticides in sediments from Changjiang Estuary and nearshore of the East China Sea," *Marine Environmental Science*, vol. 30, no. 1, pp. 52–56, 2011.

[36] X. J. Luo, S. J. Chen, B. X. Mai et al., "Distribution of organochlorine pesticites (OCPs) in surface sediments in Pearl River Delta and its adjacent coastal areas of South China Sea," *Acta Scientiae Circumstantiae*, vol. 25, no. 9, pp. 1272–1279, 2005.

[37] J. T. Wang, L. J. Tan, W. H. Zhang, and Z. R. Lian, "Concentrations and distribution characteristic of PAHs, PCBs and OCPs in the surface sediments of Qingtao coastal area," *Environmental Science*, vol. 31, no. 11, pp. 2713–2722, 2010.

[38] X. Y. Gong, S. H. Qi, C. L. Lü et al., "Vertical distribution characteristics of organochlorine pesticides in sediment core of Quanzhou Bay," *Marine Environmental Science*, vol. 26, no. 4, pp. 369–372, 2007.

[39] J. H. Guo, Y. F. Yin, L. Zheng et al., "The distribution and risk assessment of polychlorinated biphenyl in surface sediments in Estuaries of Jiaozhou bay, China," *Journal of Agro-Environment Science*, vol. 30, no. 5, pp. 965–972, 2011.

[40] Y. Xing, Y. L. Lu, W. B. Liu, Y. J. Shi, W. Luo, and H. C. Ren, "Assessment of PCB pollution in spatial distribution and analysis of the PCB sources in sediments in China," *Environmental Science*, vol. 27, no. 2, pp. 228–234, 2006.

[41] S. J. Chen, B. X. Mai, Y. P. Zeng et al., "Polybrominated diphenyl ethers (PBDEs) in surficial sediments of the Pearl River Delta and adjacent South China Sea," *Acta Scientiae Circumstantiae*, vol. 25, no. 9, pp. 1265–1271, 2005.

The *S*cientificWorldJOURNAL

Research Article

Distribution and Bioconcentration of Polycyclic Aromatic Hydrocarbons in Surface Water and Fishes

Haiyan Li[1, 2] and Yong Ran[1]

[1] *State Key Laboratory of Organic Geochemistry, Guangzhou Institute of Geochemistry, Chinese Academy of Sciences, Wushan, Guangzhou 510640, China*
[2] *University of Chinese Academy of Sciences, Beijing 100049, China*

Correspondence should be addressed to Yong Ran, yran@gig.ac.cn

To examine spatial distribution and bioconcentration of PAHs, water and fish samples were collected from Pearl River Delta in summer and spring, respectively. Particulate organic carbon, dissolved organic carbon, biodegradable DOC (BDOC), and chlorophyll a were measured. PAHs were dominated by 2- and 3-ring compounds in the water and SPM samples. Aqueous and solid-phase PAHs, respectively, showed significant correlations with total organic matter (TOC) in SPM or dissolved organic matter (DOC) in the water. The in-situ partitioning coefficients ($\log K_{oc}$, mL/g) for the samples were observed to be related to $\log K_{ow}$, implying that the hydrophobicity of PAHs is a critical factor in their distribution. It was also observed that BCF increased with the increasing K_{ow} in the viscera of tilapia ($\log \text{BCF} = 0.507 \log K_{ow} - 1.368$, $r = 0.883$). However, most of the observed log BCF values in other different fish tissues at first increased with the increasing of $\log K_{ow}$, then reached a maximum value when $\log K_{ow}$ is between 5 and 7, and then decreased when $\log K_{ow}$ is higher than 7, indicating that the value of BCF may vary due to the diversity of fish species.

1. Introduction

Polycyclic aromatic hydrocarbons (PAHs), which are listed as US-EPA and EU priority pollutants, are widely distributed in the environment. PAHs are produced primarily as a result of incomplete combustion of fossil fuels and other organic materials, as well as from forest fires [1]. PAHs in seawater depend on their chemical properties. PAHs with low molecular weight can enter atmosphere by evaporation, while nonvolatile PAHs with high molecular weight could contaminate surface water through atmospheric deposition [2]. Due to their carcinogenic and mutagenic effects to both terrestrial and aquatic organisms, PAHs have attracted much attention.

Many investigations focus on the transport and fate of PAHs in aquatic environment [3]. Qiu et al. [4] examined the level of 15 PAHs in seawater, suspended particulate matter (SPM), surface sediment, and core sediment samples of Deep Bay, South China. Recently, distributions, composition, and sources of polycyclic aromatic hydrocarbons (PAHs) in sediments and suspended particulate matter (SPM) from the Pearl River Delta have also been evaluated [5, 6]. Major

environmental factors in mediating PAH levels in the sediments as well as bioaccumulation patterns in fish were identified at Mai Po Marshes [7].

Although numerous studies have investigated the occurrence of PAHs in various compartments of the PRD, data on fish species are limited [8, 9]. PAHs in fish tissues, for example, fish liver, skin, or gills, which could provide more evidence for the bioaccumulation of PAHs and reflect the environmental conditions, have not been investigated. Previous investigations in Pearl River Delta mainly focused on the source, distribution, migration, and fate of PAHs. However, their environmental processes such as the transformation and enrichment of PAHs have rarely been conducted.

The Pearl River Delta (PRD) has three main tributaries, which are the Xijiang (West) River, the Beijiang (North) River, and the Dongjiang (East) River, and flow into the South China Sea. They form one of the largest rivers in China. PRD endures a significant urbanization and industrialization in recent three decades. It is located in the northern subtropical zone, where the climate is characterized by mild temperatures and frequent rainfalls all years around,
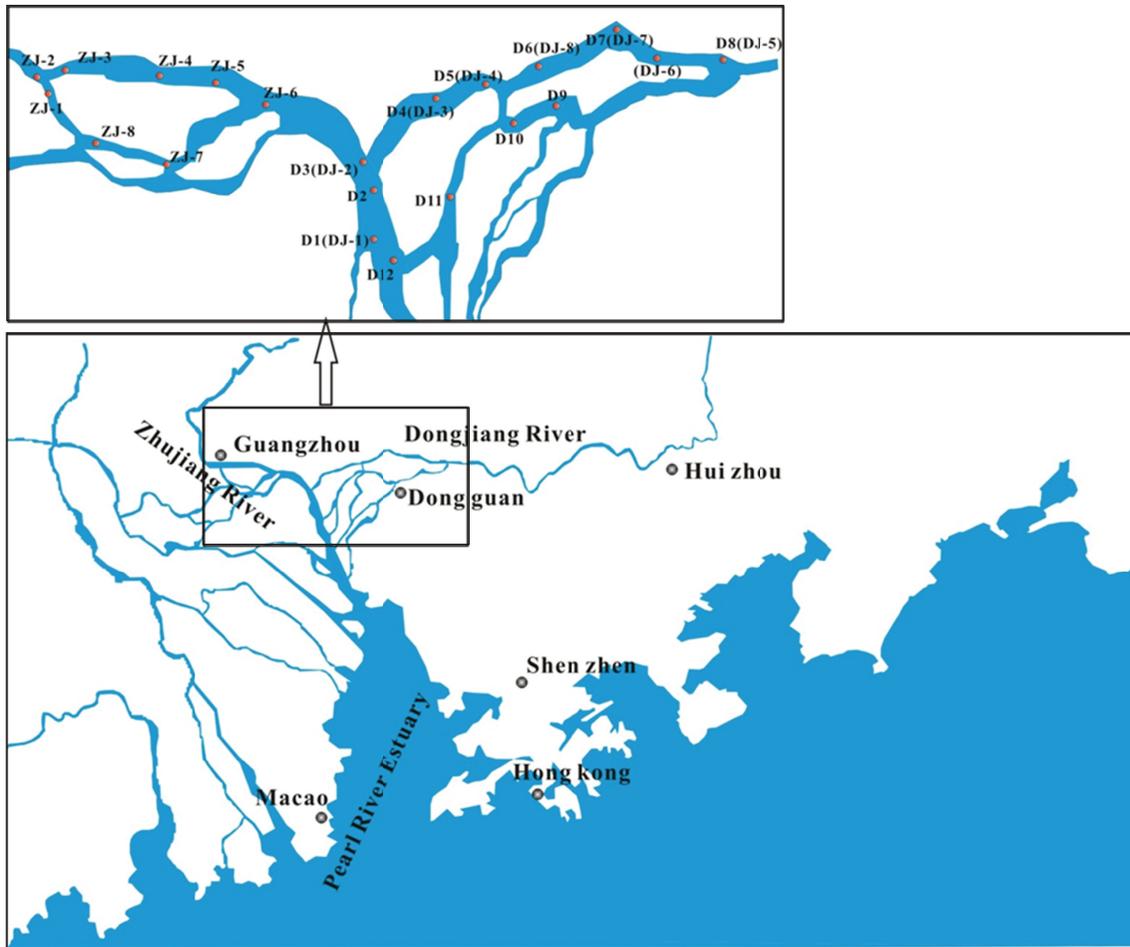
FIGURE 1: The sampling sites of the rivers from the Pearl River system.

facilitating the transport of contaminants to the aquatic environments. Owing to high population density, massive use of chemicals, and intensive industrial and agricultural development in this area, significant air and water pollutions occur [10, 11]. With dramatic increase in aquatic environment pollutions in this region, the local fishery resource, biomass, and biodiversity decline continuously. For example, fish species in the Pearl River Estuary sharply decreased from more than 200 species in 1970s to 50 species in recent years, and the proportion of the large size fish dropped from nearly 50% in 1980s to lower than 10% in this century [8, 12].

The present study aimed to determine the spatial distribution and partitioning of PAHs in water/SPM and the affecting factors, and the distribution and accumulation of PAHs in different species of fishes in order to evaluate the enrichment regularities of PAHs among water, SPM, and fish organisms.

2. Materials and Methods

2.1. Sample Collection. Water and SPM samples at 0.5 m below the surface were collected from Pearl River Delta in July 2010 and April 2011, respectively (Figure 1). Meanwhile fish samples were collected at site D7 (*xenocypris davidi*, Bleeker) and site D8 (tilapia, *blunt snout* bream, *Cirrhinus mrigala*) in July, 2010, and at site DJ-5 (red grass carp, blunt snout bream named as blunt snout bream-2, carp) in April 2011. Water samples were pumped into precleaned 10 L brown glass bottles with a stainless-steel submersible pump. NaN_3 was added to each bottle to inhibit biodegradation of PAHs. pH, conductivity, and salinity were measured immediately at the sites by using a digital pH meter with dissolved oxygen meter and salinometer (MP511,Shanghai). All of the parameters are listed in Tables 1 and 2. Some of the fish samples were also bought from small fishing boats along the river. The water samples were filtered through the 47 mm glass fiber filters (Whatman GF/F, 0.7 um pore sizes) precombusted at $450°C$ for 4 h beforehand. Then, the GF/F filters were stored at $-20°C$ until analysis. Fish samples were dissected carefully to obtain muscles, gills, and viscera. These samples were also stored at $-20°C$ until analysis.

2.2. Chemicals. HPLC-grade methanol (MeOH), hexane (Merck), ethyl acetate (Sigma), redistilled water, and analytical grade dichloromethane (DCM) and acetone were used for the analysis. Sixteen PAHs standards and deuterated

TABLE 1: Major aquatic chemical properties of the water samples collected from Dongjiang River in July 2010.

Station	DOC (mg/L)	BDOC (mg/L)	POC%	Chl a μg/L	SPM (mg/L)	Total PAHs (ng/L)	
						Dissolved	Particulate
D-1	10.20	7.32	8.49	3.11	20	16.56	116.49
D-2	2.71	0.75	9.46	4.81	31	20.24	229.82
D-3	13.91	10.9	4.93	6.14	34	21.10	321.68
D-4	1.19	−0.23	13.3	4.53	53	31.97	360.14
D-5	2.28	0.49	4.14	4.62	33	27.99	91.35
D-6	3.45	1.33	6.29	4.29	20	34.27	30.14
D-7	1.93	−0.408	4.44	3.39	16	33.91	252.75
D-8	2.11	0.555	4.76	3.43	12	25.89	25.57
D-9	1.85	0.017	5.67	3.18	11	23.26	41.36
D-10	2.77	0.771	nd	3.53	11	24.19	32.82
D-11	2.63	0.705	5.44	10.1	17	28.80	38.83
D-12	3.18	0.652	5.10	5.22	27	19.37	37.50

TABLE 2: Major aquatic chemical properties of the water samples in April 2011.

Station	Location	PH	COND μs/cm	SAL (ppt)	DO (mg/L)	DOC (mg/L)	BDOC (mg/L)	POC%	Chl a μg/L	SPM (mg/L)	$\sum_{15}$ PAHs (ng/L)	
											Dissolved	Particulate
DJ-1	23°01.372N 113°30.873E	6.92	2280	0.62	3.93	3.71	1.11	4.74	28.2	24.00	11.11	97.91
DJ-2	23°03.161N 113°31.580E	6.94	1244	0.61	3.34	4.01	0.777	6.86	21.2	23.65	12.06	93.0
DJ-3	23°05.685N 113°35.399E	6.96	327	0.16	1.72	5.24	3.06	7.08	21.7	22.32	65.21	114.9
DJ-4	23°06.672N 113°38.957E	6.9	255	0.12	2.42	5.38	3.08	9.65	3.87	13.65	46.32	80.2
DJ-5	23°07.115N 113°50.281E	7.03	177	0.08	6.60	2.42	0.902	1.59	2.93	42.86	27.48	80.1
DJ-6	23°07.843N 113°45.988E	6.92	199	0.1	7.06	3.00	1.40	1.80	2.76	34.24	11.46	65
DJ-7	23°08.121N 113°44.895E	6.76	166	0.08	6.67	2.28	0.613	1.64	2.76	24.97	14.83	53.5
DJ-8	23°08.731N 113°43.746E	6.51	179	0.08	6.00	2.62	1.06	2.29	3.30	14.72	12.75	103.6
ZJ-1		7.23	867	0.43	4.68	4.79	0.889	8.87	40.7	42.26	44.21	191.6
ZJ-2		7.16	814	0.37	5.56	4.88	0.883	14.6	48.3	46.87	38.71	223.2
ZJ-3		7.32	660	0.32	5.98	4.41	0.700	7.36	41.9	36.56	40.54	191.9
ZJ-4		7.26	696	0.33	5.6	3.60	0.415	4.05	45.1	42.10	27.34	229.2
ZJ-5		7.2	649	0.32	5.68	3.02	0.438	4.24	31.3	19.96	21.84	80.8
ZJ-6		7.08	957	0.48	6.28	2.81	0.563	5.00	26.4	26.32	22.59	105.5
ZJ-7		7.24	618	0.3	6.38	2.62	0.421	4.51	16.2	22.49	20.43	92.1
ZJ-8		7.21	492	0.25	6.49	2.62	0.441	4.81	20.9	30.44	36.49	151.7

PAHs (naphthalene-d_8, acenaphthene-d_{10}, phenanthrene-d_{10}, chrysene-d_{12}, and perylene-d_{12}) were purchased from Ultra Scientific Inc. Hexamethylbenzene was purchased from Aldrich. ENVI-C_{18} SPE cartridges (500 mg, 6 mL) were obtained from Supelco (Bellefonte, PA, USA), and glass fiber filters (GF/F, 0.7 μm pore size) were purchased from Whatman (Maidstone, England). Neutral silica gel (80–100 mesh) and alumina (100–200 mesh) were extracted with DCM for 72 h and activated at 120°C and 180°C for 12 h,

respectively. And then they were deactivated by adding 3% redistilled water. Anhydrous sodium sulfate, glasswares, and glass fiber filters were baked at 450°C for 4 hours prior to use.

2.3. Analytical Procedure. The procedures for the extraction and purification of PAHs from water, suspended particulate matter (SPM), and fish samples were published elsewhere [5, 12–14]. In brief, 4 L filtered water was spiked with deuterated internal standards (naphthalene-d_8, acenaphthene-d_{10},

phenanthrene-d_{10}, chrysene-d_{12}, and perylene-d_{12}). The Envi-C_{18} SPE cartridge was sequentially conditioned with 5 mL of ethyl acetate, 5 mL of methanol, and 5 mL distilled water containing 2% methanol. Then, the water sample passed through the preconditioned Envi-C_{18} SPE cartridge at a flow rate of 8–10 mL/min. The cartridge was cleaned with 5 mL distilled water, dried under vacuum for 15 minutes, and eluted with 3×5 mL of ethyl acetate. Finally the elution was vacuum-evaporated to 1 mL and concentrated to 100 μL under a gentle nitrogen stream.

Particle-loaded filters were freeze dried, weighed, and spiked with surrogate standards and Soxhlet extracted for 72 h with 200 mL of dichloromethane (DCM). Each extract was concentrated, solvent exchanged to hexane, and reduced to approximately 1 mL. A 1 : 2 alumina : silica gel glass column was used to purify the concentrated extracts. Then, the column was eluted with 15 mL n-hexane and 70 mL 7 : 3 hexane/DCM (v/v) successively. The second fraction containing PAHs was also finally concentrated to 100 μL under a gentle N_2 stream before GC/MS analysis.

Fish tissue samples were freeze dried, spiked with surrogate standards, and Soxhlet extracted for 72 h with 200 mL of dichloromethane (DCM). Each extract was concentrated to about 5 mL and divided into two fractions. One fraction was used to determine the content of lipid by weight method, and the remaining fraction was used to determine the concentration of PAHs in fish tissue. The remaining fraction passed through a gel permeation column to remove lipid. The elution solvent from 90 to 280 mL was collected and concentrated by a rotary evaporator. Then, the concentration extract was again cleaned by an alumina/silica gel column. And the subsequent analytical procedure was the same as that of SPM. The fraction containing PAHs was also finally concentrated to 100 μL before GC/MS analysis.

2.4. Instrumental Analysis. Sixteen PAHs were quantified by a Hewlette Packard (HP) 6890 gas chromatograph (GC) coupled to a HP 5975 mass spectrometer (MS) with a DB-5 fused silica capillary column (30 m $\times$ 0.25 μm $\times$ 0.25 mm i.d.). The system was operated in electron impact mode (EI) and detected by using selective ion monitoring mode (SIM) with helium as the carrier gas at a constant flow rate of 1 mL/min. The oven temperature was programmed from 60°C to 200°C at 10°C/min, to 214°C at a rate of 2°C/min and to 255°C at 5°C/min and held for 2 min and further increased to 290°C at 20°C/min and held at 290°C for 12 min. The concentrations of PAHs in the water and suspended particle matter were quantified by using the isotope dilution method with isotope-labeled internal standards (d8-Nap, d10-Acy, d10-Phe, d12-Chry, and d12-Per). PAHs in fish tissues were quantified with the internal calibration method based on five-point calibration curve.

Ten mL of each water sample passed through the GF/F filter was acidified with HCl to pH = 3 and then used for DOC analysis. TOC analyzer (TOC-VCPH, Shimadzu) was used to measure the DOC concentration. For the determination of TOC in SPM samples, the filters were dried at 60°C for 12 h after acidification with diluted HCl to remove carbonates. TOC in particle samples was measured using an elemental analyzer (Vario EL III Elementar, Germany) with acetanilide as external standard. For the determination of biodegradable DOC (BDOC), approximately 300 mL of filtered water was contained into 500 mL precombusted brown glass bottles and incubated in the dark at about 20°C for 30 d. The difference of DOC concentrations measured before and after incubation were regarded as the BDOC concentrations.

Samples for determining Chl a were filtered through 0.45 um cellulose acetate filters, and then the membrane samples were extracted with 90% acetone for 24 h. Chl a was determined by using a UV-VIS spectrophotometer (752, UV-2000, Shanghai). The absorbency at wavelength of 663 nm, 645 nm, 663 nm, and 750 nm were measured. Chl a was calculated by the following equation [15]:

$$
\begin{aligned}
C = [11.64 \times (D663 - D750) &- 2.16 \times (D645 - D750) \\
+ 0.1 \times (D630 - D750)] &\times \frac{V_1}{(V \times L)},
\end{aligned} \tag{1}
$$

where D630, D645, D663, and D750 represent the absorbency of 630, 645, 663, and 750 nm, respectively. The V_1, V, L, and C represent the volume of water samples (L), the thickness of cuvette (cm), and the concentration of chlorophyll a (μg/L), respectively.

2.5. Quality Assurance and Quality Control (QA/QC). Procedural blanks and spiked blanks were analyzed with field samples, and surrogate standards (d8-Nap, d10-Acy, d10-Phe, d12-Chry, and d12-Per) were also added to all the samples to monitor procedural performance. Except for Nap, 10.05 ng/L of total PAHs was detected on average in water blanks ($n = 4$), and 17.21 ng/L of total PAHs was detected in particle blanks ($n = 5$). The recoveries of 16 PAHs in spiked blanks ($n = 3$) varied from 50.9% (Nap) to 122.7% (BgP). Because of the high background values for Nap, total concentrations of PAHs did not include Nap. Phe was also not considered in the distribution of total PAHs in water and SPM samples due to the possible pollution during the process of experiments. And the reported PAHs concentrations were corrected with the blank values.

3. Results and Discussions

3.1. Major Properties of Water. The major aquatic chemical properties in the water samples including pH, conductivity, salinity, dissolved oxygen (DO), concentration of suspended particulate matters (SPM), dissolved organic carbon (DOC), particulate organic matters (POC), chlorophyll a (Chl a), and total PAHs were listed in Tables 1 and 2. The concentrations of DOC in the Dongjiang River ranged from 1.19 mg/L to 13.91 mg/L in July 2010. While in April 2011, the DOC concentrations varied from 2.28 mg/L to 5.38 mg/L in the Dongjiang River and from 2.62 to 4.88 mg/L in the Pearl River. In the Dongjiang River, SPM, POC, and Chl a varied from 11 to 53 mg/L, from 4.14% to 13.3%, and from 3.11 to 10.1 μg/L, respectively in July 2010, while they ranged from 13.65 to 42.86 mg/L, from 1.59% to 9.65%, and from 2.76 to 28.2 μg/L in April 2011. Meanwhile, the SPM, POC, and Chl a concentrations in the samples collected from Pearl River in

(a)

(b)

(c)
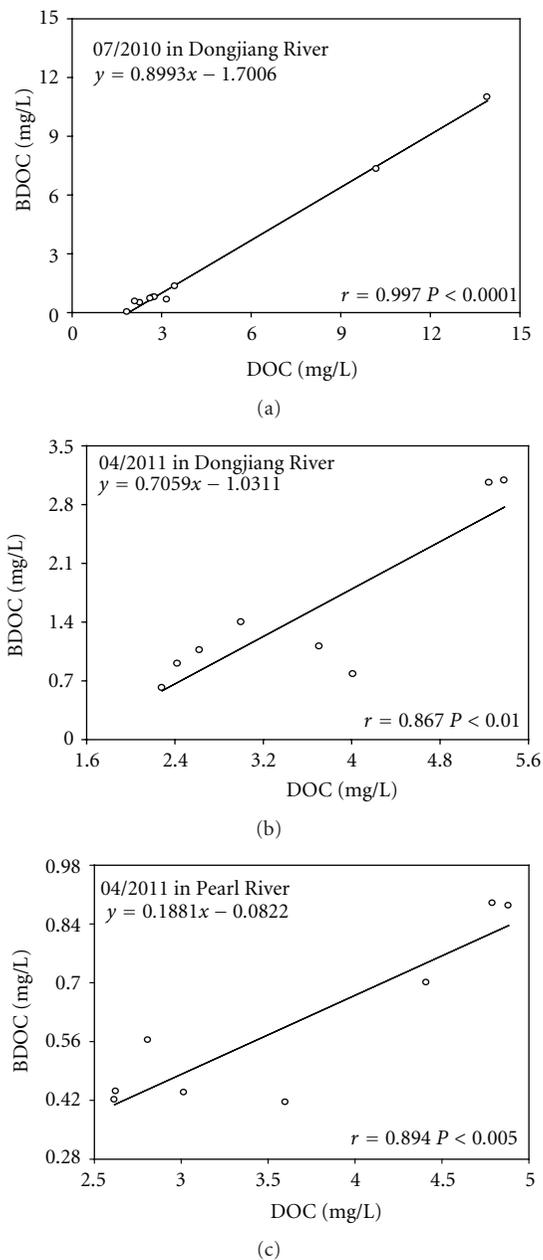
Figure 2: Correlations of DOC with BDOC of PAHs in Pearl River Delta.

April 2011 ranged from 19.96 to 46.87 mg/L, from 4.05% to 14.6%, and from 16.2 to 48.3 μg/L.

The POC distribution shows a similar pattern with the distribution of chlorophyll a (Figure 3), indicating that phytoplankton plays an important role in POC pool. Besides, the concentrations of BDOC illustrate a linear and positive relationship with the initial DOC concentrations (Figure 2), suggesting that DOC was highly biodegradable within the time scale of the incubation (1 month). Chl a concentrations were also related to the PAHs concentrations (Figure 3), which indicated that PAHs can be easily absorbed by algae in the SPM. It was also implied that algae was the dominant

composition of POC and governed the distribution of particulate PAHs. An increasing phytoplankton biomass and growth rate was reported to increase the air-water transfer of PAHs [16]. New phytoplankton production contributed to substantially longer times for air-water equilibrium, and the depletion of the dissolved phase by phytoplankton uptake prevented the equilibrium of air and water phases. The gas phase supports the concentrations of organic pollutants such as PAHs in atmospherically driven environments. Increased air-water exchange followed by phytoplankton uptake also seemed to be two of the most relevant processes increasing the vertical flux in the water column [17].

3.2. Concentrations of PAHs in the Water, SPM, Fish, Lipid Samples

3.2.1. PAHs in the Water Samples. PAHs in the water and SPM samples were listed in Figure 4. For the water samples, PAHs showed obviously seasonal variation in the Dongjiang River. They were higher in summer, ranging from 16.56 to 34.27 ng/L with an average of 25.63 ng/L, than in spring, ranging from 11.11 to 65.21 ng/L with an average of 25.15 ng/L.

Individual PAHs also showed considerable variances among the samples (Figure 5). For all the water samples, low molecular weight PAHs were the dominate compounds. The percentage of 3 and 4-ring PAHs ranged from 42.06% to 81.09% with an average of 65.38%. Acenaphthylene, fluorene, fluoranthene, and pyrene were the major constituents of PAHs in the water samples.

PAHs in the water samples are compared with those of other investigations (Table 3). The total concentration of PAHs was 2 to 3 orders of magnitude lower than those reported in Daya Bay, China (4181–27507 ng/L) [18], Jiulong River Estuary, and Western Xiamen Sea, China (6840–25620 ng/L) [19] and approximately 2 orders of magnitude lower than those found in Pearl River and the Macao Harbor, China (691–6457 ng/L) [20]. However, high PAHs in the Pearl River and the Macao Harbor [20] were related to the contamination of naphthalene in the laboratory, which accounted for about 90% of the total PAHs in dissolved phase. The aqueous concentrations in this study are similar to those of the previous investigations if Nap is excluded (13.64–106.85 ng/L). On the other hand, PAHs in this investigation were several times higher than those found in Beltic Sea (3.85–14.1 ng/L) and in the North Sea (0.63–3.51 ng/L) [21]. Similar concentrations were found in Xijiang River, China (21.7–138 ng/L) [5], Pearl River Delta (10.8–323 ng/L) [14], and Chesapeake Bay, USA (20–65.7 ng/L) [22].

3.2.2. PAHs in SPM. PAHs in SPM presented in Figure 4 also showed seasonal variation like PAHs of the water samples in the Dongjiang River. The total PAHs concentrations varied from 30.14 to 360.14 ng/L with an average of 131.5 ng/L and a standard deviation of 124.8 ng/L in summer and from 53.45 to 114.9 ng/g with an average of 85.77 ng/g and a standard deviation of 20.68 ng/L in spring. In the Pearl River, particulate PAHs were in a range of 80.8 to 229.2 ng/L with an average of 158.24 ng/L and a standard deviation of 59.4 ng/L.

(a)

(b)

(c)

(d)

(e)

(f)
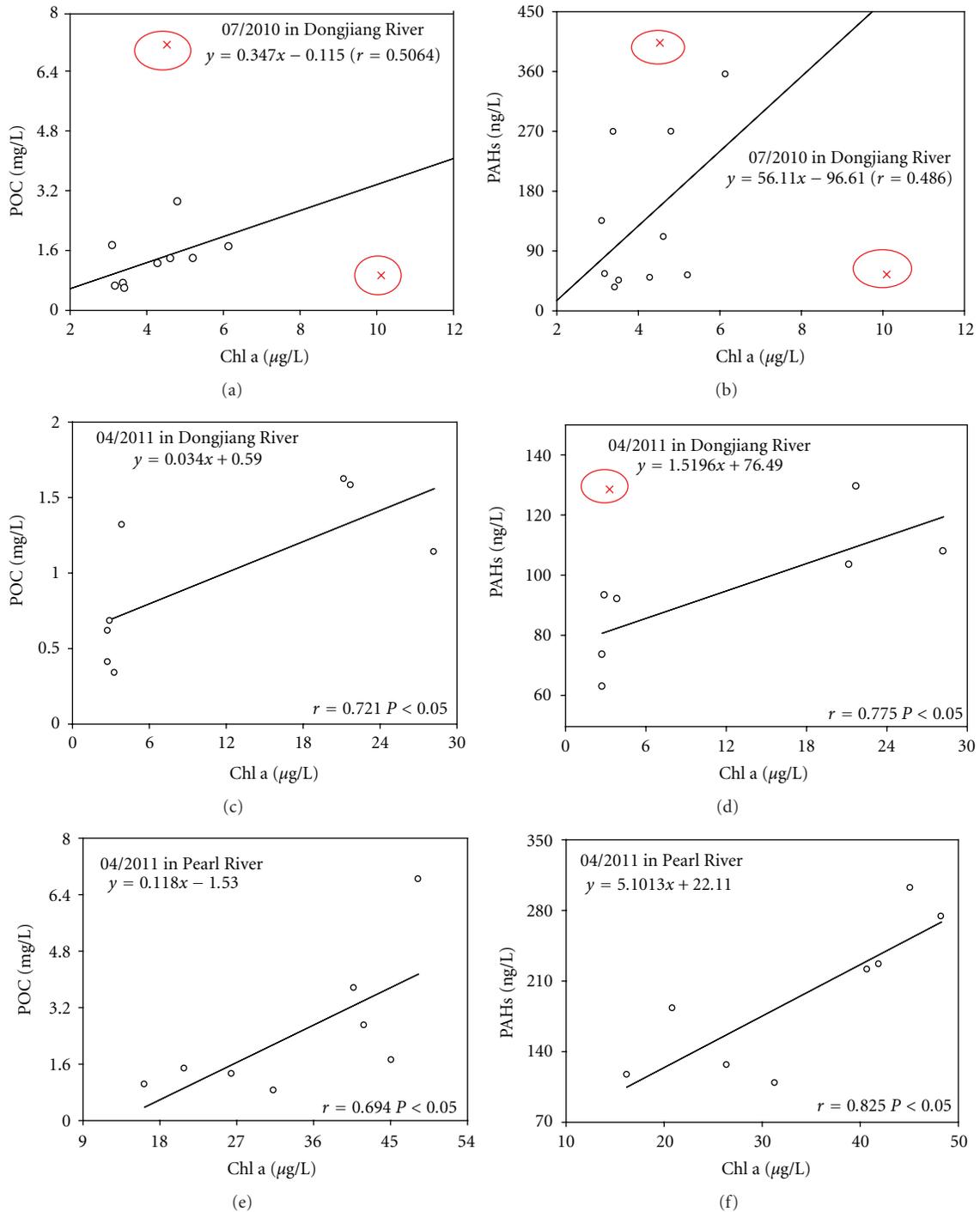
FIGURE 3: Relationship between Chl a and POC and between particulate PAHs (S-PAHs) and Chl a.

It was found that PAHs in SPM was higher in Pearl River than in Dongjiang River in spring.

Like the water samples, low molecular weight PAHs in SPM were also the dominant compounds. However, PAHs in this study are at different levels compared with the previous investigation in other areas. PAHs in SPM in this study were 2 orders of magnitude higher than those of the particulate samples collected from other regions (Table 3), such as the Xijiang River (0.17–58.2 ng/L) [5] and six to seven times

higher than York River of the VA Estuary (2.09–123 ng/L) [23]. They are at similar level to the concentrations of PAHs in Pearl River and the Macao Harbor, China (150–431 ng/L) [20] and the Seine River and Estuary, France (2–687 ng/L) [24].

3.2.3. PAHs in the Fish Species. Figure 6 shows the tissue distribution of PAHs and lipid contents in different fish species. Different levels of total PAHs in fish species were
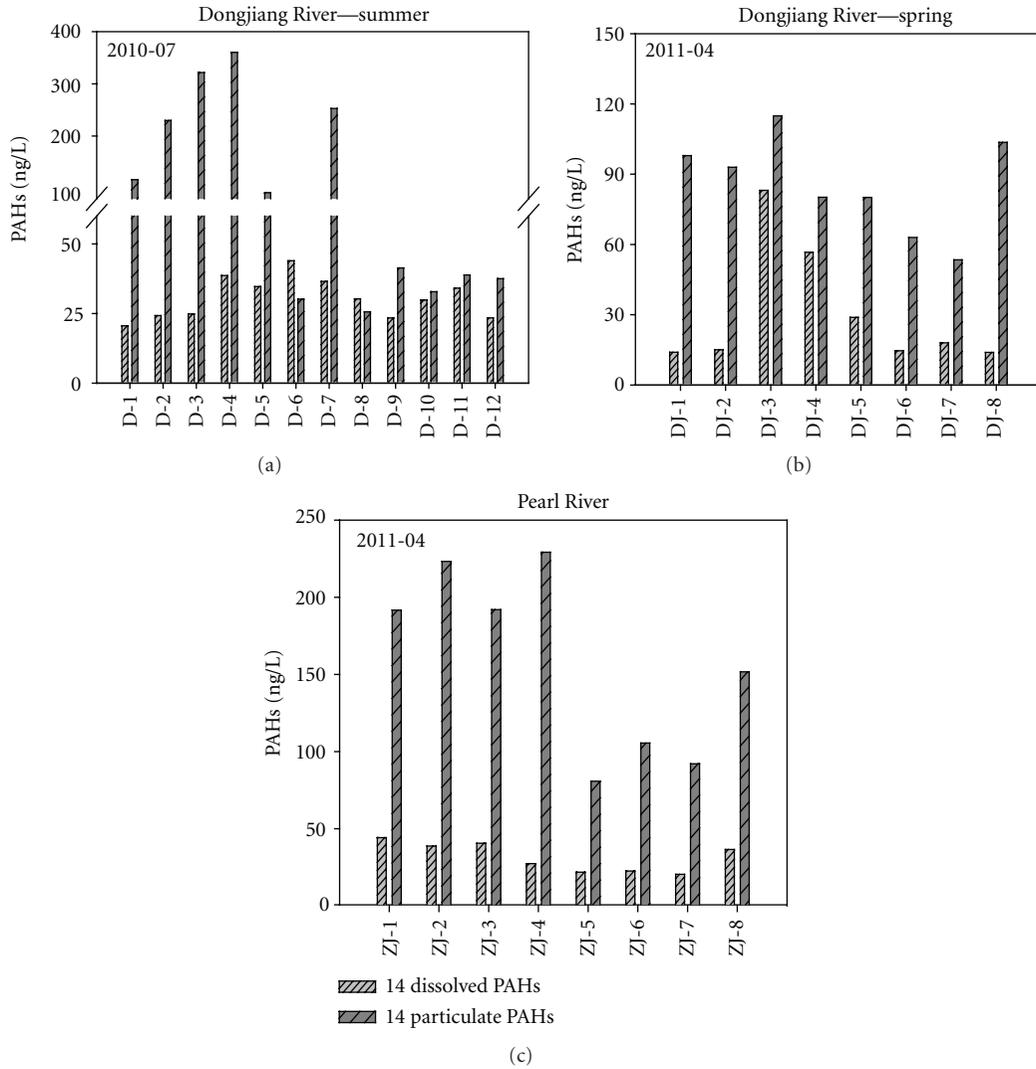
FIGURE 4: Spatial distribution of total PAHs in the riverine surface water and the SPM samples from the Pearl River Delta (except for Nap and Phe).

found. The highest concentration of PAHs was detected in red grass carp, ranging from 46.85 to 236.14 ng/g dw. It was approximately 2 to 3 times higher than other fishes. And the lowest PAHs levels occurred in tilapia (collected in summer), ranging from 14.70 to 80.51 ng/g dry weight. However, there were no significant differences among the other fish species. In terms of the individual PAHs, low molecular weight PAHs were the major compounds in the fish species, which are similar to those of the water and SPM samples. Compared with PAHs in the muscle (184–194 ng/g dw) and viscera tissues (505–854 ng/g dw) in different sized tilapia reported for Mai Po Marshes by Liang et al. [7], PAHs here both in muscle (14.55 ng/g dw) and viscera (80.51 ng/g) were much lower. This difference might be caused by the feeding habits of different fish species in different aqueous environment.

Significantly different concentrations of PAHs were also observed among fish tissues. Because the visceras of *Cirrhinus mrigala*, red grass carp, blunt snout bream-2 collected in April 2011, and carp were mashed, only the data of their muscle and gills were present. The highest concentrations of PAHs were found in the visceras, ranging from 80.51 to 180.87 ng/g dry weight, followed by the concentrations in gills, ranging from 25.43 to 236.14 ng/g dw, and those in muscle (10.52 to 46.85 ng/g dw) are the lowest. The different concentrations of PAHs in fish tissues may be affected by the physical-chemical properties of PAHs, the lipid content, and the uptake capacity of different fish tissues [9].

3.3. Association of PAHs with DOC in Water and with POC in SPM. One of the important factors affecting PAHs in the water and SPM samples was DOC and POC. Correlation analyses between PAHs and DOC or POC were illustrated in **Figure 7**. Although aqueous PAHs showed no significant correlations with DOC in summer, positive correlations were found between aqueous PAHs and DOC in both the Dongjiang River ($r = 0.736$, $P < 0.05$) and the Pearl River ($r = 0.78$, $P < 0.01$) in spring. For the particulate samples, PAHs in SPM was significantly related to POC in summer

(a)



(b)
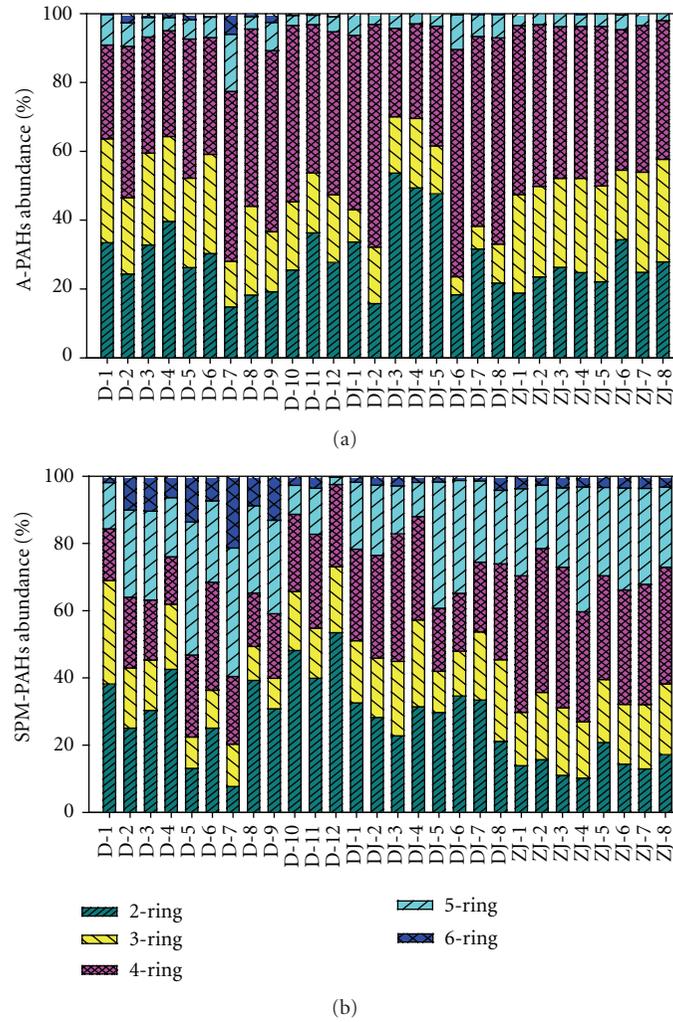
Figure 5: The composition of PAHs in (a) water samples and (b) suspended particular matters samples (both except for Nap and Phe).


(a)

(b)
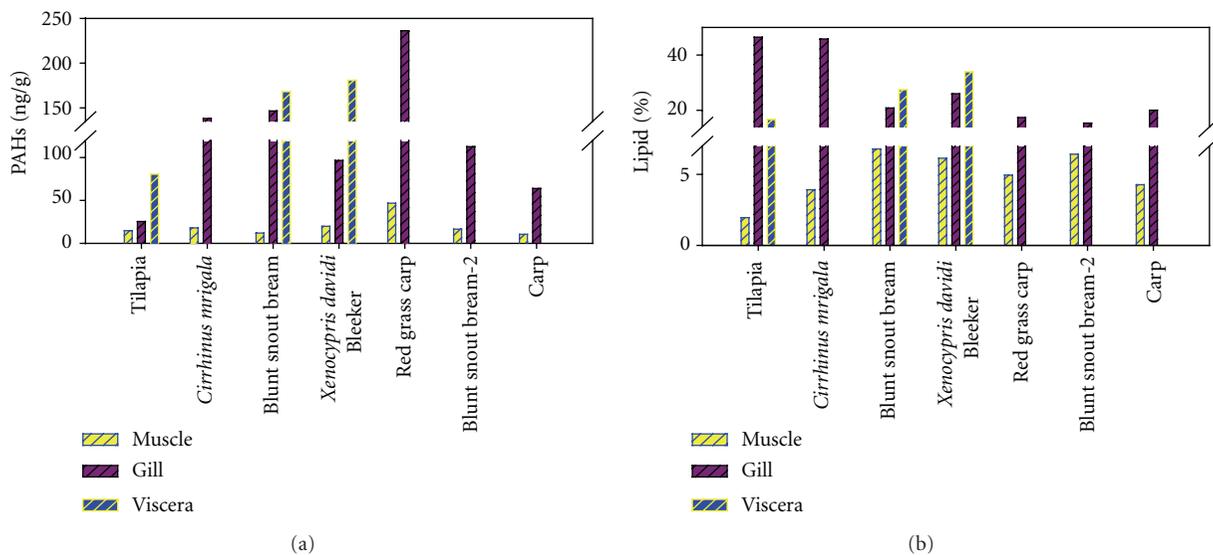
Figure 6: Distribution of total PAHs and lipid (%) in fish species from the Pearl River Delta.

TABLE 3: Summary of total PAHs concentration (ng/L) in water and SPM from different sites around the world.

	Location	Concentration (ng/L)	N	References
Water	Pearl River Delta, China	11.11–65.21	15	This study
	Xijiang River, China	21.7–138	15	Deng et al. [5]
	Pearl River and the Macao Harbor, China	13.64–106.85	15	Luo et al. [20]
	Seine River and Estuary, France	4–36	11	Fernandes et al. [24]
	Daya Bay, China	4181–27507	15	Zhou and Maskaoui [18]
	Western Xiamen Sea, China	106–945	15	Zhou et al. [33]
	Jiulong River Estuary and Western	6840–25620	15	Maskaoui et al. [19]
	Xiamen Sea, China			
	Chesapeake Bay, USA	20–65.7	17	Gustafson and Dickhut [22]
	Baltic Sea	3.85–14.1	15	Witt [21]
	North Sea	0.63–3.51	15	Witt [21]
	Pearl River Delta, China	10.8–323	15	Wang et al. [14]
SPM	Pearl River Delta China	34.68–403.12	15	This study
	Xijiang River, China	0.17–58.2	15	Deng et al. [5]
	Pearl River and the Macao Harbor, China	73.54–411.51	15	Luo et al. [20]
	York River, VA, Estuary, USA	2.09–123	20	Countway et al. [23]
	Seine River and Estuary, France	2–687	11	Fernandes et al. [24]

N: Numbers of PAHs compounds analyzed in each study.

($r = 0.695$, $P < 0.05$) in Dongjiang River and in both the Pearl River ($r = 0.625$, $P < 0.05$) and Dongjiang River ($r = 0.783$, $P < 0.05$) in spring. The highly significant correlation between PAHs and organic carbon indicated that both DOC and POC are important to the distribution of PAHs in aquatic environment.

Moreover, the slopes in Figure 7 demonstrate the importance of DOC to the association of PAHs. The slopes are -0.788, 12.19, and 7.63 ng/mg for DOC, and 50.71, 37.97, and 22.79 ng/mg for POC in the Dongjiang River in summer, in the Dongjiang River and in the Pearl River in spring, respectively. Hence, PAHs should be greatly affected by POC than by DOC in the targeted river system.

It is also widely acknowledged that K_{oc} is closely related to K_{ow} [25]. Hence, hydrophobic compounds such as PAHs with higher K_{ow} show stronger affinity to POC or DOC. The four dominant PAHs (acenaphthylene, fluorene, fluoranthene, and pyrene) in the dissolved and the particulate phases were normalized by DOC and POC, respectively (Figure 8). It was found that the mean POC-normalized concentrations for Flo, Flu, and Pyr were 21.79, 13.84, and 12.74 μg/g oc, respectively; and the mean DOC-normalized concentrations were 1.57, 1.50, and 2.67 μg/g oc, resp.). The formers were over one order of magnitude higher than the latter ones. And the POC-normalized concentration for Ace (2.25 μg/g oc) was similar to its DOC-normalized concentration (2.25 μg/g oc) (Figure 5). As Flo, Flu, and Pyr are hydrophobic nature with $\log K_{ow}$ of 4.18, 4.90, and 4.88, they are readily associated with POC and accumulated in SPM. The partitioning patterns of PAHs further reveal that POC and DOC are the most important factors in controlling their distribution, transport, and fate in the surface river water.

3.4. Distribution Coefficients of PAHs between Water and SPM.

Distribution of PAHs between SPM and water plays a very important role in the mobility and fate of PAHs in aqueous systems. The most frequently used parameter for evaluating their distribution is the organic carbon-normalized particle-water partitioning coefficients K_{oc}, which were calculated as follows:

$$K_{oc} = \frac{C_s/C_w}{f_{oc}}, \qquad (2)$$

where C_s is the solid phase concentration (ng/g), C_w is the aqueous phase concentration (ng/mL), and f_{oc} is the mass fraction of organic carbon in the particle.

From Figure 9, $\log K_{oc}$ mL/g was significantly related to $\log K_{ow}$ for the samples collected both from the Dongjiang River ($r = 0.577$) and the Pearl River ($r = 0.897$), implying that PAHs with high hydrophobicity can be adsorbed on SPM more easily. The free energy relationship between $\log K_{ow}$ and $\log K_{oc}$ was established in Figure 9. The observed equation for PAHs is similar to the previous investigation on the $\log K_{oc} - \log K_{ow}$ regression for PAHs in the water of the PRD [20].

From the slope of the equation in Figure 9, the lipophilicity of SPM relative to the reference octanol/water system may be inferred. The slope in this study is lower than the value listed in Table 4, suggesting that the lipophilicity of SPM in this is relatively low.

3.5. Bioconcentration of PAHs in Fish Species

3.5.1. Effects of Lipid on PAHs Distribution.
Lipid plays an important role in the accumulation of PAHs in aquatic

(a)

(b)

(c)

(d)

(e)

(f)
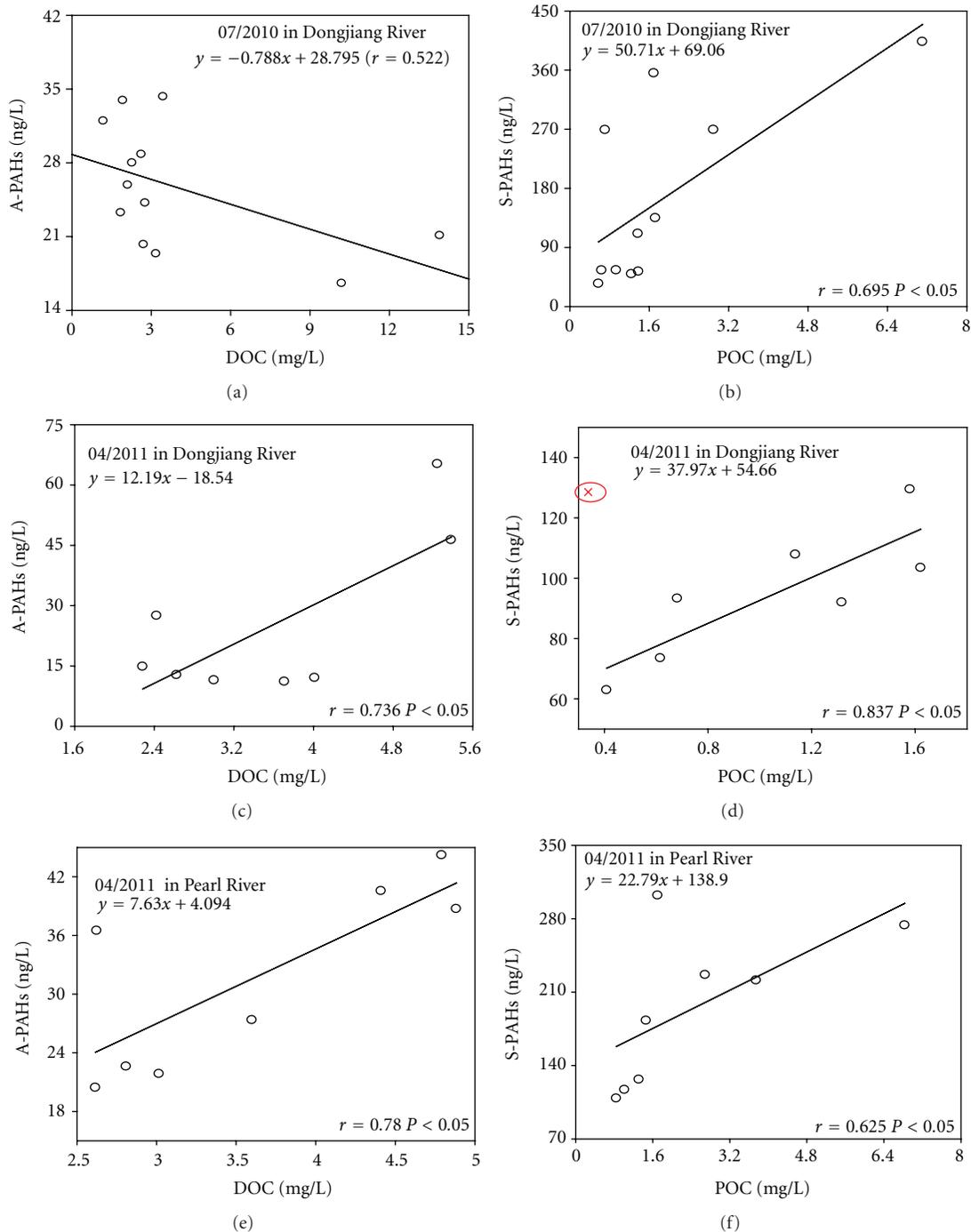
FIGURE 7: Correlations of 14 PAHs with DOC in water samples and with POC in the SPM samples. A-PAHs and S-PAHs correspond to the dissolved PAHs and particulate PAHs, respectively.

organisms, since PAHs are easily accumulated in lipid-rich tissue of fish. The lipid contents in different tissues of each fish species are shown in Figure 6. The highest lipid contents were presented in the gill tissues, ranging from 15.3% in blunt snout bream-2 (collected in spring) to 46.5% in tilapia with an average percentage of 27.4% dw, followed by those in viscera tissues ranging from 16.68% in tilapia to 33.93% in *xenocypris davidi* Bleeker with the average percentage of

26.03%. The lowest lipid contents were found in the muscle tissues, varying from 1.96% in tilapia to 6.79% in blunt snout bream with an average percentage of 4.7%. Relationship between PAHs and lipids in different tissues of fish species was showed in Figure 10. Significant positive correlations between total PAHs and lipids in different tissues of fishes from Dongjiang River were obtained ($r = 0.859$, $P < 0.0001$).

TABLE 4: Correlations of $\log K_{oc}$ against $\log K_{ow}$ values determined for selected PAHs. a, b, and R^2 correspond, respectively to slope, intercept, and square determination coefficient.

Sorbent	Sorption experiment	a	b	R^2
Coarse size fraction in sediments [34]	laboratory	1.00	−0.21	1.00
Soil and sediments [35]	laboratory	1.00	−0.317	0.98
Seine River suspensions [24]	In situ	0.70	2.75	0.95
SPM of Pearl River Delta [20]	In situ	0.58	3.41	0.98
SPM of Xijiang River [5]	In situ	0.71	1.68	0.95
SPM of Dongjiang River (This study)	In situ	0.27	5.39	0.57 (r)
SPM of Pearl River (This study)	In situ	0.51	4.03	0.897 (r)
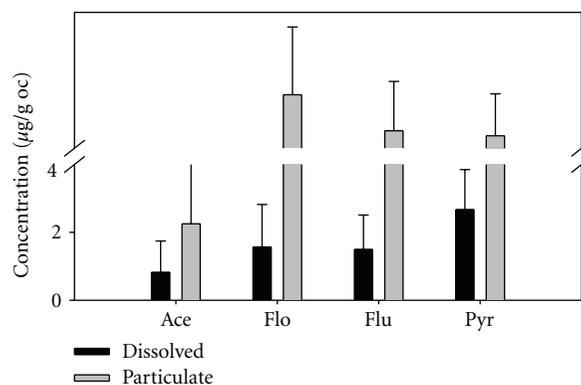
FIGURE 8: Organic carbon-normalized concentrations of Ace, Flo, Flu, and Pyr in the river water and the SPM samples.

3.5.2. Bioconcentration Factors (BCFs) in Fish Tissues. In order to compare between the bioaccumulation patterns among individual PAHs in fish, BCFs were calculated and plotted. BCF in the viscera of tilapia was observed to increase with the increasing K_{ow} ($\log \mathrm{BCF} = 0.507 \log K_{ow} + 1.631$, $r = 0.883$) (Figure 11(a)). This observation is consistent with other investigation on bioconcentration [26], suggesting that the bioaccumulation of organic chemicals in biota increases with the increasing of $\log K_{ow}$. However, measured BCF values tend to decline below the true equilibrium condition as the K_{ow} of the chemical increases.

BCF will reach the maximum value when $\log K_{ow}$ reaches 5–7 and then decreases when $\log K_{ow}$ is higher than 7. Except for the viscera of tilapia, most of the BCF values in different fish tissues follow this trend as demonstrated in Figure 11(b). This difference may depend on living habitat and trophic levels of fish and environmental behaviors of PAHs. The bioavailability, uptake, and fate of PAHs by aquatic organisms from contaminated media (water, sediments, and food) were also affected by a variety of physical (e.g., lipophilicity, temperature, etc.) and biological parameters. As a general rule, water is dominant pathway of exposure for fish if $\log K_{ow}$ of organic compounds are lower than 5, while sediment particles can be used for some fish species such as food and can contribute substantially to bioaccumulation for PAHs with $\log K_{ow}$ higher than 5 [27]. As Tilapia used to live in the bottom layer of aquatic ecosystem and in sediments PAHs in sediments may contribute to accumulation in tilapia via the dietary route and exchange with water through gills.

The previous result indicates that BCF is quite different due to the diversity of fish species.

The previous result is consistent with previous studies which illustrated that the relationship between K_{ow} and bioconcentration appeared to be relatively complex [28]. For fish with low feeding rates, the bioaccumulation of nonpolar organic compounds with $\log K_{ow}$ ranging from 2 to 6.5 is mainly determined by exchange across the gills. However, dietary uptake seems negligible because of poor absorption efficiency and rapid metabolism rates [29, 30]. For nonmetabolized PAHs, less bioaccumulation of organic compounds would appear in small fishes due to the higher oxygen uptake, which leads to much loss than uptake of organic compound, than in large ones [29]. It was also suggested that bioaccumulation of low K_{ow} PAHs (such as naphthalene) was high due to higher gill transfer efficiencies, and that of high K_{ow} was low because of enhanced biotransformation and decreased gut assimilation in fish [31, 32]. Moreover, the physicochemical properties of a chemical, the physiological components of the uptake process, biotransformation, blood flow, and fatty acid composition and lipid content in aquatic animals could all affect the uptake and accumulation of organic chemicals for fishes [28]. All of those factors contribute to the unpredictability of the bioaccumulation of POPs in fishes.

4. Conclusion

The spatial distribution and bioconcentration of PAHs in the water, SPM, and fish species from the Pearl River Delta were

(a) Dongjiang

(b) Pearl River
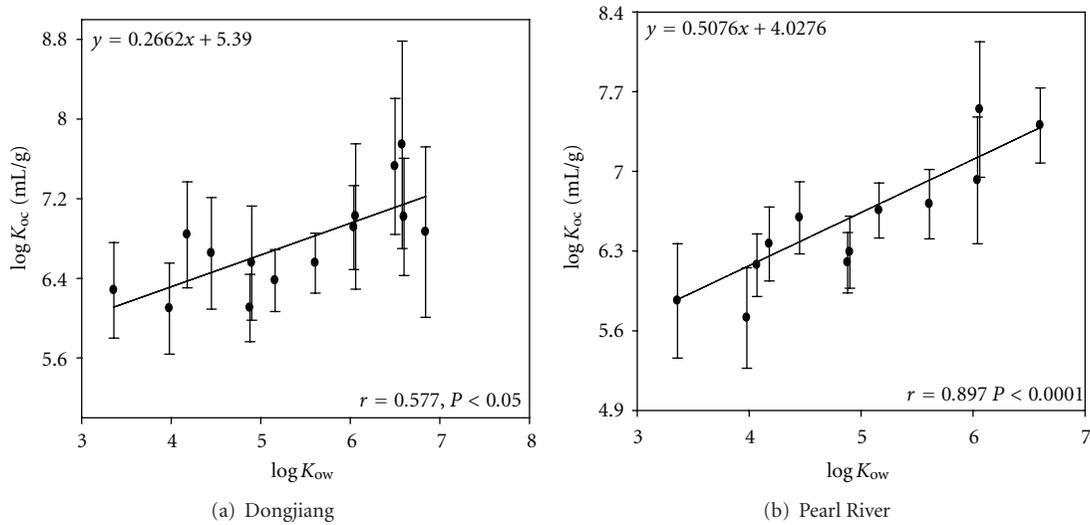
FIGURE 9: Relationship between $\log K_{oc}$ and $\log K_{ow}$ for PAHs.
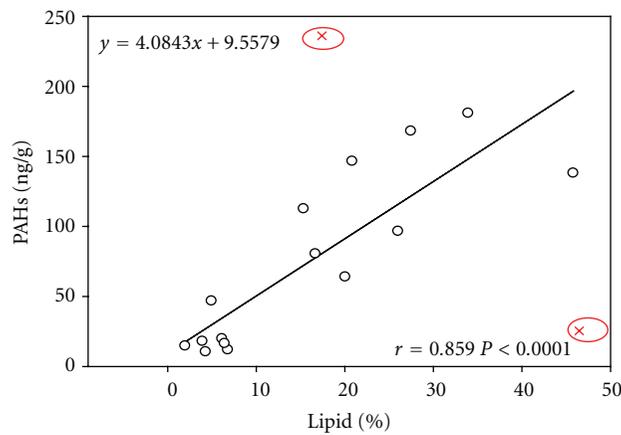
FIGURE 10: Correlations of lipid with PAHs in tissues of fishes. The two red points represent the samples (gill of tilapia and gill of red grass carp) which are not included in the correlation analysis.

(a) Tilapia—viscera

(b) Blunt snout bream—viscera
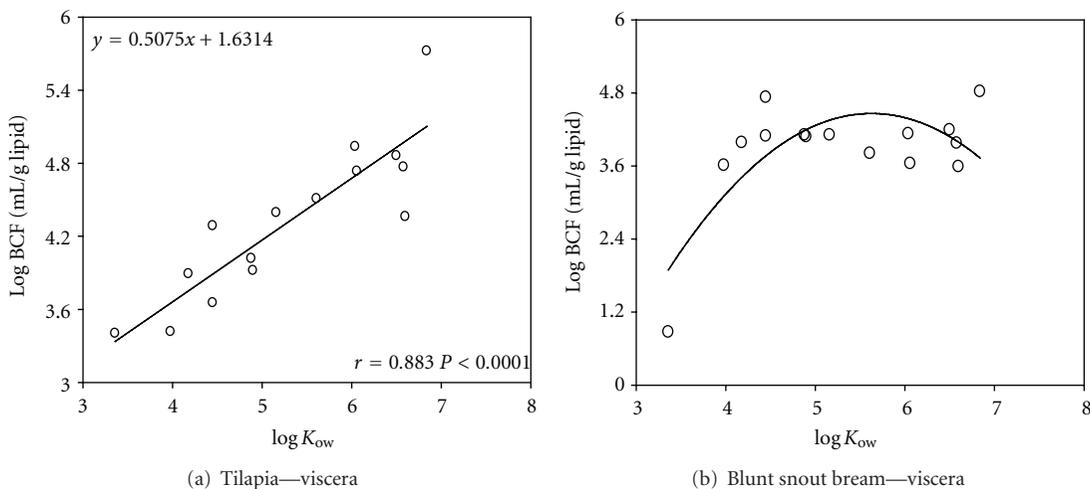
FIGURE 11: Correlations of $\log K_{ow}$ with logBCF of viscera in tilapia (a) and blunt snout bream (b).

examined. Aquatic chemical data were also determined. In both the dissolved and the particulate phases, the low molecular weight PAHs were the dominant components. Positive correlation were found between aqueous PAHs and DOC as well as particulate PAHs and POC, indicating the importance of DOC and POC to the distribution of PAHs in the aquatic environment. The in-situ partitioning coefficients ($\log K_{oc}$, mL/g) for the samples were related to $\log K_{ow}$. The relative lipophilicity of SPM could be evaluated by the slope of the observed regression equation. PAHs showed significant correlations with lipids in different tissues of fishes. BCF in the viscera of tilapia was positively related to $\log K_{ow}$. But BCF values in most of the fish samples were found to reach the maximum value when $\log K_{ow}$ reaches 5–7 and then decrease when $\log K_{ow}$ is higher than 7. The different distribution of PAHs among the fish species and their tissues were affected by $\log K_{ow}$ of PAHs and the lipid contents in fish tissues.

Acknowledgments

References

[1] C. Seruto, Y. Sapozhnikova, and D. Schlenk, "Evaluation of the relationships between biochemical endpoints of PAH exposure and physiological endpoints of reproduction in male California Halibut (*Paralichthys californicus*) exposed to sediments from a natural oil seep," *Marine Environmental Research*, vol. 60, no. 4, pp. 454–465, 2005.

[2] M. Yamada, H. Takada, K. Toyoda et al., "Study on the fate of petroleum-derived polycyclic aromatic hydrocarbons (PAHs) and the effect of chemical dispersant using an enclosed ecosystem, mesocosm," *Marine Pollution Bulletin*, vol. 47, no. 1–6, pp. 105–113, 2003.

[3] D. M. Kim, M. J. Heo, S. J. Oh et al., "Prediction of the transport and fate of polycyclic aromatic hydrocarbons (PAHs) in Masan Bay, South Korea," *Journal of the Faculty of Agriculture Kyushu University*, vol. 56, no. 2, pp. 299–305, 2011.

[4] Y. W. Qiu, G. Zhang, G. Q. Liu, L. L. Guo, X. D. Li, and O. Wai, "Polycyclic aromatic hydrocarbons (PAHs) in the water column and sediment core of Deep Bay, South China," *Estuarine, Coastal and Shelf Science*, vol. 83, no. 1, pp. 60–66, 2009.

[5] H. M. Deng, P. A. Peng, W. L. Huang, and J. Song, "Distribution and loadings of polycyclic aromatic hydrocarbons in the Xijiang River in Guangdong, South China," *Chemosphere*, vol. 64, no. 8, pp. 1401–1411, 2006.

[6] X. J. Luo, S. J. Chen, B. X. Mai, Q. S. Yang, G. Y. Sheng, and J. M. Fu, "Polycyclic aromatic hydrocarbons in suspended particulate matter and sediments from the Pearl River Estuary and adjacent coastal areas, China," *Environmental Pollution*, vol. 139, no. 1, pp. 9–20, 2006.

[7] Y. Liang, M. F. Tse, L. Young, and M. H. Wong, "Distribution patterns of polycyclic aromatic hydrocarbons (PAHs) in the sediments and fish at Mai Po Marshes Nature Reserve, Hong Kong," *Water Research*, vol. 41, no. 6, pp. 1303–1311, 2007.

[8] X. Z. Meng, E. Y. Zeng, L. P. Yu, B. X. Mai, X. J. Luo, and Y. Ran, "Persistent halogenated hydrocarbons in consumer fish of China: regional and global implications for human exposure," *Environmental Science and Technology*, vol. 41, no. 6, pp. 1821–1827, 2007.

[9] F. L. Xu, W. J. Wu, J. J. Wang et al., "Residual levels and health risk of polycyclic aromatic hydrocarbons in freshwater fishes from Lake Small Bai-Yang-Dian, Northern China," *Ecological Modelling*, vol. 222, no. 2, pp. 275–286, 2011.

[10] J. M. Fu, G. Y. Sheng, Y. Chen et al., "Preliminary study of organic pollutants in air of guangzhou, Hong Kong, and Macao," *ACS Symposium Series*, vol. 671, pp. 164–176, 1997.

[11] Y. H. Yanhong, G. Y. Sheng, J. M. Fu, and Y. S. Min, "Organochlorinated compounds in waters of the Pearl River Delta region," *Environmental Monitoring and Assessment*, vol. 44, no. 1–3, pp. 569–575, 1997.

[12] Y. Guo, X. Z. Meng, H. L. Tang, and E. Y. Zeng, "Tissue distribution of organochlorine pesticides in fish collected from the Pearl River Delta, China: implications for fishery input source and bioaccumulation," *Environmental Pollution*, vol. 155, no. 1, pp. 150–156, 2008.

[13] E. Martinez, M. Gros, S. Lacorte, and D. Barceló, "Simplified procedures for the analysis of polycyclic aromatic hydrocarbons in water, sediments and mussels," *Journal of Chromatography A*, vol. 1047, no. 2, pp. 181–188, 2004.

[14] J. Z. Wang, Y. F. Guan, H. G. Ni, X. L. Luo, and E. Y. Zeng, "Polycyclic aromatic hydrocarbons in riverine runoff of the Pearl River Delta (China): concentrations, fluxes, and fate," *Environmental Science and Technology*, vol. 41, no. 16, pp. 5614–5619, 2007.

[15] A. E. Greenberg, L. S. Clescerl, and A. D. Eaton, *Standard Methods For the Examination of Water and Wastewater*, American Public Health Association, Washington, DC, USA, 20th edition, 1998.

[16] J. Dachs, S. J. Eisenreich, J. E. Baker, F. C. Ko, and J. D. Jeremiason, "Coupling of phytoplankton uptake and air-water exchange of persistent organic pollutants," *Environmental Science and Technology*, vol. 33, no. 20, pp. 3653–3660, 1999.

[17] M. Söderström, K. Nylund, U. Järnberg, G. Lithner, G. Rosén, and H. Kylin, "Seasonal variations of DDT compounds and PCB in a eutrophic and an oligotrophic lake in relation to algal biomass," *Royal Swedish Academy of Sciences*, vol. 29, no. 4-5, pp. 230–237, 2000.

[18] J. L. Zhou and K. Maskaoui, "Distribution of polycyclic aromatic hydrocarbons in water and surface sediments from Daya Bay, China," *Environmental Pollution*, vol. 121, no. 2, pp. 269–281, 2003.

[19] K. Maskaoui, J. L. Zhou, H. S. Hong, and Z. L. Zhang, "Contamination by polycyclic aromatic hydrocarbons in the Jiulong River Estuary and Western Xiamen Sea, China," *Environmental Pollution*, vol. 118, no. 1, pp. 109–122, 2002.

[20] X. J. Luo, B. X. Mai, Q. S. Yang, J. M. Fu, G. Y. Sheng, and Z. S. Wang, "Polycyclic aromatic hydrocarbons (PAHs) and organochlorine pesticides in water columns from the Pearl River and the Macao harbor in the Pearl River Delta in South China," *Marine Pollution Bulletin*, vol. 48, no. 11-12, pp. 1102–1115, 2004.

[21] G. Witt, "Polycyclic aromatic hydrocarbons in water and sediment of the Baltic Sea," *Marine Pollution Bulletin*, vol. 31, no. 4–12, pp. 237–248, 1995.

[22] K. E. Gustafson and R. M. Dickhut, "Distribution of polycyclic aromatic hydrocarbons in southern Chesapeake Bay surface water: evaluation of three methods for determining freely dissolved water concentrations," *Environmental Toxicology and Chemistry*, vol. 16, no. 3, pp. 452–461, 1997.

[23] R. E. Countway, R. M. Dickhut, and E. A. Canuel, "Polycyclic aromatic hydrocarbon (PAH) distributions and associations with organic matter in surface waters of the York River, VA Estuary," *Organic Geochemistry*, vol. 34, no. 2, pp. 209–224, 2003.

[24] M. B. Fernandes, M. A. Sicre, A. Boireau, and J. Tronczynski, "Polyaromatic hydrocarbon (PAH) distributions in the Seine River and its estuary," *Marine Pollution Bulletin*, vol. 34, no. 11, pp. 857–867, 1997.

[25] L. P. Burkhard, "Estimating dissolved organic carbon partition coefficients for nonionic organic chemicals," *Environmental Science and Technology*, vol. 34, no. 22, pp. 4663–4668, 2000.

[26] J. P. Connolly and C. J. Pedersen, "A thermodynamic-based evaluation of organic chemical accumulation in aquatic organisms," *Environmental Science and Technology*, vol. 22, no. 1, pp. 99–103, 1988.

[27] P. F. Landrum, "Bioavailability and toxicokinetics of polycyclic aromatic hydrocarbons sorbed to sediments for the amphipod pontoporeia hoyi," *Environmental Science and Technology*, vol. 23, pp. 588–595, 1989.

[28] M. G. Barron, "Bioconcentration: will water-borne organic chemicals accumulate in aquatic animals?" *Environmental Science & Technology*, vol. 24, no. 11, pp. 1612–1618, 1990.

[29] D. J. Randall, D. W. Cornell, R. Yang, and S. S. Wu, "Concentrations of persistent lipophilic compounds in fish are determined by exchange across the gills, not through the food chain," *Chemosphere*, vol. 37, no. 7, pp. 1263–1270, 1998.

[30] B. C. Kelly, F. A. P. C. Gobas, and M. S. McLachlan, "Intestinal absorption and biomagnification of organic contaminants in fish, wildlife, and humans," *Environmental Toxicology and Chemistry*, vol. 23, no. 10, pp. 2324–2336, 2004.

[31] R. V. Thomann and J. Komlos, "Model of biota-sediment accumulation factor for polycyclic aromatic hydrocarbons," *Environmental Toxicology and Chemistry*, vol. 18, no. 5, pp. 1060–1068, 1999.

[32] R. V. Thomann, J. P. Connolly, and T. F. Parkerton, "An equilibrium model of organic chemical accumulation in aquatic food webs with sediment interaction," *Environmental Toxicology and Chemistry*, vol. 11, no. 10, p. 1509, 1992.

[33] J. L. Zhou, H. Hong, Z. Zhang, K. Maskaoui, and W. Chen, "Multiphase distribution of organic micropollutants in Xiamen Harbour, China," *Water Research*, vol. 34, no. 7, pp. 2132–2150, 2000.

[34] S. W. Karickhoff, D. S. Brown, and T. A. Scott, "Sorption of hydrophobic pollutants on natural sediments," *Water Research*, vol. 13, no. 3, pp. 241–248, 1979.

[35] J. C. Means, "Sorption of polynuclear aromatic hydrocarbons by sediments and soils 1," *Environmental Science and Technology*, vol. 14, no. 12, pp. 1524–1528, 1980.

The *Scientific* World JOURNAL

Research Article

HCHs and DDTs in Soils around Guanting Reservoir in Beijing, China: Spatial-Temporal Variation and Countermeasures

Tie-yu Wang,[1] Bing Tan,[1, 2] and Yong-long Lu[1]

[1] *State Key Laboratory of Urban and Regional Ecology, Research Center for Eco-Environmental Sciences, Chinese Academy of Sciences, Beijing 10085, China*
[2] *College of Environmental Science and Engineering, Liaoning Technical University, Fuxin, Liaoning 123000, China*

Correspondence should be addressed to Yong-long Lu, lurcees@gmail.com

The concentrations of hexachlorocyclohexanes (HCHs) and dichlorodiphenyltrichloroethanes (DDTs) in the topsoil samples around the Guanting Reservoir in Beijing were measured, and their spatial distribution and environmental risks were analyzed by GIS. The results showed that in 2003, 2007, and 2009, the HCHs concentrations were 0.66, 0.85, and 0.73 ng/g, and the DDTs concentrations were 9.50, 7.80, and 6.46 ng/g in the studied area, respectively. In the topsoil, the HCHs concentrations did not change much while the DDTs concentrations declined steadily. Most of the current residues in soil come from the POPs used in the past years but some new input is also detected in certain regions. The level of HCHs and DDTs residues in the south reservoir is lower than that in the north reservoir. The middle region has the highest HCHs and DDTs concentrations, especially near the Beixinpu town. The high risk regions of pollution of HCHs and DDTs are mainly distributed in the vicinity of Beixinpu town as well. Based on the aforementioned results, a comprehensive countermeasure is proposed entailing decision making, local implementation, scientific support, and public participation with regard to the long-term control and management of POPs around the Guanting Reservoir.

1. Introduction

Hexachlorocyclohexanes (HCHs) and dichlorodiphenyl-trichloroethanes (DDTs) have been listed as the main pesticidal persistent organic pollutants (POPs) by the United Nations Environment Program (UNEP) in the Stockholm Convention. They have been used in China on a large scale for a long time and the pesticides used in China during 1960–1980 were mainly organochlorine pesticides (OCPs). The consumption of OCPs such as DDTs and HCHs were 192,000 tons in 1970, accounting for 80.1% of the total domestic pesticide production [1, 2]. From 1972 to 1974, the agricultural consumption of HCHs and DDTs amounted to 607.8 tons and 150.8 tons, respectively, in the Beijing municipality [3]. In the early 1980s, the application of pesticidal POPs in the orchards became restricted and after 1983 the comprehensive restrictions on their production and use took effect [4]. However, the environmental problems

caused by their toxicity, nonbiodegradability, bioaccumulation, and so forth still seriously threaten human health and environmental well-being [5, 6]. Soil is a reservoir for the OCPs and has gradually changed from a major sink to an important emission source of OCPs to food and drinking water over time. Significant proportions of between 20% and 70% of a pesticide or its degradation products can remain in soil following application [7].

The Guanting Reservoir is located on the Yongding River at 100 km northwest of Beijing. It has a water capacity of 4.2 billion m^3 and includes 46,000 km^2 water shed areas. It was previously one of the most important water sources for Beijing until 1997 when its water was polluted. To enable the effective comprehensive management of the Guanting Reservoir and restore its function to supply drinking water, many studies focusing on pesticidal POPs have been carried out around the reservoir [8–10]. However, the potential nonpoint source pollution of POPs
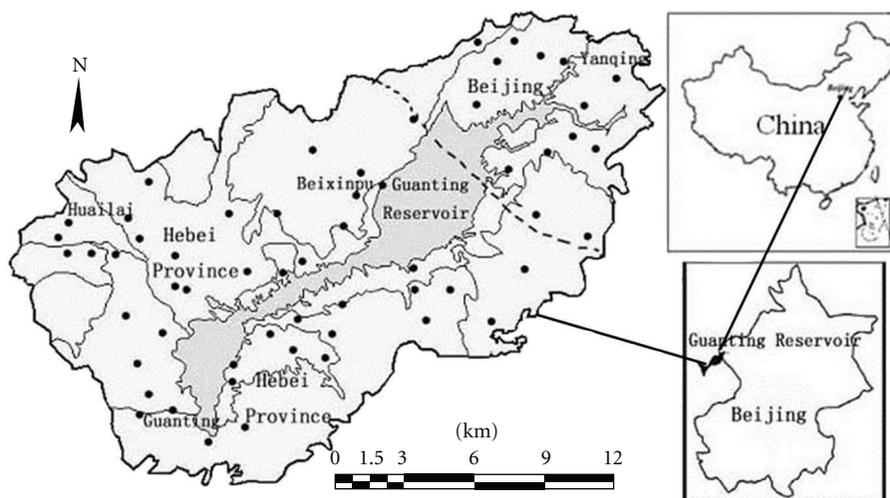
FIGURE 1: Locations of sampling sites around the Guanting Reservoir.

from farmlands around the reservoir was rarely reported. Since 2003, we embarked on the continuous integrated and systematic studies by fixing points in the soils around the reservoir [11–16]. Through multiyear monitoring and using GIS technology, we evaluated the pollution situation and risk pattern of pesticidal POPs in the soils around the water shed. The analyses presented in this paper will facilitate better understanding of the residue characteristics and tendency effects of OCPs in soils under various conditions around water sheds. Consequently, we proposed specific countermeasures to remedy regional ecological environment and provided the scientific basis for the comprehensive treatment of the reservoir and a technical framework for water source protection and management projects in the future.

2. Materials and Methods

2.1. Sample Collection. This study focused on a $920 \, km^2$ water shed within 2–10 km around the Guanting Reservoir (115.43°E–115.97°E, 40.19°N–40.50°N). The soil types are mainly brown soil, cinnamon soil, and chestnut soil. Land use in the area includes orchards, corn fields, vegetable fields, and forest shrubs. The 58 topsoil samples were collected and analyzed in 2003, 2007, and 2009, respectively. Each sample consisted of a mixture of soil collected from five subsites at a depth of 0–20 cm, each of which covering a radius of 5 m in a cross-pattern. Throughout the survey, a global positioning system (GPS) was used to locate the sampling sites to ensure the valid space registration of the sampling sites in different years. The locations of the sampling sites are shown in Figure 1.

2.2. Sample Treatment. All soil samples were air dried at room temperature, then ground with sticks, and passed through a 2 mm nylon mesh to remove grit, plant, and animal residues from the soil samples, and finally stored in polypropylene (PP) plastic bags until analysis. The analysis

method follows the previous report [15] and is summarized as follows. Each soil sample (10 g) was weighed accurately and decanted into a 150 mL Erlenmeyer flask, and an appropriate amount of high purity active copper powder and anhydrous sodium sulfate were added to the samples to remove sulfur and water. The sample was then extracted with 100 mL 7 : 3 (v/v) *n*-hexane/dichloromethane in an ultrasonic bath for several times. The extract was transferred into a glass centrifugal tube and centrifuged at 3000 rpm and then decanted into a 250 mL separating funnel where concentrated sulfuric acid was added to purify the extract. After discarding the sulfonated layer, the purified extract was washed at least twice with 10% sodium chloride solution until the pH value of the solution was close to 7 and was then concentrated under reduced pressure to about 2 mL and decanted into a 5 mL graduated test tube. The obtained residue was reduced to a final volume of 0.5 mL under a gentle stream of ultrahigh purity nitrogen (99.99%) for GC analysis.

2.3. Sample Analysis. The final extract of pesticidal POPs was analyzed on an HP 6890 gas chromatograph equipped with a ^{63}Ni electron capture detector (μECD) using an HP-1 silica capillary column (30 m $\times$ 0.32 mm i.d. $\times$ 32 μm). The injector and detector temperatures were 220 and 300°C, respectively. The oven temperature was started from 150°C and increased at 5°C/min, then maintained at 200°C for 2 min, and then increased again at 8°C/min and finally maintained at 270°C for 5 min. The injection was splitless and the injection volume was 1 μL. Ultrahigh purity nitrogen was used as the carrier gas. The Stigma pressure of nitrogen was 60 kPa, and 60 mL/min nitrogen was used as the make-up gas. The pesticidal POPs were identified by retention time and quantified using external standard.

A mixture of standard solution containing α-HCH, β-HCH, γ-HCH, δ-HCH isomers, and pp′-DDE, pp′-DDD, op′-DDT, pp′-DDT were obtained from the National Research Center for Certified Reference Materials of China.

TABLE 1: Concentrations (ng/g dw) of OCPs in soil samples in 2003, 2007, and 2009.

Variables		Mean ± SD (min–max)		
		2003	2007	2009
HCHs group	α-HCH	0.06 ± 0.14 (nd−0.78)	0.02 ± 0.05 (nd−0.27)	0.03 ± 0.08 (nd−0.48)
	β-HCH	0.36 ± 0.68 (nd−2.74)	0.59 ± 0.94 (nd−4.58)	0.69 ± 1.83 (nd−14.34)
	γ-HCH	0.06 ± 0.20 (nd−1.41)	0.16 ± 0.19 (nd−1.01)	0.01 ± 0.03 (nd−0.15)
	δ-HCH	0.19 ± 0.61 (nd−3.55)	0.07 ± 0.22 (nd−1.53)	0.02 ± 0.06 (nd−0.30)
	$\sum$ HCH	0.66 ± 1.34 (nd−7.33)	0.85 ± 1.18 (nd−5.56)	0.73 ± 1.92 (nd−14.97)
DDTs group	p,p$'$-DDE	4.71 ± 9.42 (nd−52.20)	3.88 ± 10.69 (nd−78.07)	5.07 ± 11.59 (nd−55.96)
	p,p$'$-DDD	0.24 ± 0.61 (nd−3.37)	0.11 ± 0.33 (nd−1.76)	0.73 ± 1.70 (nd−9.71)
	o,p$'$-DDT	0.84 ± 2.30 (nd−11.71)	0.75 ± 1.81 (nd−9.04)	0.08 ± 0.47 (nd−3.55)
	p,p$'$-DDT	3.67 ± 7.75 (nd−33.08)	2.98 ± 7.38 (nd−50.73)	0.58 ± 1.30 (nd−7.34)
	$\sum$ DDT	9.46 ± 17.76 (nd−76.01)	7.84 ± 17.68 (nd−116.74)	6.46 ± 13.28 (nd−64.91)
Reference		[16]	[19]	Present study

[*] nd: the value less than LOD (limits of detection) was set to nd.

TABLE 2: Composition of HCH and DDT in soil samples in 2003, 2007, and 2009.

Ratio	Year	Average	Minimum	Maximum	Percentage of sites with a ratio less than 1
α-HCH/γ-HCH	2003	1.35	0.25	3.35	8.9%
	2007	0.42	0.12	0.73	15.0%
	2009	2.76	2.25	3.26	0
(DDE + DDD)/p,p$'$-DDT	2003	2.52	0.24	25.2	23.2%
	2007	1.25	0.09	4.22	41.7%
	2009	7.07	0.24	40.1	8.2%

For quality assurance and control, procedural blanks and matrixes spiked with the standard solution were analyzed. None of the target compounds were detected in the procedural blanks. All solvents used were distilled in glass (PR grade) and were checked for interferences or contamination prior to use. The amount of substance in the extracts was quantified using the internal standard (2,4,5,6-tetrachloro-m-xylene). The recovery of the four HCH isomers (α-HCH, β-HCH, γ-HCH, δ-HCH) and four DDT homologues (pp$'$-DDE, pp$'$-DDD, op$'$-DDT, pp$'$-DDT) were 73.3%, 90.3%, 75.8%, 85.6% and 80.0%, 93.8%, 95.4%, and 96.2%, respectively. The extraction efficiency, as indicated by the recovery of the surrogate standards (TCMX), was 75% ± 10%. The detection limit was set to three times the signal-to-noise ratio (S/N). The detection limit ranged from 0.06 to 0.15 ng/g for the HCH isomers and from 0.07 to 0.19 ng/g for the DDT homologues. Reagent blanks were also analyzed simultaneously with the experimental samples.

2.4. Data Processing. The software used for the mapping and spatial analysis was ArcGis 10.0(ESRI, US). An interpolation method called Ordinary Kriging was adopted for the interpolation of geographical data. SPSS 11.5 for Windows was employed for statistical analysis. Excel (version 2007, Microsoft) was also used for preliminary data analysis and histogram graphing.

3. Results and Discussion

3.1. Temporal Variation of Residual Pesticidal POPs in Soils. Table 1 shows that, from 2003 to 2009, the HCHs concentrations in topsoil did not change much, while the DDTs concentrations declined steadily. Specifically, the β-HCH isomers were enriched in the soil, whereas the content of α-HCH isomers declined. The concentrations of γ-HCH isomer (0.01 ng/g dw) and δ-HCH isomer (0.02 ng/g dw) in 2009 are also less than those in 2003 (0.06 ng/g dw and 0.19 ng/g dw) or 2007 (0.16 ng/g dw and 0.07 ng/g dw). The ratio of α-HCH to γ-HCH is often considered the characteristic index to determine the source of the HCHs. The value of ratio between 4 and 7 in samples implies that there may be new source of HCHs; a ratio close to 1 may indicate new industrial input of lindane and a ratio greater than 7 may suggest long distance atmospheric transport of HCHs [17]. As Table 2 shows 8.9% of the samples in 2003 and 15% of the samples in 2007 had α-HCH/γ-HCH ratio less than 1. The result indicates that the main HCH input is from lindane and there may have been new industrial pollution source after restricting HCH usage. Previous studies by Wang et al. (2003), Sun et al. (2005), and Xue et al. (2005) on the Guanting Reservoir also showed that the HCHs in water may be due to the input of lindane or industrial HCHs from the upstream or surrounding regions [3, 8, 9]. However, according to the environmental monitoring in 2009, there was no new industrial lindane pollution source

(a)

(b)

(c)

(d)
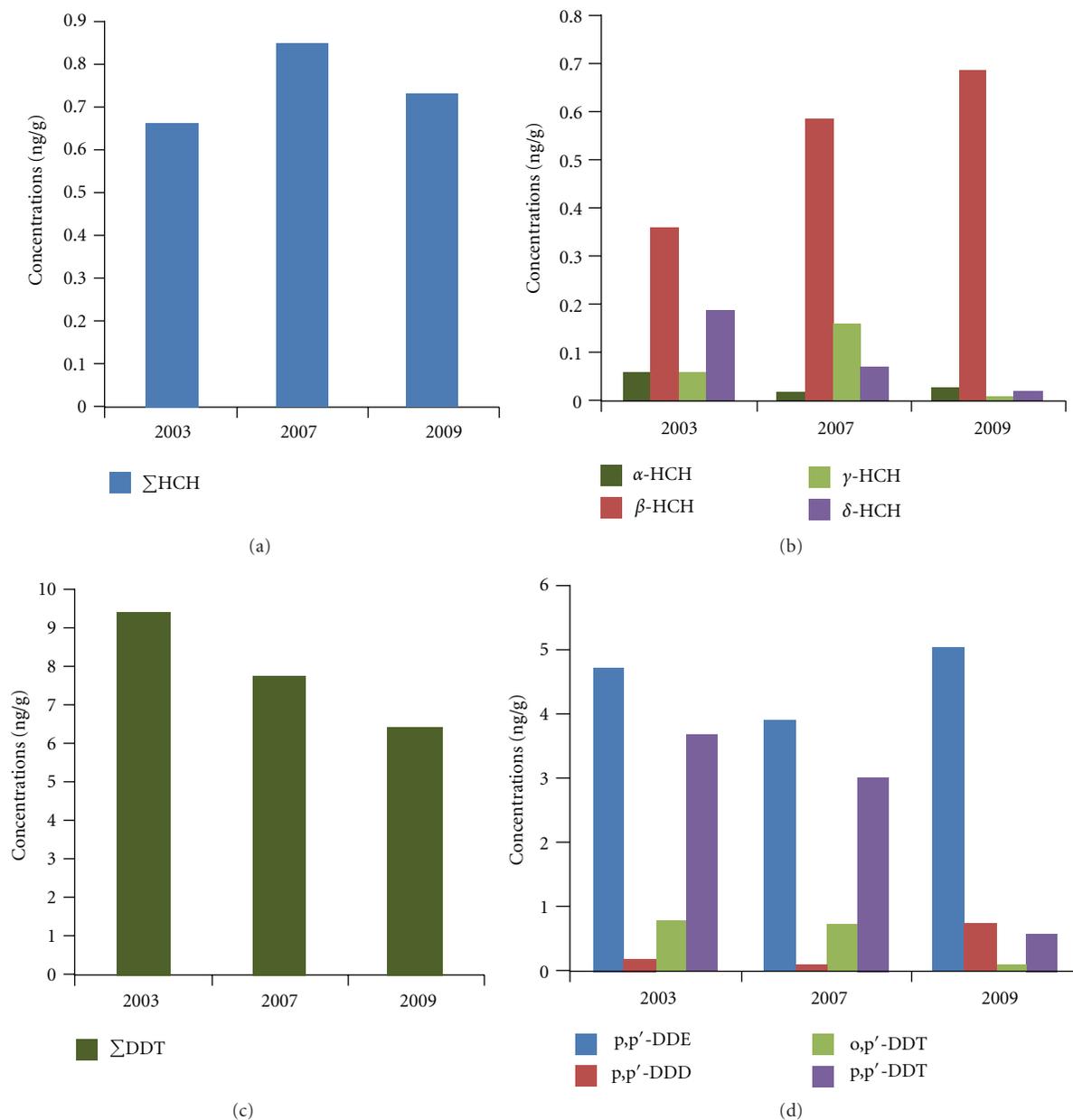
FIGURE 2: Temporal trends of HCHs and DDTs in soils from 2003 to 2009.

near the Guanting region, because α-HCH/γ-HCH ratio of each sample was much higher than 1.

By comparing with previously reported results [16, 18, 19], it can be seen that DDTs have always been the main components of pesticidal POPs in the Guanting Reservoir area, that is, 93.2% in 2003, 90.2% in 2007, and 90.6% in 2009, respectively. Figure 2 shows that the concentration of pp'-DDE in soil is the greatest in 2009. Besides, the concentration of pp'-DDT in soil gradually decreased from 2003 to 2009 while the concentration of pp'-DDD gradually increased. These results indicate that pp'-DDT has gradually degraded to pp'-DDD and pp'-DDE mainly through aerobic degradation. Although DDT can degrade relatively more easily, its degradation products DDE and DDD are more

stable and more difficult to degrade. The ratio of (DDE + DDD) to pp'-DDT is usually considered a characteristic index to determine the source of DDT in the environment [20]. Table 2 shows that 23.2% of the samples in 2003 and 41.7% of the samples in 2007 had a (DDE + DDD) to pp'-DDT ratio of less than 1. This indicates that DDTs such as dicofol or other pesticides containing DDTs as by-product were still used during that time in this region. Dicofol products have a high DDT content varying from 3.54% to 10.8%. Since the 1960 s, in each year 2000 tons of dicofol products were put into use. As a result, dicofol may be the new source of DDT pollution [21]. Table 2 also shows that only about 8.2% of the samples had a (DDE + DDD) to pp'-DDT ratio less than 1 in 2009. Hence, this new DDT source is

basically under control and the environmental exposure was mainly due to the historical use of dicofol.

Concentrations of HCHs and DDTs in soils were compared with the soil quality reference values recommended in China and The Netherlands [22]. According to the guidelines of the Chinese environmental quality standards for soil (GB 15618-1995), the limits for HCH and DDT in the soils are both 50, 500, and 1,000 ng/g dw, corresponding to Class I, II, and III, respectively. In 2003 and 2007, concentrations of HCHs in all soil samples were below the limit of Class I (50 ng/g dw) and Dutch target value (10 ng/g dw). While in 2009, HCHs concentrations were also within the limit of Class I but in several sites exceeded the Dutch target value. With regard to DDTs, mean concentrations of DDTs were within the criteria for Class I and Dutch target value in different years. In general, even concentrations of HCHs and DDTs were both less than the Chinese criteria Class I, which is set to ensure the safety of agricultural products and to prevent foods contamination from HCHs and DDTs; they still could have negative impacts on local atmosphere and aquatic ecosystem in the long term because of their nonbiodegradability and bioaccumulation.

3.2. Spatial Variation of Pesticidal POPs in Soils.
The spatial evolution patterns of HCHs and DDTs in soils were analyzed using the Geostatistical Analyst in the GS extension module of ArcGis with ordinary Kriging interpolation. The results in Figure 3 show that, in 2003, 2007, and 2009, the residual pesticidal POPs vary significantly in different areas around the Guanting Reservoir. The HCHs and DDTs are mainly concentrated in the Beixinpu town and the Huailai county, and their concentrations decreased from north to south. Generally speaking, the concentrations of HCHs and DDTs in the south reservoir were lower than those in north reservoir both before and after the pesticide restriction took effect. This is because (1) agriculture is less developed in the south reservoir and (2) the sandy and weathering soils in the south reservoir speed up the degradation and evaporation of POPs. The Beixinpu town is located in the middle of the north reservoir area. It connects the mountains in the north with the water in the south and has a decreasing geomorphological gradient from north to south. The Beixinpu town has large areas of shrub forests and orchards and used large amounts of HCH and DDT in the 1970s for forestry pest control. Currently lots of pesticides that may contain POPs isomers or degradation products (such as dicofol) are still consumed in the orchards in this area. This may explain why the residual amounts of HCH and DDT were high in the Beixinpu town compared with other areas.

The Huailai county (in Hebei province) located in the central and western Guanting Reservoir area was found to have high HCHs exposures, and the Beixinpu town was found to have the highest risk. The concentration of HCHs in the Beixinpu town was relatively high in 2003, but, after six years of degradation, it decreased to a normal level not significantly different with its surrounding. Previous studies have also shown that the concentrations of heavy metals in

the Beixinpu town are also very high [13, 23]. The Yanghe river and the Sanggan river are the major pollution sources of the Guanting Reservoir. Although the insecticide factories, chemical plants, and printing and dyeing mills located in Zhangjiakou and Xuanhua at the upstream of the Yanghe river have been partially shut down, serious pollution has already occurred. Furthermore, because of the agricultural irrigation in those water sheds, the pollutants including pesticidal POPs were spread to the surrounding soils, leading to high environmental risks. In 2003, the soil DDTs were mainly concentrated in three regions: the western reservoir (near Huailai county), the central reservoir (Beixinpu town), and the eastern reservoir (Yanqing county). The DDT concentrations in the northern regions were higher than those in the southern regions (Figure 3). In particular, the large historical use of DDTs in the Beixinpu area and the new input of pesticidal POPs resulted in much higher DDTs residues in those regions compared with their surroundings, which shows a patchy distribution of high pollution risks. Until 2007, the high pollution risk areas were still concentrated in these three regions, but the acreage of the high pollution risk areas decreased in the central Beixinpu town and Yanqing county. In 2007 the soil DDTs showed no obvious regional aggregation and its overall level declined substantially. Until 2009, the concentrations of DDTs in the high pollution risk areas in the northern Guanting Reservoir further declined from a maximum of 116.74 ng/g dw to 64.91 ng/g dw (Table 1). According to the Chinese Environmental Quality Standard for soils, the concentrations of HCHs in this area were far below the first grade (class I = 50 ng/g dw). Only two sampling sites had DDTs concentrations slightly exceeding the first grade in 2009 (64.91 ng/g dw and 59.05 ng/g dw, resp.), which accounted for only 3.3% of all samples. Overall, after years of pesticide restriction and natural degradation, the pesticidal POPs residues in the soils of studied areas decreased steadily. However, new pollution sources such as lindane and dicofol may exist in some sampling sites and should receive more attention.

3.3. Management and Control of Pesticidal POPs around the Guanting Reservoir

3.3.1. Integrated Management Framework for Regional POPs Control.
By analyzing the temporal and spatial distribution pattern of pesticidal POPs around the Guanting Reservoir based on previous and present studies, a framework of ecoenvironmental countermeasures is put forward for regional POPs control (Figure 4) [24–26]. The establishment and implementation of regional policies should be based on scientific investigation, led by policy analysis, and completed under the common goal of governmental decision-making, local implementation, scientific support, and public participation. This framework includes 18 specific regional ecoenvironmental countermeasures (1) to improve the policy and the regulation system related to pesticidal POPs; (2) improve or develop pesticidal standards and criteria in different media; (3) publicize the environmental hazards of POPs through the local government; (4) strengthen public

(a)

(b)

2003 samples HCHs
- 0–0.0772
- 0.0772–0.2477
- 0.2477–0.6238
- 0.6238–1.4538
- 1.4538–3.2853
- 3.2853–7.327

2003 samples DDTs
- 0–0.1645
- 0.1645–0.6848
- 0.6848–2.3299
- 2.3299–7.5323
- 7.5323–23.9838
- 23.9838–76.008

(c)

(d)

2007 samples HCHs
- 0–0.0681
- 0.0681–0.2132
- 0.2132–0.5219
- 0.5219–1.1791
- 1.1791–2.5782
- 2.5782–5.5564

2007 samples DDTs
- 0–1.1765
- 1.1765–1.4555
- 1.4555–2.6319
- 2.6319–7.593
- 7.593–28.5139
- 28.5139–116.7366

(e)

(f)

2009 samples HCHs
- 0–0.2202
- 0.2202–0.2806
- 0.2806–0.5008
- 0.5008–1.3051
- 1.3051–4.2421
- 4.2421–14.9674

2009 samples DDTs
- 0–0.0857
- 0.0857–0.3878
- 0.3878–1.4517
- 1.4517–5.1995
- 5.1995–18.402
- 18.402–64.9105

FIGURE 3: Spatial-temporal trend of HCHs and DDTs in soils around the Guanting Reservoir.
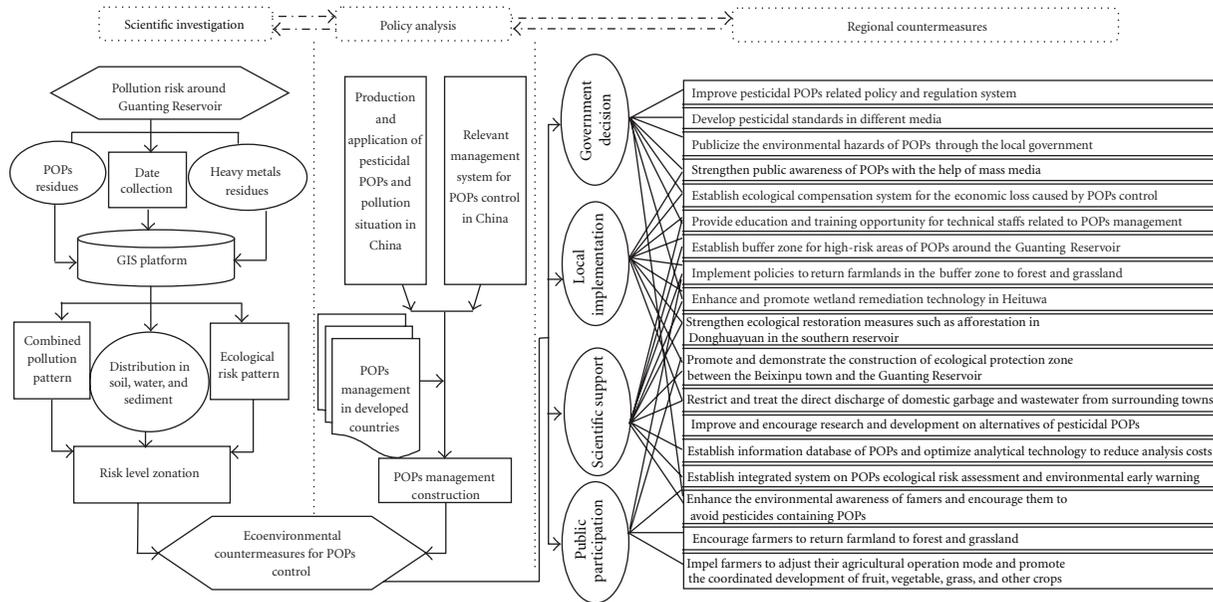
FIGURE 4: Framework of regional POPs management in the Guanting area.

awareness of POPs through mass media; (5) establish the ecological compensation system for the economic loss due to POPs control; (6) provide education and training opportunity for the technical staffs of POPs management; (7) establish buffer zones around the Guanting reservoir for high-risk areas of POPs; (8) implement policies to return farmlands in the buffer zone to forest and grassland; (9) enhance the diffuse wetland remediation technology in Heituwa; (10) strengthen the ecological restoration measures such as afforestation in Donghuayuan in the southern reservoir; (11) promote and demonstrate the construction of ecological protection zone between the Beixinpu town and the reservoir; (12) restrict and control the direct discharge of domestic garbage and wastewater from surrounding towns; (13) improve and encourage R&D on alternatives of pesticidal POPs; (14) establish the POPs information database and optimize the analytical technology for POPs; (15) establish integrated system on ecological risk assessment and environmental earlywarning of POPs; (16) enhance the environmental awareness of farmers and encourage them to avoid pesticides containing POPs; (17) encourage farmers to return farmland to forest and grassland; (18) impel farmers to adjust agricultural operation mode and promote the coordinated development of fruit, vegetable, grass, and other crops.

3.3.2. Ecoengineering Measures to Control POPs in Specific Areas.

With the use of overlay analysis in GIS, the ecological risk near the Guanting Reservoir was classified into five grades based on its spatial distribution pattern. Meanwhile, specific ecological countermeasures for typical regions are proposed in Figure 5.

Sewage Purification by Artificial Wetland between Yanghe River and Heituwa. The chemical plants located at the upstream of the Yanghe river in Zhangjiakou once caused serious pollution in the Guanting Reservoir. The Yanghe river lies between the reservoir in the Yongding river and the Huailai county and still has high concentrations of HCHs and DDTs. Therefore, to protect the water quality of the Guanting Reservoir, the environmental management and ecological restoration in this region must be strengthened. The construction of the Heituwa artificial wetland is a crucial part of the water quality improvement project of the Guanting Reservoir, and it is also the first ecological barrier to the polluted water from Yongding river flowing into the Guanting Reservoir. The construction of 84 hectares of ecological purification ponds and 7.4 hectares of wetland has been planned in the Heituwa artificial wetland. A floating-leaved plant zone of 2.52 hectares and an emergent vegetation zone of 6.84 hectares will be artificially planted, leaving the remaining areas to be covered by natural reproduction.

For ecological purification, the artificial wetland construction could also be carried out in some other areas based on the experience of the Heituwa artificial wetland. The construction of another artificial wetland at the upstream of the Guishui river near the Yanqing county is recommended to effectively prevent the pollution from industrial activities and domestic sewage discharge. The consolidated utilization of forests, arbor, shrubs, and grass can purify surface runoff, reduce reservoir sedimentation, alleviate nonpoint source pollution, recover the ecological functions, and improve the landscape around reservoir.

Forest and Grass Protection Buffer Zone between North Reservoir and Beixinpu. The large areas of orchards in the Beixinpu town are a substantial source of pesticides and fertilizers. It was reported that the Beixinpu town was once the most heavily polluted region around the Guanting Reservoir, in particular suffering from combined
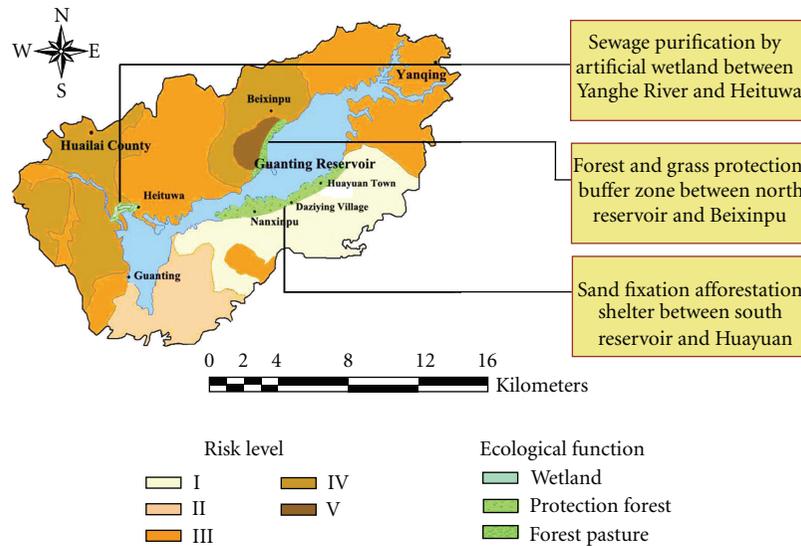
FIGURE 5: Ecological engineering projects around the Guanting Reservoir.

pollutions of DDTs and HCHs [23]. A buffer zone is strongly recommended in the sensitive areas around the reservoir between the Beixinpu town and the Huailai county. Through returning farmland to forest and grassland, the construction of a buffer strip approximately 7 km long and 200 m wide is recommended between the orchards and the water body. This buffer system can successively filtrate the pollutants through farm (orchard), forestry, shrub (grass), and water, which not only blocks the input of pesticidal POPs from the Beixinpu town due to runoffs, infiltration, and soil erosion but also fixes those POPs coming from short-distance atmospheric migration or pesticides-cemented dusts.

Sand Fixation Afforestation Shelter between South Reservoir and Huayuan. The south reservoir has poor sandy soils and is not suitable for agriculture, forestry or grass cultivation. The construction of a shelter forest approximately 14 km long and 500 m wide is proposed, using shrubs with barren resistance and low water consumption.

Meanwhile, the corresponding economic compensation system should be established for the farmers affected by the ecological protection and agriculture limitation policies. In order to transform the POPs management from passive control to active prevention, it is necessary to strengthen the public awareness of the environmental and health hazards of POPs, promote relevant policies and regulations, and foster public understanding and coordination.

4. Conclusions

This study measured the spatial and temporal variability of HCH and DDT concentrations in the soils around the Guanting Reservoir of Beijing. From 2003 to 2009, the DDT concentrations decreased significantly while the HCH concentrations did not change much. The agricultural pesticide application in this region at earlier times was the

main source of HCH and DDT. In the past several decades, China has produced and used large quantities of pesticidal POPs for agriculture purposes and for preventing infectious diseases. Therefore, monitoring databases, especially long-term systematic survey, should be expanded to fully understand this problem.

On the basis of previous and present studies on pesticidal POPs around this water shed, an integrated regional POPs control framework was established. The framework involves scientific investigation, policy analysis, and regional countermeasures, and 18 specific countermeasures are proposed that cover government decision making, local implementation, scientific and technology support, as well as public participation.

References

[1] D. Wei, T. Kameya, and K. Urano, "Environmental management of pesticidal POPs in China: past, present and future," *Environment International*, vol. 33, no. 7, pp. 894–902, 2007.

[2] W. Tieyu, L. Yonglong, Z. Hong, and S. Yajuan, "Contamination of persistent organic pollutants (POPs) and relevant management in China," *Environment International*, vol. 31, no. 6, pp. 813–821, 2005.

[3] X. T. Wang, S. G. Chu, and X. B. Xu, "Organochlorine pesticide residues in water from Guanting reservoir and Yongding River, China," *Bulletin of Environmental Contamination and Toxicology*, vol. 70, no. 2, pp. 351–358, 2003.

[4] State Environmental Protection Administration, "China's pesticide pollution and its being problems and suggestions," *Environmental Protection*, vol. 6, pp. 23–24, 2001.

[5] F. Wania and D. Mackay, "Tracking the distribution of persistent organic pollutants," *Environmental Science and Technology*, vol. 30, no. 9, pp. 390–396, 1996.

[6] H. Hung, P. Blanchard, C. J. Halsall et al., "Temporal and spatial variabilities of atmospheric polychlorinated biphenyls (PCBs), organochlorine (OC) pesticides and polycyclic aromatic hydrocarbons (PAHs) in the Canadian Arctic: results from a decade of monitoring," *Science of the Total Environment*, vol. 342, no. 1–3, pp. 119–144, 2005.

[7] K. S. B. Miglioranza, J. E. A. de Moreno, and V. J. Moreno, "Trends in soil science: organochlorine pesticides in Argentinean soils," *Journal of Soils and Sediments*, vol. 3, no. 4, pp. 264–265, 2003.

[8] N. Xue, X. Xu, and Z. Jin, "Screening 31 endocrine-disrupting pesticides in water and surface sediment samples from Beijing Guanting reservoir," *Chemosphere*, vol. 61, no. 11, pp. 1594–1606, 2005.

[9] Y. Z. Sun, X. T. Wang, and X. B. Xu, "Persistent organochlorine pesticide residues in fish from Guanting Reservoir, People's Republic of China," *Bulletin of Environmental Contamination and Toxicology*, vol. 74, no. 3, pp. 537–544, 2005.

[10] N. Xue, D. Zhang, and X. Xu, "Organochlorinated pesticide multiresidues in surface sediments from Beijing Guanting reservoir," *Water Research*, vol. 40, no. 2, pp. 183–194, 2006.

[11] H. Zhang, Y. Lu, R. W. Dawson, Y. Shi, and T. Wang, "Classification and ordination of DDT and HCH in soil samples from the Guanting reservoir, China," *Chemosphere*, vol. 60, no. 6, pp. 762–769, 2005.

[12] T. Y. Wang, Y. L. Lu, R. W. Dawson, Y. J. Shi, H. Zhang, and Y. Xing, "Effects of environmental factors on organochlorine pesticide residues in soils of the Guanting reservoir area, China," *Journal of Environmental Science and Health B*, vol. 41, no. 3, pp. 309–321, 2006.

[13] W. Luo, Y. L. Lu, J. P. Giesy et al., "Effects of land use on concentrations of metals in surface soils and ecological risk around Guanting reservoir, China," *Environmental Geochemistry and Health*, vol. 29, no. 6, pp. 459–471, 2007.

[14] T. Y. Wang, C. L. Chen, J. E. Naile, J. S. Khim, J. P. Giesy, and Y. L. Lu, "Perfluorinated compounds in water, sediment and soil from Guanting reservoir, China," *Bulletin of Environmental Contamination and Toxicology*, vol. 87, no. 1, pp. 74–79, 2011.

[15] W. Tieyu, L. Yonglong, S. Yajuan, and Z. Hong, "Spatial distribution of organochlorine pesticide residues in soils surrounding Guanting reservoir, People's Republic of China," *Bulletin of Environmental Contamination and Toxicology*, vol. 74, no. 4, pp. 623–630, 2005.

[16] T. Y. Wang, Y. L. Lu, Y. J. Shi, J. P. Giesy, and W. Luo, "Organochlorine pesticides in soils around Guanting reservoir, China," *Environmental Geochemistry and Health*, vol. 29, no. 6, pp. 491–501, 2007.

[17] J. H. Kim and A. Smith, "Distribution of organochlorine pesticides in soils from South Korea," *Chemosphere*, vol. 43, no. 2, pp. 137–140, 2001.

[18] W. Y. Hu, Y. L. Lu, G. Wang et al., "Organochlorine pesticides in soils around watersheds of Beijing reservoirs: a case study in guanting and Miyun reservoirs," *Bulletin of Environmental Contamination and Toxicology*, vol. 82, no. 6, pp. 694–700, 2009.

[19] W. Y. Hu, Y. L. Lu, T. Y. Wang et al., "Spatial variability and temporal trends of HCH and DDT in soils around Beijing Guanting reservoir, China," *Environmental Geochemistry and Health*, vol. 32, no. 5, pp. 441–449, 2010.

[20] A. Aguilar, "Relationship of DDE/SIGMA DDT in marine mammals to the chronology of DDT input into the ecosystem," *Canadian Journal of Fisheries and Aquatic Sciences*, vol. 41, no. 6, pp. 840–844, 1984.

[21] X. Qiu, T. Zhu, B. Yao, J. Hu, and S. Hu, "Contribution of dicofol to the current DDT pollution in China," *Environmental Science and Technology*, vol. 39, no. 12, pp. 4385–4390, 2005.

[22] NMH, "The Netherlands ministry of housing, spatial planning and environment's circular on target values and intervention values for soil remediation," 2000, http://www.esdat.net/Environmental%20Standards/Dutch/annexS_I2000Dutch%20Environmental%20Standards.pdf.

[23] W. Luo, T. Y. Wang, Y. L. Lu et al., "Landscape ecology of the Guanting reservoir, Beijing, China: multivariate and geostatistical analyses of metals in soils," *Environmental Pollution*, vol. 146, no. 2, pp. 567–576, 2007.

[24] S. Yajuan, L. Yonglong, Z. Hong, W. Tieyu, and X. Ying, "Persistent organic pollutants control strategy in China," *Journal of Environmental Sciences*, vol. 17, no. 2, pp. 309–314, 2005.

[25] H. Zhang, Y. Lu, Y. Shi, T. Wang, Y. Xing, and R. W. Dawson, "Legal framework related to persistent organic pollutants (POPs) management in China," *Environmental Science and Policy*, vol. 8, no. 2, pp. 153–160, 2005.

[26] M. H. Lau, K. M. Leung, S. W. Wong, H. Wang, and Z. G. Yan, "Environmental policy, legislation, and management of persistent organic pollutants (POPs) in China," *Environmental Pollution*, vol. 165, pp. 182–192, 2012.

The *s*cientificWorldJOURNAL

Research Article

Fate and Transport of Polycyclic Aromatic Hydrocarbons in Upland Irish Headwater Lake Catchments

Heidi E. M. Scott, Julian Aherne, and Chris D. Metcalfe

Environmental and Resource Studies, Trent University, Peterborough, ON, Canada K9J 7B8

Correspondence should be addressed to Heidi E. M. Scott, heidiscott@trentu.ca

Polycyclic aromatic hydrocarbons (PAHs) are a concern due to their carcinogenicity and propensity for transboundary atmospheric transport. Ireland is located on the western periphery of Europe and assumed to receive clean Atlantic air. As such, it has been used as an atmospheric reference for comparison to other regions. Nonetheless, few studies have evaluated concentrations of PAHs within the Irish environment. In the current study, PAHs were measured at five upland (500–800 masl) headwater lake catchments in coastal regions around Ireland, remote from industrial point source emissions. Semipermeable membrane devices were deployed in lakes for a 6-month period in July 2009, and topsoils were sampled from each catchment during October 2010. The concentrations of PAHs were low at most study sites with respect to other temperate regions. Homologue groups partitioned between lake and soil compartments based on their molecular weight were: "lighter" substances, such as Phenanthrene and Fluorene, were found in higher proportions in lakes, whereas "heavier" compounds, such as Chrysene and Benz[a]anthracene, were more prominent in soils. Concentrations of PAHs were highest at the east coast sites, potentially due to contributions from historical transboundary and regional combustion sources.

1. Introduction

Polycyclic aromatic hydrocarbons (PAHs) is an overarching term describing hundreds of individual chemical compounds containing two or more fused aromatic rings and are known to persist or accumulate in the environment [1]. Although PAHs occur naturally in the environment (e.g., forest fires, volcanoes, and diagenesis), their natural cycle has been significantly augmented during the past century through anthropogenic processes, such as wood and fossil fuel combustion [2–7]. Combustion is the primary source of long-range atmospheric transport of PAHs into the surrounding environment [8]. However, unlike many legacy persistent organic pollutants (POPs), that typically follow the global distillation model of accumulation in colder regions owing to atmospheric condensation and cold trapping [9], PAHs tend to decrease in concentration further from the initial point source [1]. Atmospheric concentrations of PAHs tend to be higher in temperate regions owing to seasonal heating [10]. In addition, the Arctic still exhibits

preindustrial levels of PAHs (e.g., 1–10 ng g^{-1} per individual PAH [1, 11]) largely owing to the lower atmospheric half-life [12] caused by thermal/photodegradation and propensity for particulate binding [13]. Further, regions receiving high rates of precipitation are particularly vulnerable due to the dominant "washout" of contaminants from the atmosphere [14].

The ubiquitous nature of PAHs in the environment, primarily stored in soils [1], is a major human and ecosystem health concern owing to their known carcinogenicity and potential toxicity to both aquatic and terrestrial organisms [15, 16]. Observations of PAHs in regions remote from direct emission or production provide an understanding of the influence of atmospheric transport on ecosystem integrity. Ireland is a well established background reference region for atmospheric research owing to its location on the western periphery of Europe and dominant prevailing Westerlies [17]. West coast sites are characterised by clean oceanic air while east coast sites show an anthropogenic signal from national and transboundary sources. However, there is limited knowledge on PAHs in the Irish environment;

research to date has focused only on lake sediment cores at a few sites [18].

The objective of this research was to provide a comprehensive assessment of PAHs in seminatural upland headwater lake catchments in Ireland, dominated by loadings from atmospheric deposition, catchment response, and recycling from sediments. The level of PAHs in lake water and surrounding soils was quantified in upland catchments ($n = 5$) remote from primary industrial emission sources. In addition, the variation between sites and proportions of individual PAHs was evaluated. Source apportionment and tentative relationships between PAHs and various physical, chemical, and meteorological parameters were also evaluated to assess sources and fate.

2. Materials and Methods

2.1. Study Sites. The five headwater lake catchments (Lough Cummeenoughter (CUM), Lough Adanacleveen (ADA), Mullincrick Lough (MUL), Sgilloge Lough (SGI), and Cleevaun Lough (CLE)) were located in upland regions (Figure 1, Table 1) and represented a transboundary network analogous to the atmospheric monitoring network established by the Irish Environmental Protection Agency under the European Monitoring and Evaluation Programme [19]. The study sites were located in acid-sensitive moorland regions [20]; the catchments were dominated by organic soils and the vegetation was primarily *Calluna vulgaris* along with various graminoid (e.g., sedges and grasses) and bryophyte (e.g., mosses and lichens) species. The catchments ranged in size from 1.90 to 63.4 ha (mean: 19.1 ha) and elevation ranged from 493 to 713 masl (mean: 590 masl). The lakes varied in size from 0.35 to 2.36 ha (mean: 1.37 ha) and were polymictic (well-mixed) due to their shallow nature (depth 1–8 m) and the relatively mild and windy climate. Annual wind speeds are on average 11 km hr^{-1} in the south and up to 29 km hr^{-1} in the north [17]. Long-term annual rainfall at the study sites ranged from 1600 to 3000 mm and mean air temperatures ranged between 9 and 10.3°C (Table 1) based on Met Éireann (The Irish Meteorological Service) 1960–1990 climate normals [21]. Pollutant inputs were assumed to be predominantly deposited from the atmosphere owing to their remoteness from local pollution sources.

2.2. Field Sampling. Water samples for major ion chemical analysis were collected from the shore of each lake in 250 mL plastic high density polyethylene bottles at regular intervals during the study period (July 2009–July 2011; $n = 8$), at a depth of not more than 20 cm below the surface in areas free of debris and vegetation. Each bottle was rinsed with lake water five times prior to sample collection and filled and capped underwater to avoid headspace. Supplementary physical and chemical lake parameters measured on site included water temperature, pH, conductivity, and dissolved oxygen (DO). In addition, continuous hourly water temperatures were monitored using HOBO pendant loggers.

The concentration of PAHs in lakes was monitored using semipermeable membrane devices (SPMDs) immersed in the lakes. Semipermeable membrane devices are passive
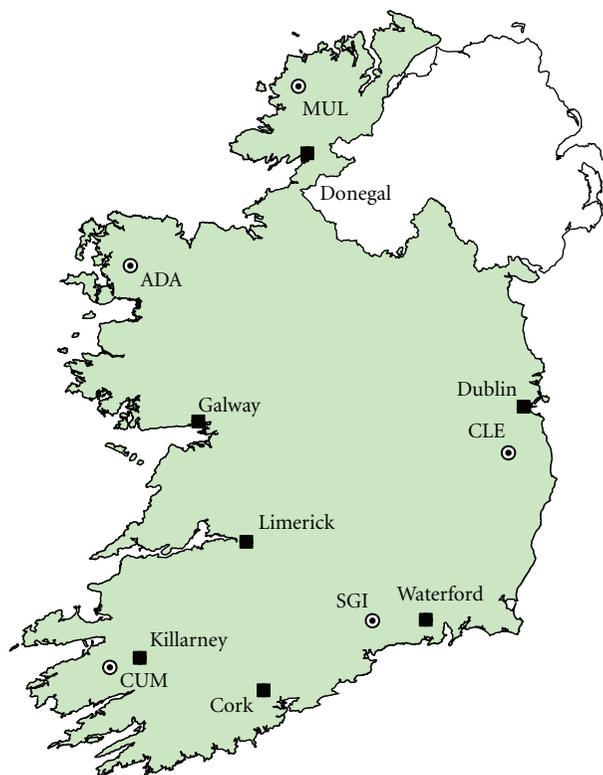
FIGURE 1: Location of the five study sites (circles) and major cities (filled squares) in the Republic of Ireland (green shading): Lough Cummeenoughter (CUM), Lough Adanacleveen (ADA), Mullincrick Lough (MUL), Sgilloge Lough (SGI), and Cleevaun Lough (CLE).

samplers used to monitor the presence of lipophilic organic contaminants at concentrations as low as parts per trillion (i.e., ng L^{-1}; [22]). These devices only measure true dissolved aqueous phase organic pollutants (and do not absorb compounds bound to organics or particulate matter), available for partitioning into synthetic lipid (triolein), given that the target pollutants are generally hydrophobic and lipophilic ($K_{ow} > 4.4$). The SPMDs were assembled in a "Class A" clean laboratory at Trent University [23]. The SPMDs contained 1 mL of high purity (95%) triolein in polyethylene bags and were prepared with performance reference compounds (PRCs): 30 ng of PCB congener 14, 32, and 155, and 25 ng of congener 203, which were used to assess the influence of environmental conditions on SPMD function [24]. Prior to deployment, three SPMDs were suspended inside a cylindrical shroud (77×10 cm) and installed in each study lake. The shrouds were constructed from galvanized metal stove pipe with holes punched to allow for water movement. The SPMDs ($n = 3$ per site) were submerged at a depth of ~1 m in each lake during July 2009 and retrieved in January 2010. Upon recovery, the SPMDs were placed back into their initial solvent-washed jars and stored in a dark cooler until they could be refrigerated. In the laboratory, SPMDs were cleaned using deionized water and separated from solution using hexane [25]. Trip blanks were exposed to air on-site during each deployment and a laboratory blank was left at

TABLE 1: Chemical, physical, and meteorological characteristics of study catchments ($n = 5$): Lough Cummeenoughter (CUM), Lough Adanacleveen (ADA), Mullincrick Lough (MUL), Sgilloge Lough (SGI), and Cleevaun Lough (CLE). Lake chemical observations represent average concentrations during the period 2010-2011 ($n = 6$).

Site characteristics	CUM	ADA	MUL	SGI	CLE
Easting (m)	80300	91900	187600	229700	307100
Northing (m)	84800	314200	416700	111500	207300
Elevation (masl)	713.0	554.0	493.0	505.1	684.7
Lake size (ha)	0.35	1.52	0.85	2.36	1.78
Catchment size (ha)	1.90	15.5	4.50	63.4	10.1
% over land (1-day mean)	11.52	11.32	14.42	21.76	27.04
Water temperature (°C)	7.59	9.35	11.07	10.53	8.43
Rainfall (mm yr^{-1})	3060	1701	2003	1895	1847
Air temperature (°C)	10.28	9.30	9.02	9.80	9.59
Lake measurements					
pH	6.44	4.75	4.96	5.93	4.70
Conductivity (μS cm^{-1})	24.95	56.46	57.89	29.79	26.00
Total organic carbon (mg L^{-1})	1.10	4.05	4.82	3.77	6.01
Gran alkalinity (mg L^{-1})	0.35	−0.75	−0.59	0.22	−0.66
Sulphate (mg L^{-1})	1.42	2.17	2.41	1.48	1.54
Chloride (mg L^{-1})	6.00	13.24	14.49	5.04	4.53
Dissolved oxygen (mg L^{-1})	11.88	11.84	11.53	11.19	11.49
Soil measurements					
Soil type	Lithosol	Peat	Peat	Peat	Peat
Bulk density (g cm^{-3})	0.54	0.13	0.14	0.16	0.12
pH (H$_2$O)	4.35	4.01	4.00	3.83	3.85
Loss-on-ignition (%)	7.04	96.25	96.00	92.95	85.13
Nitrogen (%)	0.32	1.69	1.70	2.07	2.01
Carbon (%)	3.57	47.46	47.3	47.74	44.23
Sulphur (%)	0.05	0.34	0.30	0.36	0.37

Trent University, both were used to correct for background contamination.

High molecular weight (HMW) PAHs (>4 aromatic rings) possess a strong affinity (binding) for organic matter and do not partition readily into SPMDs [26]; however, they can be monitored through catchment soil sampling. As such, soils were collected at each study site and analyzed for PAHs. Prior to sampling, all equipment was washed with Sparkleen and rinsed several times with deionized water. Reagent grade hexane and acetone were used on all equipment surfaces to ensure residues were removed prior to sampling. Soil samples were gathered with a stainless steel corer from topsoils (0–5 cm) following removal of the upper portion of vegetation [27]. The first two core samples were discarded and the subsequent three soil cores were placed in a stainless steel tray and blended into a uniform mixture. The bulk sample was placed into a 125 mL solvent-washed amber glass jar and sealed in a Ziploc bag. Jars were immediately placed in a dark cooler until they could be refrigerated and freeze dried for subsequent analysis. In the laboratory, PAHs were extracted from the soils using accelerated solvent extraction (ASE). A replicate core with a known volume was also taken at each site to determine bulk density in conjunction with additional soil samples (0–5 cm) for supplementary analysis (e.g., pH,

organic matter, etc.). Continuous soil temperature at a depth of ~10 cm was monitored during the study period using a buried HOBO pendant logger.

2.3. Laboratory Analysis. In the laboratory, water samples were analyzed for a suite of water chemistry parameters: pH was measured by low conductivity electrode, alkalinity was determined using a PC titration Plus System, total organic carbon (TOC) was analyzed on a TOCV-cph Shimazdu Analyzer, absorbance (ABS) was measured using a UV-VIS spectrometer, and chloride (Cl$^-$) and sulphate (SO$_4{}^{2-}$) ions were analyzed on an Dionex Ion Chromatograph. Oxygen18 (δ18O) and deuterium (δD) were measured with a ThermoFinnigan TC/EA Delta Plus XL Mass Spectrometer at the University of Saskatchewan and used to calculate deuterium excess (d-excess [28]), which has been shown to differentiate lake catchments characterized by slow-moving waters and high evaporation rates versus those with regular throughflow [29].

Soils were oven-dried at 60°C for 48 hours, sieved (<2 mm), and analyzed for total carbon, nitrogen, and sulphur content using a Vario MACRO-CNS Analyzer (Elementar Americas, Inc., NJ, USA), soil organic matter (SOM) was determined as loss-on-ignition (LOI) using a muffle furnace
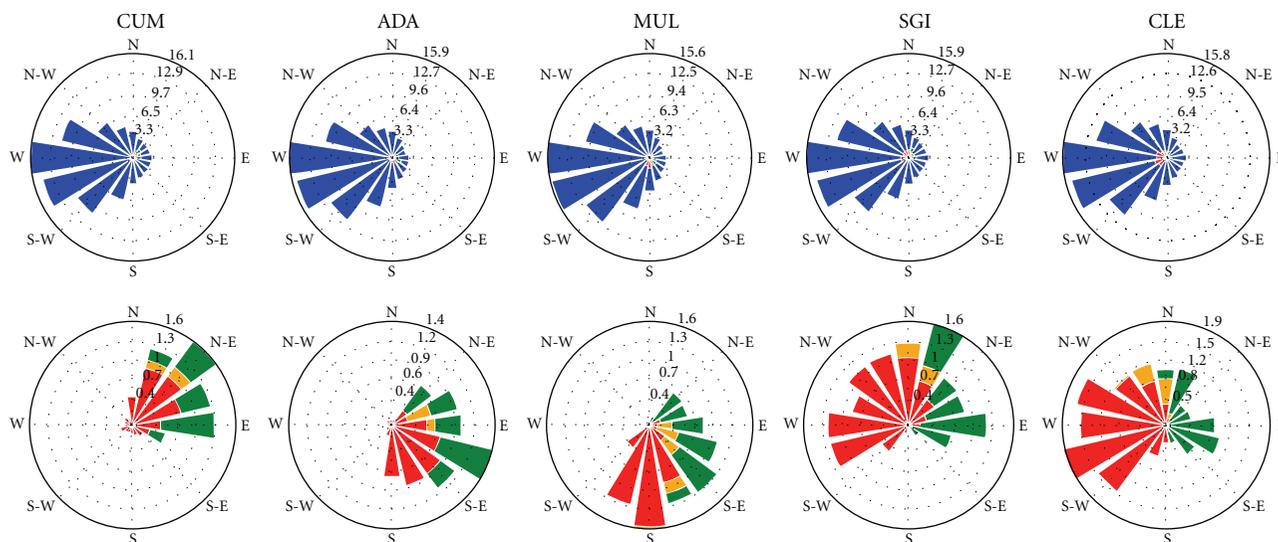
FIGURE 2: Upper: wind rose source-receptor plots showing the proportion (%) of air by direction and source (Republic of Ireland (red), Northern Ireland (orange), Great Britain (green) and marine and other regions (blue)) arriving at the study catchments (receptors; arrival height of 850 hPa) based on two-day back trajectories estimated every six hours during the period 1989–2009.

at 550°C for 8 hours, bulk density was calculated based on known volume and dry weight of the core samples, and pH was measured in distilled water using an OakTon pH/mV meter (OakTon Instruments, IL, USA).

The soil and SPMD extracts were cleaned up by gel permeation chromatography followed by fractionation via silica gel chromatography [25] to isolate PAHs. The samples were subsequently evaporated and redissolved in iso-octane prior to analysis [30]. The SPMD and soil extracts were analyzed for 15 "priority" PAHs (defined by the US EPA) using gas chromatography with low resolution mass spectrometry (GC-LRMS; [26]). Chrysene and Benz[a]anthracene were coeluted during GC-MS analysis, as such they are presented together.

2.4. Source-Receptor Analysis. The atmospheric source regions for the study sites were evaluated using back-trajectory analysis for one, two, three, and five days based on a simple single particle Lagrangian backtracking algorithm. The analysis focused on estimating the proportion of air during each back-trajectory period (1–5 days) that crossed source region land masses (e.g., Europe (EUR), Great Britain (GB), Northern Ireland (NI), Republic of Ireland (ROI), North America, etc.) before arriving at the study sites (i.e., receptors; arrival height of 850 hPa). Further, trajectory source regions were separated into 8 and 16 directional sectors (i.e., north, north east, east, etc.). Back trajectories were estimated every six hours during the period 1989–2009 using historical wind fields (based on observed data and model output) smoothed onto a 3-dimensional grid with 16 pressure levels and a horizontal resolution of 1×1 degree obtained from the ECMWF ERA Interim data set [31]. In this study, "1-day ROI+NI" was defined as the percentage of air originating from the Republic of Ireland and Northern Ireland based on a 24-hour back trajectory, "1-day GB+EUR"

as the percentage of air originating from Great Britain and Europe based on a 24-hour back trajectory, "5-day Marine" as the percentage of air originating over oceanic regions based on a 120-hour back trajectory, and "1-day overland" as air originating from the Republic of Ireland, Northern Ireland, Great Britain, and European landmasses based on a 24-hour back trajectory (Figure 2).

2.5. Data and Statistical Analysis. Average time-weighted water concentrations were estimated from measured SPMD data based on models discussed in detail by [32], and more recently by [33, 34]. Estimates accommodated PRC data, chemical uptake rates, exposure time, quantity of chemicals measured in SPMDs, and specific octanol water partition coefficients [24]. Version 5.1 of the SPMD Water Concentration Estimator [35] were used to produce estimates of water concentrations from raw SPMD data, which were calculated as average-time weighted totals based on the bulked average of three SPMD samples. Total PAHs in soils were expressed as concentration per weight of soil ($ng\,g^{-1}$) and by sample mass (i.e., pool of PAHs ($\mu g\,m^{-2}$)), estimated using soil bulk density and sample depth (5 cm). All data were tested for normality (Shapiro-Wilk). Pearson Product-Moment Correlation coefficients were used to evaluate correlations between variables and considered to be significant at $P < 0.05$. All correlations were visually assessed for outliers or skewed relationships. The limitations of statistically evaluating the tentative relationships of a small sample size ($n = 5$) using parametric procedures were outweighed by the insight offered from the analysis. Although many parameters were included in the analysis, only statistically significant results are presented. All statistical analyses were carried out using SigmaPlot 11.0 (Systat Software, Inc.). Principal component analysis (PCA) was carried out using Multibase, an Excel add-in program; a PCA is a graphical statistical analysis
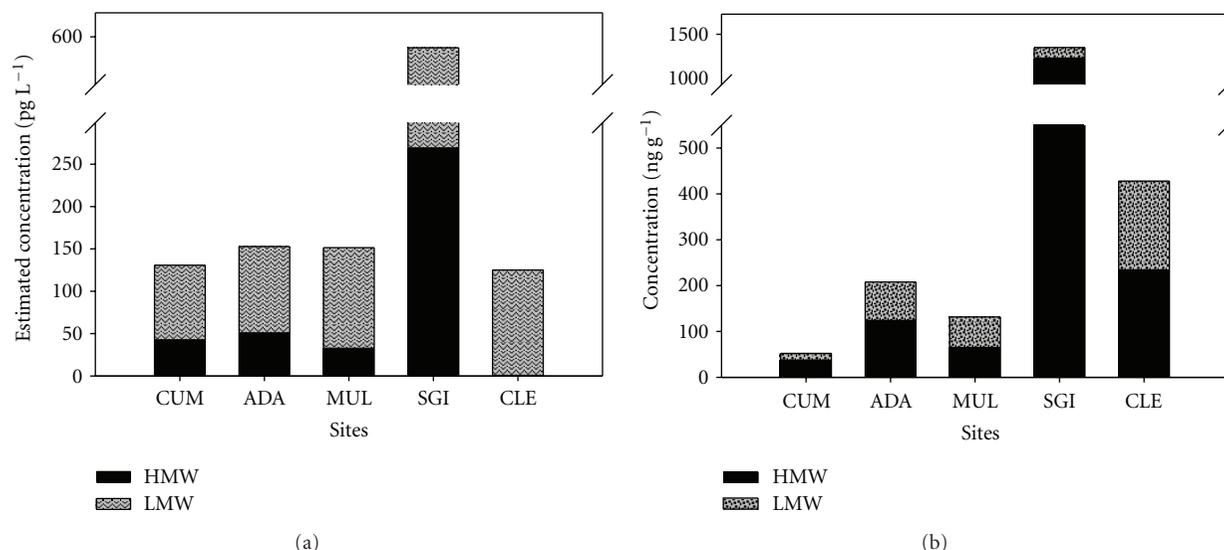
FIGURE 3: Sum of 15 PAH compounds in the five study lakes (Lough Cummeenoughter (CUM), Lough Adanacleveen (ADA), Mullincrick Lough (MUL), Sgilloge Lough (SGI), and Cleevaun Lough (CLE)) with high molecular weight (black) and low molecular weight (grey) portions shown. Concentrations of PAHs in lakes (a) estimated from SPMDs deployed during the period from July, 2009, to January, 2010. Concentrations of PAHs in soils (b) collected in October 2010.

tool used to process and visually simplify large sets of data allowing the relationships between PAHs and a wide number of physical, chemical, and meteorological site variables (e.g., lake : catchment ratio, pH, organic matter, rainfall, etc.) to be explored. Only components with eigenvalues >1 were retained to uphold reliability of the final output [36].

3. Results and Discussion

3.1. PAHs at the Study Sites. In general, low molecular weight (LMW) PAHs (2-3 rings) were dominant in the lakes (Figure 3), whereas HMW PAHs (>4 rings) contributed a larger proportion in the soils. The highest concentration of PAHs in water and soil compartments was found at SGI (east coast; see Figure 1). The levels at SGI were considerably elevated compared with the other study sites, highlighting its proximity to historic industrial emissions, and present-day agriculture sources, as evidenced by burning of heathland to promote grass growth, a significant source of PAHs to surrounding ecosystems [37, 38]. Previous studies have similarly observed higher concentrations of PAHs in sediment cores from an east coast upland lake (close to CLE) attributed to elevated historic inputs with maximum levels coinciding with European SO_2 peaks [18]. The differences in observed PAH concentrations between study sites reflected the variations in geographical location, proximity and influence of regional emissions, meteorology, and lake chemistry. Cummeenoughter is a high elevation mountain lake strongly influenced by incoming southwesterly air and high annual rainfall (>3000 mm). The soils at CUM are lithosols (shallow mineral soils) with sparse vegetation (e.g., bryophytes and graminoids) in areas. In contrast, the ADA and MUL study sites are both strongly influenced by their western exposure, as evidenced by elevated lake conductivity, Cl^- and Na^+ owing to marine inputs. Further, soils at ADA and MUL are

blanket peats overlain with *Calluna vulgaris* and graminoids, leading to high TOC and low pH in the study lakes. The eastern sites, SGI and CLE, are both more influenced by source emissions from Europe and Ireland based on back-trajectory analysis (see Figure 2).

As such, SGI and CLE exhibited a stronger anthropogenic atmospheric pollution signal, as indicated by higher concentrations of nonmarine SO_4^{2-} in lakes. Soils at both sites are also classified as blanket peat; however, vegetation in some areas of CLE is sparse owing to peat erosion.

3.2. PAHs in Lakes. Estimated PAH concentrations in lake water were three times higher at SGI (577.1 pg L^{-1}; Figure 3), with the other study sites displaying a similar range of concentrations (125–153 pg L^{-1}). A wide range in concentrations have been observed in other studies; for example, in the Neretva River in Bosnia, the concentration of 19 PAHs at the reference site was 160 pg L^{-1}, while the river mouth exhibited levels up to 4000 pg L^{-1} [39]. Similarly, a total of 23 dissolved PAHs were measured in remote mountainous lakes [40, 41] in the Alps, Austria (350 ± 190 pg L^{-1}, 2417 masl), in the Caledonian, Norway (560 ± 60 pg L^{-1}, 723 masl), Pyrenees, Spain (270 ± 190 and 580 ± 200 pg L^{-1}, 2240 masl), Tatra, Slovakia (3400 ± 400 pg L^{-1}, 2057 masl). In the Himalayas, Nepal, ΣPAHs in alpine lakes ($n = 7$) was estimated to be 1900 ± 1860 pg L^{-1} (4890–5300 masl; [42]). In a small rural lake, Esthwaite Water, UK, 14 dissolved PAHs (141000 ± 84000 pg L^{-1}; [43]). In Harbour estuary, NJ, USA, a total of 36 dissolved PAHs were measured (10713 ± 4674 pg L^{-1}; [44]).

Total PAHs in Irish lakes were comprised largely of Phenanthrene (~57%) and Fluoranthene (~22%; Table 2). Atmospheric concentrations of PAHs show higher proportions of Phenanthrene, compared with Fluorene and Fluoranthene, which is also consistent with dissolved lake

TABLE 2: Estimated lake water and measured soil concentrations (0–5 cm) of 15 PAHs for upland study catchment ($n = 5$): Lough Cummeenoughter (CUM), Lough Adanacleveen (ADA), Mullincrick Lough (MUL), Sgilloge Lough (SGI), and Cleevaun Lough (CLE).

PAHs	Rings no.	Log K_{ow}	Estimated lake concentrations (pg L^{-1})					Soil concentrations (ng g^{-1})				
			Range		Mean	SD	%ΣPAHs	Range		Mean	SD	%ΣPAHs
			Min	Max				Min	Max			
Naphthalene	2	3.45	ND	4.55	0.91	2.03	0.40	6.57	15.9	12.8	3.66	2.92
Acenaphthylene	3	4.08	ND	11.0	2.21	4.94	0.97	0.00	3.36	0.67	1.5	0.15
Acenaphthene	3	4.22	ND	8.32	1.66	3.72	0.73	0.24	3.51	1.70	1.3	0.39
Fluorene	3	4.38	ND	12.8	6.79	4.84	2.98	0.45	12.4	5.20	4.5	1.19
Phenanthrene	3	4.46	65.3	302.0	129.0	98.7	56.7	2.91	91.6	47.4	37.7	10.8
Anthracene	3	4.54	ND	38.0	7.59	17.0	3.34	1.02	70.4	25.1	27.6	5.73
Fluoranthene	4	5.2	0.63	163.1	49.6	64.6	21.8	16.8	567.8	160.8	232.2	36.7
Pyrene	4	5.3	ND	92.6	25.3	38.0	11.1	13.5	272.3	84.8	108.1	19.4
Benz[a]anthracene+Chrysene*	4	5.61–5.91	ND	12.4	3.86	0.52	1.70	4.62	158.8	41.2	66.2	9.40
Benzo[b]fluoranthene*	5	5.78	ND	ND	ND	ND	0.00	1.92	169.1	38.3	73.2	8.76
Benzo[a]pyrene*	5	6.35	ND	1.21	0.47	0.52	0.21	ND	7.44	1.61	3.3	0.37
Benzo[ghi]perylene	6	6.75	ND	ND	ND	ND	0.00	ND	63.4	13.2	28.1	3.02
Dibenz[a,h]anthracene*	5	6.51	ND	ND	ND	ND	0.00	ND	ND	ND	ND	0.00
Indeno[1,2,3-cd]pyrene*	6	6.9	ND	ND	ND	ND	0.00	ND	24.5	4.89	10.9	1.12

* known carcinogen.

samples in various mountainous lakes [40–42]. The HMW compounds are often bound to particulate (predominantly black carbon, or soot [1]) and, therefore, are more associated with soils or sediments rather than the water column and are less available for SPMD uptake; however, particle-bound PAHs will leach into surface waters via TOC transport from the catchment [1]. In addition, HMW compounds also have higher K_{ow} coefficients and experience longer sorption rates to reach equilibrium in SPMDs [45]. In contrast, LMW compounds are more susceptible to seasonality and temperature, possessing higher vapour pressures and lower K_{ow} coefficients, which increases solubility in water and bioavailability. This increased availability leads to higher exchange in media (i.e., water, air, sediments, etc.), which favours leaching and degradation via microbes or photooxidation compared with HMW compounds [40, 46].

Estimated concentrations of HMW PAHs in the study lakes were negatively correlated with lake : catchment ratio ($R = -0.87$), highlighting increased inputs from relatively larger drainage areas, whereas LMW PAH estimates in lake water exhibit a positive correlation with 1-day overland ROI+NI air ($R = 0.88$), indicative of a potential source region originating from within Ireland, likely attributable to more local combustion sources. In addition, Naphthalene in lakes showed a negative correlation with TOC ($R = -0.88$) and SOM ($R = -0.99$), and a positive correlation with soil pH ($R = 0.92$) and annual rainfall ($R = 0.98$). The association with organic matter and relationship with precipitation underscores the elevated volatility and solubility coefficient (30.2 versus <3.93; [45]) of Naphthalene compared with "heavier" PAH compounds.

3.3. PAHs in Soils. Similar to lake water, the level of PAHs in soils was at least three-fold higher at SGI (1369 ng g^{-1} (109.5

μg m^{-2})) compared with the other study sites, which ranged from 52.2–428.0 ng g^{-1} (9.20–25.7 μg m^{-2}; Figure 3). The concentrations were similar to grassland soils from a transect study between the UK and Norway (15 PAHs; 63 (Norway)–700 (UK) ng g^{-1}; [47]), and on the lower end compared with concentrations observed in higher elevation European mountain ranges, which analyzed a greater number of PAHs in soils (Teide, Pyrenees, and Tatra; 23 PAHs between 750 and 2500 ng g^{-1}: [48]). Soil organic carbon (OC) was high in the study sites (median: 47.3% OC) compared with other studies, as such, pool sizes were smaller. Alpine catchments observed mean PAH concentrations at Montseny 1000 ng g^{-1} (324 masl; 1.6% OC), Pyrenees 550 ng g^{-1} (1516 masl; 15.8% OC), Alps 1600 ng g^{-1} (1101 masl; 2.1% OC), Tatra 1400 ng g^{-1} (1413 masl; 12% OC [49]), and the Chilean Andes 600–4243 ng g^{-1} (1368 masl; [50]). Lower mean values for 16 PAHs measured in the Canadian Rocky Mountains, 68.3 ng g^{-1} [51] were more consistent with values representative of tropical regions (e.g., Costa Rica 1–36 ng g^{-1} [52]) rather than temperate background regions >200 ng g^{-1} [1].

Total PAHs in the study soils were dominated by Fluoranthene (~31%) and Pyrene (~20%; Table 2). This proportional pattern was also observed in Montseny soils (394 masl; [49]) despite the substantial difference in SOM (2.8%, compared with average ~75% in this study). Soil properties can lead to major differences in PAH spatially and temporally; for instance, PAHs often undergo sorption to organic-rich substrate; however, particle size, polarity, soil pH, temperature, and moisture greatly affect their degradation and transport [1, 53]. In addition, total PAHs tend to be lower in mineral soils with a higher proportion consisting of HMW [54], which is consistent with observations in the mineral soils at CUM compared with the other organic-rich study

catchments based on concentration per weight rather than pool size. Organic soils have a lower overall density but larger surface area, and the higher density of binding sites increases sorption capacity [46]. Further, PAHs with similar physio-chemical properties are generally correlated [55], as observed in the study catchment (e.g., Fluorene and Anthracene ($R = 0.90$)). In contrast to water estimates of Naphthalene, concentrations in soils were positively correlated with TOC ($R = 0.93$) and negatively correlated with lake and soil pH ($R = 0.88$) and rainfall ($R = -0.97$), whereas Phenanthrene exhibited a negative correlation with soil pH ($R = -0.88$), related to organic acids, suggesting an association with SOM. Benz[a]anthracene+Chrysene was also correlated with lake : catchment ratio ($R = -0.88$), again demonstrating the influence of a relatively larger drainage basin.

3.4. Source Diagnosis. Concentrations of PAHs in soils and estimated concentrations in water were highest at SGI, suggesting proximity to local emission sources in the east of the country as PAHs are produced primarily as a byproduct of various combustion processes. In contrast, the lowest soil concentrations were observed at CUM, suggesting the site predominantly received clean Atlantic air; further, the catchment is located in a mountainous region compared with SGI which is located in an agricultural region where vegetation burning is common. In general, PAHs typically have a lower volatility and therefore a shorter atmospheric residence time owing to their transport in association with particles [48]; as such, national emission sources potentially contribute the majority of these pollutants. Fluoranthene : Fluoranthene + Pyre ratios (Figure 4) among sites were consistent with sources originating from combustion of grass, coal, or wood rather than fossil fuels (e.g., diesel or petroleum). Ratios <0.4 are considered petrogenic, while ratios between 0.4-0.5 are pyrogenic, and ratios >0.5 are attributed to combustion of organic matter [56]. Ratios provide an indication of source; however, they can vary greatly even from the same source owing to different atmospheric conditions [10]. Further, discrepancies in wind speeds, moisture, sunlight, and temperature among sites highly influence volatilization [57]. Correlations between LMW PAHs in lakes and soils and 1-day overland air originating from ROI and NI ($R = 0.88$ and 0.89, resp.) further suggest local combustion sources, supporting the higher concentrations measured in the eastern-southeastern sites. Back trajectory analysis showed higher proportions of 1-day overland air originating from ROI and NI at CLE (21.1%) and SGI (17.6%) compared with CUM (9.6%), ADA (9.2%), and MUL (10.9% (Figure 2 and Supporting Information Figure SI-1 available online at doi:10.1100/2012/828343)).

3.5. Principal Component Analysis. The PCA (Figure 5) illustrated codistributed parameters (lake characteristics, and lake and soil PAH concentrations) and their relation to the five study sites. The ordination did not separate compounds with similar concentrations among sites; however, the ordination was strongly influenced by the high concentrations of some compounds at SGI. Component 1 (PC1), which described 41% of the variability in the parameters, was
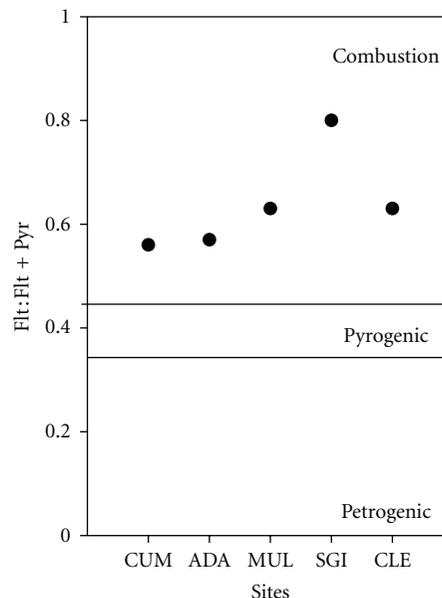
Figure 4: Ratios of Fluoranthene : Fluoranthene + Pyrene in soils and potential emission sources for the study catchments (Lough Cummeenoughter (CUM), Lough Adanacleveen (ADA), Mullincrick Lough (MUL), Sgilloge Lough (SGI), and Cleevaun Lough (CLE)).

most highly influenced by Fe lake concentration (positively), and lake : catchment ratio and DO (negatively). Positive correlations with PC1 were observed for HMW compounds (soil and water) and LMW compounds (water). Component 2 (PC2), which described 28% of the variability in the parameters, was characterized by positive loadings for TOC, SOM, Al lake concentrations and Fe soil concentrations as well as negative loadings from pH (soil and water), and rainfall. Positive correlations with the PC2 axis were seen for LMW PAHs in soil (e.g., Naphthalene, Anthracene, and Fluorene), indicating their codistribution with organic matter and potentially reduced leaching rates with less precipitation. Component 3 (PC3, ~23% (not shown)), was most strongly influenced by the proportion of 1-day overland air, nonmarine SO_4^{2-}, and elevation (positively) and conductivity and water temperature (negatively). Acenaphthene, Fluorene, and Anthracene in lakes were positively correlated with this axis indicating their codistribution and association with the eastern-most sites (CLE and SGI) and therefore 1-day overland air, which was significantly correlated with anthropogenic emissions.

4. Conclusion

Although higher concentrations were observed at the south-eastern-most site (SGI), the results suggest that upland semi-natural headwater catchments in Ireland are representative of midlatitude background regions (>200 ng g^{-1}; [1]), owing to the low levels of PAHs (solely from atmospheric deposition). Furthermore, PAH concentrations were well within, or below, the range of "background" values observed in
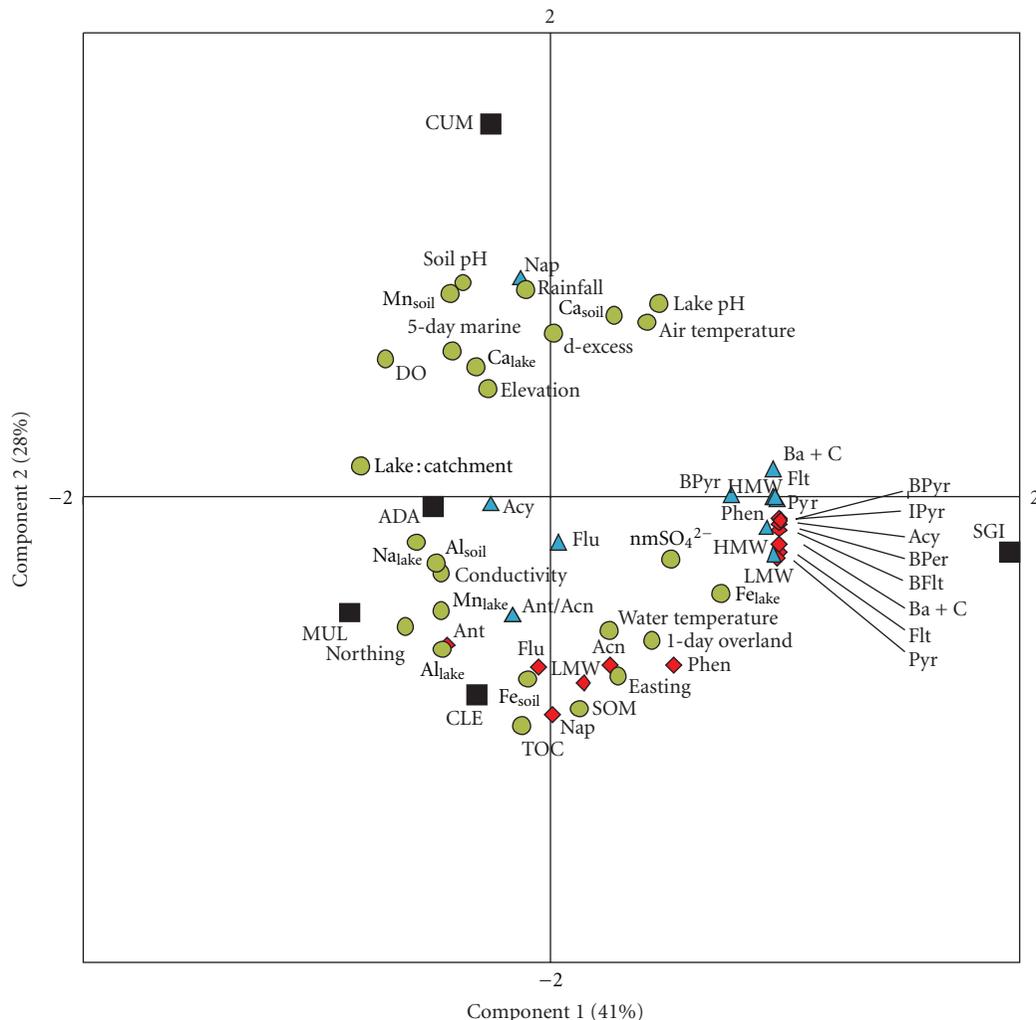
FIGURE 5: Principle component analysis (PCA) showing study catchments (black-filled square), lake characteristics (green-filled circles), lake PAH concentrations (blue-filled triangles), and soil PAH concentrations (red-filled diamonds). PC1 (41%), PC2 (28%), and PC3 ((not shown) 23%). Study sites: Lough Cummeenoughter (CUM), Lough Adanacleveen (ADA), Mullincrick Lough (MUL), Sgilloge Lough (SGI), and Cleevaun Lough (CLE).

continental Europe and internationally. Airshed movement and SOM strongly influenced the fate and transport of PAHs in headwater lakes in Ireland. Individual site physical, meteorological, and chemical parameters exhibited correlations with PAHs in SPMDs and soil samples, for example, lake : catchment ratio, rainfall, TOC, and source air, which highlighted the propensity of some compounds to washout, bind to organic matter, or undergo atmospheric transport. Further, Fluoranthene : Fluoranthene + Pyrene ratios suggested that wood, coal, and grass combustion were the primary source of PAH to the study sites. Media partitioning was evident in the study catchments; that is, even in highly organic soils, Naphthalene has a tendency to revolatilize or washout more readily and is more likely to be captured in SPMDs, whereas "heavier" HMW compounds bind to soil and sediments.

Although the responses of individual PAHs in water are well known [58], few studies have been conducted in Ireland.

This study is the first catchment-based study to quantify PAHs in soils in combination with lake waters (using passive sampling techniques). It provides baseline data for future research and also provides a reference for other land-covers (e.g., urban, industrial, etc.). The vulnerability of PAHs to climate change should be investigated (i.e., [59, 60]). Increasing levels of DOC, altered hydrological processes, and land use changes may ultimately influence the release of long-term stores from organic-rich soils [61], which may have profound effects on PAH cycling in ecosystems. In particular, the breakdown of SOM leading to increased DOC in surface waters [62] will influence the remobilization of these compounds from their peaty reservoirs into the surrounding environment.

Conflict of Interests

The authors declare that no competing interests exist.

Acknowledgments

References

[1] W. Wilcke, "Polycyclic aromatic hydrocarbons (PAHs) in soil—a review," *Journal of Plant Nutrition and Soil Science*, vol. 163, no. 3, pp. 229–248, 2000.

[2] R. A. Hites, R. E. Laflamme, and J. W. Farrington, "Sedimentary polycyclic aromatic hydrocarobons: the historical record," *Science*, vol. 198, no. 4319, pp. 829–831, 1977.

[3] P. Fernández, R. M. Vilanova, C. Martínez, P. Appleby, and J. O. Grimalt, "The historical record of atmospheric pyrolytic pollution over Europe registered in the sedimentary PAH from remote mountain lakes," *Environmental Science and Technology*, vol. 34, no. 10, pp. 1906–1913, 2000.

[4] N. L. Rose and B. Rippey, "The historical record of PAH, PCB, trace metal and fly-ash particle deposition at a remote lake in north-west Scotland," *Environmental Pollution*, vol. 117, no. 1, pp. 121–132, 2002.

[5] S. Usenko, S. L. M. Simonich, K. J. Hageman et al., "Sources and deposition of polycyclic aromatic hydrocarbons to western U.S. national parks," *Environmental Science and Technology*, vol. 44, no. 12, pp. 4512–4518, 2010.

[6] X. Wang, H. Yang, P. Gong et al., "One century sedimentary records of polycyclic aromatic hydrocarbons, mercury and trace elements in the Qinghai Lake, Tibetan Plateau," *Environmental Pollution*, vol. 158, no. 10, pp. 3065–3070, 2010.

[7] C. Bogdal, T. D. Bucheli, T. Agarwal et al., "Contrasting temporal trends and relationships of total organic carbon, black carbon, and polycyclic aromatic hydrocarbons in rural low-altitude and remote high-altitude lakes," *Journal of Environmental Monitoring*, vol. 13, no. 5, pp. 1316–1326, 2011.

[8] A. Ribes, J. O. Grimalt, C. J. Torres García, and E. Cuevas, "Polycyclic aromatic hydrocarbons in mountain soils of the subtropical Atlantic," *Journal of Environmental Quality*, vol. 32, no. 3, pp. 977–987, 2003.

[9] F. Wania, "On the origin of elevated levels of persistent chemicals in the environment," *Environmental Science and Pollution Research*, vol. 6, no. 1, pp. 11–19, 1999.

[10] P. Masclet, M. A. Bresson, and G. Mouvier, "Polycyclic aromatic hydrocarbons emitted by power stations, and influence of combustion conditions," *Fuel*, vol. 66, no. 4, pp. 556–562, 1987.

[11] N. T. Edwards, "Polycyclic aromatic hydrocarbons (PAH's) in the terrestrial environment—a review," *Journal of Environmental Quality*, vol. 12, no. 4, pp. 427–441, 1983.

[12] P. Gramatica, F. Consolaro, and S. Pozzi, "QSAR approach to POPs screening for atmospheric persistence," *Chemosphere*, vol. 43, no. 4-7, pp. 655–664, 2001.

[13] K. Nikolaou, P. Masclet, and G. Mouvier, "Sources and chemical reactivity of polynuclear aromatic hydrocarbons in the atmosphere—a critical review," *Science of the Total Environment*, vol. 32, no. 2, pp. 103–132, 1984.

[14] J. M. Blais, D. W. Schindler, D. C. G. Muir, L. E. Kimpe, D. B. Donald, and B. Rosenberg, "Accumulation of persistent organochlorine compounds in mountains of western Canada," *Nature*, vol. 395, no. 6702, pp. 585–588, 1998.

[15] C. E. Boström, P. Gerde, A. Hanberg et al., "Cancer risk assessment, indicators, and guidelines for polycyclic aromatic hydrocarbons in the ambient air," *Environmental Health Perspectives*, vol. 110, no. 3, pp. 451–488, 2002.

[16] L. A. Kapustka, "Establishing Eco-SSLs for PAHs: lessons revealed from a review of literature on exposure and effects to terrestrial receptors," *Human and Ecological Risk Assessment*, vol. 10, no. 2, pp. 185–205, 2004.

[17] Met Éireann, "Wind over Ireland," The Irish Meteorological Service Online, Glasnevin Hill, Dublin, Ireland, 2012, http://www.met.ie/climate/wind.asp.

[18] B. O'Dwyer and D. Taylor, "Paleolimnological evidence of variations in deposition of atmosphere-borne Polycyclic Aromatic Hydrocarbons (PAHs) in Ireland," *Chemosphere*, vol. 77, no. 10, pp. 1374–1380, 2009.

[19] S. Leinert, F. McGovern, and S. G. Jennings, *New Transboundary Air Pollution Monitoring Capacity for Ireland*, Environmental Research Centre Report Series no.10, Environmental Protection Agency, Wexford, Ireland, 2008.

[20] A. W. Burton and J. Aherne, "Changes in the chemistry of small irish lakes," *Ambio*, vol. 41, pp. 170–179, 2012.

[21] D. Fitzgerald and F. Forrestal, *Monthly and Annual Averages of Rainfall 1961–1990*, Meteorological Service, Climatological Note no. 10, 1996.

[22] J. N. Huckins, G. K. Manuweera, J. D. Petty, D. Mackay, and J. A. Lebo, "Lipid-containing semipermeable membrane devices for monitoring organic contaminants in water," *Environmental Science and Technology*, vol. 27, no. 12, pp. 2489–2496, 1993.

[23] S. O'Toole, C. Metcalfe, I. Craine, and M. Gross, "Release of persistent organic contaminants from carcasses of Lake Ontario Chinook salmon (Oncorhynchus tshawytscha)," *Environmental Pollution*, vol. 140, no. 1, pp. 102–113, 2006.

[24] D. A. Alvarez, M. R. Rosen, S. D. Perkins, W. L. Cranor, V. L. Schroeder, and T. L. Jones-Lepp, "Bottom sediment as a source of organic contaminants in Lake Mead, Nevada, USA," *Chemosphere*, vol. 88, pp. 605–611, 2012.

[25] T. L. Metcalfe, P. J. Dillon, and C. D. Metcalfe, "Detecting the transport of toxic pesticides from golf courses into watersheds in the precambrian shield region of Ontario, Canada," *Environmental Toxicology and Chemistry*, vol. 27, no. 4, pp. 811–818, 2008.

[26] T. L. Metcalfe, C. D. Metcalfe, E. R. Bennett, and G. D. Haffner, "Distribution of toxic organic contaminants in water and sediments in the Detroit River," *Journal of Great Lakes Research*, vol. 26, no. 1, pp. 55–64, 2000.

[27] S. N. Meijer, E. Steinnes, W. A. Ockenden, and K. C. Jones, "Influence of environmental variables on the spatial distribution of PCBs in Norwegian and U.K. soils: implications for global cycling," *Environmental Science and Technology*, vol. 36, no. 10, pp. 2146–2153, 2002.

[28] W. Dansgaard, "Stable isotopes in precipitation," *Tellus*, vol. 16, pp. 436–468, 1964.

[29] C. J. Whitfield, J. Aherne, and H. M. Baulch, "Controls on greenhouse gas concentrations in polymictic headwater lakes in Ireland," *Science of the Total Environment Journal*, vol. 410-411, pp. 217–225, 2011.

[30] C. D. Metcalfe, P. A. Beddows, G. G. Bouchot, T. L. Metcalfe, H. Li, and H. Van Lavieren, "Contaminants in the coastal

karst aquifer system along the Caribbean coast of the Yucatan Peninsula, Mexico," *Environmental Pollution*, vol. 159, no. 4, pp. 991–997, 2011.

[31] D. P. Dee, S. M. Uppala, A. J. Simmons et al., "The ERA-Interim reanalysis: configuration and performance of the data assimilation system," *Quarterly Journal of the Royal Meteorological Society*, vol. 137, no. 656, pp. 553–597, 2011.

[32] J. N. Huckins, J. D. Petty, and K. Booij, *Monitors of Organic Chemicals in The Environment—Semipermeable Membrane Devices*, Springer, New York, NY, USA, 2006.

[33] W. L. Cranor, D. A. Alvarez, J. N. Huckins, and J. D. Petty, "Uptake rate constants and partition coefficients for vapor phase organic chemicals using semipermeable membrane devices (SPMDs)," *Atmospheric Environment*, vol. 43, no. 20, pp. 3211–3219, 2009.

[34] D. A. Alvarez, *Use of the Semipermeable Membrane Device (SPMD) and the Polar Organic Chemical Integrative Sampler (POCIS) in Environmental Monitoring Studies*, U.S. Geological Survey, Techniques and Methods 1–D4, 2010.

[35] D. A. Alvarez, Estimated Water Concentration Calculator from SPMD Data Using Multiple PRCs: Version 5.1. Microsoft Excel spreadsheet, 2010, http://www.cerc.usgs.gov/Branches.aspx?BranchId=8.

[36] H. F. Kaiser, "The application of electronic computers to factor analysis," *Educational and Psychological Measurement*, vol. 20, pp. 141–151, 1960.

[37] F. Mitchell, "The impact of grazing and human disturbance on the dynamics of woodland in SW Ireland," *Journal of Vegetation Science*, vol. 1, pp. 245–254, 1990.

[38] M. Mandalakis, O. Gustafsson, T. Alsberg et al., "Contribution of biomass burning to atmospheric polycyclic aromatic hydrocarbons at three european background sites," *Environmental Science and Technology*, vol. 39, no. 9, pp. 2976–2982, 2005.

[39] J. Djedjibegovic, A. Marjanovic, M. Sober et al., "Levels of persistent organic pollutants in the Neretva River (Bosnia and Herzegovina) determined by deployment of semipermeable membrane devices (SPMD)," *Journal of Environmental Science and Health B*, vol. 45, no. 2, pp. 128–136, 2010.

[40] R. Vilanova, P. Fernández, C. Martínez, and J. O. Grimalt, "Organochlorine pollutants in remote mountain lake waters," *Journal of Environmental Quality*, vol. 30, no. 4, pp. 1286–1295, 2001.

[41] P. Fernández, G. Carrera, and J. O. Grimalt, "Persistent organic pollutants in remote freshwater ecosystems," *Aquatic Sciences*, vol. 67, no. 3, pp. 263–273, 2005.

[42] L. Guzzella, G. Poma, A. De-Paolis, C. Roscioli, and G. Viviano, "Organic persistent toxic substances in soils, waters and sediments along an altitudinal gradient at Mt. Sagarmatha, Himalayas, Nepal," *Environmental Pollution*, vol. 159, pp. 2552–2564, 2011.

[43] B. Gevao, J. Hamilton-Taylor, and K. C. Jones, "Polychlorinated biphenyl and polycyclic aromatic hydrocarbon deposition to and exchange at the air-water interface of Esthwaite Water, a small lake in Cumbria, UK," *Environmental Pollution*, vol. 102, no. 1, pp. 63–75, 1998.

[44] C. L. Gigliotti, P. A. Brunciak, J. Dachs et al., "Air-water exchange of polycyclic aromatic hydrocarbons in the New York-New Jersey, USA, Harbor Estuary," *Environmental Toxicology and Chemistry*, vol. 21, no. 2, pp. 235–244, 2002.

[45] J. N. Huckins, J. D. Petty, C. E. Orazio et al., "Determination of uptake kinetics (sampling rates) by lipid-containing semipermeable membrane devices (SPMDs) for polycyclic aromatic hydrocarbons (PAHs) in water," *Environmental Science and Technology*, vol. 33, no. 21, pp. 3918–3923, 1999.

[46] G. Guggenberger, M. Pichler, R. Hartmann, and W. Zech, "Polycyclic aromatic hydrocarbons in different forest soils: mineral horizons," *Zeitschrift fur Pflanzenernahrung und Bodenkunde*, vol. 159, no. 6, pp. 565–573, 1996.

[47] J. J. Nam, A. J. Sweetman, and K. C. Jones, "Polynuclear aromatic hydrocarbons (PAHs) in global background soils," *Journal of Environmental Monitoring*, vol. 11, no. 1, pp. 45–48, 2009.

[48] P. Fernández and J. O. Grimalt, "On the global distribution of persistent organic pollutants," *Chimia*, vol. 57, no. 9, pp. 514–521, 2003.

[49] R. Quiroz, J. O. Grimalt, P. Fernandez et al., "Polycyclic aromatic hydrocarbons in soils from European high mountain areas," *Water, Air, and Soil Pollution*, vol. 215, no. 1–4, pp. 655–666, 2011.

[50] R. Barra, P. Popp, R. Quiroz, C. Bauer, H. Cid, and W. V. Tümpling, "Persistent toxic substances in soils and waters along an altitudinal gradient in the Laja River Basin, Central Southern Chile," *Chemosphere*, vol. 58, no. 7, pp. 905–915, 2005.

[51] S. D. Choi, C. Shunthirasingham, G. L. Daly, H. Xiao, Y. D. Lei, and F. Wania, "Levels of polycyclic aromatic hydrocarbons in Canadian mountain air and soil are controlled by proximity to roads," *Environmental Pollution*, vol. 157, no. 12, pp. 3199–3206, 2009.

[52] G. L. Daly, Y. D. Lei, L. E. Castillo, D. C. G. Muir, and F. Wania, "Polycyclic aromatic hydrocarbons in Costa Rican air and soil: a tropical/temperate comparison," *Atmospheric Environment*, vol. 41, no. 34, pp. 7339–7350, 2007.

[53] R. K. Hitch and H. R. Day, "Unusual persistence of DDT in some Western USA soils," *Bulletin of Environmental Contamination and Toxicology*, vol. 48, no. 2, pp. 259–264, 1992.

[54] I. T. Cousins, B. Gevao, and K. C. Jones, "Measuring and modelling the vertical distribution of semi-volatile organic compounds in soils. I: PCB and PAH soil core data," *Chemosphere*, vol. 39, no. 14, pp. 2507–2518, 1999.

[55] Z. Wang, X. Ma, G. Na, Z. Lin, Q. Ding, and Z. Yao, "Correlations between physicochemical properties of PAHs and their distribution in soil, moss and reindeer dung at Ny-Ålesund of the Arctic," *Environmental Pollution*, vol. 157, no. 11, pp. 3132–3136, 2009.

[56] M. B. Yunker, R. W. Macdonald, R. Vingarzan, R. H. Mitchell, D. Goyette, and S. Sylvestre, "PAHs in the Fraser River basin: a critical appraisal of PAH ratios as indicators of PAH source and composition," *Organic Geochemistry*, vol. 33, no. 4, pp. 489–515, 2002.

[57] R. C. Sims and M. R. Overcash, "Fate of polynuclear aromatic compounds (PNAs) in soil-plant systems," *Residue Reviews*, vol. 88, pp. 1–68, 1983.

[58] J. N. Huckins, J. D. Petty, J. A. Lebo et al., "Development of the permeability/performance reference compound approach for in situ calibration of semipermeable membrane devices," *Environmental Science and Technology*, vol. 36, no. 1, pp. 85–91, 2002.

[59] J. Ma, H. Hung, C. Tian, and R. Kallenborn, "Revolatilization of persistent organic pollutants in the Arctic induced by climate change," *Nature Climate Change*, vol. 1, pp. 255–260, 2011.

[60] United Nations Environment Programme/Arctic Monitoring and Assessment Programme (UNEP/AMAP), "Climate change and POPs: predicting the impacts," 2011, http://chm.pops.int/Programmes/GlobalMonitoringPlan/ClimateChangeandPOPsPredictingtheImpacts/tabid/1580/language/en-US/Default.aspx.

[61] D. T. Monteith, J. L. Stoddard, C. D. Evans et al., "Dissolved organic carbon trends resulting from changes in atmospheric deposition chemistry," *Nature*, vol. 450, no. 7169, pp. 537–540, 2007.

[62] C. D. Evans, D. T. Monteith, and D. M. Cooper, "Long-term increases in surface water dissolved organic carbon: observations, possible causes and environmental impacts," *Environmental Pollution*, vol. 137, no. 1, pp. 55–71, 2005.

Research Article

Levels, Distribution, and Health Risks of Polycyclic Aromatic Hydrocarbons in Four Freshwater Edible Fish Species from the Beijing Market

Wen-Jing Wu, Ning Qin, Wei He, Qi-Shuang He, Hui-Ling Ouyang, and Fu-Liu Xu

MOE Laboratory for Earth Surface Processes, College of Urban and Environmental Sciences, Peking University, Beijing 100871, China

Correspondence should be addressed to Fu-Liu Xu, xufl@urban.pku.edu.cn

We first estimated the content of polycyclic aromatic hydrocarbons (PAHs) in the brain, liver, bladder, roe, and muscle of four species of edible freshwater fish from the Beijing market. The distribution characteristics of PAHs in these tissues and organs were analyzed to determine their health risks to humans. The results showed that the residual levels of wet weight and lipid-normalized weight $\sum$PAHs in various tissues of these fish ranged from $0.51\,\text{ng}\cdot\text{g}^{-1}$ to $28.78\,\text{ng}\cdot\text{g}^{-1}$ and from $93.62\,\text{ng}\cdot\text{g}^{-1}$ to $8203.43\,\text{ng}\cdot\text{g}^{-1}$, respectively. The wet weight contents of $\sum$PAHs were relatively higher in the brain and lower in the liver and muscle. But the differences were not significant. And the differences of lipid-normalized weight PAHs were significant, which in the bighead carp were found significantly the highest, followed in crucian carp, and the lowest in grass carp and carp. The contents of $\sum$PAHs were the highest in the liver and the lowest in the brain. In the tissues with a higher lipid content, higher residual levels of PAHs were found. The carcinogenic risks for humans from residual $\sum$PAHs in the various fish tissues were far below 10^{-5}.

1. Introduction

Polycyclic aromatic hydrocarbons (PAHs) are a typical form of persistent organic pollutants with a wide range of distribution in various environmental media in China, particularly in the northern part of the country [1]. The emission sources of PAHs in the environment mainly include fossil fuels, wood fuels [2–4], oil spills [5], and metal smelting, among others [6, 7]. Hydrophoby and low water-solubility are two typical characteristics of PAHs [8, 9]. In addition, lipid solubility, carcinogenicity, and mutagenicity will increase when the number of rings grows larger [10]. Although PAHs will rapidly degrade once they access the body of a fish [11], research has documented that residuals of PAHs were found in the tissues and organs of various species of fish [11, 12].

PAHs can affect human health through various routes of exposure, such as air, food, and water, as well as in- and outdoor ambient soil and dust; and the populations' Chronic Daily Intake (CDI) of PAHs through various routes mainly depends on the PAHs levels in exposure medium, the time-behavior patterns, and physiological characteristics of human bodies [1, 13–16]. It was reported that, in the United

States, the PAHs exposure through food consumptions accounted for 96% for the aged 19–50 nonsmokers [15]. In Montreal, Canada, the children's exposure to PAHs through food consumptions accounted for 93% to 97% [16]. However, in Tianjin, China, populations' exposure to PAHs through dietary intake, respiratory, and skin contact accounted approximately for 75%, 20%, and 5% of the total exposure, respectively [1]. These reports suggest that dietary intake is a predominant route of PAHs exposure to harm human health. Because fish plays a key role in the food chain in comparison to other types of food media of PAHs intake such as vegetables [17], it is a primary intermediary through which these pollutants access the human body, even though fish only constitutes approximately ten percent of the dietary intake of humans [18]. Therefore, the residual level of PAHs in fish, and particularly in edible fish, has a great effect on human health. This paper will estimate the content of PAHs in various tissues and organs of four commonly found edible fish species at the Beijing market. These fish tissues and organs, although not all harvested by all peoples across the world, are all ingested by the Chinese people to a larger or smaller extent, according to the dietary habit. In addition,

TABLE 1: Fish species and their characteristics collected from a local market in Beijing.

Common name	Scientific name	Feeding mode	Average length (cm)	Average weight (g)	Lipid contents
Crucian carp	*Carassius auratus*	Omnivorous	20	250	0.6%~22.5%
Bighead carp	*Aristichthys nobilis*	Filter feeder	34	750	0.6%~24.1%
Carp	*Cyprinus carpio*	Omnivorous	25	450	2.4%~35.0%
Grass carp	*Ctenopharyngodon idellus*	Herbivorous	34	650	2.9%~26.8%

we will show how the content is distributed in the tissues and organs of the fish and how it is distributed across the various species that we are studying. We will also discuss the potential risks for human health through an analysis of wet weight contents and lipid-normalized contents.

2. Materials and Methods

2.1. Sample Collection. 50 specimens from each of four commonly consumed freshwater fish species, namely, crucian carp (*Carassius auratus*), bighead carp (*Aristichthys nobilis*), carp (*Cyprinus carpio* L), and grass carp (*Ctenopharyngodon idellus*) were collected from the Yuegezhuang wholesale market, which is the largest aquatic product market in the Beijing region. Five tissues and organs from these specimens, including the brain, liver, bladder, roe, and a muscle mixture from the dorsal and chest were sampled. To eliminate individual diversity, tissues from five specimens of each species were combined into one sample. All of the samples were freeze-dried for three to four days after weighing and then preserved in the desiccator prior to analysis. The general physiological information of the fish is shown in Table 1.

2.2. Sample Pretreatment. The freeze-dried fish tissue samples, each weighing approximately 3 grams, were first ground with anhydrous sodium sulfate. The samples were then Soxhlet extracted with 100 mL of mixed solvent of dichloromethane and n-hexane (v : v, 4 : 1) for 24 h at 60°C. The extracted mixed solvent was then transformed into an n-hexane solvent and concentrated into 3 mL. The next step was the liquid-liquid extraction followed by Haruhiko's procedure [19]. The lipid content within the tissues and organs was measured using the quality-subtraction method. A silica gel column was used for the sample cleanup. The cleanup column was eluted with 50 mL of n-hexane followed by 50 mL of a 3 : 2 mixture of n-hexane and dichloromethane. The eluate collected from the silica column during cleanup was concentrated into 0.2 mL using a vacuum rotary evaporator. The samples were sealed in vials and stored at −4°C prior to analysis.

2.3. Sample Analysis. 16 priority PAHs identified by the USEPA including naphthalene (Nap), acenaphthylene (Acy), acenaphthene (Ace), fluorene (Flo), phenanthrene (Phe), anthracene (Ant), fluoranthene (Fla), pyrene (Pyr), chrysene (Chr), benzo[a]anthracene (BaA), benzo[b]fluoranthene (BbF), benzo[k]fluoranthene (BkF), benzo[a]pyrene (BaP), indeno[1,2,3-cd]pyrene (IcdP), benzo[ghi]perylene (BghiP), and dibenz[a,h]anthracene (DahA) were analyzed in this study. The analysis was conducted using an Agilent 6890 GC, coupled with an Agilent 5973 mass spectrometer and a 7683 autosampler (Agilent Technology). An HP-5 MS capillary column with 30 m × 0.25 mm × 0.25 μm film thickness was used. High-purity helium was used as the carrier gas. Samples of 1 μL were injected using the splitless mode at a flow rate of 1.0 mL/min. The temperatures of the injection port and ion source were maintained at 220°C and 280°C, respectively. GC temperature was programmed from an initial 60°C at 6°C/min up to 260°C, with a final holding time of 20 min. The mass spectrometer was operated in scan mode with an electron impact ionization of 70 eV. The quality range is from 45 to 600 amu, an electron multiplier voltage of 1288 V and an ion source at 280°C.

2.4. Quality Control. Prior to the sample analysis, a mixed stock standard with 16 PAHs (PAH-Mixture, 610/525/550, Chem. Service Co.) was used to make the standard curve with the concentration of 1 ppb, 10 ppb, 100 ppb, and 1000 ppb. The procedural blank was determined by going through the extraction and cleanup procedures using glass beads instead of fish samples. Recoveries of PAHs were determined by spiking fish samples with standards at both higher and lower concentrations. Recovery rates and detection limits (dry weight data and PAH content in freeze-dried samples of unit mass) for PAHs in fish samples are shown in Table 2. With regard to sample data that are lower than detection limits, one-third of this value was counted in the statistics (BkF is an exception because of its high detection limits, and therefore detected value was used). Dry weight content was transformed into wet weight content and lipid-normalized content (dry weight content divided by the percentage of lipid in the dry weight sample).

2.5. Data Processing. The software used was SPSS 13.0. The Shapiro-Wilk test was used to estimate data normality, under which we found that PAH data from the wet weight basis fit neither normal distribution nor logarithmic normal distribution. Moreover, PAH data from the lipid-normalized weight basis did not fit into the normal distribution but it did, to an extent, present as a logarithmic normal distribution. A log-transformation was performed to ensure the normality of the distribution of data in all tissues. A two-way ANOVA (analysis of variance) was conducted to detect differences in data among tissues and species. The relationship between the data was determined by Pearson's sample correlation, and when the value of P was below 0.05, the linear regression was regarded as significant.

Table 2: Recovery rates and detection limits for PAHs in fish samples.

|	Nap	Ace	Acy	Flo	Phe	Ant	Fla	Pyr	BaA	Chr	BbF	BkF	BaP	DahA	IcdP	BghiP
Recovery rates	63.7%	90.0%	97.8%	116.0%	114.0%	124.3%	139.8%	145.5%	140.5%	108.6%	138.7%	133.4%	149.6%	132.6%	130.9%	119.6%
Detection limits (ng·g^{-1})	1.02	0.61	0.65	0.65	0.60	0.41	0.38	0.38	0.51	0.70	1.14	0.39	0.45	0.30	0.48	0.34
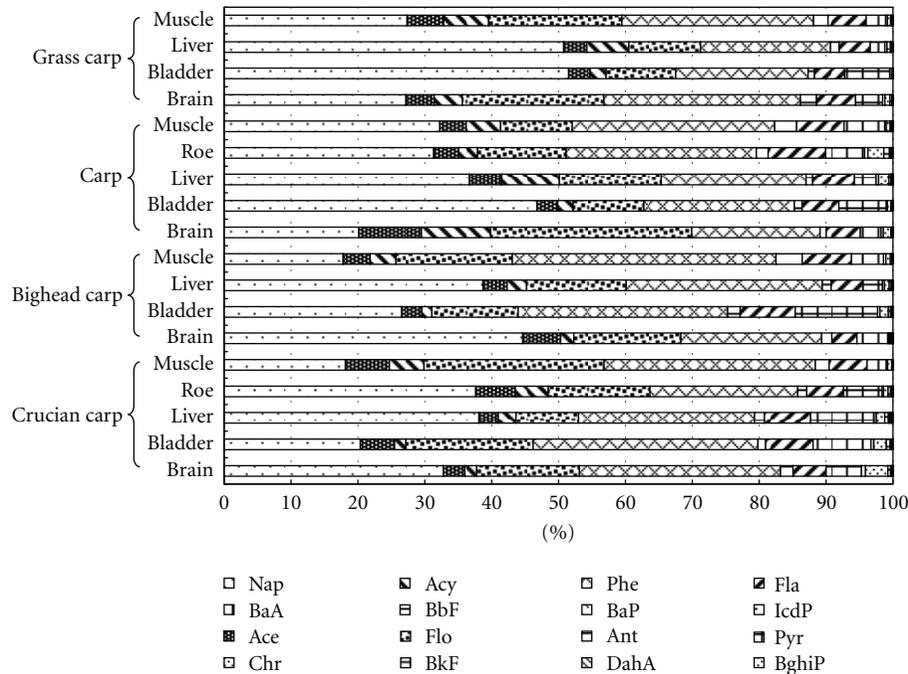
Figure 1: Percentage composition of 16 priority PAHs congeners in the fish from Beijing market.

3. Results

3.1. Wet Weight Contents and Composition Patterns of 16 Types of PAHs. Residual levels of sixteen types of PAHs ($\sum$PAHs) on a wet weight basis in various tissues of the four types of fish species ranged from $0.51\,\text{ng}\cdot\text{g}^{-1}$ to $28.78\,\text{ng}\cdot\text{g}^{-1}$, with a mean of $10.17 \pm 0.67\,\text{ng}\cdot\text{g}^{-1}$. Figures 1 and 2 show percentages and contents of all sixteen types of PAHs in various tissues of the four fish species, respectively. Low molecular weight PAHs (LMWPAHs) with two or three rings (Nap, Acy, Ace, Flo, Phe, Ant, Fla) took the largest share as 85.4%~96.6%. The proportion of middle molecular weight PAHs (MMWPAHs) with four rings (Pyr, BaA, Chr, BbF, BkF) ranged from 3.3% to 14.4%; Pyr dominated this segment with a share of 2.2% to 12.3%. High molecular weight PAHs (HMWPAHs) with five rings (BaP, IcdP, DahA, BghiP) only accounted for a share of approximately 0 to 0.5 percent. Residual levels of Nap, Flo, and Phe were high in the tissues of the various species, of which Nap measured approximately 32%, Phe approximately 27%, and Flo approximately 17%. Correlational studies also found that the main forms of PAH residuals in living creatures in general were PAHs with two or three rings [18, 20–22]. By contrast, general residual levels of PAHs with four rings were lower and those of PAHs with five rings were extremely low. For example, the proportion of low molecular weight PAHs, middle molecular weight PAHs, and high molecular weight PAHs residuals in fish from Italy (Adriatic Sea) were 62%, 37%, and 1%, respectively [23]. A similar tendency in the levels of PAHs residuals was also found by Binelli [18] in research on European shellfish. Vives found that Phe contents in salmon liver from lakes in Europe and Greenland were as high as 52% [11]. He also found high levels of Phe

residuals in various environmental media, such as water, suspended matter, and deposit sediment.

The content of Nap, Flo, and Phe in various tissues of all four species in our study is relatively high, as shown in Figure 2, with the exception of the crucian carp liver. The distribution of Nap varied significantly among different tissues, ranging from $1.1\,\text{ng}\cdot\text{g}^{-1}$~$7.2\,\text{ng}\cdot\text{g}^{-1}$ and was generally lower in the muscle. Flo levels were higher in the brain than in other tissues ($2.0\,\text{ng}\cdot\text{g}^{-1}$~$3.5\,\text{ng}\cdot\text{g}^{-1}$). With regard to the levels of Phe content, higher values were in the brain of crucian carp, bighead carp, and grass carp and in the bladder of carp ($3.5\,\text{ng}\cdot\text{g}^{-1}$~$6.0\,\text{ng}\cdot\text{g}^{-1}$). The contents of PAHs in the liver of crucian carp were significantly lower than in other tissues. Residual levels of Chr were the highest among all the four ring PAHs ($0.03\,\text{ng}\cdot\text{g}^{-1}$~$0.66\,\text{ng}\cdot\text{g}^{-1}$). However, residual levels of HMWPAHs were extremely low.

In comparison with similar studies, the wet weight PAH16 contents in the freshwater fish of this study are lower than those found in most other studies, with a mean level of $10.17\,\text{ng}\cdot\text{g}^{-1}$ ranging from $0.51\,\text{ng}\cdot\text{g}^{-1}$ to $28.78\,\text{ng}\cdot\text{g}^{-1}$. For instance, the levels of PAH on a wet weight basis were found to range from $19.7\,\text{ng}\cdot\text{g}^{-1}$ to $154.3\,\text{ng}\cdot\text{g}^{-1}$ in Bolti fish and mallet fish collected from markets in Ismailia city, Egypt [12]. The contents of $\sum$PAHs in fish from Lake Victory in Africa were between of $0.035\,\text{ng}\cdot\text{g}^{-1}$ and $3.934\,\text{ng}\cdot\text{g}^{-1}$ [24]. And $\sum$PAHs contents in Mullus barbatus from the Sicily Channel in Italy had a mean of $26.47\,\text{ng}\cdot\text{g}^{-1} \pm 34.16\,\text{ng}\cdot\text{g}^{-1}$ [25]. In China, PAHs content levels in the freshwater and marine fish collected from the Hong Kong market varied from $15.5\,\text{ng}\cdot\text{g}^{-1}$ to $118\,\text{ng}\cdot\text{g}^{-1}$ (ww) [26], while PAHs content levels in freshwater fish from the Pearl River delta were 30.94–410.06 ng$\cdot$g^{-1} (ww) [27].
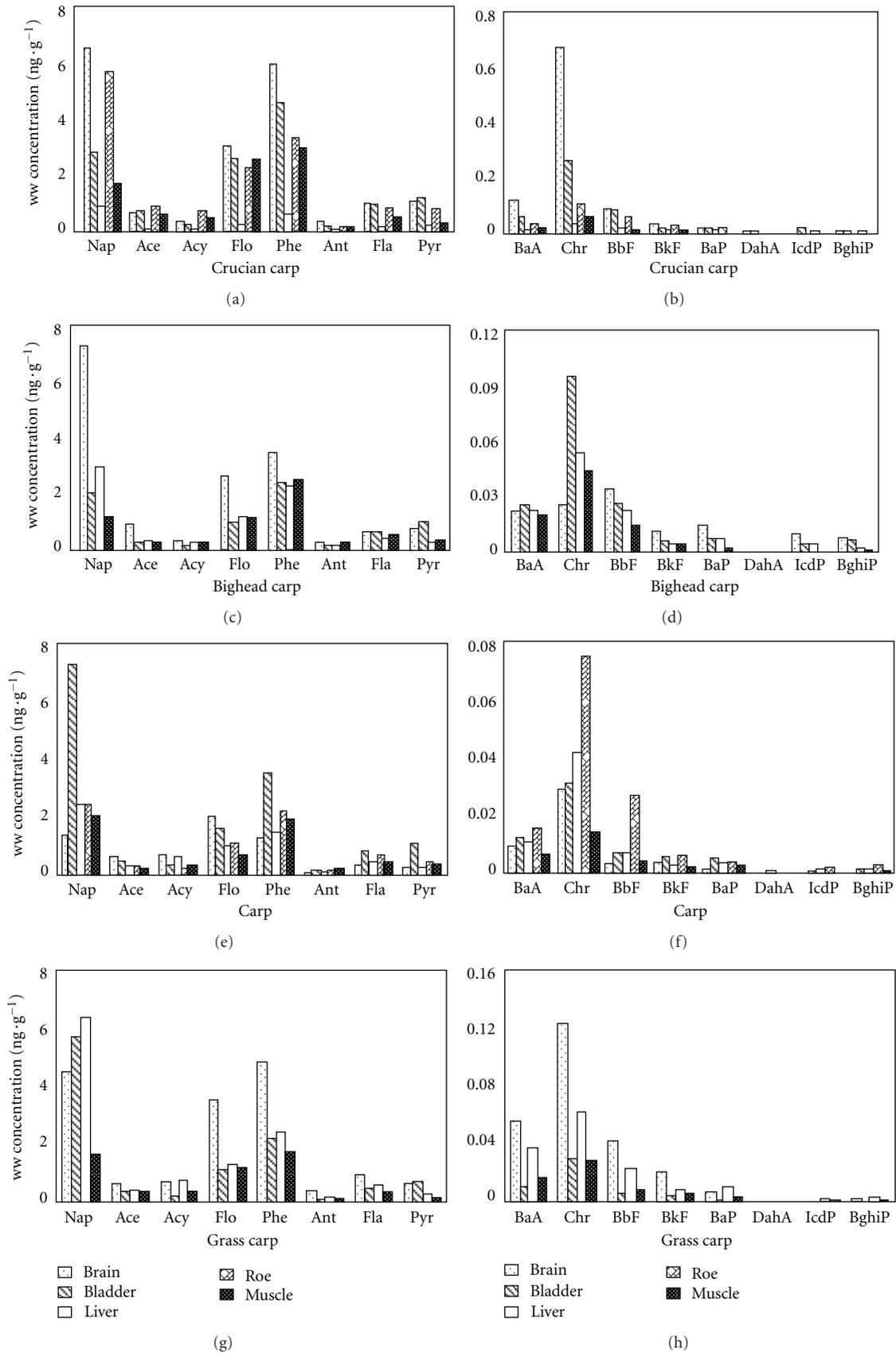
FIGURE 2: Distribution pattern of PAH congeners in the tissues and organs of four fish species.

Table 3: Residual levels of PAHs (wet weight) (ng·g^{-1}) in freshwater fish samples.

PAHs	Species	Brain	Bladder	Liver	Roe	Muscle
$\sum$PAHs	Crucian carp	19.77 ± 4.71	13.63	2.28 ± 1.65	14.90 ± 9.33	9.40 ± 1.94
	Bighead carp	16.10 ± 9.59	7.52 ± 1.65	7.63 ± 2.63	—[b]	6.26 ± 0.62
	Carp	6.65 ± 1.71	15.46 ± 2.33	6.74 ± 1.82	7.84 ± 2.28	6.34 ± 1.63
	Grass carp	16.50 ± 4.80	11.01 ± 5.22	12.57 ± 2.47	—	6.13 ± 0.62
LMWPAHs	Crucian carp	17.81 ± 5.74	12.00	2.01 ± 1.41	13.79 ± 8.81	9.04 ± 1.78
	Bighead carp	15.24 ± 9.01	6.42 ± 0.97	7.29 ± 2.53	—	5.87 ± 0.47
	Carp	6.32 ± 1.70	14.21 ± 2.16	6.35 ± 1.78	7.06 ± 2.12	5.87 ± 1.53
	Grass carp	15.58 ± 4.34	10.22 ± 4.78	12.14 ± 2.44	—	5.89 ± 0.73
MMWPAHs	Crucian carp	1.93 ± 1.12	1.59	0.27 ± 0.25	1.06 ± 0.53	0.37 ± 0.16
	Bighead carp	0.84 ± 0.59	1.08 ± 0.77	0.33 ± 0.11	—	0.38 ± 0.17
	Carp	0.33 ± 0.017	1.23 ± 0.78	0.38 ± 0.081	0.76 ± 0.19	0.46 ± 0.093
	Grass carp	0.91 ± 0.54	0.80 ± 0.51	0.41 ± 0.096	—	0.25 ± 0.17
HMWPAHs	Crucian carp	0.033 ± 0.031	0.03	0.005 ± 0.01	0.027 ± 0.015	0.0025 ± 0.005
	Bighead carp	0.033 ± 0.017	0.018 ± 0.015	0.01 ± 0.00	—	0.0025 ± 0.005
	Carp	0.0025 ± 0.005	0.015 ± 0.013	0.01 ± 0.0082	0.028 ± 0.005	0.01 ± 0.00
	Grass carp	0.008 ± 0.0084	0.00 ± 0.00	0.013 ± 0.0082	—	0.0033 ± 0.0052

[a]Levels of PAHs are presented as mean ± standard deviation.
[b]"—" means no samples were collected.

3.2. PAHs Distribution in Various Fish Tissues on a Wet Weight Basis.

The mobility of PAHs in the environment is normally determined by molecular weight. Related researches have shown that the mobility of low molecular weight PAHs in the atmosphere is relatively higher than that of middle and high molecular weight PAHs [28, 29]. However, middle and high molecular weight PAHs usually have higher carcinogenicity and mutagenicity [28, 29]. Considering this, we categorized PAHs by the number of their rings. PAHs with two or three rings are defined as low molecular weight PAHs (LMWPAHs). Those PAHs with four rings belong to middle molecular weight PAHs (MMWPAHs), and those with five rings belong to high molecular weight PAHs (HMWPAHs). Residual levels of PAHs on a wet weight basis in various fish tissues are illustrated in Table 3.

The distribution of LMWPAHs and total PAHs share a similar pattern, as shown in Figure 3. Residual levels of PAHs on a wet weight basis were found slightly higher in crucian carp and grass carp and relatively lower in bighead carp and carp. Nevertheless, the variances of PAHs residuals on a wet weight basis among the species studied were not wide. The distribution of MMWPAHs on a wet weight basis was found higher in crucian carp and was approximately equal in the other three species. A decreasing pattern of HMWPAHs distribution was found among crucian carp, bighead carp, carp, and grass carp, respectively. However, these differences were not significant at a 95% confidence level ($P > 0.05$), under the two-way ANOVA.

Residual PAH levels in various tissues are shown in Figure 4. The distribution of total PAHs and LMWPAHs was found to be highest in the brain, lower in the bladder and roe, and the lowest was found in the liver and muscle. With regard to the distribution of MMWPAHs, the highest levels of content were found in the bladder, lower levels in the brain and roe, and the lowest were found in the liver and

Table 4: ANOVA results of wet weight-based PAH contents.

PAHs		Square	F value	Sig.
$\sum$PAHs	Species	44.93	1.81	0.154
	Tissues and organs	161.31	6.51	0.000
LMWPAHs	Species	42.26	1.90	0.138
	Tissues and organs	132.40	5.96	0.000
MMWPAHs	Species	0.44	1.84	0.150
	Tissues and organs	1.85	7.80	0.000
HMWPAHs	Species	0.00033	2.21	0.095
	Tissues and organs	0.00072	4.78	0.002

muscle. Finally, the distribution of HMWPAHs was found to be highest in the roe, lower in the brain, and the lowest was found in the bladder, liver, and muscle. The result of the two-way ANOVA is shown in Table 4, which showed that residual levels of PAHs on a wet weight basis were tested to be significant under a 95% confidence level ($P < 0.05$).

3.3. PAH Distribution in Various Fish Tissues on a Lipid-Normalized Weight Basis.

The distribution of sixteen types of PAHs in various fish tissues on a lipid-normalized weight basis shown in Table 5 ranges from 93.62 ng·g^{-1} to 8203.43 ng·g^{-1}, with a mean value of 1204.18 ng·g^{-1} ± 144.16 ng·g^{-1}. Figure 5 shows the differences on a lipid-normalized weight basis of the various species. Residual levels of PAHs on a lipid-normalized weight basis were found to be highest in bighead carp, lower in crucian carp, and the lowest in carp and grass carp. The distribution of total PAHs, LMWPAHs, and MMWPAHs shared similar patterns. According to the two-way ANOVA results (Table 6), the residual level of PAHs on a wet weight basis was tested to be significant under a 95% confidence level ($P < 0.05$).

TABLE 5: Residual levels of PAHs (lipid normalized) (ng·g^{-1} lw) in freshwater fish samples.

PAHs	Species	Brain	Bladder	Liver	Roe	Muscle
$\sum$PAHs	Crucian carp	685.92 ± 163.49	1233.83	2168.78 ± 1566.04	1469.73 ± 920.61	1496.40 ± 308.88
	Bighead carp	523.01 ± 311.46	2281.04 ± 500.70	6593.50 ± 2276.79	—	2317.51 ± 228.61
	Carp	148.35 ± 38.20	665.95 ± 100.33	394.66 ± 106.71	527.30 ± 153.16	1230.44 ± 315.89
	Grass carp	81.78 ± 140.27	762.68 ± 361.76	967.79 ± 190.42	—	101.36 ± 100.69
LMWPAHs	Crucian carp	617.55 ± 199.01	1086.74	1901.88 ± 1329.31	1361.42 ± 869.41	1438.56 ± 283.38
	Bighead carp	494.86 ± 292.80	1947.79 ± 293.57	6297.75 ± 2188.34	—	2174.14 ± 172.63
	Carp	141.12 ± 38.06	612.17 ± 93.25	371.90 ± 104.54	474.34 ± 142.55	1140.44 ± 297.25
	Grass carp	454.95 ± 126.86	707.60 ± 331.12	934.95 ± 187.91	—	961.22 ± 118.39
MMWPAHs	Crucian carp	67.21 ± 38.66	143.36	255.98 ± 242.39	105.40 ± 52.52	57.43 ± 26.44
	Bighead carp	27.08 ± 19.06	327.50 ± 234.74	283.10 ± 87.72	—	141.96 ± 59.88
	Carp	7.13 ± 0.39	53.10 ± 33.71	21.87 ± 4.45	51.38 ± 12.68	88.17 ± 18.53
	Grass carp	26.54 ± 15.72	54.95 ± 35.39	31.52 ± 7.52	—	39.27 ± 27.54
HMWPAHs	Crucian carp	1.17 ± 0.73	3.73	10.92 ± 5.54	2.91 ± 1.50	0.42 ± 0.60
	Bighead carp	1.07 ± 0.49	5.74 ± 2.53	12.65 ± 0.74	—	1.41 ± 1.53
	Carp	0.10 ± 0.049	0.68 ± 0.49	0.89 ± 0.43	1.59 ± 0.26	1.82 ± 0.36
	Grass carp	0.29 ± 0.29	0.12 ± 0.095	1.32 ± 0.64	—	0.87 ± 1.35
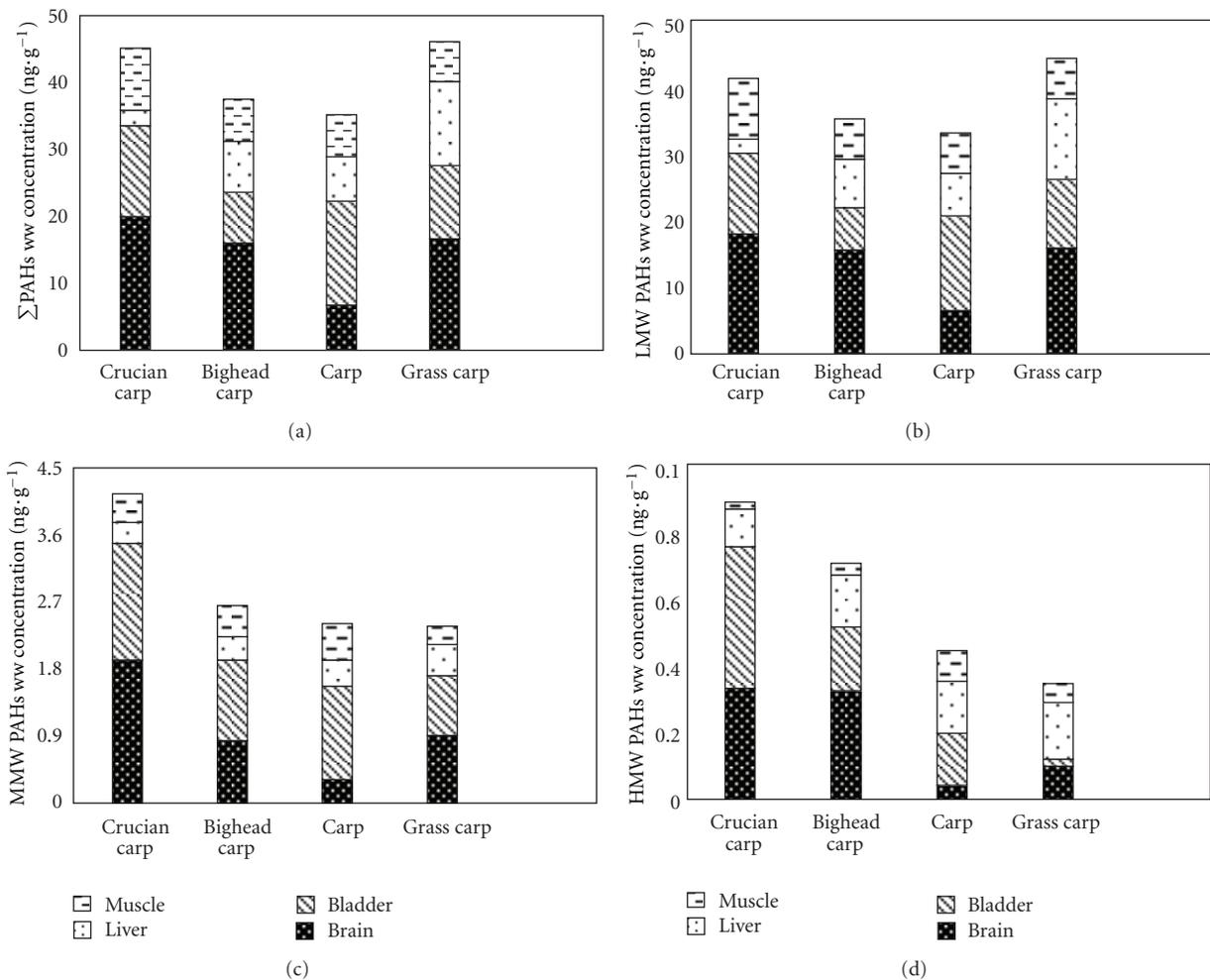
FIGURE 3: Wet weight contents of (a) total PAHs (PAH16), (b) LMW-PAHs, (c) MMW-PAHs, and (d) HMW-PAHs in four fish species.
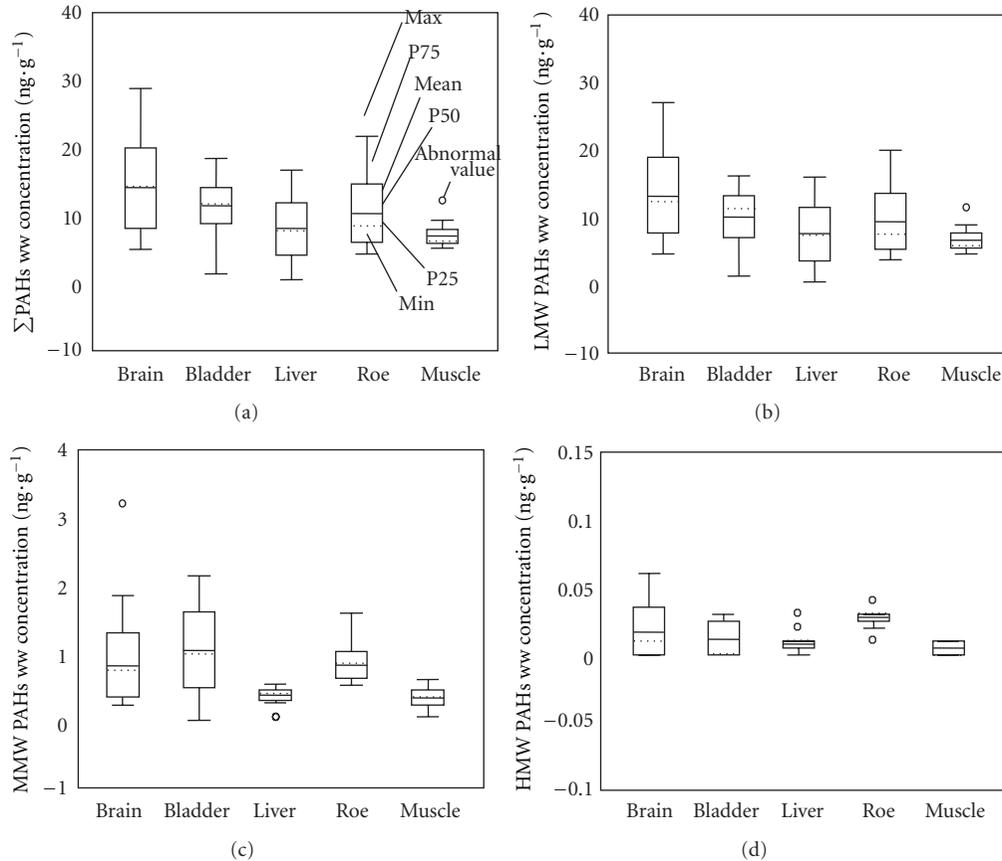
FIGURE 4: Wet weight contents of (a) total PAHs (PAH16), (b) LMW-PAHs, (c) MMW-PAHs, and (d) HMW-PAHs in four fish tissues.

TABLE 6: ANOVA results of lipid normalized-based ∑PAHs contents.

PAHs		Mean square	F value	Sig.
∑PAHs	Species	11741830.31	13.93	0.000
	Tissues and organs	4989904.44	5.92	0.000
LMWPAHs	Species	9814905.47	13.18	0.000
	Tissues and organs	4410348.16	5.92	0.000
MMWPAHs	Species	88756.14	9.69	0.000
	Tissues and organs	31423.44	3.43	0.013
HMWPAHs	Species	70.79	10.50	0.000
	Tissues and organs	53.68	7.96	0.000

This is most likely related to the different feeding habits of the various species. Bighead carp is a filter feeder, feeding on zooplankter, leading to the highest residual levels of PAHs on a lipid-normalized weight basis. Crucian carp and carp are omnivorous fish and therefore the residual level of PAHs on a lipid-normalized weight basis was found to be lower. Grass carps are herbivorous, and they were found to contain the lowest residual level of PAHs on a lipid-normalized weight basis.

The different residual levels of PAHs on a lipid-normalized weight basis in various tissues and organs are shown in Figure 6. In general, the distribution of total PAHs, LMWPAHs, MMWPAHs, and HMWPAHs shared a similar tendency, which is that residual levels of PAHs were the highest in the liver, lower in the muscle, bladder, and roe, and lowest in the brain. A one-way analysis of variance reflected that the differences of PAH residual levels on a lipid-normalized weight basis in various tissues were significant at a 95% confidence level ($P < 0.05$). An ideal illustration for this is the liver block phenomenon, which holds that pollutants in the living body will integrate with related proteins to form a compound. This compound, consisting mainly of various cytochromes of P450, will subsequently be transferred into the liver, causing pollutants to accumulate and concentrate there [30]. In comparison, the low concentration of pollutants in the brain is thought to be related to the blood-brain barrier, which consists of a layer of endothelial cells that exists in many organisms [31]. The main biological function of this blood-brain barrier is to resist various pathogens and poisonous substances. The selective entry of molecules in the brain lies in its structural characteristics of being both highly complex and highly ordered. This can ensure an accurate identification of outgoing substances in its biological, chemical, and physical properties, as well as in its spatial structure [32].

3.4. Relation between Lipid Content and Residual Level of PAHs in Fish. Table 7 illustrates the related coefficient and significance levels between lipid content and the residual

TABLE 7: Correlation between LMPAHs contents in dry, wet, and Ln-transformed lipid contents.

	Ln($\sum$PAHs)	Ln(LMWPAHs)	Ln(MMWPAHs)	Ln(HMWPAHs)
Pearson correlation coefficient (R)	0.659	0.663	0.528	0.249
Significance level (P)	<0.001	<0.001	<0.001	0.051

(a)

(b)

(c)

(d)

Muscle   Bladder
Liver   Brain
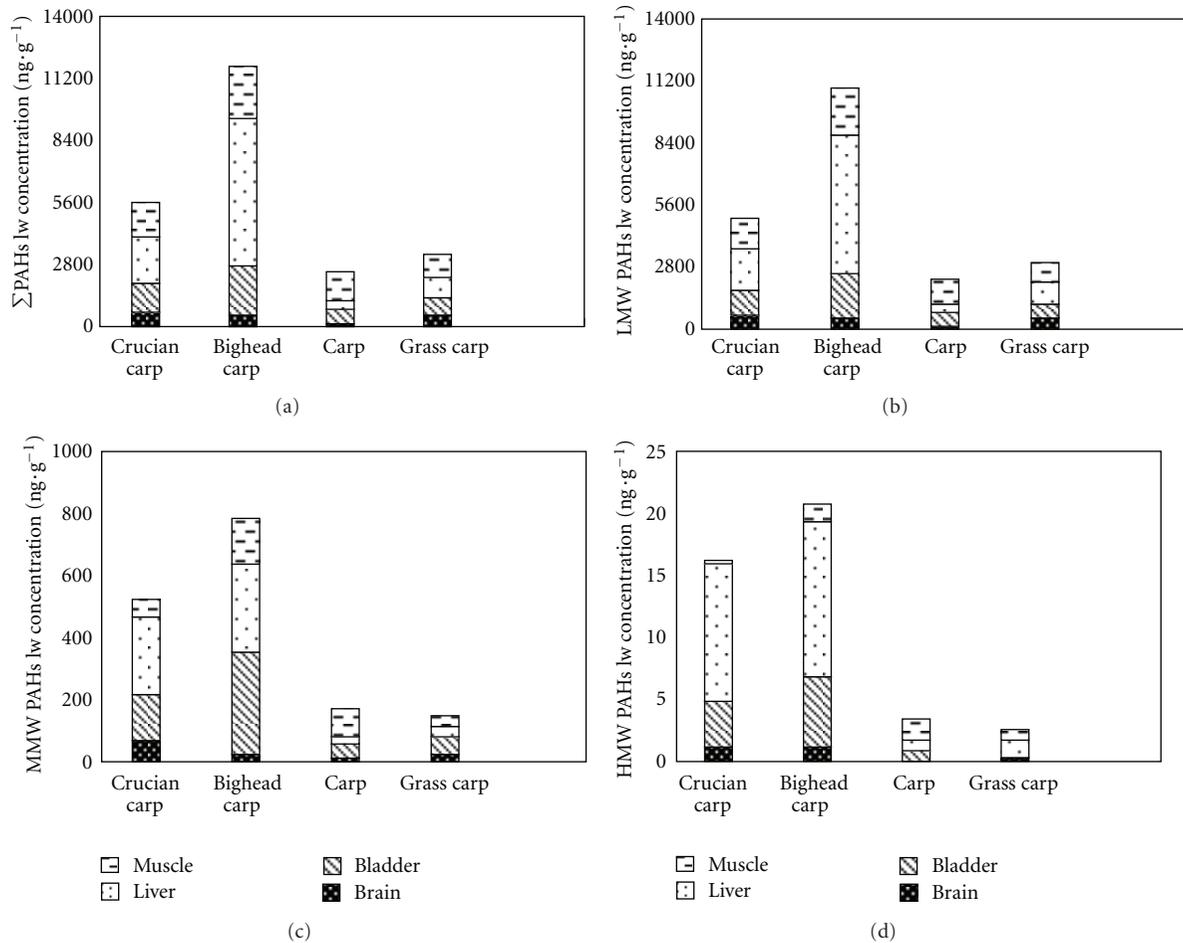
FIGURE 5: Lipid normalized contents of (a) total PAHs (PAH16), (b) LMW-PAHs, (c) MMW-PAHs, and (d) HMW-PAHs in four fish species.

level of PAHs in the specimens we studied. The relation between lipid content and residual level of total PAHs, LMWPAHs, and MMWPAHs was found significant at a 0.01 confidence level. However, the correlation between lipid content and the residual level of HMWPAHs is lower ($R = 0.249$, $P = 0.051$). In tissues with high lipid content, higher residual levels of PAHs were also found. For instance, lipid content is as high as 22.5%~35.0% in the brain and 4.6%~6.8% in the roe, and residual level of PAHs in these tissues was also high (see Figure 3).

3.5. Risks to Human Health from PAHs in Fish. Our research adopted a screen value (SV) to assess the health risks of PAHs to humans from eating these four fish species. Screen value is defined as the concentration of chemicals in edible tissue that are a potential public health concern. The SV indicator is calculated according to the following formula [26, 33–35]:

$$SV = \frac{[(RL/SF) * BW]}{CR}, \quad (1)$$

where SV is the screening value ($\mu g \cdot g^{-1}$) that is used as a threshold value against the residue level in similar tissue collected from the environment; RL is the maximum acceptable risk level (dimensionless, using 10^{-5}); SF is the oral slope factor ($\mu g \cdot g^{-1} \cdot d^{-1}$) and the SF value of BaP is 7.3 ($\mu g \cdot g^{-1} \cdot d^{-1}$)$^{-1}$; BW is body weight (kg) and an average of 70 kg is used for the calculations; and CR refers to the consumption rate ($g \cdot d^{-1}$) and is substituted by the USEPA standard value for the average intake rate of fish, which is 142.2 $g \cdot d^{-1}$.

When the carcinogenic risk is 10^{-5}, the calculated SV threshold is 0.67 ng $\cdot g^{-1}$ (wet weight, the potency equivalent concentration) [36–39], which is far higher than the wet weight contents of PAHs in various tissues and organs acquired from this research. Therefore, we can clarify that the carcinogenic risk from the four main fish species found in the Beijing market is significantly lower than 10^{-5} (Table 8).

In addition, BaP equivalent concentrations of PAHs in the fish measured in this research were also below

TABLE 8: Risk assessment on BaP and potency equivalent concentration of PAHs for human consumption of fish.

|	Species	Brain	Bladder	Liver	Roe	Muscle
BaP	Crucian carp	5.5×10^{-7}	4.0×10^{-7}	1.5×10^{-7}	4.3×10^{-7}	1.9×10^{-7}
	Bighead carp	4.3×10^{-7}	2.2×10^{-7}	2.2×10^{-7}	—	2.1×10^{-7}
	Carp	1.6×10^{-7}	3.3×10^{-7}	2.4×10^{-7}	3.1×10^{-7}	2.2×10^{-7}
	Grass carp	2.7×10^{-7}	2.7×10^{-7}	3.3×10^{-7}	—	3.0×10^{-7}
PEC of PAHs	Crucian carp	1.14×10^{-6}	7.7×10^{-7}	1.7×10^{-7}	6.4×10^{-7}	2.6×10^{-7}
	Bighead carp	6.2×10^{-7}	3.5×10^{-7}	3.3×10^{-7}	—	2.4×10^{-7}
	Carp	2.2×10^{-7}	5.3×10^{-7}	3.4×10^{-7}	5.2×10^{-7}	2.9×10^{-7}
	Grass carp	6.1×10^{-7}	2.3×10^{-7}	5.0×10^{-7}	—	2.2×10^{-7}
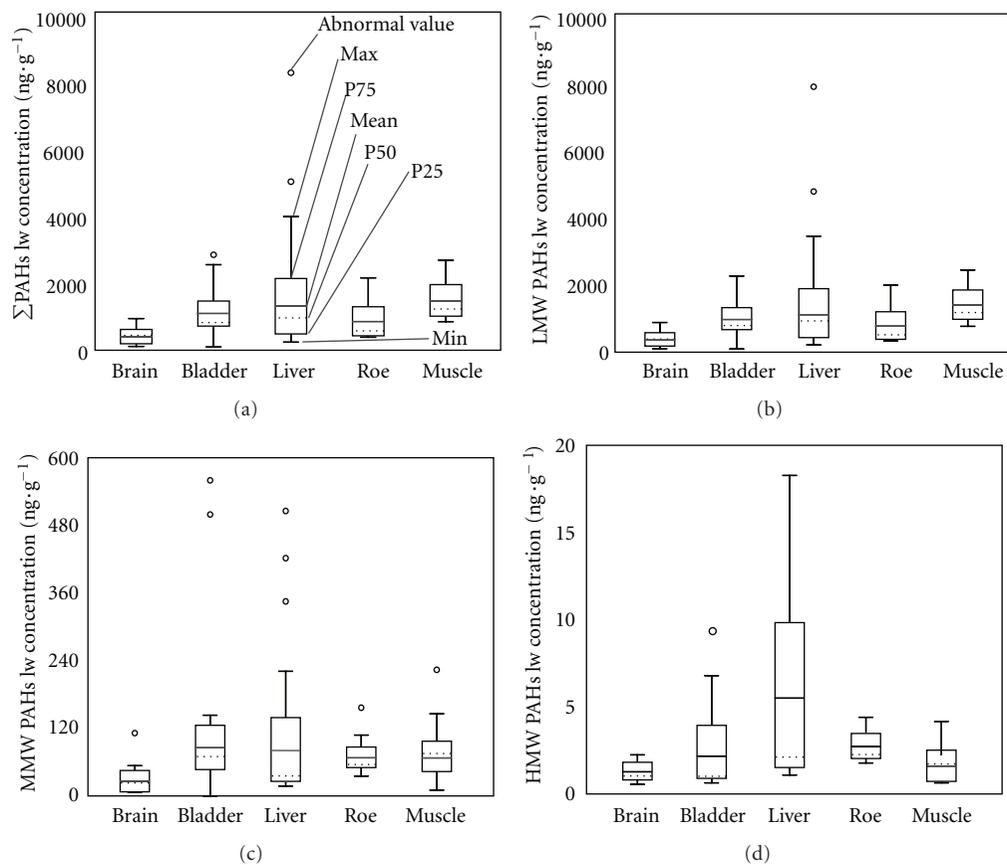
FIGURE 6: Lipid-normalized contents of (a) total PAHs (PAH16), (b) LMW-PAHs, (c) MMW-PAHs, and (d) HMW-PAHs in four fish tissues.

the national standards limiting pollutants, in which BaP equivalent concentrations are suggested below $5 \, ng \cdot g^{-1}$ for grain and meat and $10 \, ng \cdot g^{-1}$ for vegetables [35, 40].

4. Conclusions

The residual levels of PAHs in fish on a wet weight basis ranged from $0.51 \, ng \cdot g^{-1}$ to $28.78 \, ng \cdot g^{-1}$, while the residual levels of PAHs on a lipid-normalized basis ranged between $93.62 \, ng \cdot g^{-1}$ and $8203.43 \, ng \cdot g^{-1}$. LMWPAHs took a dominant percentage of the total of the PAH residuals.

The residual levels of PAHs in fish on a wet weight basis had no significant differences among various fish species but did show differences among the various fish tissues. The

highest residual levels of total PAHs and LMWPAHs were found in the brain, they were lower in the roe and bladder, and they were the lowest in the liver and muscle. With regard to residual levels of MMWPAHs, the highest value was found in the bladder, lower values in the brain and roe, and the lowest values in the liver and muscle. For HMWPAHs, the highest value was found in the roe, lower values in the brain, and the lowest values in the bladder, liver, and muscle.

The residual levels of PAHs on a lipid-normalized weight basis had significant differences both for various fish species and for various fish tissues. In all of the four fish species, the highest total residual levels of PAHs was found in bighead carp, lower levels in crucian carp and the lowest values in carp, and grass carp. As for the five tissues, the highest

residual levels of PAHs were found in the liver, lower levels in the muscle, roe, and bladder, and the lowest levels in the brain. No significant differences were found for PAH distribution in HMWPAH, MMWPAHs, and LMWPAHs.

The potency equivalent concentration of PAHs on a wet weight basis in various tissues was found to be lower than the SV value from USEPA (0.67 ng·g^{-1}, wet weight). Therefore, its carcinogenic risk for humans was far lower than 10^{-5}.

Acknowledgments

References

[1] X. R. Li, B. G. Li, S. Tao et al., "Population exposure to PAHs in Tianjin area," *Acta Scientiae Circumstantiae*, vol. 25, no. 7, pp. 989–993, 2005 (Chinese).

[2] E. R. Christensen and P. A. Bzdusek, "PAHs in sediments of the Black River and the Ashtabula River, Ohio: source apportionment by factor analysis," *Water Research*, vol. 39, no. 4, pp. 511–524, 2005.

[3] H. B. Moon, K. Kannan, S. J. Lee, and G. Ok, "Atmospheric deposition of polycyclic aromatic hydrocarbons in an urban and a suburban area of Korea from 2002 to 2004," *Archives of Environmental Contamination and Toxicology*, vol. 51, no. 4, pp. 494–502, 2006.

[4] D. Lin and L. Zhu, "Polycyclic aromatic hydrocarbons: pollution and source analysis of a black tea," *Journal of Agricultural and Food Chemistry*, vol. 52, no. 26, pp. 8268–8271, 2004.

[5] J. Koyama, S. Uno, and K. Kohno, "Polycyclic aromatic hydrocarbon contamination and recovery characteristics in some organisms after the Nakhodka oil spill," *Marine Pollution Bulletin*, vol. 49, no. 11-12, pp. 1054–1061, 2004.

[6] S. Tao, X. Li, Y. Yang et al., "Dispersion modeling of polycyclic aromatic hydrocarbons from combustion of biomass and fossil fuels and production of coke in Tianjin, China," *Environmental Science and Technology*, vol. 40, no. 15, pp. 4586–4591, 2006.

[7] S. Tao, Y. H. Cui, F. L. Xu et al., "Polycyclic aromatic hydrocarbons (PAHs) in agricultural soil and vegetables from Tianjin," *Science of the Total Environment*, vol. 320, no. 1, pp. 11–24, 2004.

[8] S. Xu, W. Liu, and S. Tao, "Emission of polycyclic aromatic hydrocarbons in China," *Environmental Science and Technology*, vol. 40, no. 3, pp. 702–708, 2006.

[9] Y. Zhang and S. Tao, "Global atmospheric emission inventory of polycyclic aromatic hydrocarbons (PAHs) for 2004," *Atmospheric Environment*, vol. 43, no. 4, pp. 812–819, 2009.

[10] Y. Tian and T. L. Zheng, "PAH-degrading microorganisms in marine environment," *Marine Sciences*, vol. 28, no. 9, pp. 50–55, 2004 (Chinese).

[11] I. Vives, J. O. Grimalt, P. Fernández, and B. Rosseland, "Polycyclic aromatic hydrocarbons in fish from remote and high mountain lakes in Europe and Greenland," *Science of the Total Environment*, vol. 324, no. 1–3, pp. 67–77, 2004.

[12] N. Loutfy, M. Fuerhacker, P. Tundo, S. Raccanelli, and M. T. Ahmed, "Monitoring of polychlorinated dibenzo-p-dioxins and dibenzofurans, dioxin-like PCBs and polycyclic aromatic hydrocarbons in food and feed samples from Ismailia city, Egypt," *Chemosphere*, vol. 66, no. 10, pp. 1962–1970, 2007.

[13] K. Sexton, D. E. Kleffman, and M. A. Callahan, "An introduction to the National Human Exposure Assessment Survey (NHEXAS) and related phase I field studies," *Journal of Exposure Analysis and Environmental Epidemiology*, vol. 5, no. 3, pp. 229–232, 1995.

[14] R. Van den Berg, *Human Exposure to Soil Contamination: A Qualitative Analysis Towards Proposals for Humane Toxicological Intervention Values*, National Institute of Public Health and Environmental Protection, Bilthoven, The Netherlands, 1994.

[15] C. A. Menzie, B. B. Potocki, and J. Santodonato, "Ambient concentrations and exposure to carcinogenic PAHs in the environment," *Environmental Science and Technology*, vol. 26, no. 7, pp. 1278–1284, 1992.

[16] A. Vyskocil, Z. Fiala, V. Chénier et al., "Assessment of multipathway exposure of small children to PAH," *Environmental Toxicology and Pharmacology*, vol. 8, no. 2, pp. 111–118, 2000.

[17] S. Khan and Q. Cao, "Human health risk due to consumption of vegetables contaminated with carcinogenic polycyclic aromatic hydrocarbons," *Journal of Soils and Sediments*, vol. 12, no. 2, pp. 178–184, 2012.

[18] A. Binelli and A. Provini, "Risk for human health of some POPs due to fish from Lake Iseo," *Ecotoxicology and Environmental Safety*, vol. 58, no. 1, pp. 139–145, 2004.

[19] H. Nakata, Y. Sakai, T. Miyawaki, and A. Takemura, "Bioaccumulation and toxic potencies of polychlorinated biphenyls and polycyclic aromatic hydrocarbons in tidal flat and coastal ecosystems of the Ariake Sea, Japan," *Environmental Science and Technology*, vol. 37, no. 16, pp. 3513–3521, 2003.

[20] B. X. Mai, J. M. Fu, G. Y. Sheng et al., "Chlorinated and polycyclic aromatic hydrocarbons in riverine and estuarine sediments from Pearl River Delta, China," *Environmental Pollution*, vol. 117, no. 3, pp. 457–474, 2002.

[21] A. R. Schneider, H. M. Stapleton, J. Cornwell, and J. E. Baker, "Recent declines in PAH, PCB, and toxaphene levels in the Northern Great Lakes as determined from high resolution sediment cores," *Environmental Science and Technology*, vol. 35, no. 19, pp. 3809–3815, 2001.

[22] K. Pointet and A. Milliet, "PAHs analysis of fish whole gall bladders and livers from the Natural Reserve of Camargue by GC/MS," *Chemosphere*, vol. 40, no. 3, pp. 293–299, 2000.

[23] M. Perugini, P. Visciano, A. Giammarino, M. Manera, W. Di Nardo, and M. Amorena, "Polycyclic aromatic hydrocarbons in marine organisms from the Adriatic Sea, Italy," *Chemosphere*, vol. 66, no. 10, pp. 1904–1910, 2007.

[24] A. Onyango, J. Lalah, S. Wandiga, and J. Gichuki, "Assessment of polycyclic aromatic hydrocarbons in lates niloticus, oreochromis niloticus and rastrineobola argentea as sources of human exposure in Kisumu Bay, Winam Gulf of Lake Victoria," *The Bulletin of Environmental Contamination and Toxicology*, vol. 88, pp. 747–751, 2012.

[25] G. Conti, C. Copat, C. Ledda et al., "Evaluation of heavy metals and polycyclic aromatic hydrocarbons (PAHs) in Mullus barbatus from sicily channel and risk-based consumption limits," *The Bulletin of Environmental Contamination and Toxicology*, vol. 88, pp. 946–950, 2012.

[26] K. C. Cheung, H. M. Leung, K. Y. Kong, and M. H. Wong, "Residual levels of DDTs and PAHs in freshwater and marine fish from Hong Kong markets and their health risk assessment," *Chemosphere*, vol. 66, no. 3, pp. 460–468, 2007.

[27] J. Dong, T. G. Luan, S. C. Zou et al., "Residues and risk assessment of DDTs and PAHs in sediments and fish from pearl river delta area," *Ecology and Environment*, vol. 15, no. 4, pp. 693–696, 2006 (Chinese).

[28] Y. Zhang, S. Tao, J. Cao, and R. M. Coveney, "Emission of polycyclic aromatic hydrocarbons in China by county," *Environmental Science and Technology*, vol. 41, no. 3, pp. 683–687, 2007.

[29] Y. Zhu, W. J. Wu, J. J. Wang et al., "The distributions, sources and ecological risks of polycyclic aromatic hydrocarbons in water-sediment system in Lake Small Baiyangdian," *Journal of Lake Science*, vol. 21, no. 5, pp. 44–53, 2009 (Chinese).

[30] Y. Wan, J. Hu, W. An et al., "Congener-specific tissue distribution and hepatic sequestration of PCDD/Fs in wild herring gulls from Bohai Bay, North China: comparison to coplanar PCBs," *Environmental Science and Technology*, vol. 40, no. 5, pp. 1462–1468, 2006.

[31] P. Ballabh, A. Braun, and M. Nedergaard, "The blood-brain barrier: an overview: structure, regulation, and clinical implications," *Neurobiology of Disease*, vol. 16, no. 1, pp. 1–13, 2004.

[32] C. Roney, P. Kulkarni, V. Arora et al., "Targeted nanoparticles for drug delivery through the blood-brain barrier for Alzheimer's disease," *Journal of Controlled Release*, vol. 108, no. 2-3, pp. 193–214, 2005.

[33] M. G. Barron, R. Heintz, and S. D. Rice, "Relative potency of PAHs and heterocycles as aryl hydrocarbon receptor agonists in fish," *Marine Environmental Research*, vol. 58, no. 2–5, pp. 95–100, 2004.

[34] S. O. Baek, R. A. Field, M. E. Goldstone, P. W. Kirk, J. N. Lester, and R. Perry, "A review of atmospheric polycyclic aromatic hydrocarbons: sources, fate and behavior," *Water, Air, and Soil Pollution*, vol. 60, no. 3-4, pp. 279–300, 1991.

[35] Y. N. Wu, X. Q. Wang, H. F. Yang et al., *Maximum Residue Limits For Pesticides in Food*, Chinese Standards Press, Beijing, China, 2005.

[36] UNEP (United Nations Environment Programme), *Europe Regional Report: Regionally Based Assessment of Persistent Toxic Substances*, 2002.

[37] USEPA, "Risk assessment guidance for superfund," in *Human Health Evaluation Manual*, vol. 1, Environmental Protection Agency, Office of Emergency and Remedial Response, Washington, DC, USA, 1989.

[38] USEPA, "Guidance for assessing chemical contaminant, data for use in fish advisories," in *Fish Sampling and Analysis*, vol. 1, EPA 823-R-95-007 Office of Water, Washington, DC, USA, 3rd edition, 2000.

[39] J. C. White and T. Triplett, "Polycyclic aromatic hydrocarbons (PAHs) in the sediments and fish of the Mill River, New Haven, Connecticut, USA," *Bulletin of Environmental Contamination and Toxicology*, vol. 68, no. 1, pp. 104–110, 2002.

[40] R. Ke, Y. Xu, S. Huang, Z. Wang, and J. N. Huckins, "Comparison of the uptake of polycyclic aromatic hydrocarbons and organochlorine pesticides by semipermeable membrane devices and caged fish (Carassius carassius) in Taihu Lake, China," *Environmental Toxicology and Chemistry*, vol. 26, no. 6, pp. 1258–1264, 2007.

The *J*cientificWorldJOURNAL

Research Article

Simulation of the Fate and Seasonal Variations of *α*-Hexachlorocyclohexane in Lake Chaohu Using a Dynamic Fugacity Model

Xiang-zhen Kong, Wei He, Ning Qin, Qi-Shuang He, Bin Yang, Huiling Ouyang, Qingmei Wang, Chen Yang, Yujiao Jiang, and Fuliu Xu

MOE Laboratory for Earth Surface Processes, College of Urban and Environmental Sciences, Peking University, Beijing 100871, China

Correspondence should be addressed to Fuliu Xu, xufl@urban.pku.edu.cn

Fate and seasonal variations of *α*-hexachlorocyclohexane (*α*-HCH) were simulated using a dynamic fugacity model in Lake Chaohu, China. Sensitivity analyses were performed to identify influential parameters and Monte Carlo simulation was conducted to assess model uncertainty. The calculated and measured values of the model were in good agreement except for suspended solids, which might be due to disregarding the plankton in water. The major source of *α*-HCH was an input from atmospheric advection, while the major environmental outputs were atmospheric advection and sediment degradation. The net annual input and output of *α*-HCH were approximately 0.294 t and 0.412 t, respectively. Sediment was an important sink for *α*-HCH. Seasonal patterns in various media were successfully modeled and factors leading to this seasonality were discussed. Sensitivity analysis found that parameters of source and degradation were more important than the other parameters. The sediment was influenced more by various parameters than air and water were. Temperature variation had a greater impact on the dynamics of the model output than other dynamic parameters. Uncertainty analysis showed that the model uncertainty was relatively low but significantly increased in the second half of the simulation period due to the increase in the gas-water diffusion flux variability.

1. Introduction

Organochlorine pesticides (OCPs) have been under increasing scrutiny due to their refractory qualities and high ecotoxicity. Hexachlorocyclohexanes (HCHs), a type of OCPs, have already been listed by the Stockholm Convention on Persistent Organic Pollutants in the first batch of control compounds [1]. During the 1960s and 1970s, there was a substantial amount of production and usage of HCH pesticides in China, resulting in high level of residues in the soil [2]. Through surface runoff, undercurrent, osmosis, leaching, and other transport mechanisms from the soil into the surface water, the water bodies, such as lakes, have also been severely polluted by HCH pesticides. According to historical data, the quantity of emitted OCPs in the Lake Chaohu water bodies amounted to 1.16 tons in 1984. Among

the isomers of HCHs, *α*-HCH can cause human neurological disorders and gastrointestinal discomfort, resulting in liver and kidney damage, human endocrine system disorders and immune system abnormalities [1]. Therefore, an understanding of the distribution and dynamics of *α*-HCH in lake environments is extremely crucial.

The multimedia model is a mathematical model developed in the 1980s based on the concept that the physical and chemical properties of environmental systems and pollutants synergistically determine the concentration, distribution, and migration of contaminants throughout the transformation process between environmental compartments [3]. Mackay [4] and Mackay and Paterson [5, 6] proposed a fugacity model to simplify the structure of the multi-media model and the calculation process. This model has been widely used in describing the environmental behaviors of
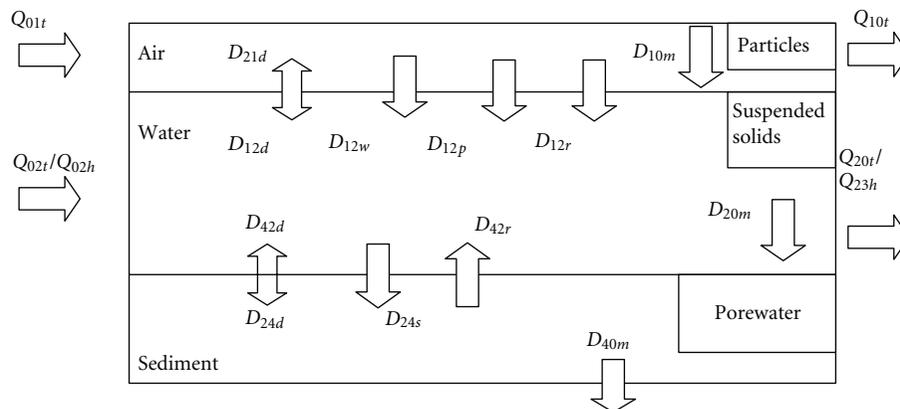
FIGURE 1: Transport fluxes of α-HCH in and out of the Lake Chaohu area and between the adjacent compartments. D_{12d}, D_{21d}, D_{24d}, and D_{42d} represent the diffusion processes between air/water and water/sediment. D_{12p} and D_{12w} represent the dry and wet deposition from air to water, respectively. D_{12r} represents scavenging by precipitation. Q_{01t}, Q_{02t}, and Q_{02h} represent the input from air advection, water inflows, and waste water discharge, respectively. Q_{10t}, Q_{20t}, and Q_{23h} represent the output from air advection, water outflows and water reuse by industry, and agriculture, respectively. D_{10m}, D_{20m}, and D_{40m} represent the degradation occurring in the air, water, and sediment, respectively.

TABLE 1: Volume and properties of the phases and sub-phases.

Main phase	Area (m^2)	Depth (m)	Organic carbon (%)	Subphases and volume fraction (X_{ij})		
				Air (1)	Water (2)	Solid particles (3)
Air (1)	$7.5810E+08$	$1.0000E+02$	—	$1.0000E+00$	—	$7.6278E-11$[a]
Water (2)	$7.5810E+08$	$3.0124E+00$[a]	$1.6700E-01$	—	$1.0000E+00$	$1.2631E-05$[a]
Sediment (3)	$7.5810E+08$	$1.0000E-01$	$4.6077E-03$	—	$7.0000E-01$	$3.0000E-01$

a: annually average value; seasonal data were available in simulation.

pollutants in global, regional, and local environments [7–9]. There are four levels in the fugacity model. A level IV fugacity model is appropriate when continuous changes in the concentrations of particular pollutants are studied over a period of time [8, 10].

Few studies have been conducted that focus on the seasonal variation in α-HCH using the level IV fugacity model. In this study, the fate and seasonal variation of α-HCH in the air, water, and sediment of Lake Chaohu were examined. Since the usage of industrial HCHs was banned in 1983 and lindane was applied instead [10], the α-HCH emissions can be assumed to be zero. The results of this model can reveal the main source, the migration and transformation processes, and the most influential parameters on the fate and seasonal variations of α-HCH in the of Lake Chaohu environment. The uncertainty of the model was also assessed using a Monte Carlo simulation.

2. Materials and Methods

2.1. Model Development. The framework of the model in this study was based on the quantitative water, air, sediment interaction (QWASI) fugacity model [11], with the major difference being the inclusion of atmospheric advection input and output of the system. This model included three main compartments: atmosphere, water, and sediment, which were represented by the subscripts 1, 2, and 4,

respectively. The atmospheric phase was comprised of two subphases: gaseous and particulate matter. The aqueous phase also comprised two sub-phases: water and suspended solids. The sediment phase consisted of porewater and a solid phase. The model framework is shown in Figure 1. The basic characteristics of the model for Lake Chaohu are shown in Table 1.

Model parameter symbols, units, values and data sources are shown in Tables S1 and S2 in supplementary materials available online at doi:10.1100/2012/691539. The model had a total of 46 parameters, including 23 environmental parameters, 12 interface mass transfer parameters, and 11 physicochemical parameters for the pollutant. The environmental parameters included temperature, lake area, height and sub-phase volume fraction determined by the literature or laboratory measurements. The physicochemical parameters, such as the gas constant, Henry's constant, and saturated vapor pressure, were obtained from the literature. The environmental kinetics of the process parameters, including the rate of degradation, the rate of diffusion, migration constant, molecular diffusion path length, atmospheric wet and dry deposition rates, deposition rate, and cleaning coefficients, were obtained from the relevant literature. Fifteen parameters had annually changing values, including the environmental parameters (h_2, X_{13}, $Q_{01t}Q_{10t}$, Q_{02t}, Q_{20t}, Q_{23h}, Q_{02h}, T, C_1, and X_{23}) and the mass transfer parameters (K_{12}, K_{21}, K_{42r}, and K_w). The parameter h_2 included hourly

data; T, K_{12}, K_{21}, K_{42r}, and K_w had daily data, and X_{13}, $Q_{01t}(Q_{10t})$, Q_{02t}, Q_{20t}, Q_{23h}, Q_{02h}, C_1, and X_{23} had monthly data. Other parameters were used in terms of annual average values, and they remained constant during the simulation. In addition, Henry's constant, saturated vapor pressure, and the fugacity rate of the pollutant were primarily obtained using a temperature of 25°C. The temperature correction required for these parameters and the correction equation are shown in (1) [12]:

$$\log_{10} P_T = \log_{10} P_{25} + A \times \left(\frac{1}{298} - \frac{1}{T + 273} \right), \qquad (1)$$

where P_T is the physical and chemical parameter values at T (°C) (Henry's constant, the saturation vapor pressure, or fugacity rate); P_{25} is the physical and chemical parameters at 25°C; A is the temperature correction coefficient (for Henry's constant, saturated vapor pressure, and fugacity rate). To obtain the total river inflows of Lake Chaohu from May 2010 to February 2011, monthly data from May 1987 to April 1988 were collected [13] along with the corresponding daily precipitation data from the China Meteorological Data Sharing Service System [14]. There was a significant linear relationship between the river inflow and the precipitation data. Using this linear relationship and the monthly precipitation data from May 2010 to February 2011 for Lake Chaohu, the river inflow (Q_{02t}) for the simulation period was easily calculated. This calculation was based on the assumption that there were no significant landscape level changes which largely modifies fate of precipitation at catchment area since 1980s. In addition, the values of water inflow were not important to the fate of α-HCH in the lake, which will be revealed in the sensitive analysis (Section 3.3). The average monthly river outflow (Q_{02t}) of Lake Chaohu was based on the water balance calculation of inflow and water level in addition to the rates of industrial and agricultural water consumption (Q_{23h}) [13].

Taking into consideration that industrial HCHs were banned in 1983 and lindane (γ-HCH) was applied instead [10], emissions of α-HCH in the vicinity of Lake Chaohu were assumed to be zero during the simulation. Atmospheric α-HCH input originated from atmospheric advection. The α-HCH concentration in the advection within the study area (C_1) was determined according to the sampled values on the lake side (four samples in total). The daily average wind speed and direction during the simulation period in Lake Chaohu area were obtained from the China Meteorological Data Sharing Service System [14]. The volumes of atmospheric advections (Q_{01t}, Q_{10t}) were calculated according to the corresponding atmospheric height, the area of Lake Chaohu, and the wind speed. α-HCH input originated from water inflows was determined by the summation of the input amount from all the rivers around the lake [15].

The mass transfer coefficients of both sides of the gas-water interface (K_{12} and K_{21}) were calculated according to the method proposed by Southworth [16]. The resuspension coefficient (K_{42r}) was calculated according to the formula from Tu et al. [13]. The specific equations are as follows:

$$K_{12} = 11.375 \cdot (\text{WS} + \text{RS}) \cdot \left(\frac{18}{\text{MW}} \right)^{0.5}, \qquad (2)$$

$$K_{21} = 0.2351 \cdot \text{RS}^{0.969} \cdot \left(\frac{32}{\text{MW}} \right)^{0.5} \frac{a}{h_W^{0.673}}$$

$$(\text{if WS} \leq 1.9 \, m/s, a = 1; \text{else } a = \exp[0.529(\text{WS} - 1.9)]), \qquad (3)$$

$$K_{42r} = 3 \times 10^{-8} \cdot \frac{\text{WS}}{h_W}, \qquad (4)$$

where WS is the average wind speed (m/s); RS is the surface flow velocity (m/s); MW is the molecular weight (g/mol); and h_W is the water depth (m).

The transfer and transformation processes defined in the model are shown in Table S3 (Supplementary Material). Details can be found in Mackay and Paterson [17]. The level IV fugacity model can be expressed by (5), where fugacity is symbolized by f (Pa). The processes considered in the model included the advection of the air and water phases, diffusion and dry/wet deposition between the air and water, diffusion, sedimentation, and resuspension between the water and sediment, and the degradation process during the main phase. In this study, the fourth-order Runge-Kutta method was applied to solve the differential equations by simulating step of 1-hour. The time period of the dynamic simulation was from May 1, 2010 to February 28, 2011. The seasonal variation of the α-HCH concentration for each compartment of the environment was simulated and compared to the measured values. Validation data were obtained from the monthly samples of atmospheric aerosols on an island in the lake, water and suspended solids (four sample sites in total) collected from May 2010 to February 2011 [18, 19] and from the 14 sediment samples collected in August 2008 from Lake Chaohu [20].

$$\frac{V_1 Z_1 df_1}{dt}$$
$$= T_{01t} - \left(D_{12d} + D_{12p} + D_{12r} + D_{12w} + D_{10m} - D_{10t} \right) f_1$$
$$+ D_{21d} f_2,$$

$$\frac{V_2 Z_2 df_2}{dt}$$
$$= T_{02t} + \left(D_{12d} + D_{12p} + D_{12g} + D_{12w} \right) f_1$$
$$- (D_{21d} + D_{24d} + D_{24s} + D_{20m} + D_{20t} + D_{23h}) f_2$$
$$+ (D_{42d} + D_{42r}) f_4,$$

$$\frac{V_4 Z_4 df_4}{dt}$$
$$= (D_{24d} + D_{24s}) f_2 - (D_{42d} + D_{42r} + D_{40m}) f_4. \qquad (5)$$

2.2. Sensitive Analysis. When a system error of the model cannot be eliminated, the accuracy of the parameters is the most important factor in model accuracy, particularly regarding some sensitive parameters [2]. Therefore, a sensitivity analysis was conducted for all parameters involved in the model (except the gas constant, R). For constant parameters, a local sensitivity analysis was applied which implemented a "perturbation" near the best estimate value of a parameter, and the variation of model outputs was studied under the condition that other parameters remained unchanged. The Morris classification screening method, a widely applied local sensitivity analysis method, was used [21]. A variable was selected, and the value changed to the fixed step size, while the other parameters remained the same. The sensitivity index of the parameter was the average of the multiple disturbance calculated Morris coefficient:

$$S = \sum_{i=0}^{n-1} \frac{(Y_{i+1} - Y_i)/Y_0}{(P_{i+1} - P_i)/100}/(n-1), \qquad (6)$$

where S is the Morris coefficient; Y_i is the model output value in the ith simulation; Y_0 is the model calculation result when the parameter is set at the initial value; P_i is the percentage change of the parameter value the for ith simulation ; and n is the number of runs.

Cao et al. [2] proposed that when the step size is small enough, the nonlinear effects of the parameters of the model output are negligible. In this study, it was assumed that the parameters increased and decreased by 10% on the basis of the original value. $Y_{0.9}$, Y_0, and $Y_{1.1}$ are the output results when the parameter was multiplied by 0.9, 1 and 1.1, respectively. The sensitivity coefficient (C_s) is as follows:

$$C_s = \text{Abs}\left(\frac{Y_{1.1} - Y_{0.9}}{0.2 \times Y_0}\right). \qquad (7)$$

The effect of the parameters on the model output was not only associated with corresponding C_s values of the parameters but was also related to the fluctuation range of the parameters in the environment [2]. With the same C_s value, those parameters with higher variability have greater impacts on the model than those with lower variability. In this study, the sensitivity coefficient after the correction of the coefficient of variation (C_n) for the parameters was also calculated by [2], such that $C_n = C_s \times \text{CV}$, where CV is the coefficient of variation of the parameter.

For the dynamic parameters in the model, the dynamic sensitivity coefficient (SCV) is calculated as follows [22]:

$$\text{SCV}_i = \frac{\Delta CV_i^Y / CV_i^Y}{\Delta CV_i^X / CV_i^X}, \qquad (8)$$

where CV_i^X and CV_i^Y indicate the corresponding coefficients of variation of the ith input parameter and the output parameter, respectively, and ΔCV_i^X and ΔCV_i^Y represent the variations of the corresponding coefficients of variation of the ith input parameter and the output parameter, respectively.

2.3. Uncertainty Analysis. A Monte Carlo simulation was utilized to study the impact of the simultaneous changes in the parameters on the model results, that is, the uncertainty of the model. Based on an analysis of the collected parameter values, all of the parameters except for temperature (T) were assumed to follow the lognormal distribution [22].

A total of 2200 Monte Carlo simulation runs were conducted. Both static and dynamic parameters with higher sensitivity coefficients were selected and the original values were retained for the remaining parameters in the simulation process. The geometric mean and standard deviation could be calculated for static parameters with multiple values. Conversely, if only one value was obtained, the corresponding coefficients of variation for the parameters were assigned using values based on the literature [2, 22]. For dynamic parameters, the monthly geometric mean and standard deviation were calculated from hourly or daily data. When only monthly data were available, the coefficients of variation were manually assigned. Each run was implemented with values for each parameter that were randomly selected in the range of the mean ± standard deviation. Semi-interquartile ranges for the monthly model output were obtained for the uncertainty analysis.

3. Results and Discussion

3.1. Concentrations of α-HCH in Various Media and Models Validation. The simulated annually average concentrations of α-HCH in the air, water, and sediment are shown in Figure 2 and were found to be in agreement with the measured data. The differences in the main phases were 0.21, 0.06, and 0.07 logarithmic units for the air, water, and sediment, respectively, which were all within 0.5 log units during the simulation. The air concentrations were underestimated, which might be due to various factors. On the other hand, in addition to the uncertainty of the model, the underestimation in the sediment may be due to the fact that the samples were collected in 2008, while the model simulation period was 2010-2011. The overestimation of the concentration in the water may have been due to the absence of a biological phase. Aquatic organisms, especially plankton, can substantially affect the fate of persistent organic pollutants (POPs) in the water environment [23]. It can be observed that the α-HCH concentration in the sediment particles was much higher than that in the atmosphere or in the water bodies. It was concluded that sediment is an important sink of α-HCH [24].

The simulation results for the atmospheric particulates and the suspended solids in the water were not satisfactory. The differences between the measured and simulated data are 0.6 and 1.69 orders of magnitude, respectively. The underestimation of the α-HCH concentration in atmospheric particulates may be associated with the underestimation of the organic carbon content or the volume ratio of the atmospheric particulates. It was always acceptable if the deviations between the simulated and observed data were less than 0.5 or 0.7 orders of magnitude for multimedia fugacity model [2]. Thereby, the results in the air particles should be
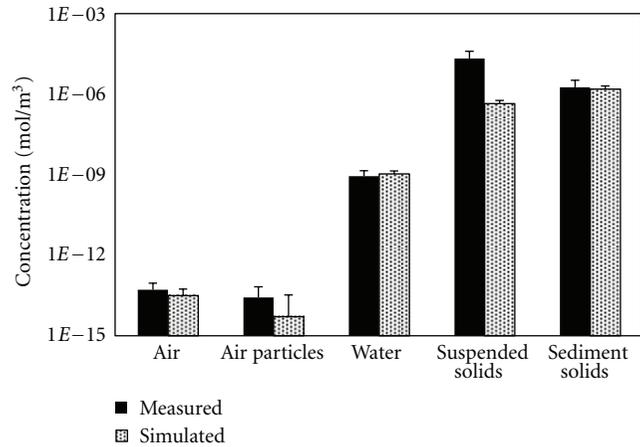
FIGURE 2: Comparison between the simulated and measured α-HCH concentrations in the air, water, and sediment of Lake Chaohu. The error bars included in this figure represent the standard deviations.

(a)

(b)

(c)

(d)
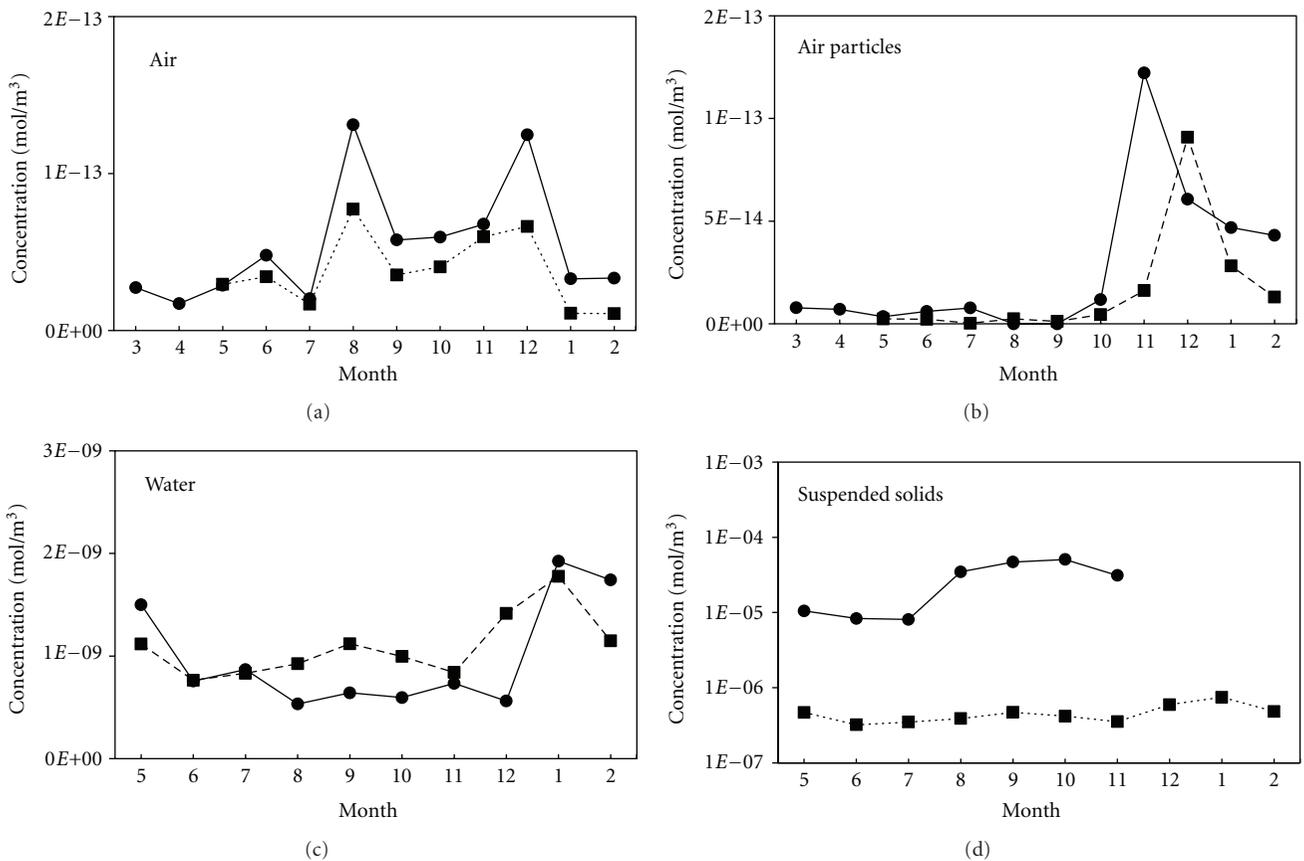
FIGURE 3: Seasonal variations of α-HCH concentrations in the various environmental media. Both the simulated (dashed) and measured (solid) concentrations are presented for model validation.

acceptable. The underestimation of the α-HCH concentration in the suspended solids in the water may be related to similar processes as those that caused the overestimation in the water.

The simulation results regarding the monthly α-HCH concentration in different compartments are shown in Figure 3. The model output of the α-HCH concentrations in the atmosphere and the atmospheric particles was consistent with the measured values. However, the α-HCH concentration in the atmospheric particles peaked in November according to the measured values, while the calculated value peaked in December, which corresponded

to the peak of gaseous α-HCH concentration but failed to capture the November peak. This discrepancy may be due to higher concentrations of α-HCH in the remote input of atmospheric particulate matter in November. The specific mechanisms underlying this difference require further study.

Gaseous α-HCH concentrations in the summer and winter, notably in August and December, were higher than in other seasons. Ridal et al. [25] also observed relatively high concentrations of gaseous α-HCH in Lake Ontario in August. The most likely cause of higher α-HCH concentrations in the summer may be the higher temperatures in summer months [26], which favor volatilization. High values in the winter may be due to remote inputs from the atmosphere [27]. Haugen et al. [28] suggested that when the regression coefficient R^2 for $\ln P$ and $1/T$ is high, local gaseous α-HCH is mainly derived from surface volatilization. Otherwise, remote input is typically the dominant source of gaseous α-HCH. In this study, the regression coefficient for $\ln P$ and $1/T$ was 0.004, indicating that the gaseous α-HCH in Lake Chaohu was influenced to a greater extent by remote input than by lake volatilization. Agricultural land accounted for 61.12% of the total land area in the Lake Chaohu watershed [13]. Consequently, large amounts of α-HCH residues remain in the soils. After volatilization, the α-HCH is able to be transported to the lake by air advection. In addition, there was a slight decline of gaseous α-HCH in July (Figure 3), which corresponded to a marked increase in the wet deposition flux (T_{12r}) during this period. The reason for the slight decline may be increased precipitation. It can be concluded that both temperature and precipitation are key factors affecting gaseous α-HCH. This conclusion was quantitatively verified using the sensitivity analysis. It is worth noting that wet deposition (T_{12w}) was higher in the summer, particularly in August, and lower during the other seasons. In contrast, dry deposition (T_{12p}) was higher in the winter, notably in December, and lower during the other seasons.

α-HCH in atmospheric particulate matter was lower in the summer and higher in the winter. The primary reason behind this difference may be that as the temperature rises in the summer, the gas-solid balance of α-HCH in the air shifts toward the gaseous phase. The situation is opposite in the winter [15]. In addition, the atmospheric particulate matter content in the summer is lower due to a decrease in the remote inputs when compared to winter.

The measured and simulated values of α-HCH in the water were also in good agreement. The model captured the high value in the winter and the variation in the other seasons, which was also consistent with the data Ridal et al. [25] observed in Lake Ontario. The peak in the winter values may be attributed to several causes. First, although the winter temperatures are lower, leading to reduced water fugacity capacity [15], the precipitation and water inflow are also lower in the winter, resulting in a significant decrease in water levels, which may cause a concentration effect. Furthermore, the gas-to-water diffusion process flux (T_{12d}) is higher in the winter, which may also be important. Conversely, lower concentrations were simulated in the summer and the autumn. A noticeable decline occurred in June, which

may be due to the dilution effect caused by the rising water levels and elevated water-to-air diffusion (T_{12d}) caused by increasing temperatures. The α-HCH concentrations in water begin to be overestimated from August through December, which coincides with an observed increase in the seasonal distribution of cyanobacteria in Lake Chaohu [29]. In addition, the calculated value of the α-HCH concentration in the suspended solids was much less than the measured value by a factor of more than one order of magnitude every month. It can be speculated that disregarding aquatic organisms, particularly the phytoplankton phase, can lead to a significant deviation between the measured data and simulation results. Phytoplankton uptake is strongly affecting the fate of persistent organic pollutants (POPs) in aquatic environments [23], which was not included in this model. Only absorption by the organic matter in the suspended solids was considered in the model. Dachs et al. [23] proposed a model combining POPs in the air-water exchange and phytoplankton absorption processes. However, currently there is no data on the parameters of HCH exchange between water and phytoplankton [30, 31]. A modification in the model structure and further research are needed in the future.

The annual averages of the sampled values of α-HCH content in the sediment particles were consistent with the simulated results. Similar seasonal variations in the water bodies were obtained, showing the trends of higher values in the summer and lower values in the winter. With smaller seasonal changes, the α-HCH content in the sediment was relatively stable compared to that in the water.

3.2. Transfer Fluxes of α-HCH between Compartments. As shown in Figure 4, the net input of α-HCH into the Lake Chaohu environment is approximately 0.115 mol/h (approximately 0.294 t/a), while the net output is 0.162 mol/h (approximately 0.412 t/a). It can be observed that the α-HCH content in the Lake Chaohu watershed is diminishing. The atmospheric advection input was found to be the main source (T_{01t}) (0.278 t/a), which corresponded to the atmospheric advection output (T_{10t}) (0.277 t/a). By contrast, the α-HCH input from water inflows was very small (0.016 t/a). An important output was the degradation in the sediments (0.119 t/a), which accounted for 89.05% of the total degradation in the environment, while the degradation in the water was 0.015 t/a, which accounted for 10.86% of the total degradation.

For interface processes, the atmospheric input to the water was 0.030 t/a, and the dominant process of atmospheric input to the water was precipitation scavenging (T_{12w}), which accounted for 57.80% of the gas-to-water flux. The flux of diffusion from the water to the atmosphere (T_{21d}) was 0.014 t/a. Therefore, there was an annual net input from the atmosphere to the water. The seasonal variations in the air-water exchange were shown in Figure 5. There was a net volatilization from the water into the atmosphere in May, which was consistent with the results obtained by Taihu [32]. During the other seasons, however, there is a net input from the atmosphere to the water, which is
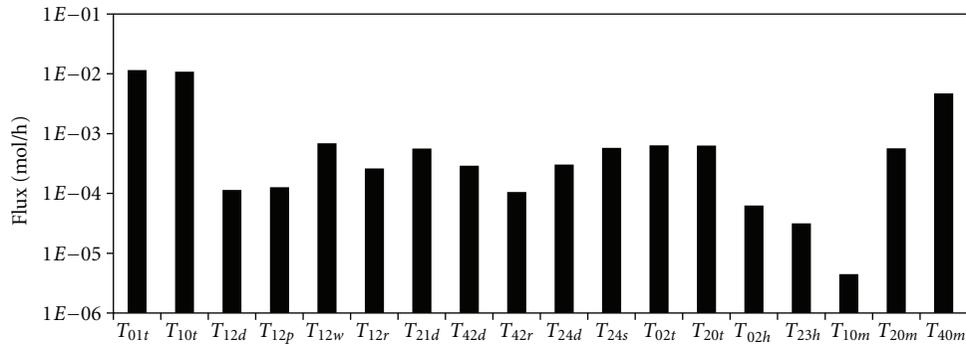
Figure 4: α-HCH fluxes in and out of the Lake Chaohu area and between the adjacent compartments. T_{01t}: air advection flows into the area; T_{10t}: air advection flows out of the area; T_{12d}: diffusion from air to water; T_{12p}: dry deposition from air to water; T_{12w}: wet deposition from air to water; T_{12r}: rain scavenging; T_{21d}: diffusion from water to air; T_{42d}: diffusion from sediment to water; T_{42r}: resuspension from sediment to water; T_{24d}: diffusion from water to sediment; T_{24s}: sedimentation from water to sediment; T_{02t}: water advection flows into the area; T_{20t}: water advection flows out of the area; T_{02h}: locative wastewater discharge; T_{23h}: industry and agriculture water usage; T_{10m}: degradation in air; T_{20m}: degradation in water; T_{40m}: degradation in sediment.

(a)

(b)
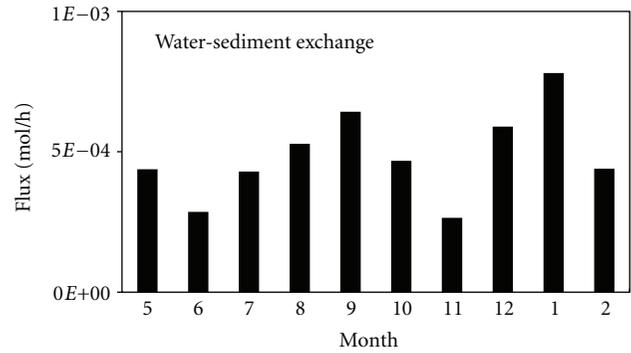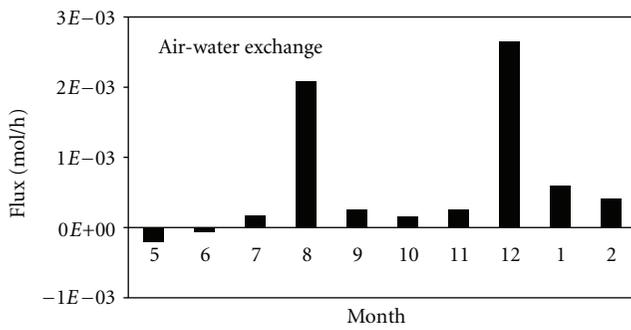
Figure 5: α-HCH fluxes over the air-water interface (a) and the water-sediment interface (b). The positive values indicate net inputs from air to water or from water to sediment.

the converse of the results observed in Lake Taihu. The main cause of this difference may be that the research in Lake Taihu did not include deposition from air to water. It is also worth noting that the α-HCH concentrations in the Lake Taihu atmosphere and water are $32 \pm 28\,\text{pg/m}^3$ and $1887 \pm 1372\,\text{pg/L}$, respectively, while in Lake Chaohu, the corresponding concentrations are $16 \pm 11\,\text{pg/m}^3$ and $423 \pm 395\,\text{pg/L}$, which are 50.0% and 22.4% of the values of Lake Taihu, respectively. The lower α-HCH concentration in the water of Lake Chaohu may be due to historically lower HCH pesticide usage. The results are also opposite from the findings for Lake Ontario [25]. Ridal et al. [25] proposed that, due to a reduction in the atmospheric concentration, the α-HCH flux in Lake Ontario has shifted from net settlement to net volatilization when compared with the years prior to 1990. For Chaohu, however, due to a reduction in the water α-HCH concentration, the air-water interface may have still been net settlement. Therefore, despite the net volatile flux in the summer, the annual net flux is from the gas to the water.

The flux from the water to the sediment was 0.022 t/a, and sedimentation (T_{24s}) accounted for 65.49% of this flux.

In addition, the flux from the sediment to the water was 0.010 t/a, and diffusion flux (T_{42d}) accounted for 73.28% of this flux. There was a net input from the water to the sediment (Figure 5). Although the sediment resuspension flux was 0.003 t/a, which accounted for 26.72% of the flux from the sediment to the water, this flux still reflects the strong resuspension process in Lake Chaohu [13].

In the sensitivity analysis, those parameters related to relatively important processes will always be observed with higher sensitivity (see Section 3.3).

3.3. Sensitivity Analysis. For the static parameters, the sensitivity coefficients changed significantly after correction with the coefficients of variation (Figure 6). Thus, despite the high sensitivities regarding $K_{oc}, r_{23}, r_{43}, B_{ps}, B_H, A_2$, and Sc, the corrected sensitivity coefficients for those parameters with lower variability were significantly reduced, such that these eight parameters were considered to be insensitive. The sensitivity reductions in K_{oc} and A_2 were also observed by Cao et al. [2]. In contrast, due to higher variability, the sensitivity coefficients of h_4, k_{m4}, k_{m2}, and L_4 increased after correction,
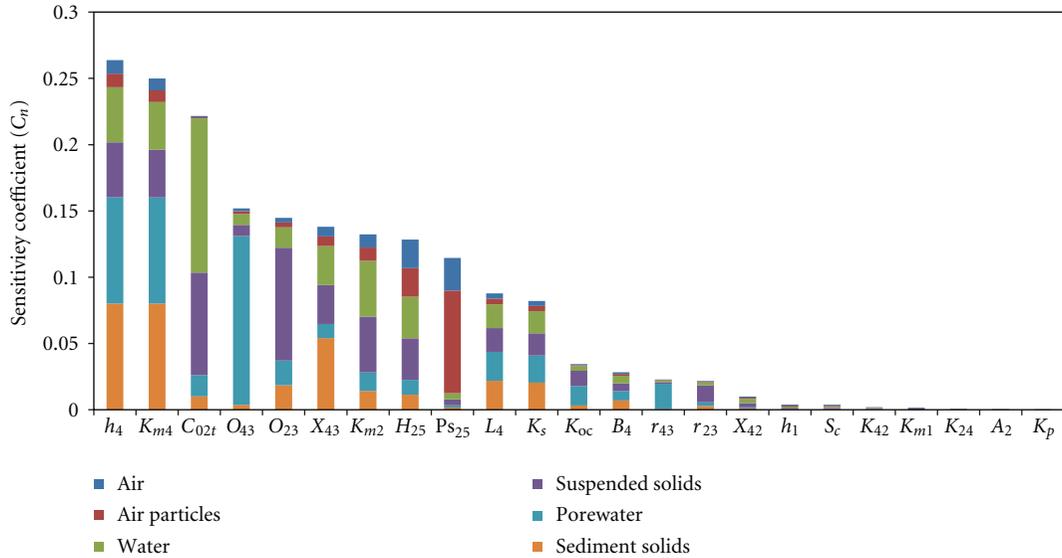
(a)
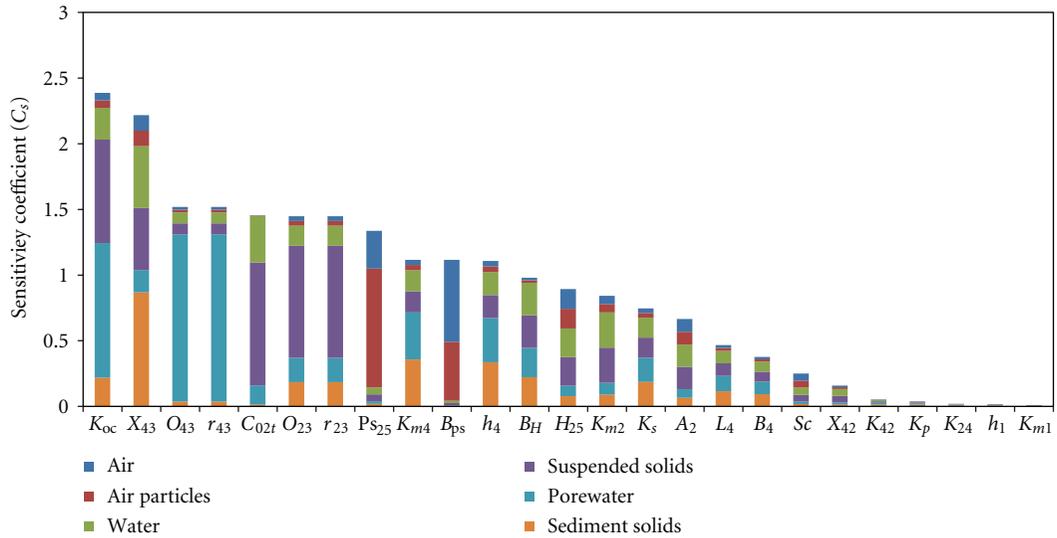
(b)

FIGURE 6: Coefficients of sensitivity of the calculated concentrations of the environmental compartments to the input static parameters with (C_n) (a) and without (C_s) (b) CV normalization.

and they were found to be important parameters. h_4 is related to sediment volume, and sediment is found as the sink for α-HCH in lakes; k_{m4} is directly related to the degradation of α-HCH in the sediments, which has been found to be the most important degradation process in the environment (Section 3.2). Thus, the two static parameters exerted considerable influence on the model results. L_4 and k_{m2} become more important parameters due to their high variability. Other parameters, including C_{02t}, O_{23}, O_{43}, X_{43}, Ps$_{25}$, and H_{25}, had relatively similar high sensitivity coefficients before and after correction. C_{02t} strongly affects the α-HCH content in the water and suspended matter. O_{23} and O_{43} determine the adsorption capacity of the particles in the suspended solids and sediments, while X_{43} is related to the amount

of sediment adsorption. Therefore, these parameters exert a great influence on the model output. Ps$_{25}$ determines the fugacity capacity of the atmospheric particulates [33], and H_{25} plays a decisive role in the fate of POPs in the environment [34]. Although the variability of these two parameters is negligible, the collected values in this study are based on the results from different time periods using different methods. Therefore, the sensitivities of these two parameters remain high after the correction.

Each of the parameters has a different influence on the various environmental compartments. For example, k_{m4} has a higher sensitivity coefficient for the sediment than for the water or atmosphere, while k_{m2} has the highest sensitivity coefficient for the water. Overall, the average values of C_n for
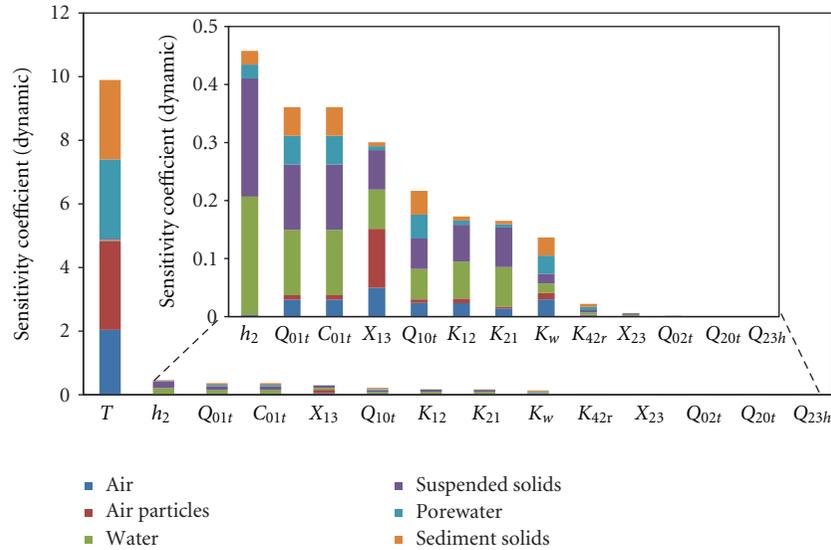
FIGURE 7: Dynamic coefficients of sensitivity of the calculated concentrations of the environmental compartments to the input dynamic parameters.

the air, water, and sediment were 1.17%, 2.78%, and 3.42%, respectively. Although water contains the most parameters among the three main phases [10], the sediment serves as an important sink for α-HCH and is influenced by all of the parameters to a greater extent than either the air or the water.

The dynamic sensitivity coefficients (SCV) are shown in Figure 7. The model output was much more sensitive to temperature (T) than to the other parameters because temperature had very strong effects on Ps and H, the two important parameters in the model. Consequently, temperature played a decisive role in the distribution of α-HCH between the gaseous and particulate phases as well as between the air and water [24]. In addition, h_2, Q_{01t}, Q_{10t}, C_{01t}, X_{13}, K_{12}, K_{21}, and K_w also had strong influences on the dynamic changes of the model output. h_2 strongly affected the variation of α-HCH concentrations in the water and suspended solids; Q_{01t}, Q_{10t}, and C_{01t} were associated with the atmospheric advection, which was the main source of the α-HCH in Lake Chaohu. Thus, the seasonal variations in these three parameters also had significant impacts. Cao et al. [2] found that the parameters related to source and degradation in the fugacity model were relatively more important, which was consistent with the relatively high sensitivities of Q_{01t}, Q_{10t}, C_{01t}, k_{m4}, and k_{m2}. X_{13} had a relatively strong influence on the seasonal changes in the concentration in the atmosphere and the water bodies as well as the particulate and suspended matter content, which is in agreement with the conclusion of the Pearl River Delta study [22]; K_{12}, K_{21}, and K_w were the main parameters influencing the air-water interface flux due to their direct impacts and significant seasonal variations, and these three parameters are also important parameters generally. In addition, due to the insignificant effect of water inflows on the model, parameters such as Q_{02t}, Q_{20t}, and Q_{23h} had little effect on the variability of the model output. Without considering

the biological phase, the importance of X_{23} was also reduced. The low sensitivity coefficient of K_{42r} was due to the corresponding low resuspension flux.

3.4. Uncertainty Analysis. The results of the uncertainty analysis for each phase are shown in Figure 8. It was found that the uncertainty of the model was relatively small from May to September, as represented by the small semi-interquartile ranges of the Monte Carlo simulation results. The uncertainty of the model output began to increase in October and peaked in December or January. This increase was attributed to our finding that from October to December, the coefficients of variation in the gas-water diffusion rate (K_{12} and K_{21}) significantly increased, leading to an increase of variation in the air-water diffusion flux. This also contributed to a significant increase in the uncertainty of the other phases. Lang et al. [22] similarly found that the coefficient of variability of diffusion is associated with wide variability in the gaseous PAHs concentrations. The rates of diffusion across the gas-water interface (K_{12} and K_{21}) were related to wind speed and water depth, and the coefficient of variation of water depth (h_2) did not increase during October–December. It can be speculated that elevated variation in the wind speed in this period causes the increasing uncertainty.

4. Conclusions

A dynamic quantitative water, air, and sediment interaction (QWASI) fugacity model was utilized to simulate the fate and seasonal variations of α-HCH in the air, water, and sediment, as well as various environmental fluxes in Lake Chaohu. The calculated and measured values of the model were in good agreement. However, disregarding the effects of aquatic organisms resulted in large deviations between

(a)

(b)

(c)

(d)

(e)

(f)
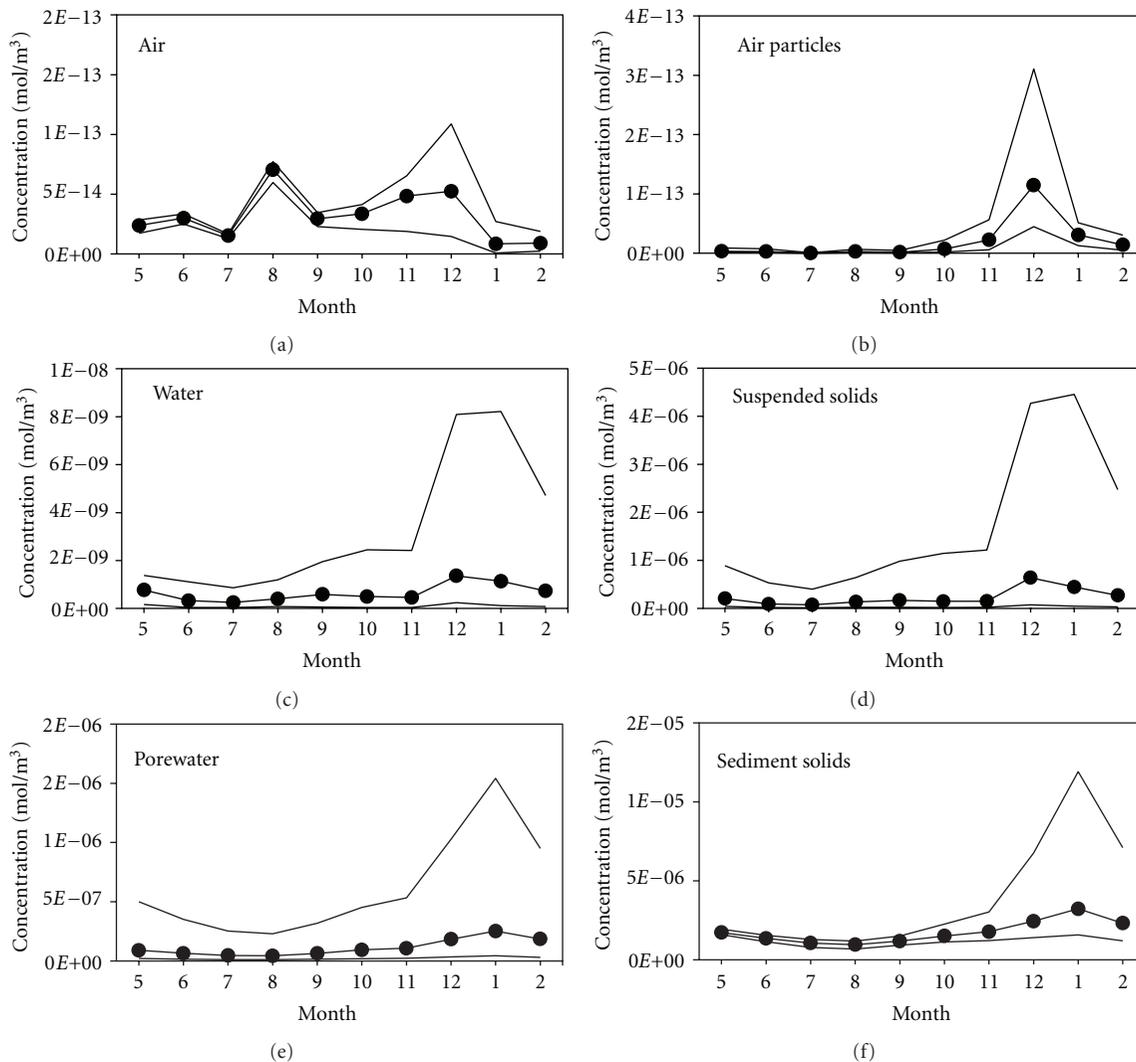
Figure 8: Uncertainties of the predicted seasonal variations of α-HCH concentrations in various environmental media. The results are presented as median values (lines with dots) and semi-interquartile ranges (solid lines).

the simulated and measured values of α-HCH in suspended solids in water. The major source of α-HCH in Lake Chaohu was an input from atmospheric advection, while the major environmental outputs were atmospheric advection and sediment degradation. The net annual input of α-HCH into the lake area was approximately 0.294 t, while the net output was approximately 0.412 t. The factors leading to the seasonal variations of α-HCH in various compartments were revealed. For the fluxes at the air-water interface, atmospheric inputs into the water were dominant for most of the year with the deposition processes included, while the water and sediment interface was mainly influenced by the net input from the water to the sediment. Thus, sediment is an important sink for α-HCH. Sensitivity analysis found that parameters of source and degradation were more important than the other parameters. The sediment was influenced more by the combined effects of the various parameters than air and water were. In addition, temperature variation had a much greater impact on the dynamics of the model output than

other dynamic parameters. Uncertainty analysis showed that the model uncertainty was relatively low, especially in the first half of the simulation period. Due to the increase in the gas-water diffusion flux variability, uncertainty of the model significantly increased for all of the compartments.

Acknowledgments

References

[1] Stockholm Convention on persistent organic pollutants (SCPOPs), 2009, The Nine New POPs: an introduction to the nine chemicals added to the Stockholm Convention by the

Conference of the Parties at its fourth meeting, http://chm.pops.int/Programmes/NewPOPs/Publications/tabid/695/ctl/Download/mid/2784/language/en-US/Default.aspx?id=2.

[2] H. Cao, S. Tao, F. Xu et al., "Multimedia fate model for hexachlorocyclohexane in Tianjin, China," *Environmental Science and Technology*, vol. 38, no. 7, pp. 2126–2132, 2004.

[3] D. Mackay, *Multimedia Environmental Models: The Fugacity Approach*, Lewis Publishers, NewYork, NY, USA, 2nd edition, 2001.

[4] D. Mackay, "Finding fugacity feasible," *Environmental Science and Technology*, vol. 13, no. 10, pp. 1218–1223, 1979.

[5] D. Mackay and S. Paterson, "Calculating fugacity," *Environmental Science and Technology*, vol. 15, no. 9, pp. 1006–1014, 1981.

[6] D. Mackay and S. Paterson, "Fugacity revisited," *Environmental Science and Technology*, vol. 16, no. 12, pp. A654–A660, 1982.

[7] F. Wania and D. Mackay, "A global distribution model for persistent organic chemicals," *Science of the Total Environment*, vol. 160-161, pp. 211–232, 1995.

[8] Z. Liu, X. Quan, and F. Yang, "Long-term fate of three hexachlorocyclohexanes in the lower reach of Liao River basin: dynamic mass budgets and pathways," *Chemosphere*, vol. 69, no. 7, pp. 1159–1165, 2007.

[9] S. Tao, H. Cao, W. Liu et al., "Fate modeling of phenanthrene with regional variation in Tianjin, China," *Environmental Science and Technology*, vol. 37, no. 11, pp. 2453–2459, 2003.

[10] S. Tao, Y. Yang, H. Y. Cao et al., "Modeling the dynamic changes in concentrations of γ- hexachlorocyclohexane (γ-HCH) in Tianjin region from 1953 to 2020," *Environmental Pollution*, vol. 139, no. 1, pp. 183–193, 2006.

[11] D. Mackay, M. Joy, and S. Paterson, "A quantitative water, air, sediment interaction (QWASI) fugacity model for describing the fate of chemicals in lakes," *Chemosphere*, vol. 12, no. 7-8, pp. 981–997, 1983.

[12] J. Paasivirta, S. Sinkkonen, P. Mikkelson, T. Rantio, and F. Wania, "Estimation of vapor pressures, solubilities and Henry's law constants of selected persistent organic pollutants as functions of temperature," *Chemosphere*, vol. 39, no. 5, pp. 811–832, 1999.

[13] Q. Y. Tu, D. X. Gu, C. Q. Yi, Z. R. Xu, and G. Z. Han, *The Researches on the Lake Chaohu Eutrophication*, University of Science and Technology of China, Hefei, China, 1990.

[14] China Meteorological Data Sharing Service System (CMDSSS), 2010-2011. Daily Meteorological Data, http://www.cma.gov.cn/2011qxfw/2011qsjgx/index.htm.

[15] D. L. Carlson, I. Basu, and R. A. Hites, "Annual variations of pesticide concentrations in great lakes precipitation," *Environmental Science and Technology*, vol. 38, no. 20, pp. 5290–5296, 2004.

[16] G. R. Southworth, "The role of volatilization in removing polycyclic aromatic hydrocarbons from aquatic environments," *Bulletin of Environmental Contamination and Toxicology*, vol. 21, no. 4-5, pp. 507–514, 1979.

[17] D. Mackay and S. Paterson, "Evaluating the multimedia fate of organic chemicals: a level III fugacity model," *Environmental Science and Technology*, vol. 25, no. 3, pp. 427–436, 1991.

[18] W. X. Liu, W. He, N. Qin et al., "Residues, distributions, sources and ecological risks of OCPs in the water from Lake Chao, China," *The Scientific World Journal*, vol. 2012, Article ID 897697, 16 pages, 2012.

[19] H. L. Ouyang, W. He, N. Qin et al., "Levels temporal-spatial variations and sources of organochlorine pesticides in ambient air of Lake Chaohu, China," *The Scientific World Journal*, vol. 2012, Article ID 504576, 12 pages, 2012.

[20] Y. Wang, W. He, N. Qin, and Q. S. He, "Residual levels and ecological risks of organochlorine pesticides in surface sediments from Lake Chaohu," *Acta Scientiae Circumstantiae*, vol. 32, no. 2, pp. 308–316, 2012 (Chinese).

[21] M. D. Morris, "Factorial sampling plans for preliminary computational experiments," *Technometrics*, vol. 33, no. 2, pp. 161–174, 1991.

[22] C. Lang, S. Tao, X. Wang, G. Zhang, J. Li, and J. Fu, "Seasonal variation of polycyclic aromatic hydrocarbons (PAHs) in Pearl River Delta region, China," *Atmospheric Environment*, vol. 41, no. 37, pp. 8370–8379, 2007.

[23] J. Dachs, S. J. Eisenreich, J. E. Baker, F. C. Ko, and J. D. Jeremiason, "Coupling of phytoplankton uptake and air-water exchange of persistent organic pollutants," *Environmental Science and Technology*, vol. 33, no. 20, pp. 3653–3660, 1999.

[24] K. Walker, D. A. Vallero, and R. G. Lewis, "Factors influencing the distribution of lindane and other hexachlorocyclohexanes in the environment," *Environmental Science and Technology*, vol. 33, no. 24, pp. 4373–4378, 1999.

[25] J. J. Ridal, B. Kerman, L. Durham, and M. E. Fox, "Seasonally of air-water fluxes of hexachlorocyclohexanes in lake Ontario," *Environmental Science and Technology*, vol. 30, no. 3, pp. 852–858, 1996.

[26] X. Zheng, D. Chen, X. Liu et al., "Spatial and seasonal variations of organochlorine compounds in air on an urban-rural transect across Tianjin, China," *Chemosphere*, vol. 78, no. 2, pp. 92–98, 2010.

[27] Y. F. Li, R. W. Macdonald, L. M. M. Jantunen, T. Harner, T. F. Bidleman, and W. M. J. Strachan, "The transport of β-hexachlorocyclohexane to the western Arctic Ocean: a contrast to α-HCH," *Science of the Total Environment*, vol. 291, no. 1–3, pp. 229–246, 2002.

[28] J. E. Haugen, F. Wania, N. Ritter, and M. Schlabach, "Hexachlorocyclohexanes in air in southern Norway. Temporal variation, source allocation, and temperature dependence," *Environmental Science and Technology*, vol. 32, no. 2, pp. 217–224, 1998.

[29] P. Xie, *Reading about the Histories of Cyanobacteria, Eutrophication and Geological Evolution in Lake Chaohu*, Science Press, Beijing, China, 2009.

[30] N. Berrojalbiz, J. Dachs, S. Del Vento et al., "Persistent organic pollutants in mediterranean seawater and processes affecting their accumulation in plankton," *Environmental Science and Technology*, vol. 45, no. 10, pp. 4315–4322, 2011.

[31] S. del Vento and J. Dachs, "Prediction of uptake dynamics of persistent organic pollutants by bacteria and phytoplankton," *Environmental Toxicology and Chemistry*, vol. 21, no. 10, pp. 2099–2107, 2002.

[32] X. Qiu, T. Zhu, F. Wang, and J. Hu, "Air-water gas exchange of organochlorine pesticides in Taihu Lake, China," *Environmental Science and Technology*, vol. 42, no. 6, pp. 1928–1932, 2008.

[33] D. Mackay, S. Paterson, and W. H. Schroeder, "Model describing the rates of transfer processes of organic chemicals between atmosphere and water," *Environmental Science and Technology*, vol. 20, no. 8, pp. 810–816, 1986.

[34] M. Odabasi, B. Cetin, E. Demircioglu, and A. Sofuoglu, "Air-water exchange of polychlorinated biphenyls (PCBs) and organochlorine pesticides (OCPs) at a coastal site in Izmir Bay, Turkey," *Marine Chemistry*, vol. 109, no. 1-2, pp. 115–129, 2008.

The **S**cientificWorldJOURNAL

Research Article

Residues, Distributions, Sources, and Ecological Risks of OCPs in the Water from Lake Chaohu, China

Wen-Xiu Liu, Wei He, Ning Qin, Xiang-Zhen Kong, Qi-Shuang He, Hui-Ling Ouyang, Bin Yang, Qing-Mei Wang, Chen Yang, Yu-Jiao Jiang, Wen-Jing Wu, and Fu-Liu Xu

MOE Laboratory for Earth Surface Processes, College of Urban and Environmental Sciences, Peking University, Beijing 100871, China

Correspondence should be addressed to Fu-Liu Xu, xufl@urban.pku.edu.cn

The levels of 18 organochlorine pesticides (OCPs) in the water from Lake Chaohu were measured by a solid phase extraction-gas chromatography-mass spectrometer detector. The spatial and temporal distribution, possible sources, and potential ecological risks of the OCPs were analyzed. The annual mean concentration for the OCPs in Lake Chaohu was 6.99 ng/L. Aldrin, HCHs, and DDTs accounted for large proportions of the OCPs. The spatial pollution followed the order of Central Lakes > Western Lakes > Eastern Lakes and water area. The sources of the HCHs were mainly from the historical usage of lindane. DDTs were degraded under aerobic conditions, and the main sources were from the use of technical DDTs. The ecological risks of 5 OCPs were assessed by the species sensitivity distribution (SSD) method in the order of heptachlor > γ-HCH > p,p′-DDT > aldrin > endrin. The combining risks of all sampling sites were MS > JC > ZM > TX, and those of different species were crustaceans > fish > insects and spiders. Overall, the ecological risks of OCP contaminants on aquatic animals were very low.

1. Introduction

As typical persistent organic pollutants (POPs), organochlorine pesticides (OCPs) were widely used and have threatened the ecosystem and human health due to the need for pest control. There are 15 OCPs in the list produced by the Stockholm Convention on Persistent Organic Pollutants, which forbids the production and use of 22 of chemical substances, including DDT, chlordane, mirex, aldrin, dieldrin, endrin, hexachlorobenzene, heptachlor, toxaphene, α-HCH, β-HCH, lindane (γ-HCH), chlordecone (kepone), pentachlorobenzene, and endosulfan [1, 2]. Although these OCPs have been banned (especially DDT) and the residual levels have gradually decreased since the 1980s, OCPs can still be detected in various environmental and biological media [3–5].

OCPs can enter the water, one of the environmental media that is most vulnerable to OCP contaminants through a variety of routes, such as surface runoff and atmospheric wet and dry deposition. At present, there are residues of OCPs in the surface water including rivers, lakes, and oceans,

such as the Küçük Menderes River in Turkey [6], the Ebro River in Spain [7], the Gomti River in India [8], and the section from the Sea of Japan to the Bering Sea [9]. There has also been much research on the distribution of organochlorine pesticides in the environment, such as that in the Huaihe River [10], the Pearl River [11], the Guanting Reservoir in Beijing [12], and Lake small Baiyangdian [13]. The residue concentrations in these regions were different.

Lake Chaohu, located in the center of Anhui Province (Figure 1), is the fifth-largest freshwater lake in China, with a water area of approximately 760 km^2. In addition to the development of fisheries and agricultural irrigation, Lake Chaohu is also the drinking water source for the 9.6 million residents in the surrounding areas, and the water quality will affect the health and safety of the residents directly. Therefore, this study on the residual levels of the organochlorine pesticides (especially HCHs and DDTs), their spatial and temporal distributions, the source analysis, and the ecological risks will not only contribute to understanding the environmental behavior and potential hazards of persistent toxic pollutants but also provide the necessary theoretical
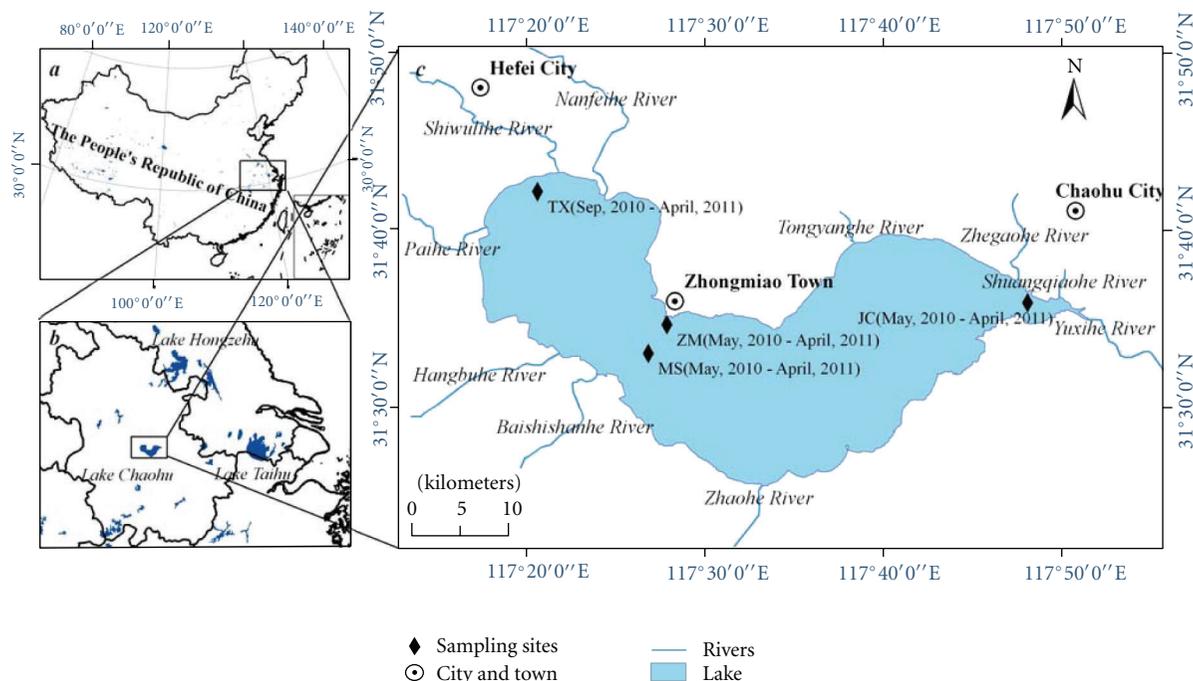
FIGURE 1: The location of Lake Chaohu and the distribution of the sampling sites.

basis for persistent toxic pollution prevention and lake environmental management.

2. Materials and Methods

2.1. Measurement of OCPs in the Water. The water samples were collected from May 2010 to February 2011 monthly, and the distribution of the sample sites is shown in Figure 1. The MS and ZM are located at 200 meters south of the Zhongmiao Temple and 200 meters east of Mushan Island, respectively; the JC and TX represent the city water intake near the Chaohu automatic monitoring station and western TangXi, 150 meters south of the intake of original waterworks, respectively.

The surface, middle, and bottom water samples were collected separately and then mixed together. In the sampling sites having depths of more than 1 meter, the water samples were collected from the surface water (0–0.15 m below the surface), the midwater (0.5–0.65 m below surface), and, the bottom water (0–0.15 m above the sediment) and mixed. In the sites having depths of less than 1 meter, the surface water and the bottom water were collected and mixed. The water samples were stored in brown glass jars that were washed with deionized water and the water samples before use. From each site, 1 liter of water was collected.

As a recovery indicator, 100 ng 1-Bromo-2-nitrobenzene was added to the water samples, which were then filtered through a glass fiber filter (ashed at 450°C for 4 h) using a peristaltic pump (80EL005, Millipore Co., USA) and a filter plate with a 142 mm diameter to remove the suspended particles. A solid phase extraction system was used to extract the filtered water samples. Before extraction, the octadecylsilane

SPE cartridges (SPE, C18, 6 mL, 500 mg, Supelco, Co., USA) were first washed with 6 mL dichloromethane and conditioned with 6 mL methanol and 6 mL ultrapure water, and the cartridges were not dried before loading the samples. After the activation, the water samples were loaded using a large volume sampler (Supelco Co., USA) that was connected to the SPE vacuum manifold (Supelco Co., USA), and the cartridges were dried by vacuum pump after the extraction step. The SPE cartridges were sealed and delivered back to laboratory prior to the elution and purification.

Each cartridge was connected to an anhydrous sodium sulfate (5 g) cartridge and eluted using DCM (three times, 6 mL per elution). The extracts were concentrated to approximately 1 mL with a vacuum rotary evaporator (Eyela N-1100, Tokyo Rikakikai Co., Japan). The solvent was changed to hexane, and then the samples were again concentrated to approximately 1 mL. PCNB (pentachloronitrobenzene) was added to the sample as an internal standard. The samples were concentrated to 10 μL with flowing nitrogen, transferred to micro volume inserts, and sealed until analysis.

The samples were analyzed using an Agilent 7890A-5975C gas chromatography and mass spectrometer detector and a HP-5MS fused silica capillary column (30 m × 0.25 mm × 0.25 μm, Agilent Co., USA). Helium was used as the carrier gas at a flow rate of 1 mL/min. Samples (1 μL) were injected by the autosampler under a splitless mode at a temperature of 220°C. The oven temperature program was the following: 50°C for 2 min, 10°C/min to 150°C, 3°C/min for 240°C, 240°C for 5 min, 10°C/min for 300°C, and 300°C for 5 min. The ion source temperature of the mass spectrometer was 200°C, the temperature of the transfer line was 250°C, and the temperature of the quadrupole was

TABLE 1: The method recoveries and the instrument detection limits.

Pollutants	Recovery %	Detection limit (ng/mL)
α-HCH	100.4	0.05
β-HCH	99.1	0.05
γ-HCH	88.7	0.06
δ-HCH	90.3	0.06
o,p$'$-DDE	87.1	0.2
p,p$'$-DDE	60.4	0.18
o,p$'$-DDD	80.1	0.06
p,p$'$-DDD	84.2	0.59
o,p$'$-DDT	66.4	1.2
p,p$'$-DDT	84.6	0.07
HCB	54.0	0.01
Heptachlor	68.0	0.1
Aldrin	71.6	0.07
Isodrin	74.7	0.03
γ-chlordane	66.6	0.1
Endosulfan I	89.4	0.06
Endosulfan II	95.7	0.05
Endrin	107.4	0.47

150°C. The compounds were quantified in the selected ion mode, and the calibration curve was quantified with the internal standard.

There were two parallel samples in each sampling site. The samples, the method blanks, and the procedure blanks were prepared in the same manner. The test for recovery and the detection limit of the method should be performed before the sample analysis (Table 1).

2.2. Ecological Risk Assessment. In this study, the species sensitivity distribution (SSD) model was applied to evaluate the separate and combining ecological risks of typical OCPs, following these basic steps: (1) toxicological data acquisition and processing, (2) SSD curve construction, (3) calculation of the potentially affected fraction (PAF) to assess the ecological risk of a single pollutant, and (4) calculation of the multiple substances potentially affected fraction (msPAF) to assess the combining risks of multiple pollutants [14, 15].

2.2.1. Toxicity Data Acquisition and Processing. Acute toxicity data (such as LC50 and EC50) or chronic toxicity data (NOEC) can be used to conduct an SSD curve, and in this study, acute toxicity data were used due to the lack of chronic toxicity data for OCPs. The toxicity data were collected from the ECOTOX database (http://www.epa.gov/ecotox/), and the search criteria included the LC50 endpoint, the exposure duration of less than 10 days, and the type of freshwater and tests in laboratories, and all species were considered. Because of the differences between the personnel and laboratory environment, there are many toxicity data on the same pollutant for the same species. In this study, the data point was the geometric mean of the toxicity data for the same species [16]. To understand the ecological risks to different types of freshwater organisms comprehensively,

the toxicity data for the OCPs were classified into three patterns: (1) all species were not subdivided, (2) all species were subdivided into vertebrates and invertebrates, and (3) three subcategories for which the toxicity data were rich were selected, which included fish, insects and spiders, and crustaceans. According to the availability of the OCP toxicity data and the levels of exposure to the water of Lake Chaohu, this study selected five typical OCPs, which were p,p$'$-DDT, γ-HCH, heptachlor, aldrin, and endrin, to assess the ecological risks. Table 2 shows the statistical characteristics of the toxicity data.

2.2.2. SSD Curve Fitting. The basic assumption of the SSD is that the toxicity data of the pollutants can be described by a mathematical distribution and that the available toxicity data are considered as a sample from the distribution that can be used to estimate the parameters of the distribution [17]. First, the species toxicity data (e.g., LC50 or NOEC) were sorted according to the concentration values (μg/L), and the cumulative probabilities of each species were calculated in accordance with the following formula [18, 19]:

$$\text{Cumulative Probabilities} = \frac{i}{n+1}, \qquad (1)$$

where i is the rank of species sorting and n is the sample size. Then, after placing the concentrations on the X-axis and the cumulative probabilities on the Y-axis in the coordinate system, these toxicity data points are marked according to the exposure concentration and cumulative probability of different organisms and fitted on the SSD curves by selecting a distribution. There are a variety of models, including parametric methods such as lognormal, log-logistic, and Burr III [20–22] and nonparametric methods such as bootstrapping [23]. At present, there is no principle for choosing the method when fitting an SSD curve because no research can prove to which specific curve form that the SSD belongs. Therefore, different researchers may choose different fitting methods [21]; for example, the researchers in the US and Europe recommended using a lognormal distribution to conduct the SSD curves, whereas others in Australia and New Zealand recommended the Burr III. Taking into account that the Burr III type requires less data and has a flexible distribution pattern that can be flexibly converted into ReWeibull and Burr III, depending on the size of the parameter values, and be conducted well using the species toxicity data [14], this study used a Burr III distribution to fit the SSD curves. In this paper, the software BurrliOZ, which was designed by Australia's Commonwealth Scientific and Industrial Research Organization (CSIRO) [24], was employed to fit the SSD curves and calculate the relevant parameters. Five OCP SSD curves for vertebrates, invertebrates, fish, crustaceans, and insects and spiders are shown in Figure 2.

2.2.3. Calculation of the Single Pollutant's PAF. The PAF of the single pollutant can be calculated by the following Burr III equation:

$$F(x) = \frac{1}{\left[1 + (b/x)^c\right]^k}, \qquad (2)$$

TABLE 2: The statistical characteristics of the log-transformed toxicity data for typical OCPs (μg/L).

	p,p′-DDT			γ-HCH			Heptachlor		
	Numbers	Mean	SD	Numbers	Mean	SD	Numbers	Mean	SD
All species	151	1.782	1.148	122	2.323	1.068	48	2.08	1.11
Vertebrates	62	1.802	1.083	60	2.475	0.896	32	2.11	0.65
Invertebrates	89	1.769	1.196	62	2.175	1.201	16	1.79	0.93
Fishes	57	1.678	1.022	54	2.352	0.854	31	2.09	0.65
Crustaceans	28	1.496	1.127	20	2.048	1.151	8	1.67	0.48
Insects and spiders	50	1.516	0.939	28	1.509	0.663	6	1.48	1.14

	Aldrin			Endrin		
	Numbers	Mean	SD	Numbers	Mean	SD
All species	55	2.08	1.11	83	83	83
Vertebrates	31	1.72	0.66	46	46	46
Invertebrates	24	2.54	1.39	37	37	37
Fishes	29	1.64	0.58	40	40	40
Crustaceans	13	2.59	1.71	10	10	10
Insects and spiders	6	1.71	0.55	21	21	21

SD = Standard deviation.

where x is the concentration of the pollutant (μg/L) in the environment and b, c, and k are the three parameters of the model (the same as below). When k tends to infinity, the Burr III distribution model transforms into a ReWeibull distribution model:

$$F(x) = \exp\left(-\frac{b}{x^c}\right). \quad (3)$$

When c tends to infinity, it transforms into a RePareto distribution:

$$F(x) = \left(\frac{x}{x_0}\right)^{\theta}, \quad I\{x \leq x_0\} \ (x_0, \theta > 0). \quad (4)$$

The parameters are calculated by the BurrliOZ program. When k is greater than 100 or c is greater than 80, the software will use ReWeibull or RePareto to calculate the relevant parameters automatically. The fitting parameters for p,p′-DDT, γ-HCH, heptachlor, aldrin, and endrin are given in Table 3.

2.2.4. The Calculation of mSPAF. The advantage of the SSD is that the mSPAF can be calculated and consequently the combining ecological risks of multiple pollutants can be evaluated. According to the toxic mode of action (TMoA) by different pollutants, the mSPAF was calculated using concentration addition or response addition [25]. In this study, the TMoAs of the five OCPs were different, and thus the response addition was adopted. The equation is as follows:

$$\text{mSPAF} = 1 - (1 - \text{PAF}_1)(1 - \text{PAF}_2) \cdots (1 - \text{PAF}_n). \quad (5)$$

3. Results and Discussion

3.1. The Residues of OCPs in the Water. Eighteen OCPs were found in the water from Lake Chaohu (Table 4),

which were the following: HCH isomers (α-, β-, γ-, and δ-HCH), DDT and its metabolites (o,p′-, p,p′-DDE, DDT and DDD), heptachlor, hexachlorobenzene (HCB), aldrin, isodrin, endosulfan isomers (endosulfan I, endosulfan II), γ-chlordane, and endrin. The annual mean concentration of the region's total OCPs was 6.99 ng/L, and the arithmetic mean was 7.14 ± 4.19 ng/L. The detection rates of aldrin, HCB, α-HCH, β-HCH, and γ-HCH were 100%, while the rates of γ-chlordane and endrin were less than 50%; the rates of the other pollutants ranged from 64.86% to 97.3%. The residual level of aldrin (2.83 ± 2.87 ng/L) was the highest, followed by the DDTs (1.91 ± 1.92 ng/L) and the HCHs (1.76 ± 1.54 ng/L); together, these residual levels accounted for 91% of the total OCPs. The residual levels of the pollutants are illustrated in Figure 3.

Compared with other studies, the level of aldrin in Lake Chaohu was lower than that in the Pearl River artery estuary during the low flow season (4.17 ± 3.07 ng/L) [11], the Karst Subterranean River in Liuzhou (9.22 ± 1.90 ng/L) [26], and the Kucuk Menderes River in Turkey (17–1790 ng/L) [6], higher than that in the Changsha section of the Xiangjiang River (0.22–0.51 ng/L) [27] and the Wuhan section of the Yangtze River (1.88 ng/L) [28], and comparable with that in the Huaxi River in Guizhou (2.079 ng/L) [29] and the Guanting Reservoir in Beijing (2.26 ± 2.84 ng/L) [30]. The levels of HCHs were similar to those in Lake Baiyangdian (2.1 ± 0.8 ng/L) [31], considerably lower than those in the Qiantang River in Zhejiang (33.07 ± 14.64 ng/L) [32], the Chiu-lung River in Fujian (71.1 ± 85.5 ng/L) [33], and the Kucuk Menderes River in Turkey (187–337 ng/L) [6], and higher than those in Meiliang Bay in Lake Taihu (>0.4 ng/L) [34], Lake Co Ngoin in Tibet (0.3 ng/L) [35], and Lake Baikal in Russia (0.056–0.96 ng/L) [36]. The concentrations of DDTs were also at low levels, which were roughly equal to those in the Nanjing section of the Yangtze River (1.57–1.79 ng/L) [37] and lower than those in the Guanting
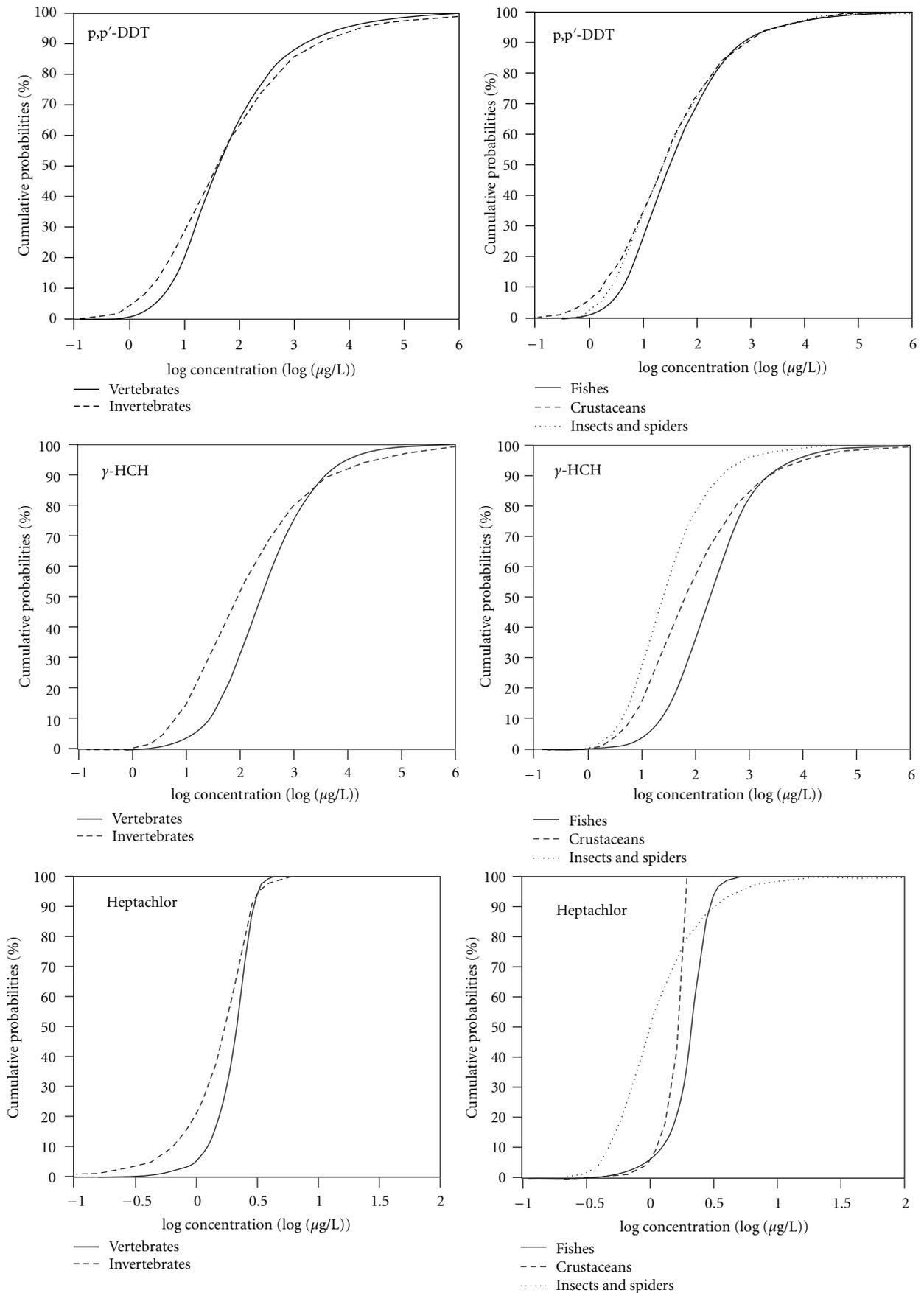
Figure 2: Continued.
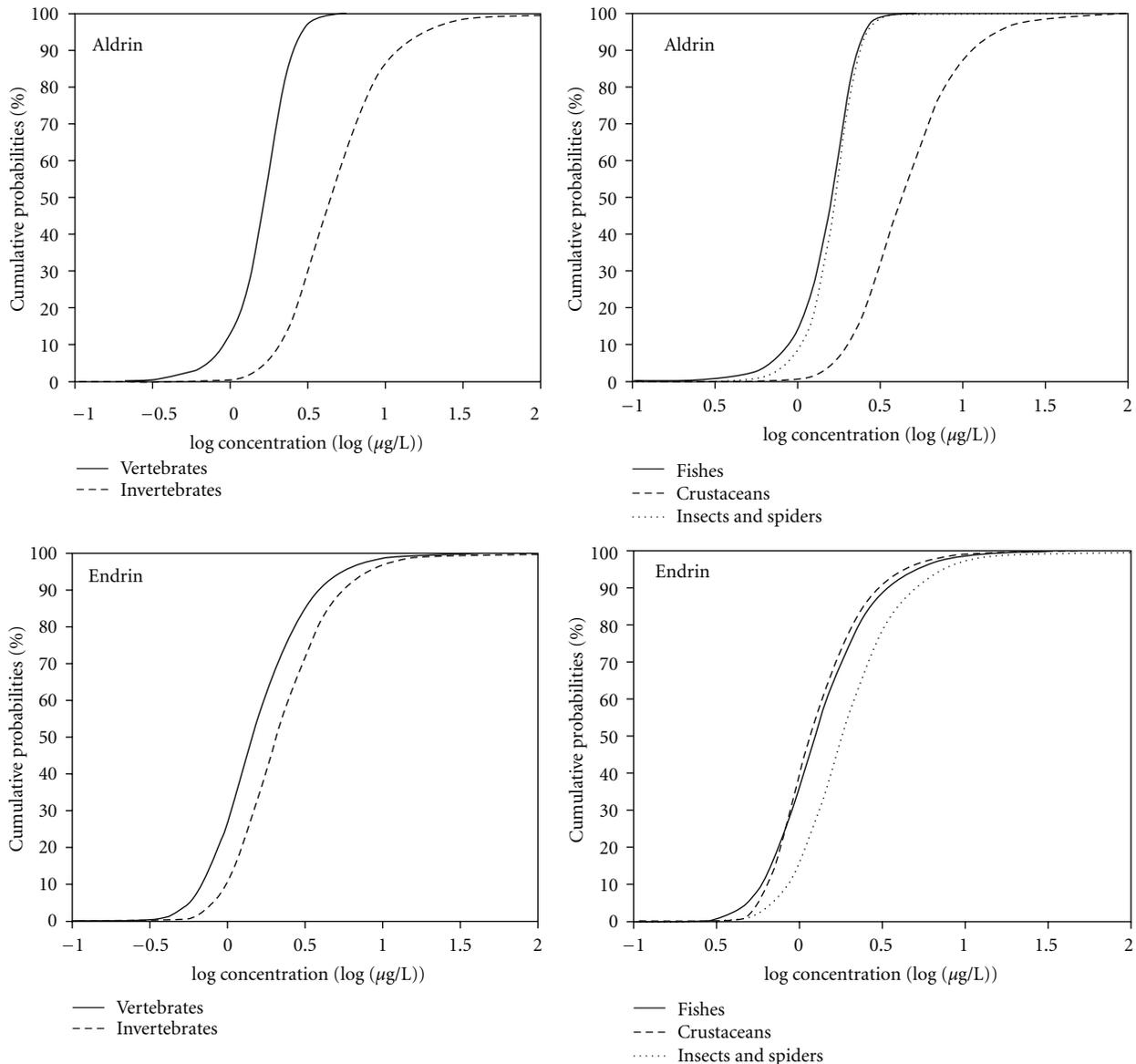
FIGURE 2: The SSD curves of typical OCPs for different species.

Reservoir (3.71–16.03 ng/L) [38], the Huangpu River (3.83–20.90 [11.97] ng/L) [39], the Pearl River artery estuary during the low flow season (5.85–9.53 ng/L) [11], the Kucuk Menderes River in Turkey (ND-120 ng/L) [6], and the Lake Baikal in Russia (ND-0.015 μg/L) [36].

3.2. The Spatial and Temporal Distribution of OCPs in the Water. The changes in the concentrations of the total OCPs and the three main pollutants (HCHs, DDTs, and aldrin) in Lake Chaohu and the three subregions from May 2010 to February 2011 are shown in Figure 4. There were similar trends for the OCPs over time both in the entire lake and in the Central Lake. The OCP levels increased jaggedly from May to September, and the peak was in September. Then, the residues declined rapidly, reached the bottom in November, and rose again from December to February. The trend in

the Western Lake from September to February was the same, but the trend in the Eastern Lake was different. One of the main causes was that the concentrations of DDT in July were excessive, resulting in the higher OCPs from the Eastern Lake in July than that in the other months. There was presumably a temporary point source pollution in July. Moreover, the high values of aldrin both in the Western and the Central Lake in September, which were not observed in the Eastern Lake, made the overall trends of the Eastern Lake different from the other subregions.

Ten months were divided into four seasons, with spring just using the data of May as a reference. The concentrations of HCHs in the four seasons were 1.44 ng/L, 1.25 ng/L, 1.19 ng/L, and 2.81 ng/L, and the concentrations of DDTs were 3.61 ng/L, 3.75 ng/L, 1.53 ng/L, and 0.24 ng/L. The variable trends of the HCHs and the DDTs were similar

Table 3: The parameters of SSD curves calculated by BurrliOZ.

	p,p′-DDT				Lindane (γ-HCH)			
	Fitted curve	Parameters and values			Fitted curve	Parameters and values		
All species	Burr III	0.082(b)	0.489(c)	14.626(k)	Burr III	2.519(b)	0.515(c)	6.043(k)
Vertebrates	ReWeibull	5.146(b)	0.541(c)		Burr III	58.638(b)	0.708(c)	2.259(k)
Invertebrates	Burr III	0.146(b)	0.468(c)	9.786(k)	ReWeibull	5.450(b)	0.456(c)	
Fishes	ReWeibull	5.365(b)	0.593(c)		Burr III	57.899(b)	0.784(c)	2.085(k)
Crustaceans	Burr III	1.960(b)	0.577(c)	3.214(k)	ReWeibull	6.430(b)	0.526(c)	
Insects and spiders	ReWeibull	3.906(a)	0.551(b)		Burr III	1.560(b)	0.780(c)	6.655(k)

	Heptachlor				Aldrin			
	Fitted curve	Parameters and values			Fitted curve	Parameters and values		
All species	Burr III	2.704(b)	8.188(c)	0.280(k)	Burr III	1.860(b)	2.000(c)	3.000(k)
Vertebrates	Burr III	2.614(a)	8.839(b)	0.357(k)	Burr III	2.086(b)	6.654(c)	0.413(k)
Invertebrates	Burr III	2.586(b)	5.919(c)	0.284(k)	Burr III	2.230(b)	2.000(c)	3.000(k)
Fishes	Burr III	2.490(b)	7.902(c)	0.429(k)	Burr III	2.042(b)	8.036(c)	0.343(k)
Crustaceans	RePareto	2.000(x_0)	4.093(θ)		Burr III	2.180(b)	2.000(c)	3.000(k)
Insects and spiders	ReWeibull	0.699(b)	1.636(c)		Burr III	1.956(b)	7.174(c)	0.521(k)

	Endrin			
	Fitted curve	Parameters and values		
All species	Burr III	0.987(b)	2.000(c)	3.000(k)
Vertebrates	Burr III	0.724(b)	2.000(c)	3.000(k)
Invertebrates	Burr III	1.041(b)	2.000(c)	3.000(k)
Fishes	Burr III	0.634(b)	2.000(c)	3.000(k)
Crustaceans	ReWeibull	0.957(b)	2.011(c)	
Insects and spiders	Burr III	0.924(b)	2.000(c)	3.000(k)

The letter in parentheses mean the parameters b, c, k, x_0, and θ.

Table 4: The residual levels of OCPs in the water from Lake Chaohu (ng/L).

|	SD	Maximum	Minimum	Arithmetic mean	Geometric mean	Detection rate
α-HCH	0.53	2.40	0.11	0.47	0.33	100.00%
β-HCH	0.51	2.19	0.36	0.92	0.80	100.00%
γ-HCH	0.38	1.77	0.06	0.29	0.19	100.00%
δ-HCH	0.13	0.60	N.D.	0.08	0.06	83.78%
HCHs	1.45	6.92	0.55	1.76	1.41	100.00%
o,p′-DDE	1.93	7.03	N.D.	1.42	1.01	62.16%
p,p′-DDE	0.04	0.16	N.D.	0.02	0.03	32.43%
o,p′-DDD	0.08	0.38	N.D.	0.03	0.18	16.22%
p,p′-DDD	0.22	1.06	N.D.	0.06	0.07	24.32%
o,p′-DDT	0.46	2.32	N.D.	0.16	0.15	35.14%
p,p′-DDT	0.30	1.15	N.D.	0.23	0.30	62.16%
DDTs	1.92	7.03	N.D.	1.91	1.10	97.30%
HCB	0.08	0.35	0.06	0.17	0.15	100.00%
Heptachlor	0.25	1.09	N.D.	0.17	0.15	64.86%
Aldrin	2.87	12.22	0.15	2.83	1.76	100.00%
Isodrin	0.17	0.63	N.D.	0.16	0.12	91.89%
γ-chlodane	0.02	0.14	N.D.	0.01	0.01	32.43%
Endosulfan I	0.03	0.15	N.D.	0.02	0.03	62.16%
Endosulfan II	0.45	2.70	N.D.	0.09	0.01	48.65%
Endosulfan	0.46	2.80	N.D.	0.10	0.30	86.26%
Endrin	0.08	0.37	N.D.	0.03	0.08	27.03%
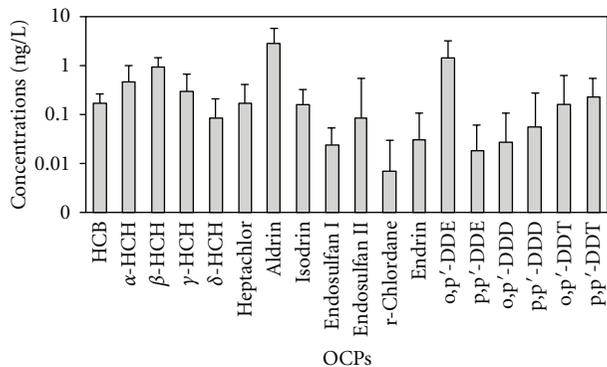
FIGURE 3: Annual mean concentrations of 18 OCPs in the water from Lake Chaohu.

except during winter, and the concentrations were higher in spring and summer than in autumn. The levels of HCHs in winter were greater than those in any other season, but the levels of DDTs were the opposite and with an order of magnitude lower in winter than in the other seasons. The possible reasons for this phenomenon included water changes and the use of related pesticides. Beginning in June, the input amount of water from Lake Chaohu was higher than the output amount, reaching the highest level in July and August. After September, the output amount of water was greater than the input, and the water of Lake Chaohu was gradually reduced. On the one hand, the increase in water diluted the pollutants in the lake, and on the other hand, new pollutants were added to the lake from the area along the river. Furthermore, the use of OCPs around the lake would result in an increase in the OCP residues in spring and summer, when there are more agricultural activities. Additionally, other technical products that include HCHs or DDTs may result in this irregular seasonal variation.

Seasonal differences in the remaining pollutants were analyzed as follows: the seasonal trends of hexachloroben- zene and heptachlor, which were similar to those of HCHs, were the highest residues in winter; the residue of aldrin was at a high concentration, but the seasonal variation was inconspicuous; the pollution of isodrin and γ-chlordane was severe in summer while the concentrations of endosulfan and endrin had high values in spring. These values may have certain relationships with the application characteristics of these pollutants in general without uniform trends.

Based on the spatial distribution, the sampling site JC represented the Eastern Lake and its water source areas, MS and ZM represented the Central Lake and the lakeside area of the Zhongmiao Temple, and TX represented the Western Lake region, which was near the region of the water intake. The data in TX just included September 2010 to February 2011. To ensure the comparability among the sampling sites, the monitoring data of the other three sites were also selected from this period (Table 5). The concentration of the OCPs was 3.33 ng/L from the Eastern Lake, 7.56 ng/L from the Central Lake, and 6.83 ng/L from the Western Lake. The pollution levels, from heavy to light, followed the order of Central Lake > Western Lake > Eastern Lake and the water

source area, and the levels of OCPs in the Western and Central Lakes were more than twice those in the Eastern Lake and the water source area. The main pollutants in each region of the lake were different. The main pollutants were HCHs and DDTs in the Eastern Lake and the water source area and aldrin in the Western Lake and the Central Lake in addition to HCHs and DDTs. Because of fewer sampling sites, the spatial differences they reflected may be influenced by the environment around the sites. There was an unpopulated region near the site of JC, whereas the relatively dense residential areas were located near the sites of ZM and MS. The life or industrial emissions were also one of the factors that led to the high pollution levels of the lake.

3.3. The Composition and Source of the OCPs in the Water

3.3.1. The Composition of the OCPs in the Water. The compositions of the OCPs, particularly the HCHs and DDTs, are shown in Figures 5(a), 5(b), and 5(c). Figure 5(a) shows that a greater than high proportion of the OCPs (85%) was shared by aldrin, HCHs, and DDTs in the water. The level of aldrin was the highest, accounting for 54.04% in autumn and 24.94% to 37.66% in the other seasons. The highest levels of HCHs were observed (46.43%) in winter, with seasonal HCHs being the main pollutants and the levels being approximately 15% in the other three seasons. In contrast, the level of DDTs was the lowest in winter at 4.32% and higher than the other pollutants in spring and summer at 43.54% and 46.40%, respectively.

As shown in Figure 5(b), β-HCH was the main HCH isomer in each season, ranging from 46.20% to 63.44%, followed by α-HCH (20.88%–30.84%). There were no sig- nificant seasonal differences between the HCH isomers. The levels of γ-HCH and δ-HCH were relatively lower, ranging from 10.60% to 18.56% and 3.20% to 7.29%, respectively.

Figure 5(c) illustrates that o, p′-DDE occupied more than 90% of the DDTs in spring and summer. In autumn o, p′- DDE accounted for 41.39%, and o, p′-DDT and p, p′-DDT, the two other isomers of DDT, accounted for 26.31% and 22.22%, respectively. The major pollutant in the winter was p, p′-DDT (79.87%), whereas o, p′-DDE accounted for only 11.50%, and the proportion of the remaining isomers was less than 8% collectively.

3.3.2. Source Identification of HCHs and DDTs. The HCH residues in the environment may come from the early use of the technical HCH or lindane and/or recent input, which can be identified according to their proportions, such as the α-/γ-HCH ratio or the β-/(α + γ)-HCH ratio. Technical HCH consists of 60–70% α-HCH, 5–12% β-HCH, and 10– 15% γ-HCH, with an α-/γ-HCH ratio of approximately 4– 7 and a β-/(α + γ)-HCH ratio of approximately 0.06–0.17. For lindane, which contains more than 99% γ-HCH, the α- /γ-HCH ratio is less than 0.1 and the β-/(α + γ)-HCH is less than 0.06. Because of the high vapor pressures, α-HCH is the main isomer in the air and could be transported for long distances. Hence, the α-/γ-HCH ratio can be used to identify the source of the HCHs [36, 40]. If the α-/γ-HCH ratio is between 4 and 7, the source of the HCH may be
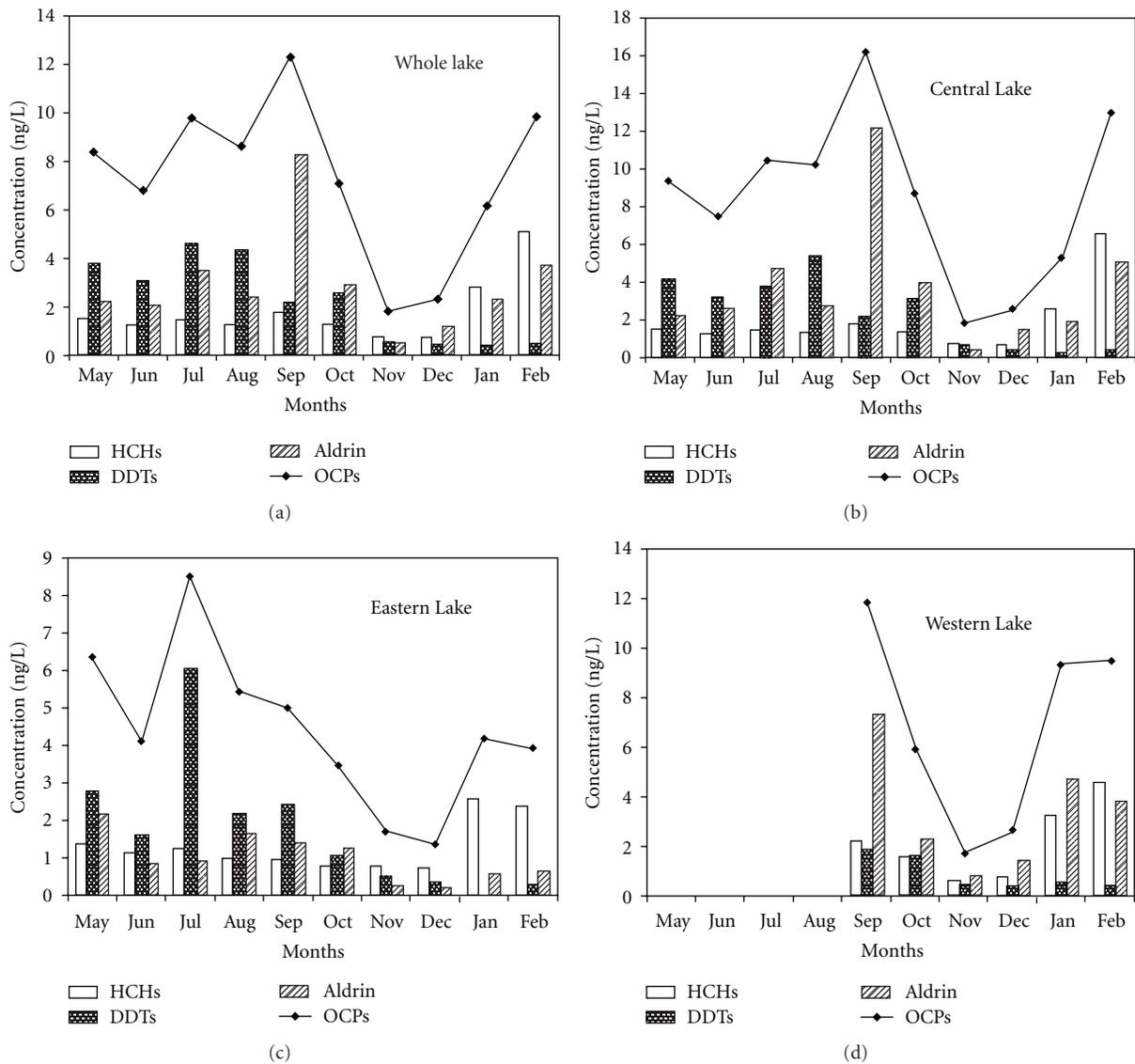
Figure 4: The temporal and spatial variation of OCPs in the water from Lake Chaohu.

Table 5: The spatial distributions of OCPs in the water from September 2010 to February 2011 (ng/L).

Pollutants	MS	ZM	JC	TX
HCB	0.16	0.17	0.15	0.20
HCHs	2.30	2.13	1.36	2.14
DDTs	0.87	1.01	0.78	0.78
Heptachlor	0.29	0.23	0.22	0.14
Aldrin	3.90	3.84	0.68	3.36
Isodrin	0.08	0.07	0.11	0.09
γ-chlordane	0.00	0.00	0.00	0.00
Endosulfan	0.03	0.02	0.03	0.10
Endrin	0.01	0.01	0.01	0.03
OCPs	7.65	7.48	3.33	6.83

(a)

(b)

(c)
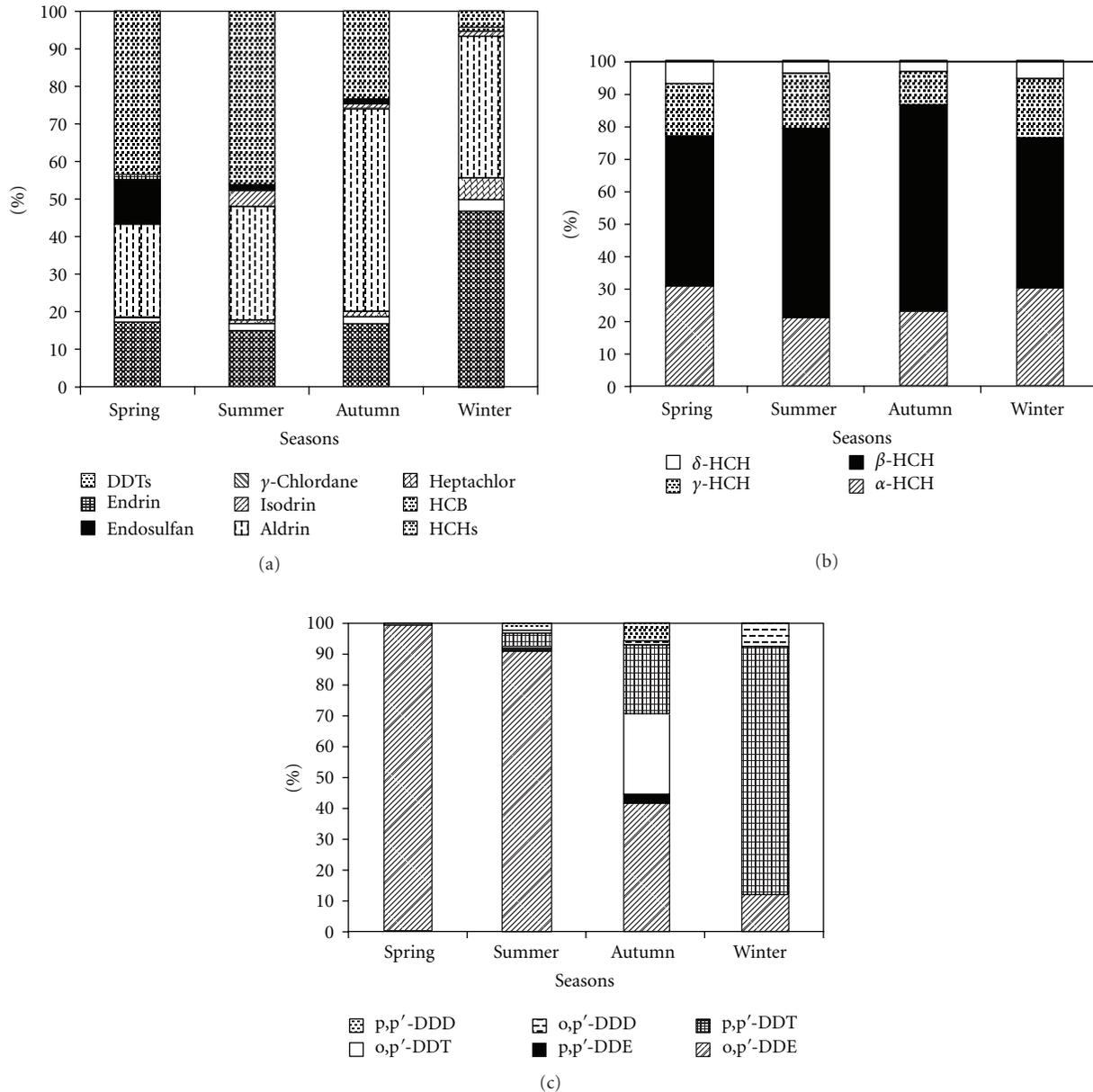
Figure 5: Seasonal changes of the composition of (a) OCPs, (b) HCHs, and (c) DDTs in the water.

from an industrial product, while the ratio for lindane is less than 4 [41]. β-HCH is the major isomer in water, soil, and sediment because of its stable physical and chemical properties. Therefore, the β-/$(\alpha + \gamma)$-HCH ratio can be used to identify the history of the HCH use. The high ratio indicates the source of the historical use of technical HCH or lindane [42]. However, there is no acknowledged ratio threshold to illustrate either the historical use or the recent input. Based on the references from other studies [43], 0.5 was used as a threshold. When the β-/$(\alpha + \gamma)$-HCH ratio is less than 0.5, a recent use of lindane or an atmospheric source for the input exists, and when the ratio is greater than or equal to 0.5, HCH comes from the historical use of technical HCH or lindane. According to the analysis above, we can

illustrate the source of the HCH in the graph with the ratios as the axes (Figure 6).

Figure 6 shows that the α-/γ-HCH ratios of the sampling sites from May 2010 to February 2011 ranged from 0.78 to 4.16 and that only the ratio of the Zhongmiao Temple in October 2010 was greater than 4. β-HCH accounted for a high proportion of the total HCHs, and the β-/$(\alpha + \gamma)$-HCH ratios of all sites were greater than 0.5. These observations indicated that the sources of the HCHs were mainly from the historical use of lindane after a period of degradation.

The sources of the DDTs can be identified by analyzing their composition in the environment. Technical DDT contains approximately 14 compounds, including 75% p, p′-DDT and 15% o, p′-DDT, with the o, p′-/p, p′-DDT ratio

TABLE 6: The spatial variation of the mean ecological risk of typical OCPs (PAF).

Pollutant	Site	Mean value (μg/L)	PAF					
			All species	Vertebrates	Invertebrates	Fishes	Crustaceans	Insects and spiders
p,p′-DDT	MS	$3.556E-4$	$4.692E-18$	$7.440E-165$	$6.083E-13$	$2.494E-259$	$1.128E-07$	$1.329E-135$
	ZM	$2.897E-4$	$1.187E-18$	$4.218E-184$	$2.503E-13$	$9.462E-293$	$7.730E-08$	$9.952E-152$
	JC	$2.237E-4$	$2.072E-19$	$1.247E-211$	$8.114E-14$	$0.000E+00$	$4.799E-08$	$7.572E-175$
	TX	$3.470E-4$	$3.983E-18$	$4.823E-167$	$5.472E-13$	$4.123E-263$	$1.078E-07$	$1.957E-137$
γ-HCH	MS	$1.940E-4$	$1.508E-13$	$1.717E-09$	$2.159E-117$	$1.123E-09$	$4.103E-251$	$5.312E-21$
	ZM	$1.911E-4$	$1.440E-13$	$1.676E-09$	$3.391E-118$	$1.096E-09$	$4.184E-253$	$4.913E-21$
	JC	$1.555E-4$	$7.615E-14$	$1.205E-09$	$8.951E-130$	$7.825E-10$	$5.199E-282$	$1.686E-21$
	TX	$2.282E-4$	$2.490E-13$	$2.226E-09$	$4.571E-109$	$1.465E-09$	$1.286E-230$	$1.233E-20$
Heptachlor	MS	$1.436E-4$	$1.582E-10$	$3.606E-14$	$7.024E-08$	$4.264E-15$	$1.094E-17$	$0.000E+00$
	ZM	$1.603E-4$	$2.036E-10$	$5.102E-14$	$8.450E-08$	$6.191E-15$	$1.717E-17$	$0.000E+00$
	JC	$2.039E-4$	$3.535E-10$	$1.090E-13$	$1.266E-07$	$1.400E-14$	$4.595E-17$	$0.000E+00$
	TX	$1.176E-4$	$1.001E-10$	$1.920E-14$	$5.020E-08$	$2.166E-15$	$4.831E-18$	$0.000E+00$
Aldrin	MS	$2.446E-3$	$5.172E-18$	$8.825E-09$	$1.741E-18$	$8.852E-09$	$1.995E-18$	$1.412E-11$
	ZM	$2.412E-3$	$4.755E-18$	$8.492E-09$	$1.601E-18$	$8.517E-09$	$1.835E-18$	$1.340E-11$
	JC	$7.304E-4$	$3.667E-21$	$3.186E-10$	$1.235E-21$	$3.164E-10$	$1.415E-21$	$1.542E-13$
	TX	$2.580E-4$	$7.123E-24$	$1.825E-11$	$2.398E-24$	$1.797E-11$	$2.748E-24$	$3.154E-15$
Endrin	MS	$8.664E-5$	$4.575E-25$	$2.937E-24$	$3.324E-25$	$6.513E-24$	$0.000E+00$	$6.796E-25$
	ZM	$1.177E-4$	$2.876E-24$	$1.846E-23$	$2.089E-24$	$4.094E-23$	$0.000E+00$	$4.272E-24$
	JC	$3.000E-5$	$7.885E-28$	$5.062E-27$	$5.728E-28$	$1.123E-26$	$0.000E+00$	$1.171E-27$
	TX	$7.348E-5$	$1.703E-25$	$1.093E-24$	$1.237E-25$	$2.424E-24$	$0.000E+00$	$2.529E-25$
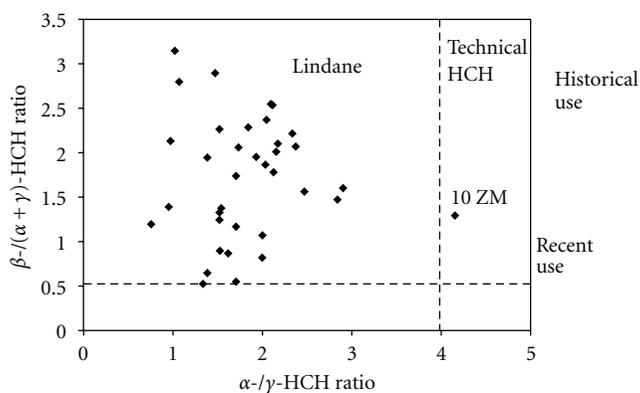
FIGURE 6: The identification of HCHs sources in the water from Lake Chaohu.

being approximately 0.2. dicofol, a substitute for DDT that contained considerable impurities of DDTs, was widely used after the prohibition of technical DDT in 1983. o, p′-DDT is the major DDT impurity, and the o, p′-/p, p′-DDT ratio is 7 ± 2. A high ratio in the environment is considered to indicate pollution by dicofol [44], and a ratio of 0.2 indicates that technical DDT is the main source. Otherwise, the relative proportions of the DDT metabolites can be used to identify the source. In the environment, DDT can be degraded to DDE and DDD, and the percentage of DDT will decrease as DDE and DDD increase over time [45]. Therefore, the DDT/(DDE + DDD) ratio can indicate when the DDT was used. New inputs are indicated when the ratio is greater than or equal to 1, and historical use is indicated when the

ratio is less than 1. Because DDT will be metabolized into DDE under aerobic conditions and DDD under anaerobic conditions, the DDD/DDE ratio can be used to estimate the metabolic environment of DDT. The condition is anaerobic when the ratio is greater than 1 and aerobic when the ratio is less than 1 [46, 47]. According to the analysis above, the DDT triangular graph can indicate the historical use and metabolic environment of DDT [48]. The chart with the o, p′-/p, p′-DDT and DDT/(DDE + DDD) ratios as axes can illustrate the source and use history of DDT [46].

Figure 7 shows that there were 12 samples without DDT in the 36 samples in which DDTs were detected, and the o, p′-/p, p′-DDT ratios of the remaining samples ranged from 0 to 2.17, except the two samples at the JC site in June and August. These results indicated that the detectable DDTs were derived from technical DDT, while the use of dicofol made less contribution to the concentrations of DDT in the water from Lake Chaohu, which was affected near the JC site. The DDT/(DDD + DDE) ratios were less than 1 from May to September, ranging from 0 to 0.11 and increased rapidly from October, ranging from 1.10 to 13.40. On the one hand, the degradation of DDT in spring and summer was relatively significant, and on the other hand, there were new inputs in autumn and winter because the ratio was greater than 1. In addition, the low detectable rate of DDD (20.83%) indicated that the metabolic environment was aerobic, which is associated with the higher oxygen content of surface water.

3.4. The Ecological Risks of OCPs in Water. The SSD model was employed to assess the ecological risks for all species at four sampling sites. The average and maximum ecological

(a)

(b)
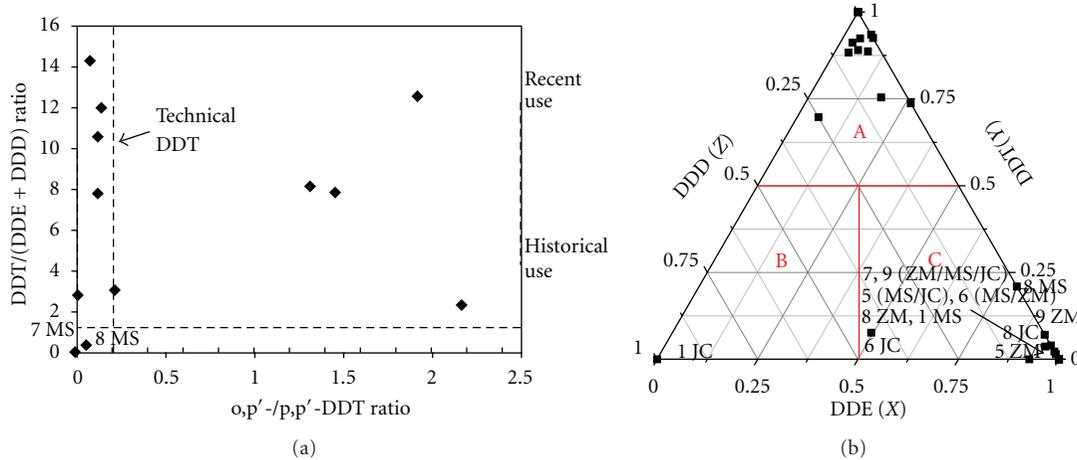
Figure 7: The identification of the DDT sources in the water from Lake Chaohu.

Table 7: The spatial variation of the maximum ecological risk of typical OCPs (PAF).

Pollutant	Site	Max. value (μg/L)	Month	PAF					
				All species	Vertebrates	Invertebrates	Fishes	Crustaceans	Insects and spiders
p,p′-DDT	MS	$1.145E-3$	8	$9.797E-15$	$6.536E-88$	$8.683E-11$	$5.427E-130$	$9.655E-07$	$1.537E-71$
	ZM	$1.067E-3$	10	$6.248E-15$	$2.650E-91$	$6.476E-11$	$1.628E-135$	$8.485E-07$	$2.397E-74$
	JC	$3.700E-4$	10	$6.117E-18$	$2.285E-161$	$7.220E-13$	$2.590E-253$	$1.213E-07$	$1.100E-132$
	TX	$4.967E-4$	10	$4.326E-17$	$1.040E-137$	$2.561E-12$	$7.684E-213$	$2.086E-07$	$6.401E-113$
γ-HCH	MS	$1.770E-3$	2	$1.333E-10$	$5.887E-08$	$2.691E-43$	$4.167E-08$	$5.447E-79$	$4.983E-16$
	ZM	$1.467E-3$	2	$7.530E-11$	$4.361E-08$	$4.212E-47$	$3.066E-08$	$4.093E-87$	$1.889E-16$
	JC	$2.833E-4$	6	$4.853E-13$	$3.145E-09$	$6.840E-99$	$2.086E-09$	$6.763E-206$	$3.784E-20$
	TX	$1.053E-3$	2	$2.738E-11$	$2.567E-08$	$1.134E-54$	$1.783E-08$	$1.417E-103$	$3.400E-17$
Heptachlor	MS	$1.087E-3$	2	$1.639E-08$	$2.143E-11$	$2.110E-06$	$4.072E-12$	$4.337E-14$	$0.000E+00$
	ZM	$4.867E-4$	2	$2.598E-09$	$1.697E-12$	$5.466E-07$	$2.672E-13$	$1.618E-15$	$0.000E+00$
	JC	$6.300E-4$	1	$4.695E-09$	$3.832E-12$	$8.435E-07$	$6.409E-13$	$4.651E-15$	$0.000E+00$
	TX	$4.400E-4$	1	$2.062E-09$	$1.235E-12$	$4.613E-07$	$1.898E-13$	$1.070E-15$	$0.000E+00$
Aldrin	MS	$1.201E-2$	9	$7.246E-14$	$6.996E-07$	$2.440E-14$	$7.111E-07$	$2.796E-14$	$5.407E-09$
	ZM	$1.222E-2$	9	$8.041E-14$	$7.338E-07$	$2.707E-14$	$7.459E-07$	$3.102E-14$	$5.769E-09$
	JC	$2.140E-3$	5	$2.320E-18$	$6.112E-09$	$7.810E-19$	$6.124E-09$	$8.948E-19$	$8.570E-12$
	TX	$7.313E-3$	9	$3.694E-15$	$1.790E-07$	$1.244E-15$	$1.812E-07$	$1.425E-15$	$8.466E-10$
Endrin	MS	$3.225E-4$	7	$1.217E-21$	$7.812E-21$	$8.840E-22$	$1.732E-20$	$0.000E+00$	$1.808E-21$
	ZM	$3.667E-4$	5	$2.630E-21$	$1.688E-20$	$1.911E-21$	$3.744E-20$	$0.000E+00$	$3.907E-21$
	JC	$3.000E-5$	10	$7.885E-28$	$5.062E-27$	$5.728E-28$	$1.123E-26$	$0.000E+00$	$1.171E-27$
	TX	$9.000E-5$	9	$5.748E-25$	$3.690E-24$	$4.176E-25$	$8.183E-24$	$0.000E+00$	$8.539E-25$

risks are given in Tables 6 and 7, respectively. By comparing the mean values, the ecological risk of site MS, where the pollution of p,p′-DDT and aldrin was heavy, was slightly higher than those of the other sites. The potential risk of γ-HCH at site TX was relatively higher, while at sites JC and ZM, the risks of heptachlor and isodrin were higher. In 5 OCPs, the ecological risk of heptachlor was the highest, followed by γ-HCH, p,p′-DDT, aldrin, and endrin. However, Tables 6 and 7 indicate that the potential risks of the OCPs for all species at the four sites were very low, ranging from 7.885×10^{-28} to 1.639×10^{-8}. The maximum

risk probability of a single pollutant was less than 10^{-7}. Comparing by species, the risks of p,p′-DDT and heptachlor for vertebrates were less than those for invertebrates, and the risks of the other three pollutants for vertebrates were higher. For further classification of the three subcategories, the risk of p,p′-DDT for crustaceans was 10^{-7}, which was the highest, whereas the risk of p,p′-DDT was mostly harmless for fish and insects and spiders. The risk of γ-HCH was highest for fish (10^{-8}) and was up to 10^{-16} for insects and spiders and less for crustaceans. Heptachlor had no risk for insects and spiders, but its risk for fish was two orders

TABLE 8: The spatial and temporary variation of combining ecological risks (msPAF).

Site	Month	All species	Vertebrates	Invertebrates	Fishes	Crustaceans	Insects and spiders
MS	2010.5	$1.926E-13$	$1.011E-08$	$0.000E+00$	$9.464E-09$	$0.000E+00$	$1.270E-11$
	2010.6	$1.414E-13$	$1.263E-08$	$0.000E+00$	$1.210E-08$	$0.000E+00$	$1.899E-11$
	2010.7	$1.449E-11$	$2.659E-08$	$1.192E-08$	$2.576E-08$	$1.954E-08$	$5.418E-11$
	2010.8	$5.499E-09$	$3.986E-09$	$9.473E-07$	$3.632E-09$	$9.655E-07$	$3.243E-12$
	2010.9	$3.067E-11$	$7.012E-07$	$2.099E-08$	$7.121E-07$	$2.798E-14$	$5.407E-09$
	2010.10	$5.895E-11$	$1.259E-08$	$3.408E-08$	$1.239E-08$	$6.597E-07$	$2.120E-11$
	2010.11	$5.894E-11$	$4.801E-10$	$3.404E-08$	$3.270E-10$	$1.316E-07$	$1.732E-14$
	2010.12	$1.728E-12$	$3.372E-09$	$2.555E-09$	$3.274E-09$	$4.271E-08$	$3.417E-12$
	2011.1	$1.689E-09$	$9.302E-09$	$3.986E-07$	$8.156E-09$	$0.000E+00$	$8.082E-12$
	2011.2	$1.652E-08$	$1.056E-07$	$2.109E-06$	$8.880E-08$	$2.892E-08$	$1.364E-10$
	Mean	**$1.584E-10$**	**$1.054E-08$**	**$7.024E-08$**	**$9.976E-09$**	**$1.128E-07$**	**$1.412E-11$**
ZM	2010.5	$4.681E-13$	$6.548E-09$	$0.000E+00$	$5.509E-09$	$0.000E+00$	$3.955E-12$
	2010.6	$7.053E-12$	$9.245E-09$	$7.078E-09$	$8.706E-09$	$0.000E+00$	$1.159E-11$
	2010.7	$3.411E-13$	$9.264E-08$	$0.000E+00$	$9.266E-08$	$8.477E-09$	$3.325E-10$
	2010.8	$1.130E-13$	$2.610E-08$	$0.000E+00$	$2.574E-08$	$0.000E+00$	$5.703E-11$
	2010.9	$3.008E-10$	$7.356E-07$	$1.125E-07$	$7.473E-07$	$2.788E-08$	$5.775E-09$
	2010.10	$4.374E-14$	$6.094E-08$	$6.467E-11$	$6.118E-08$	$8.481E-07$	$1.920E-10$
	2010.11	$3.754E-11$	$2.460E-10$	$2.446E-08$	$1.563E-10$	$1.884E-07$	$0.000E+00$
	2010.12	$2.436E-10$	$1.099E-09$	$9.637E-08$	$9.890E-10$	$5.187E-08$	$5.504E-13$
	2011.1	$1.444E-09$	$4.838E-09$	$3.553E-07$	$3.832E-09$	$0.000E+00$	$1.708E-12$
	2011.2	$2.673E-09$	$1.249E-07$	$5.465E-07$	$1.127E-07$	$1.076E-07$	$2.893E-10$
	Mean	**$2.038E-10$**	**$1.017E-08$**	**$8.451E-08$**	**$9.613E-09$**	**$7.730E-08$**	**$1.340E-11$**
JC	2010.5	$1.744E-13$	$7.963E-09$	$0.000E+00$	$7.338E-09$	$0.000E+00$	$8.570E-12$
	2010.6	$4.855E-13$	$3.589E-09$	$0.000E+00$	$2.527E-09$	$0.000E+00$	$2.413E-13$
	2010.7	$3.836E-13$	$3.308E-09$	$0.000E+00$	$2.362E-09$	$8.930E-09$	$3.029E-13$
	2010.8	$7.927E-14$	$4.147E-09$	$0.000E+00$	$3.716E-09$	$0.000E+00$	$3.134E-12$
	2010.9	$4.730E-14$	$2.677E-09$	$0.000E+00$	$2.340E-09$	$0.000E+00$	$1.546E-12$
	2010.10	$2.770E-10$	$1.692E-09$	$1.059E-07$	$1.536E-09$	$1.213E-07$	$1.017E-12$
	2010.11	$1.116E-10$	$3.722E-10$	$5.439E-08$	$2.388E-10$	$7.582E-08$	$0.000E+00$
	2010.12	$4.545E-11$	$4.205E-10$	$2.814E-08$	$2.681E-10$	$6.636E-08$	$0.000E+00$
	2011.1	$4.695E-09$	$2.838E-09$	$8.435E-07$	$1.923E-09$	$4.663E-15$	$5.462E-14$
	2011.2	$8.353E-10$	$2.243E-09$	$2.378E-07$	$1.538E-09$	$4.654E-08$	$7.860E-14$
	Mean	**$3.536E-10$**	**$1.524E-09$**	**$1.266E-07$**	**$1.099E-09$**	**$4.799E-08$**	**$1.542E-13$**
TX	2010.9	$2.189E-11$	$1.822E-07$	$1.620E-08$	$1.833E-07$	$0.000E+00$	$8.468E-10$
	2010.10	$9.437E-14$	$8.476E-09$	$2.560E-12$	$8.024E-09$	$2.086E-07$	$1.057E-11$
	2010.11	$4.774E-15$	$6.127E-10$	$1.243E-13$	$5.042E-10$	$5.747E-08$	$1.592E-13$
	2010.12	$2.461E-12$	$2.107E-09$	$3.311E-09$	$1.980E-09$	$7.582E-08$	$1.589E-12$
	2011.1	$2.068E-09$	$6.356E-08$	$4.614E-07$	$6.032E-08$	$1.692E-07$	$1.575E-10$
	2011.2	$9.511E-10$	$5.529E-08$	$2.561E-07$	$4.766E-08$	$9.465E-08$	$7.329E-11$
	Mean	**$1.003E-10$**	**$2.244E-09$**	**$5.021E-08$**	**$1.483E-09$**	**$1.078E-07$**	**$3.109E-15$**

of magnitude higher than those for crustaceans, at 10^{-12} and 10^{-14}, respectively. The risk of aldrin, and endrin was ranked as followed: fish > insects and spiders ≫ crustaceans. The risk of aldrin for fish was up to 10^{-7}, whereas endrin generally had a low risk.

The results of the combining ecological risk of each site are shown in Table 8. The mean combining ecological risk probability of each site for all species was approximately 10^{-10}, following the order of MS > JC > ZM > TX. The site of the highest combining risk was MS in February (1.652×10^{-10}). A species-by-species comparison revealed that the potential combining ecological risk probability for invertebrates was 10^{-6} at the MS site in February, which was higher than that for vertebrates. Among the three subcategories, the probability of the combining ecological risks was ranked as crustaceans > fish > insects and spiders, with the maximum probability being close to 10^{-6} at the MS and ZM sites. Nevertheless, the risk was actually very low

because of its order of magnitude, and the pollutants had little influence on aquatic organisms. Overall, the ecological risk of OCPs for aquatic organisms in Lake Chaohu was very low.

4. Conclusions

(1) The annual mean concentration of the total OCPs in the water from Lake Chaohu was 6.99 ng/L. The level of the total HCHs was 1.76 ng/L, which was the highest in winter, and the level of the total DDTs was 1.91 ng/L, which was higher in spring and summer than that in autumn and winter. The spatial pollutions followed from heavy to light as follows: Central Lakes > Western Lakes > Eastern Lakes and water resource district. The residues of the HCHs and DDTs were lower compared with those from other studies.

(2) Aldrin, HCHs, and DDTs accounted for the majority of the OCPs, and their peak values appeared in the autumn, winter, and spring and summer, respectively. In each season, β-HCH was the main HCH isomer, followed by α-HCH, and there were no significant seasonal differences between the two. The main metabolite of DDT was o,p$'$-DDE in the spring and summer, there were two additional isomers of DDT in autumn, and p,p$'$-DDT was the major metabolite in winter.

(3) The sources of the HCHs were mainly from the historical usage of lindane after a period of degradation. The DDTs were degraded under aerobic conditions, and the main sources were from the use of technical DDTs. The concentration of the DDTs was slightly influenced by the use of dicofol. In spring and summer, the degradation was relatively significant, but there were new DDT inputs in autumn and winter.

(4) The ecological risks of 5 OCPs were assessed by the species sensitivity distribution (SSD) method in the following order: heptachlor > γ-HCH > p,p$'$-DDT > aldrin > endrin. The combining risks of all the sampling sites in decreasing order were as follows: MS > JC > ZM > TX. The combining ecological risks of different species were in the order: crustacean > fish > insects and spiders. Overall, the ecological risks of OCPs contaminants on aquatic animals were very low.

Acknowledgments

References

[1] UNEP, *Final Act of the Plenipotentiaries on the Stockholm Convention on Persistent Organic Pollutants*, United Nations Environment Programme, Geneva, Switzerland, 2001.

[2] UNEP, *Report of the Conference of the Parties to the Stockholm Convention on Persistent Organic Pollutants on the work of its fifth meeting*, United Nations Environment Programme, Geneva, Switzerland, 2011.

[3] H. J. Gao and X. Jiang, "Bioaccumulation of organochlorine pesticides and quality safety in vegetables from Nanjing suburb," *Acta Scientiae Circumstantiae*, vol. 25, no. 1, pp. 90–93, 2005.

[4] A. G. Frenich, J. L. M. Vidal, A. D. C. Sicilia, M. J. González Rodríguez, and P. Plaza Bolaños, "Multiresidue analysis of organochlorine and organophosphorus pesticides in muscle of chicken, pork and lamb by gas chromatography-triple quadrupole mass spectrometry," *Analytica Chimica Acta*, vol. 558, no. 1-2, pp. 42–52, 2006.

[5] P. Furst, C. Furst, and K. Wilmers, "PCDDs and PCDFs in human milk—statistical evaluation of a 6-years survey," *Chemosphere*, vol. 25, no. 7-10, pp. 1028–1038, 1992.

[6] C. Turgut, "The contamination with organochlorine pesticides and heavy metals in surface water in Küçük Menderes River in Turkey, 2000–2002," *Environment International*, vol. 29, no. 1, pp. 29–32, 2003.

[7] M. A. Fernández, C. Alonso, M. J. González, and L. M. Hernández, "Occurrence of organochlorine insecticides, PCBs and PCB congeners in waters and sediments of the Ebro River (Spain)," *Chemosphere*, vol. 38, no. 1, pp. 33–43, 1999.

[8] K. P. Singh, A. Malik, D. Mohan, and R. Takroo, "Distribution of persistent organochlorine pesticide residues in Gomti River, India," *Bulletin of Environmental Contamination and Toxicology*, vol. 74, no. 1, pp. 146–154, 2005.

[9] S. M. Chernyak, L. L. McConnell, and C. P. Riee, "Fate of some chlorinated hydrocarbons in arctic and far eastern ecosystems in the Russian Federation," *Science of the Total Environment*, vol. 160-161, pp. 75–85, 1995.

[10] K. Feng, B. Y. Yu, D. M. Ge, M. H. Wong, X. C. Wang, and Z. H. Cao, "Organo-chlorine pesticide (DDT and HCH) residues in the Taihu Lake region and its movement in soil-water system I. Field survey of DDT and HCH residues in ecosystem of the region," *Chemosphere*, vol. 50, no. 6, pp. 683–687, 2003.

[11] Q. S. Yang, B. X. Mai, J. M. Fu, G. Y. Sheng, and J. X. Wang, "Spatial and temporal distribution of organochlorine pesticides (OCPs) in surface water from the Pearl River Artery estuary," *Environmental Science*, vol. 25, no. 2, pp. 150–156, 2004.

[12] X. T. Wang, S. G. Chu, and X. B. Xu, "Organochlorine pesticide residues in water from Guanting reservoir and Yongding River, China," *Bulletin of Environmental Contamination and Toxicology*, vol. 70, no. 2, pp. 351–358, 2003.

[13] Y. Wang, W. J. Wu, W. He, N. Qin, Q. S. He, and F. L. Xu, "Residues and ecological risks of organochlorine pesticides in Lake Small Baiyangdian, North China," *Environmental Monitoring and Assessment*. In press.

[14] Y. Wang, J. J. Wang, N. Qin, W. J. Wu, Y. Zhu, and F. L. Xu, "Assessing ecological risks of DDT and lindane to freshwater organisms by species sensitivity distributions," *Acta Scientiae Circumstantiae*, vol. 29, no. 11, pp. 2407–2414, 2009.

[15] L. Liu, X. P. Yan, Y. Wang, and F. L. Xu, "Assessing ecological risks of polycyclic aromatic hydrocarbons (PAHs) to freshwater organisms by species sensitivity distributions," *Asian Journal of Ecotoxicology*, vol. 4, no. 5, pp. 647–654, 2009.

[16] M. C. Newman, D. R. Ownby, L. C. A. Mézin et al., "Applying species-sensitivity distributions in ecological risk assessment: assumptions of distribution type and sufficient numbers of species," *Environmental Toxicology and Chemistry*, vol. 19, no. 2, pp. 508–515, 2000.

[17] L. Posthuma, T. P. Traas, and G. W. Suter, *Species Sensitivity Distributions in Ecotoxicology*, Lewis Publishers, Boca Raton, Fla, USA, 2002.

[18] N. M. van Straalen, "Threshold models for species sensitivity distributions applied to aquatic risk assessment for zinc," *Environmental Toxicology and Pharmacology*, vol. 11, no. 3-4, pp. 167–172, 2002.

[19] P. J. van den Brink, L. Posthuma, and T. C. M. Brock, "The value of the species sensitivity distribution concept for predicting field effects: (non-) confirmation of the concept using semi-field experiments," in *Species Sensitivity Distributions in Ecotoxicology*, L. Posthuma, T. P. Traas, and G. W. Suter, Eds., pp. 155–193, Lewis Publisher, Boca Raton, Fla, USA, 2002.

[20] Q. Shao, Y. D. Chen, and L. Zhang, "An extension of three-parameter Burr III distribution for low-flow frequency analysis," *Computational Statistics and Data Analysis*, vol. 52, no. 3, pp. 1304–1314, 2008.

[21] B. Wang, G. Yu, J. Huang, and H. Hu, "Development of species sensitivity distributions and estimation of HC 5 of organochlorine pesticides with five statistical approaches," *Ecotoxicology*, vol. 17, no. 8, pp. 716–724, 2008.

[22] T. I. Hayashi and N. Kashiwagi, "A bayesian method for deriving species-sensitivity distributions: selecting the best-fit tolerance distributions of taxonomic groups," *Human and Ecological Risk Assessment*, vol. 16, no. 2, pp. 251–263, 2010.

[23] Q. X. Shao, "Estimation for hazardous concentrations based on NOEC toxicity data: an alternative approach," *Environmetrics*, vol. 11, no. 5, pp. 583–595, 2000.

[24] CSIRO, (Australia's Commonwealth Scientific and Industrial Research Organisation): a flexible approach to species protection, 2008, http://www.cmis.csiro.au/envir/burrlioz.

[25] T. P. Traas, D. van de Meent, L. Posthuma et al., "The potentially affected fraction as a measure of ecological risk," in *Species Sensitivity Distributions in Ecotoxicology*, L. Posthuma, T. P. Traas, and G. W. Suter, Eds., pp. 315–343, Lewis Publisher, Boca Raton, Fla, USA, 2002.

[26] L. L. Wei, F. Guo, J. Z. Wang, and C. X. Kang, "Distribution characteristics of organochlorine pesticides in karst subterranean river in Liuzhou," *Carsologica Sinica*, vol. 30, no. 1, pp. 16–21, 2011.

[27] G. Tian, Y. Q. Chen, X. Z. Wan, and S. C. Wang, "Investigations and control measures on seven persistent organic pollutants in protected region of drinking water sources of Xiangjiang in Changsha," *Environmental Monitoring in China*, vol. 26, no. 1, pp. 58–62, 2010.

[28] X. Zhi, J. F. Niu, and Z. W. Tang, "Ecological risk assessment of typical organochlorine pesticides in water from the Wuhan reaches of the Yangtze River," *Acta Scientiae Circumstantiae*, vol. 28, no. 1, pp. 168–173, 2008.

[29] R. Ban and Y. M. Li, "Contamination of OCPs in Huaxi River in Guiyang, China," in *Persistent Organic Pollutants Forum 2009 and the 4th Persistent Organic Pollutants in National Academic Symposium*, pp. 1–43, 2009.

[30] Y. H. Kang, P. B. Liu, Z. J. Wang, Y. B. Lv, and Q. J. Li, "Persistent organochlorine pesticides in water from Guanting Reservoir and Yongdinghe River, Beijing," *Journal of Lake Sciences*, vol. 15, no. 2, pp. 125–132, 2003.

[31] G. C. Hu, X. J. Luo, F. C. Li et al., "Organochlorine compounds and polycyclic aromatic hydrocarbons in surface sediment from Baiyangdian Lake, North China: concentrations, sources profiles and potential risk," *Journal of Environmental Sciences*, vol. 22, no. 2, pp. 176–183, 2010.

[32] R. B. Zhou, L. Z. Zhu, and Y. Y. Chen, "Levels and source of organochlorine pesticides in surface waters of Qiantang River, China," *Environmental Monitoring and Assessment*, vol. 136, no. 1–3, pp. 277–287, 2008.

[33] K. Maskaoui, J. L. Zhou, T. L. Zheng, H. Hong, and Z. Yu, "Organochlorine micropollutants in the Jiulong River Estuary and Western Xiamen Sea, China," *Marine Pollution Bulletin*, vol. 51, no. 8–12, pp. 950–959, 2005.

[34] T. Na, Z. Fang, G. Zhanqi, Z. Ming, and S. Cheng, "The status of pesticide residues in the drinking water sources in Meiliangwan Bay, Taihu Lake of China," *Environmental Monitoring and Assessment*, vol. 123, no. 1–3, pp. 351–370, 2006.

[35] W. L. Zhang, G. Zhang, S. H. Qi, and P. A. Peng, "A preliminary study of organochlorine pesticides in water and sediments from two Tibetan lakes," *Geochimica*, vol. 32, no. 4, pp. 363–367, 2003.

[36] H. Iwata, S. Tanabe, K. Ueda, and R. Tatsukawa, "Persistent organochlorine residues in air, water, sediments, and soils from the Lake Baikal Region, Russia," *Environmental Science and Technology*, vol. 29, no. 3, pp. 792–801, 1995.

[37] X. Jiang, S. F. Xu, D. Martens, and L. S. Wang, "Polychlorinated organic contaminants in waters, suspended solids and sediments of the Nanjing section, Yangtze River," *China Environmental Science*, vol. 20, no. 3, pp. 193–197, 2000.

[38] Y. W. Wan, T. F. Kang, Z. L. Zhou, P. N. Li, and Y. Zhang, "Health risk assessment of volatile organic compounds in water of Beijing Guanting reservoir," *Research of Environmental Sciences*, vol. 22, no. 2, pp. 150–154, 2009.

[39] F. Xia, X. X. Hu, Z. H. Han, and W. H. Wang, "Distribution characteristic s of organochlorine pesticides in surface water from the Huangpu River," *Research of Environmental Sciences*, vol. 19, no. 2, pp. 11–15, 2006.

[40] H. Iwata, S. Tanabe, and R. Tatsukawa, "A new view on the divergence of HCH isomer compositions in oceanic air," *Marine Pollution Bulletin*, vol. 26, no. 6, pp. 302–305, 1993.

[41] K. Walker, D. A. Vallero, and R. G. Lewis, "Factors influencing the distribution of lindane and other hexachlorocyclohexanes in the environment," *Environmental Science and Technology*, vol. 33, no. 24, pp. 4373–4378, 1999.

[42] K. L. Willett, E. M. Ulrich, and R. A. Hites, "Differential toxicity and environmental fates of hexachlorocyclohexane isomers," *Environmental Science and Technology*, vol. 32, no. 15, pp. 2197–2207, 1998.

[43] W. X. Liu, Y. Li, Q. Zuo et al., "Residual characteristics of HCHs and DDTs in surface soils from the western zone of Bohai Bay," *Acta Scientiae Circumstantiae*, vol. 28, no. 1, pp. 142–149, 2008.

[44] X. H. Qiu, T. Zhu, B. Yao, J. X. Hu, and S. W. Hu, "Contribution of dicofol to the current DDT pollution in China," *Environmental Science and Technology*, vol. 39, no. 12, pp. 4385–4390, 2005.

[45] G. G. Pandit, S. K. Sahu, S. Sharma, and V. D. Puranik, "Distribution and fate of persistent organochlorine pesticides in coastal marine environment of Mumbai," *Environment International*, vol. 32, no. 2, pp. 240–243, 2006.

[46] R. K. Hitch and H. R. Day, "Unusual persistence of DDT in some Western USA soils," *Bulletin of Environmental Contamination and Toxicology*, vol. 48, no. 2, pp. 259–264, 1992.

[47] Y. Z. Sun, X. T. Wang, X. H. Li, and X. B. Xu, "Distribution of persistent organochlorine pesticides in tissue/organ of silver carp (Hypophthalmichthys molitrix) from Guanting reservoir, China," *Journal of Environmental Sciences*, vol. 17, no. 5, pp. 722–726, 2005.

[48] Y. Zhang, *The Spatial and Temporal Distribution of DDTs Contents in Water, Suspended Solids and Sediments in Western Region Around Bohai Bay*, Peking University, Beijing, China, 2006.

The *scientific* World JOURNAL

Research Article

Levels, Temporal-Spatial Variations, and Sources of Organochlorine Pesticides in Ambient Air of Lake Chaohu, China

Hui-Ling Ouyang, Wei He, Ning Qin, Xiang-Zhen Kong, Wen-Xiu Liu, Qi-Shuang He, Qing-Mei Wang, Yu-Jiao Jiang, Chen Yang, Bin Yang, and Fu-Liu Xu

MOE Laboratory for Earth Surface Process, College of Urban & Environmental Sciences, Peking University, No. 5 Yiheyuan Road, Haidian District, Beijing 100871, China

Correspondence should be addressed to Fu-Liu Xu, xufl@urban.pku.edu.cn

The residual levels of OCPs in the gas phase and particle phase in Lake Chaohu, China, were measured using GC-MS from March 2010 to February 2011. The temporal-spatial variations and sources of OCPs were also analyzed. Twenty types of OCPs were detected in the gas phase with a total concentration of 484.8 ± 550.4 pg/m^3. Endosulfan, DDTs and chlordane were the primary OCPs in the gas phase. The mean concentration of OCPs in the gas phase was significantly higher in the summer than in the winter. Seventeen types of OCPs were detected in the particle phase with a total concentration of 18.3 ± 26.1 pg/m^3. DDTs were major OCPs in the particle phase. The mean concentration of OCPs in the particle phase decreased at first and then increased during the period. The potential source of the HCHs in ambient air of Lake Chaohu might come from recent lindane usage. DDTs mainly came from historical dicofol usage, and an input of DDT was observed in the spring, which may result from the present use of marine paint that contains technical DDT. Endosulfan and chlordane in the air may be due to the present use of technical endosulfan and chlordane.

1. Introduction

Organochlorine pesticides (OCPs), which are typical persistent organic pollutants (POPs), are persistent in the environment and have serious impacts on ecosystems and human health [1–3]. Although some OCPs (e.g., DDT, chlordane, HCB, mirex, aldrin, and dieldrin) have been banned from production and use since the 1980s, numerous surveys have reported that these OCPs can still be detected in the environment (e.g., [4–7]) and even exhibited an upward trend of concentration and harmfulness in some regions [5].

Atmospheric transport plays an important role in the distribution of OCPs on a global scale. The atmospheric "distillation effect" allows the detection of OCPs in the environment and organisms in Polar Regions where there has been no historical usage of OCPs [8–10]. Approximately 97 tons of α-HCH and 13 tons of β-HCH were imported to the North Pole [11]. Through volatilization, diffusion, and atmospheric transport, the OCPs used for farmland pest control and epidemic prevention could transport from the land to the ocean and be detected in the ambient air above the ocean. According to a survey conducted by Wu et al., the atmospheric concentrations of DDTs measured from Shanghai, China, to the Arctic Ocean were 2 to 110 pg/m^3 [12]. The atmospheric concentrations of α-HCH and γ-HCH in North America were 1.5–170 pg/m^3 and 5–400 pg/m^3, respectively [13].

Lake Chaohu, which is located in the center of the Anhui province and in the southeast of China (Figure 1), is the fifth-largest freshwater lake in China, with a water area of 760 km^2 and a basin area of 13350 km^2. This area is one of the most developed agricultural regions [14, 15], and considerable amounts of OCPs have been used in agricultural activities. Studies have shown that the residual levels of OCPs in the water and sediment were relatively high in Lake Chaohu [16, 17]; however, the residual levels and distributions of OCPs in the atmosphere in Lake Chaohu still remain to

be studied. The objectives of this study are to measure the concentrations of OCPs in the gas phase and particle phase and to study the components, temporal-spatial variations, and sources of OCPs in Lake Chaohu to determine the residual characteristics of OCPs and provide a theoretical basis for the prevention and control of OCPs in Lake Chaohu.

2. Materials and Methods

2.1. Sample Collections. Sample collections were conducted in the center of the lake (Mushan Island, Lake Chaohu, China) and the side of the lake (Environmental Protection Agency of Chaohu, HB). The sampling sites are marked in Figure 1.

Samples were collected once per month from March 2010 to February 2011. Polyurethane foam plugs (PUF, 60 mm $\times$ 100 mm) and glass fiber filters (GFF) were used in a high-volume sampler (PM10-PUF-300) to collect gas-phase and particle-phase OCPs based on Method TO-13A provided by the USEPA [18]. Before sampling, the PUFs were Soxhlet extracted successively with acetone, dichloromethane, and n-hexane for 8 hours each, and GFFs were calcined at 450°C for 6 hours and weighed. After sampling, both the PUFs and GFFs were packed in aluminum foil and returned to the laboratory for further analyses.

2.2. Sample Preparation. In the laboratory, the PUF with a recovery indicator was Soxhlet extracted with 100 mL of a 1 : 1 mixture of n-hexane and acetone at 70°C for 24 h. The GFF was placed in a desiccator for 24 h and then weighed and cut into pieces for microwave extraction. The GFF was extracted with 25 mL of a hexane/acetone mixture (1 : 1) using a microwave-accelerated reaction system (CEM Corporation, Matthews, NC, USA). The microwave power was set at 1200 W, and the temperature program was as follows: ramped to 100°C over the course of 10 min and held at 100°C for another 10 min. Both the PUF and GFF extracts were concentrated to 1 mL by rotary evaporation first and then reconcentrated to 1 mL after adding 10 mL of n-hexane. The extracts were subsequently transferred to a silica/alumina chromatography column for cleanup. The initial solution that was eluted with 20 mL of n-hexane was discarded, and the subsequent eluate was collected, while 50 mL of a 1 : 1 mixture of n-hexane and DCM was used to elute the OCPs. The eluate was first concentrated to 1 mL by rotary evaporation and then reconcentrated to 1 mL after adding 10 mL of n-hexane. PCNB was added to the sample as an internal standard. The samples were concentrated to 100 μL with flowing nitrogen, transferred to microvolume inserts, and sealed for analysis.

2.3. Sample Analyses and Quality Control. The samples were analyzed using an Agilent 7890A/5975C gas chromatography and mass spectrometer detector and a HP-5MS fused silica capillary column (30 m $\times$ 0.25 mm $\times$ 0.25 μm, Agilent Co., USA). Helium was used as a carrier gas at a flow rate of 1 mL/min. The samples (1 μL) were injected by an autosampler under a splitless mode at a temperature of 220°C. The column temperature program was as follows: 50°C for

2 min, 10°C/min for 150°C, 3°C/min for 240°C, 240°C for 5 min, 10°C/min for 300°C, and 300°C for 5 min. The ion source temperature of the mass spectrometer was 200°C, the quadrupole temperature was 150°C. The compounds were quantified using the selected ion mode and a calibration curve with an internal standard.

There were two parallel samples in each sampling site, and the values from the parallel samples were averaged to get one value per sample. The samples, method blanks, and procedure blanks were prepared in the same manner. Method recoveries and detection limits were measured before sample analysis and are shown in Table 1.

3. Results and Discussion

3.1. Residual Levels of the OCPs in Ambient Air. The residual levels of OCPs in the gas phase and particle phase are shown in Table 2.

Twenty types of OCPs were detected in the gas phase at Lake Chaohu, including HCHs (α-, β-, γ-, δ-HCH), DDTs (o, p$'$-, p, p$'$-DDE, DDT, DDD), HCB, heptachlor, aldrin, isodrin, endrin, chlordane (α-, γ-chlordane), endosulfan (endosulfan I, II) and mirex, with a total concentration of 484.8 $\pm$ 550.4 pg/m^3. Endosulfan (245.6 $\pm$ 309.0 pg/m^3), DDTs (108.6 $\pm$ 122.9 pg/m^3), and chlordane (60.7 $\pm$ 138.0 pg/m^3) were the primary OCPs in the gas phase, which accounted for 50.7%, 22.4%, and 12.5%, respectively, whereas the other OCPs only occupied 14.4%. Endosulfan I (81.7%) and α-chlordane (93.0%) were the dominant isomers of endosulfan and chlordane, respectively. o, p$'$-DDE was the primary metabolite of DDT, which accounted for 64.9% of the DDTs. The proportions of α-HCH, γ-HCH, and β-HCH in the gas phase were 44.9%, 28.0%, and 20.3%, respectively.

Seventeen types of OCPs were detected in the particle phase at Lake Chaohu, including HCHs (α-, γ-, δ-HCH), DDTs (o, p$'$-, p, p$'$-DDE, DDT, DDD), HCB, heptachlor, aldrin, isodrin, endrin, endosulfan (endosulfan I, II), and dieldrin, with a total concentration of 28.9 $\pm$ 28.7 pg/m^3, which was approximately 6% of the total OCPs in the gas phase. DDTs (18.3 $\pm$ 26.1 pg/m^3), HCHs (2.4 $\pm$ 3.1 pg/m^3), and endosulfan (2.3 $\pm$ 1.7 pg/m^3) were the primary OCPs in the particle phase, which accounted for 63.4%, 8.3%, and 7.8%, respectively. p, p$'$-DDT (46.5%) and o, p$'$-DDT (17.9%) were the dominant DDTs and α-HCH (51.2%) and γ-HCH (40.0%) were the dominant HCHs in the particle phase.

The concentration of endosulfan (245.6 $\pm$ 309.0 pg/m^3) was the highest among the OCPs in the gas phase, which was similar to the result reported by Pozo et al. [19]. The residual level of endosulfan was less than that in Xi'an (472.7 pg/m^3) [20] and Lake Taihu (320 pg/m^3) [21] and greater than that in the Northern South China Sea (131 pg/m^3) [21]. The concentration of chlordane (60.7 $\pm$ 138.0 pg/m^3) was considerably less than that in Guangzhou (209 pg/m^3) [4], Hong Kong (769 pg/m^3) [22] and Japan (314 pg/m^3) [23], and greater than that in Qingdao (32 pg/m^3) [24] and Korea (4.2 pg/m^3) [25]. The residual levels of HCHs and DDTs in the gas phase at
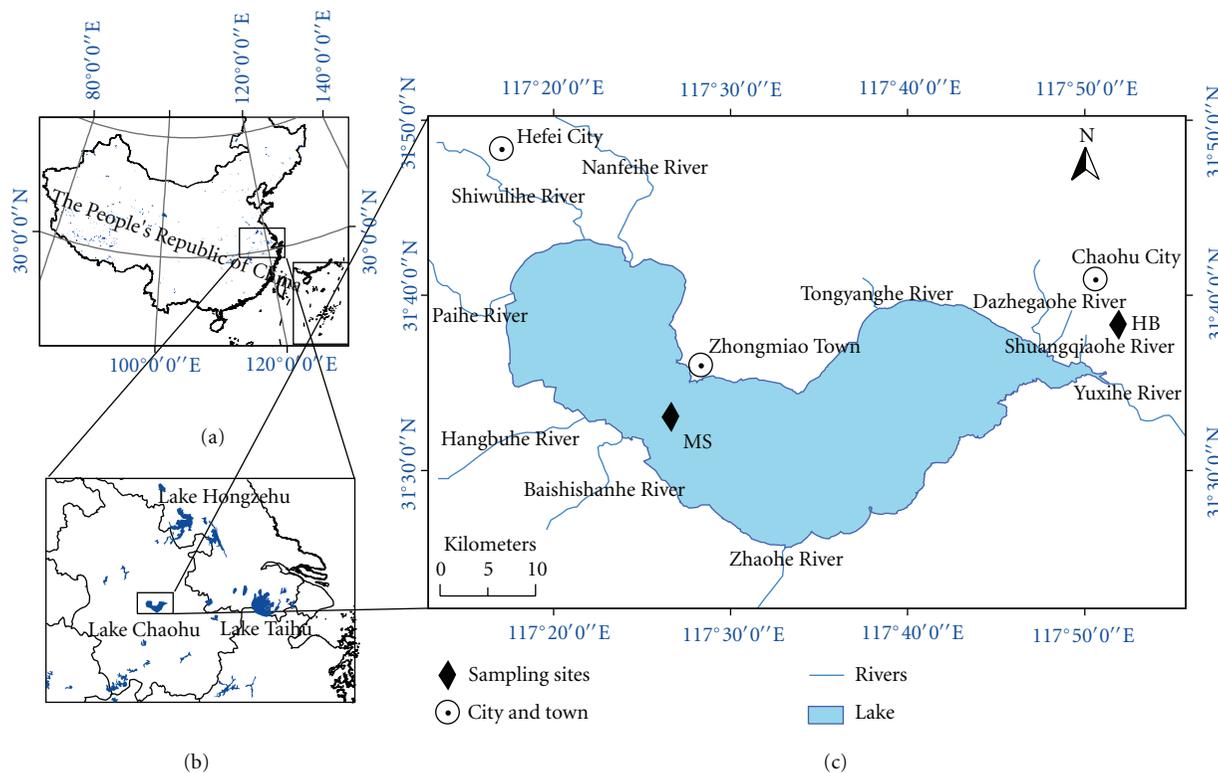
FIGURE 1: Geographical locations of (a) Lake Chaohu in China, (b) Lake Chaohu in Eastern China, and (c) the sampling sites.

TABLE 1: Recoveries and detection limits.

	Recoveries %		Detection limits (pg/m^3)	
	Gas phase	Particle phase	Gas phase	Particle phase
α-HCH	79.5	87.5	0.06	0.05
β-HCH	98.8	107.7	0.05	0.04
γ-HCH	89.6	93.1	0.05	0.05
δ-HCH	89.4	94.1	0.05	0.05
o, p′-DDE	115.7	112	0.08	0.08
p, p′-DDE	113.2	117.7	0.04	0.04
o, p′-DDD	113	114.1	0.04	0.04
p, p′-DDD	64.8	84.5	0.7	0.5
o, p′-DDT	116.8	115.8	0.4	0.4
p, p′-DDT	135.8	135.8	0.03	0.03
HCB	69.6	76.3	0.01	0.01
Heptachlor	121.4	110.4	0.04	0.04
Aldrin	95.1	96.6	0.05	0.05
Isodrin	93.3	95.5	0.02	0.02
α-Chlordane	109.9	104.2	0.08	0.09
γ-Chlordane	94.6	98.7	0.05	0.05
Endosulfan I	67.4	84.7	0.07	0.05
Endosulfan II	90	98.1	0.05	0.05
Dieldrin	83.1	90.5	0.05	0.05
Endrin	162.1	142.4	0.3	0.3
Mirex	97.8	108.2	0.09	0.08

TABLE 2: Residual levels of OCPs in ambient air at Lake Chaohu from March 2010 to February 2011.

	Gas phase		Particle phase		Total
	AM $\pm$ SD (pg/m^3)	Detection ratio	AM $\pm$ SD (pg/m^3)	Detection ratio	AM $\pm$ SD (pg/m^3)
α-HCH	16.1 $\pm$ 12.4	95.8%	1.2 $\pm$ 1.9	66.7%	17.3 $\pm$ 12.8
β-HCH	7.3 $\pm$ 12.4	87.5%	ND	ND	7.3 $\pm$ 12.4
γ-HCH	10.0 $\pm$ 9.8	95.8%	1.0 $\pm$ 0.9	75.0%	11.0 $\pm$ 9.5
δ-HCH	2.4 $\pm$ 3.7	75.0%	0.2 $\pm$ 0.5	20.8%	2.7 $\pm$ 3.7
HCHs	35.8 $\pm$ 29.7	95.8%	2.4 $\pm$ 3.1	75.0%	38.2 $\pm$ 29.3
o, p$'$-DDE	70.5 $\pm$ 90.6	91.7%	0.1 $\pm$ 0.5	8.3%	70.7 $\pm$ 90.9
p, p$'$-DDE	22.1 $\pm$ 22.3	83.3%	1.4 $\pm$ 1.5	66.7%	23.5 $\pm$ 21.6
o, p$'$-DDD	1.4 $\pm$ 3.2	25.0%	1.7 $\pm$ 3.6	29.2%	3.0 $\pm$ 4.5
p, p$'$-DDD	1.3 $\pm$ 1.4	62.5%	3.3 $\pm$ 7.5	58.3%	4.6 $\pm$ 7.1
o, p$'$-DDT	7.7 $\pm$ 9.1	83.3%	3.3 $\pm$ 3.7	70.8%	10.9 $\pm$ 9.0
p, p$'$-DDT	5.6 $\pm$ 7.5	79.2%	8.5 $\pm$ 23.9	50.0%	14.1 $\pm$ 27.2
DDTs	108.6 $\pm$ 122.9	95.8%	18.3 $\pm$ 26.1	79.2%	126.9 $\pm$ 126.6
HCB	10.4 $\pm$ 15.1	95.8%	1.6 $\pm$ 0.7	100.0%	12.0 $\pm$ 15.6
Heptachlor	5.0 $\pm$ 5.8	62.5%	0.2 $\pm$ 0.6	20.8%	5.3 $\pm$ 6.1
Aldrin	13.5 $\pm$ 27.9	62.5%	1.2 $\pm$ 2.1	37.5%	14.7 $\pm$ 27.7
Isodrin	2.4 $\pm$ 2.7	79.2%	1.2 $\pm$ 1.2	70.8%	3.6 $\pm$ 2.7
α-Chlordane	56.4 $\pm$ 137.2	87.5%	ND	ND	56.4 $\pm$ 137.2
γ-Chlordane	4.2 $\pm$ 4.0	83.3%	ND	ND	4.2 $\pm$ 4.0
Chlordane	60.7 $\pm$ 138.0	95.8%	ND	ND	60.7 $\pm$ 138.0
Endosulfan I	200.6 $\pm$ 246.5	91.7%	0.8 $\pm$ 0.8	66.7%	201.4 $\pm$ 246.2
Endosulfan II	45.0 $\pm$ 66.3	79.2%	1.5 $\pm$ 1.2	83.3%	46.4 $\pm$ 66.1
Endosulfan	245.6 $\pm$ 309.0	91.7%	2.3 $\pm$ 1.7	87.5%	247.8 $\pm$ 308.4
Endrin	1.3 $\pm$ 2.2	29.2%	0.2 $\pm$ 0.5	16.7%	1.5 $\pm$ 2.2
Mirex	1.4 $\pm$ 1.5	66.7%	ND	ND	1.4 $\pm$ 1.5
Dieldrin	ND	ND	1.6 $\pm$ 2.3	33.3%	1.6 $\pm$ 2.3
Total	484.8 $\pm$ 550.4	100%	28.9 $\pm$ 28.7	100%	513.7 $\pm$ 545.0

AM: arithmetic mean, SD: standard deviation, ND: not detected.

Lake Chaohu were less than those in other regions, such as Guangdong (HCHs 0.655 ng/m^3, DDTs 1.458 ng/m^3), Hong Kong (HCHs 0.161 ng/m^3, DDTs 0.444 ng/m^3), Anhui (HCHs 0.185 ng/m^3, DDTs 0.297 ng/m^3), Hebei (HCHs 0.117 ng/m^3, DDTs 0.336 ng/m^3), Jiangsu (HCHs 0.0948 ng/m^3, DDTs 0.771 ng/m^3), Seoul in Korea (HCHs 0.262 ng/m^3, DDTs 0.033 ng/m^3), Japan (HCHs 0.124 ng/m^3), Alabama in America (HCHs 0.168 ng/m^3, DDTs 0.011 ng/m^3), Mexico (HCHs 0.103 ng/m^3, DDTs 0.574 ng/m^3), Belize in America (DDTs 1.159 ng/m^3), and India (HCHs 0.91 $\sim$ 35.57 ng/m^3) [23, 26–29].

The concentrations of HCHs and DDTs in the particle phase in Lake Chaohu were less than those in other cities in China, such as Beijing (HCHs 0.506 $\pm$ 0.334 ng/m^3, DDTs 1.559 $\pm$ 2.021 ng/m^3) [30], Tianjin (HCHs 1.05 $\pm$ 1.88 ng/m^3, DDTs 0.839 $\pm$ 1.88 ng/m^3) [31], Guangdong (HCHs 0.002 ng/m^3, DDTs 0.091 ng/m^3) [22], Hong Kong (HCHs 0, DDTs 0.0185 ng/m^3) [22], and Hohhot (HCHs 1.68 ng/m^3) [32]. Compared to Sweden (HCHs 0.882 ng/m^3, DDTs 0.001 ng/m^3), the Gulf of Mexico (p, p$'$-DDT 0.008–0.018 ng/m^3), and Paris (HCHs 0.3–6.3 ng/m^3) [33, 34], the residual level of HCHs was relatively low, but the level of DDTs was relatively high.

3.2. Components of the OCPs in Ambient Air. The seasonal distributions of the OCPs components in the gas phase and particle phase are shown in Figure 2. In the gas phase, HCHs (28.2%) and HCB (26.2%) were the primary OCPs in winter, whereas endosulfan (39.9%–54.1%) and DDTs (17.8%–35.2%) were the dominant types in the other three seasons. The other OCPs also exhibited seasonal variations; for example, the proportion of heptachlor was approximately 20 times greater in the winter than in the other seasons, and chlordane was two times greater in the summer and autumn than in the spring and winter. In the particle phase, HCHs (32.0%) and DDTs (27.3%) were the predominant types of OCPs, and the proportion of DDTs was significantly greater than the other OCPs in the other three seasons, which accounts for 49.9%–85.0%. The proportions of HCHs and dieldrin were significantly greater in the autumn and winter. Aldrin was higher in the spring, and HCB was higher in autumn.

The proportions of the HCHs and DDTs components are shown in Figures 3 and 4. In the gas phase (Figure 3(a)), α-HCH (29.6%–71.3%) was the predominant isomer, the second one was γ-HCH (14.3%–33.3%), and δ-HCH (4.1%–8.2%) was the lowest. The percentage of α-HCH increased in

(a)

(b)
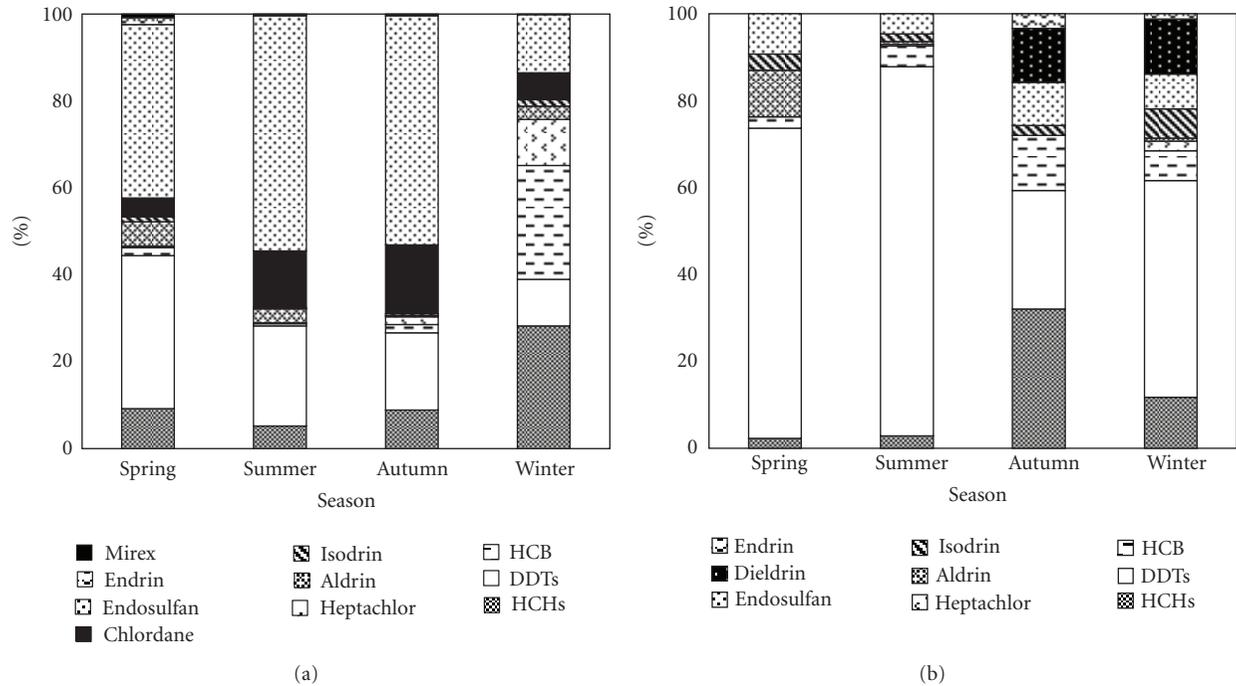
FIGURE 2: Seasonal variations of OCPs in the gas phase (a) and particle phase (b) at Lake Chaohu from March 2010 to February 2011.

the autumn and winter while β-HCH and γ-HCH exhibited an opposite trend, and the proportion of δ-HCH decreased in winter. In the particle phase (Figure 3(b)), γ-HCH was the dominant HCHs in the spring and summer (73.0% and 56.4%), whereas α-HCH was the primary isomer in the autumn and winter (59.5% and 54.2%). β-HCH was not detected in any of the seasons, and δ-HCH was not detected in the spring. The percentage of δ-HCH was higher in the summer and lower in the winter.

In the gas phase (Figure 4(a)), the majority of the DDTs were DDE (61.5%–92.6%); p, p′-DDE was the dominant type in the winter while o, p′-DDE was the primary one in the other seasons. The proportion of DDE was considerably lower in the particle phase, which only accounted for 3.1%–18.4%, and the highest proportion was in winter. In the particle phase (Figure 4(b)), DDT was the dominant type in spring and summer, accounting for 61.5% and 96.9%, whereas DDD was the major type in autumn and winter, occupying 70.8% and 45.8%. The majority of DDT existed as p, p′-DDT in the spring and summer, especially in the summer, when 93.1% of the DDTs was p, p′-DDT, and the concentration of p, p′-DDT decreased sharply in the autumn and winter. p, p′-DDD was greater than o, p′-DDD in the spring and summer, and it was lower in the autumn and winter.

3.3. Temporal-Spatial Variations of OCPs in Ambient Air.
The residual levels and temporal variations of OCPs at the lakeside (HB) and central lake (MS) sampling sites are shown in Table 3 and Figures 5 and 6.

In the gas phase, the total concentrations of OCPs at the HB and MS sampling sites were 457.1 ± 553.4 pg/m^3 (36.5–1838.1 pg/m^3) and 512.4 ± 570.6 pg/m^3 (44.3–1573.9 pg/m^3), respectively. The residual level of OCPs was greater in the central lake than in the lakeside site, expect for o, p′-DDT, HCB, heptachlor, isodrin, γ-chlordane, and endosulfan II (Table 3). As illustrated in Figure 5, the temporal distributions of the total OCPs at the HB and MS sampling sites are unimodal, with significantly higher mean concentrations in the summer than in the winter, which may be due to the high temperature in the summer that promotes volatilization from the water to the atmosphere. The correlations between atmospheric temperature and total OCPs concentration in the gas phase at HB and MS sampling sites are 0.868 ($P < 0.01$) and 0.782 ($P < 0.01$), respectively. The HCHs (except in July), DDTs, and endosulfan present similar distributions to that of the total OCPs.

In the particle phase, the total concentrations of OCPs at the HB and MS sampling sites were 34.3 ± 35.0 pg/m^3 (1.2–127.7 pg/m^3) and 23.4 ± 20.8 pg/m^3 (1.3–64.1 pg/m^3), respectively. An opposite spatial variation was observed in the particle phase in that the residual level of OCPs was lower in the central lake (MS) than in the lakeside (HB), which was primarily due to the discrepancy of the concentration of DDTs. As shown in Figure 6, an extremely high level of DDTs (120.8 pg/m^3) appeared in July 2010 at the HB sampling site. If the extremum was excluded, the concentration and temporal variation of the total OCPs in the lakeside would exhibit no significant difference with those in the central lake. The temporal distribution of OCPs in the particle phase was opposite with that in the gas phase, presenting a low concentration in the summer and high concentrations in the spring and winter, which may be due to the temperature discrepancy that affects the distribution of pollutants in the gas phase and particle phase. The correlation between

(a)

(b)
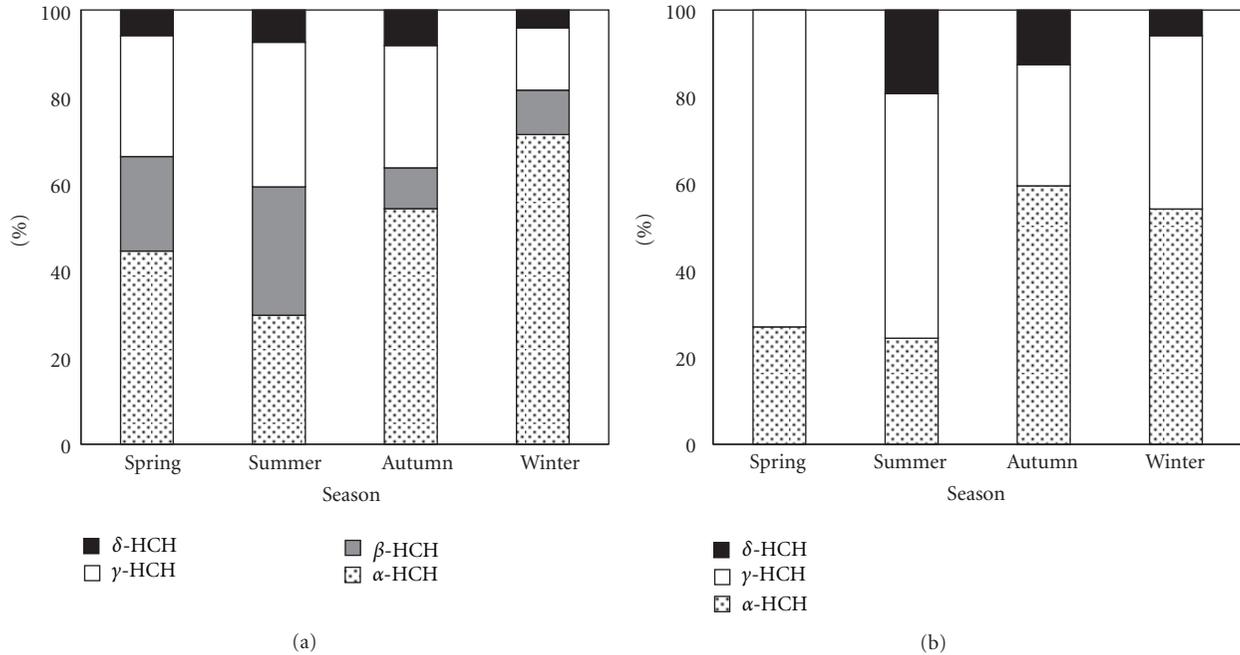
FIGURE 3: Seasonal variations of HCHs in the gas phase (a) and particle phase (b) at Lake Chaohu from March 2010 to February 2011.


(a)

(b)
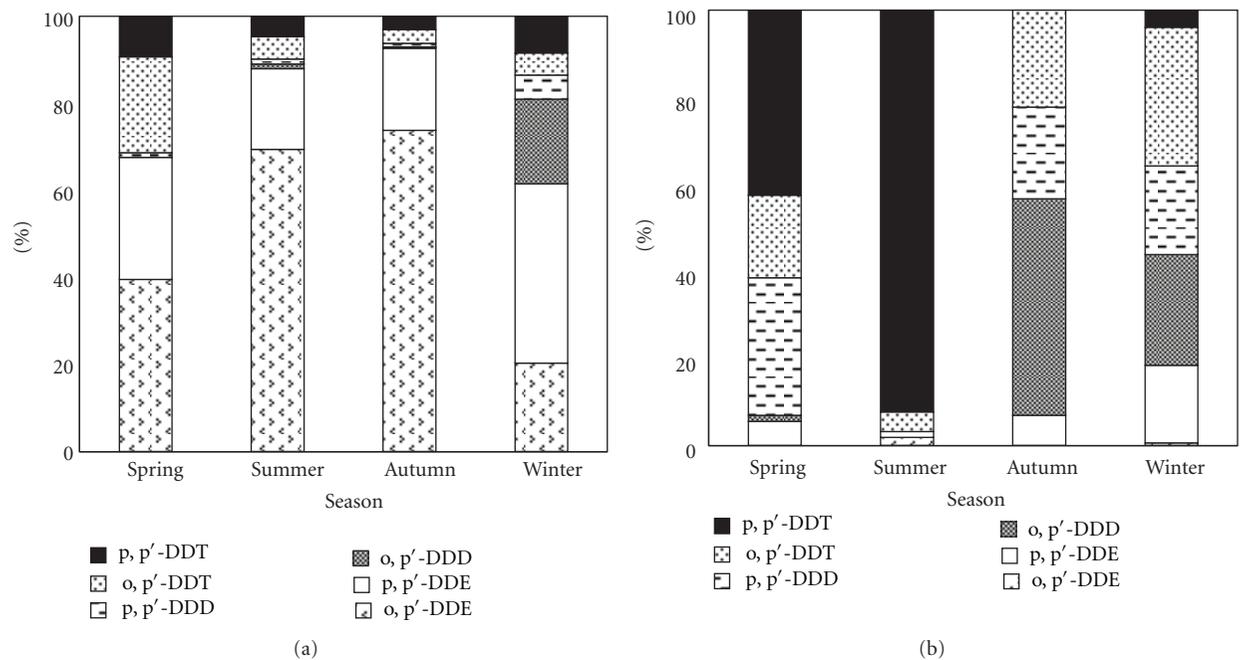
FIGURE 4: Seasonal variations of DDTs in the gas phase (a) and particle phase (b) at Lake Chaohu from March 2010 to February 2011.

atmospheric temperature and total OCPs concentration in the particle phase at MS sampling site is -0.703 ($P = 0.011$).

3.4. Sources of OCPs in Ambient Air

3.4.1. HCHs. Technical HCH consists of 60–70% α-HCH, 5–12% β-HCH, and 10–15% γ-HCH [35], with an α-/γ-HCH ratio of approximately 4–7 and a β-/($\alpha + \gamma$)-HCH ratio

of approximately 0.06–0.17. For lindane, which contains more than 99% γ-HCH, the α-/γ-HCH ratio is less than 0.1, and the β-/($\alpha + \gamma$)-HCH is less than 0.06. Because of a high vapor pressure, α-HCH tends to be residual in the atmosphere and could be transported for long distances. Consequently, the α-/γ-HCH ratio can be used to identify the source of the HCHs. If the α-/γ-HCH ratio is greater than 7, the HCHs may come from atmospheric transport

Table 3: Residual levels of OCPs in ambient air at the HB and MS from March 2010 to February 2011.

	HB (AM ± SD, pg/m³)			MS (AM ± SD, pg/m³)		
	Gas phase	Particle phase	Total	Gas phase	Particle phase	Total
α-HCH	14.7 ± 12.2	1.1 ± 1.5	15.8 ± 12.9	17.5 ± 13	1.4 ± 2.3	19.2 ± 15.2
β-HCH	4.6 ± 8.1	ND	4.6 ± 8.1	9.9 ± 15.6	ND	10.7 ± 17.4
γ-HCH	6.7 ± 5.1	0.9 ± 1.0	7.6 ± 4.8	13.3 ± 12.2	1 ± 0.9	15.0 ± 13.6
δ-HCH	1.8 ± 2.7	0.2 ± 0.6	2.1 ± 2.8	3.1 ± 4.6	0.2 ± 0.4	3.5 ± 5.4
HCHs	27.9 ± 20.0	2.2 ± 2.9	30.1 ± 20.6	43.8 ± 36.1	2.5 ± 3.4	48.4 ± 42.2
o, p′-DDE	67.0 ± 89.0	0.1 ± 0.2	67 ± 88.9	74.1 ± 96.0	0.2 ± 0.7	78.4 ± 102
p, p′-DDE	19.6 ± 19.3	1.4 ± 1.3	21 ± 18.6	24.7 ± 25.6	1.4 ± 1.7	27.6 ± 27.7
o, p′-DDD	0.3 ± 1.0	1.4 ± 2.4	1.7 ± 2.4	2.4 ± 4.3	1.9 ± 4.6	4.2 ± 5.4
p, p′-DDD	1.1 ± 1.1	4 ± 9.1	5.2 ± 8.8	1.4 ± 1.7	2.7 ± 5.7	4.2 ± 5.5
o, p′-DDT	8.0 ± 10.7	3.0 ± 3.0	11.1 ± 9.5	7.3 ± 7.7	3.5 ± 4.4	11.2 ± 9.3
p, p′-DDT	4.6 ± 5.9	13.9 ± 33.3	18.5 ± 37.3	6.6 ± 9.0	3.1 ± 4.1	10.3 ± 11.1
DDTs	100.7 ± 112.8	23.8 ± 33.9	124.5 ± 127.6	116.5 ± 136.8	12.8 ± 14.5	136 ± 140.1
HCB	11.2 ± 16.8	1.6 ± 0.7	12.7 ± 17.3	9.7 ± 13.9	1.6 ± 0.8	11.3 ± 14.1
Heptachlor	6.4 ± 7.2	0.2 ± 0.4	6.6 ± 7.5	3.7 ± 3.7	0.3 ± 0.7	3.9 ± 3.8
Aldrin	12.8 ± 26.9	1.2 ± 2.0	14.0 ± 26.9	14.3 ± 30.1	1.2 ± 2.2	16 ± 31.6
Isodrin	3.0 ± 3.4	1.2 ± 1.3	4.2 ± 3.2	1.9 ± 1.8	1.2 ± 1.2	3.2 ± 2.2
α-Chlordane	45.3 ± 146.9	ND	45.3 ± 146.9	67.6 ± 132.3	ND	73.5 ± 153.8
γ-Chlordane	4.9 ± 4.5	ND	4.9 ± 4.5	3.6 ± 3.4	ND	3.8 ± 3.7
Chlordane	50.2 ± 148.6	ND	50.2 ± 148.6	71.1 ± 132.3	ND	77.3 ± 154.1
Endosulfan I	196.6 ± 253.3	0.9 ± 0.8	197.5 ± 252.9	204.6 ± 250.7	0.7 ± 0.8	217.1 ± 271.9
Endosulfan II	46.0 ± 65.3	1.4 ± 1.1	47.4 ± 65.2	43.9 ± 70.2	1.5 ± 1.3	47.6 ± 71.2
Endosulfan	242.6 ± 315.5	2.3 ± 1.6	244.9 ± 315.0	248.5 ± 316.3	2.2 ± 1.9	264.7 ± 338.2
Endrin	1.2 ± 2.1	0.2 ± 0.6	1.4 ± 2.0	1.3 ± 2.5	0.2 ± 0.4	1.6 ± 2.5
Mirex	1.2 ± 1.4	ND	1.2 ± 1.4	1.6 ± 1.6	ND	1.7 ± 1.7
Dieldrin	ND	1.6 ± 2.4	1.6 ± 2.4	ND	1.5 ± 2.3	1.4 ± 2.1
Total	457.1 ± 553.4	34.3 ± 35.0	491.4 ± 555.7	512.4 ± 570.6	23.4 ± 20.8	535.9 ± 557.9

AM: arithmetic mean, SD: standard deviation, ND: not detected.

[36, 37]; if the α-/γ-HCH ratio is between 4 and 7, technical HCH might be the source of HCHs; if the α-/γ-HCH ratio is less than 4, lindane may be the primary source of the HCHs [38]. β-HCH is the primary isomer in the water, soil, and sediment because of its stable physical and chemical characteristics. Therefore, the β-/$(\alpha + \gamma)$-HCH ratio can be used to identify the historical HCH usage. A high β-/$(\alpha + \gamma)$-HCH ratio indicates a historical usage of technical HCH and lindane [39]. However, there is no consensus of a threshold to distinguish between historical usage and recent input. Based on previous studies [40], 0.5 was used as the threshold in this study. When the β-/$(\alpha + \gamma)$-HCH ratio is less than 0.5, the source of the HCHs may be the recent usage of lindane or atmospheric transport, whereas historical usage of technical HCH and lindane may result in a higher β-/$(\alpha + \gamma)$-HCH ratio. Therefore, the source of the HCHs can be analyzed by calculating the α-/γ-HCH and β-/$(\alpha+\gamma)$-HCH ratios (Figure 7(a)).

Based on the α-/γ-HCH ratio, only one sample had a ratio greater than 7 and two samples between 4 and 7; the majority of the samples fell into the region that was less than 4. Based on the β-/$(\alpha+\gamma)$-HCH ratio, only three samples were greater than 0.5. Therefore, the potential source of the HCHs at Lake Chaohu might come from recent lindane usage. The

α-/γ-HCH ratio of the sample collected in December 2010 at the HB sampling site was greater than 7, which indicated an atmospheric transport of α-HCH from North China.

3.4.2. DDTs. Technical DDT contains approximately 14 compounds, including 75% p, p′-DDT and 15% o, p′-DDT, with the o, p′-/p, p′-DDT ratio being approximately 0.2. Dicofol, which is a substitute for DDT, was widely used after the prohibition of technical DDT in 1983, and it contains considerable impurities of DDTs with o, p′-DDT being the primary DDT isomer. The o, p′-/p, p′-DDT ratio in dicofol is 7 ± 2; therefore, a high o, p′-/p, p′-DDT ratio in the environment is a result of dicofol usage [41], whereas a ratio of 0.2 indicates technical DDT usage. In addition, the proportion of DDT and its metabolites can help to analyze the source of DDTs in the environment. By degrading into DDE and DDD, the amount of DDT will decrease while the amounts of DDE and DDD increase [42]. Therefore, a small value of DDT/(DDE + DDD) is an indicator of historical DDT usage, and a value >1 indicates recent input. Consequently, the source of the DDTs can be analyzed by calculating the o, p′-/p, p′-DDT and DDT/(DDE + DDD) ratios (Figure 7(b)).
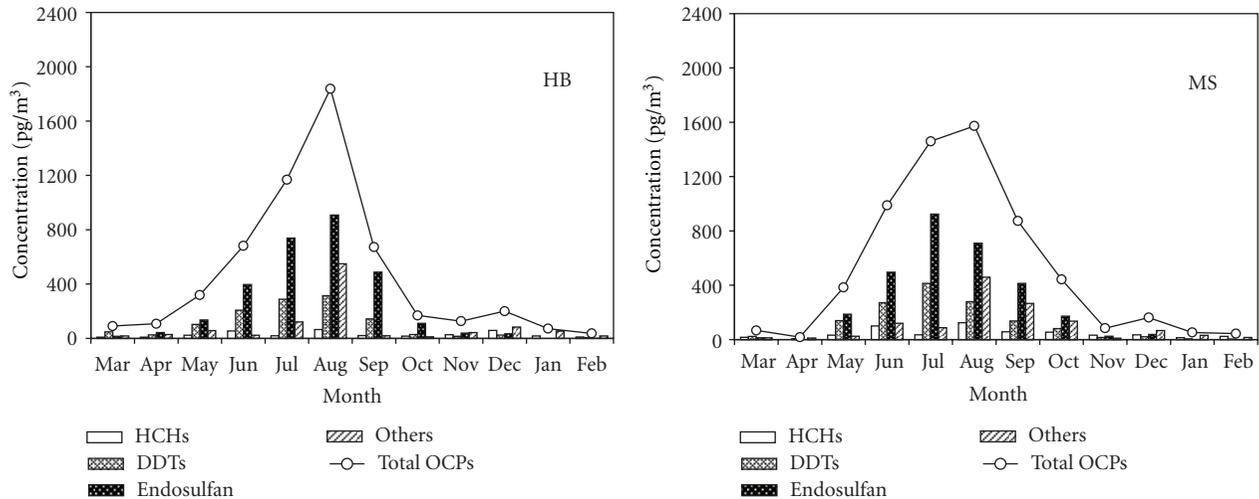
FIGURE 5: Temporal distributions of OCPs in the gas phase at the HB and MS sampling sites from March 2010 to February 2011.
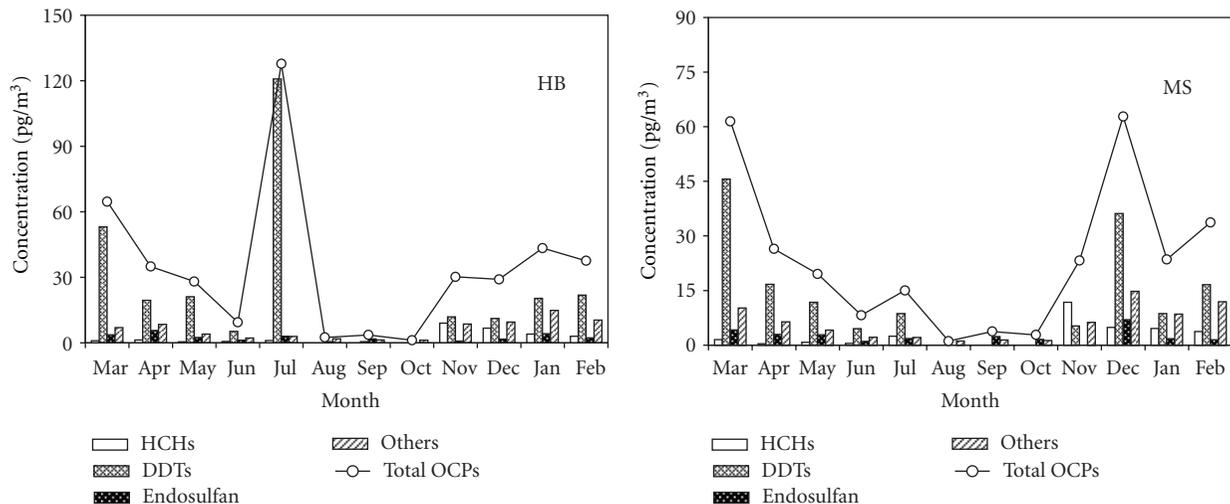

FIGURE 6: Temporal distributions of OCPs in the particle phase at the HB and MS sampling sites from March 2010 to February 2011.

As shown in Figure 7(b), the DDT/(DDE + DDD) ratios of three samples were >1, indicating that there were fresh DDT inputs in the spring, which might come from the use of marine paint during closed seasons (between February and June) (e.g., HB and MS sampling sites in March 2010), or dicofol usage for soaking seeds during the spring sowing (e.g., MS sampling site in April 2010). Except for the above three samples, the DDT/(DDE + DDD) ratios of other samples were <1, which indicated historical DDT usage. For these samples, the o, p′-/p, p′-DDT ratios of them were as follows: only one sample was <0.2, and six samples were >0.2, which implied that the source of the DDTs may be historical usage of technical DDT and dicofol.

In addition to being an important food and aquatic product base for the Anhui province, Chaohu also has a developed ship building industry, which has become one of the pillar industries, and there are more than 4000 boats engaged in fishing. Since DDT was prohibited for agriculture

use in 1983, DDT is primarily used as a material for producing dicofol and for making marine paint, mosquito coils, and for epidemic prevention, such as malaria. Dicofol is a widely used organochlorine acaricide because of its wide acaricidal range, high activity, and low price. All of these activities lead to the usage and distribution of DDTs.

3.4.3. Endosulfan. Endosulfan exists as either endosulfan I or endosulfan II. Because endosulfan II is more stable in the environment than endosulfan I [43], the ratio of endosulfan I/II will be <1 if there is no endosulfan input. Technical endosulfan is a 7 : 3 mixture of endosulfan I and endosulfan II [44]; therefore, technical endosulfan input will increase the endosulfan I/II ratio. Consequently, the ratio of endosulfan I/II can be used as an indicator for the age of endosulfan. As shown in Figure 7(c), the ratios of endosulfan I/II were >2.33 for all of the gas samples, except for those without detection, which indicates recent technical endosulfan input.
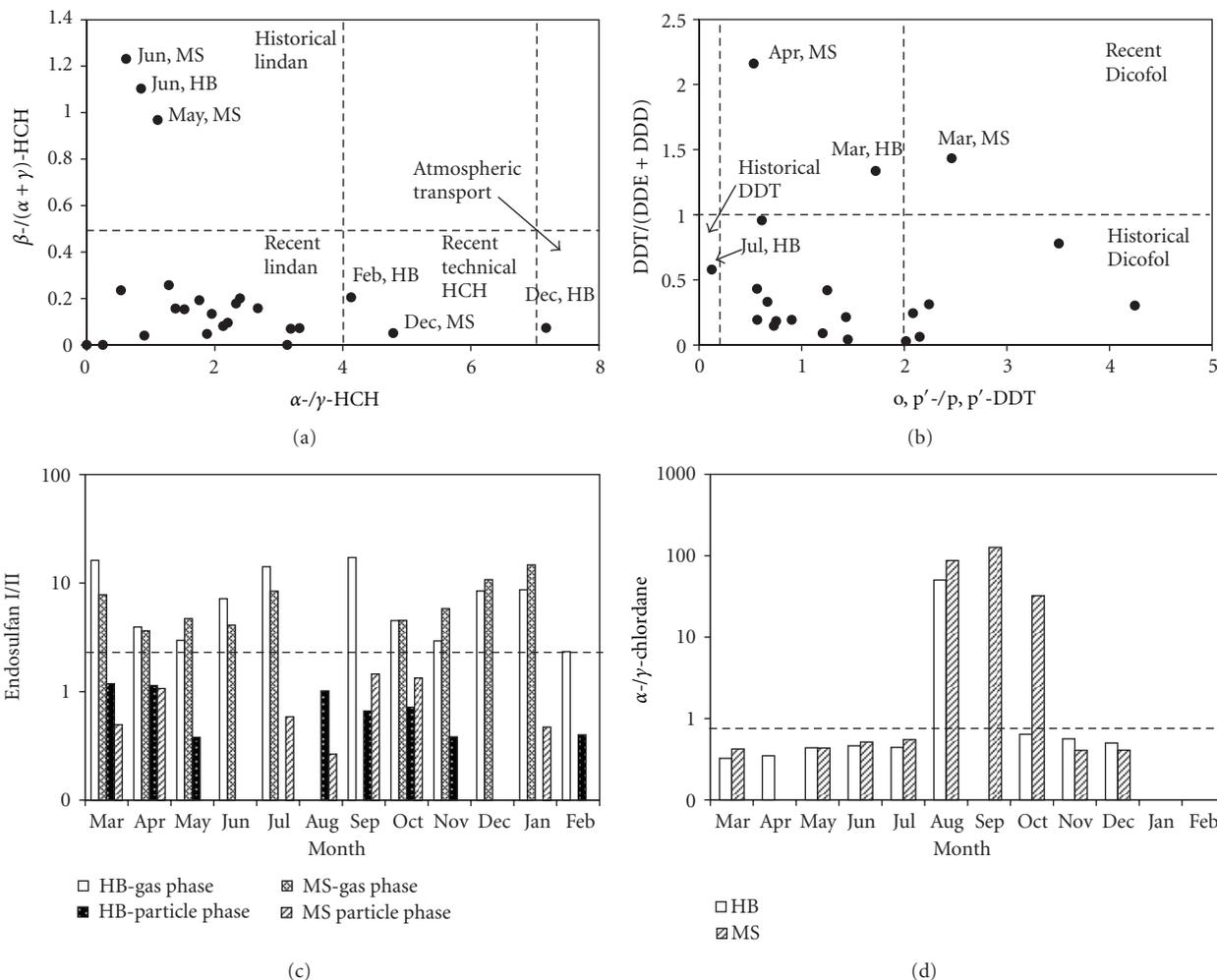
FIGURE 7: Source analyses of HCHs (a), DDTs (b), endosulfan (c), and chlordane (d) in ambient air at the HB sampling site and the MS sampling site from March 2010 to February 2011.

Endosulfan, which is an organochlorine acaricide, is still widely used in China to control insect pests for cotton, wheat, tea, tobacco, vegetable, fruit, and so forth. Endosulfan production in China is the second largest in the world after India. Between 1994 and 2004, the total amount of endosulfan usage was 25700 tons, and the usage in Anhui was the fifth largest (1900 tons), which was the less than Henan (4000 tons), Xinjiang (3200 tons), Shandong (3000 tons), and Hebei (2100 tons) [45]. Chaohu basin is a primary base for cotton, tea, vegetable, and fruit plantations in the Anhui province, which suggests a large amount of endosulfan usage in this area, which may be why endosulfan was the primary type of OCPs in the atmosphere.

3.4.4. Chlordane.
γ-chlordane degrades more rapidly than α-chlordane, and a ratio of α-/γ-chlordane >1 is generally believed to come from aged chlordane [46]. In technical chlordane, the α-/γ-chlordane ratio is approximately 0.77 [47]. When a ratio of α-/γ-chlordane is <0.77, there may be fresh technical chlordane input. Therefore, the ratio of

α-/γ-chlordane can be used as an indicator of aged chlordane. As shown in Figure 7(d), the ratios of α-/γ-chlordane were <0.77 for most of the samples, which indicates recent technical chlordane input.

In China, especially South China, chlordane is still the primary pesticide for termite control although an Integrated Pest Management (IPM) program has come into use. Chaohu basin is located in the north-south air flow intersection and northern subtropical humid monsoon climate zone, with an annual average temperature of 15-16°C, which is suitable for the growth of termites. The length of the dams of the rivers, such as the Yangtze River, the lakes, such as Lake Chaohu, and the reservoirs has reached 2870 km, with more than 70% suffering from termite damage, especially during the termites' reproduction peaks in April, May, and June [48]. The relatively high concentration of chlordane in the atmosphere may be a result of termite control.

3.4.5. Other OCPs

HCB. China began HCB synthesis in 1951 and has had six HCB production companies in its history. Because of

the prohibition of HCH in 1983, only one company has remained (Tianjin Dagu Chemical Company). Between 1988 and 2002, the cumulative production of HCB was 75756 tons, among which 98.6% were used to synthesize sodium pentachlorophenate and pentachlorophenate [49]. Sodium pentachlorophenate is effective for snail control and is applied in epidemic prevention to kill snails, miracidia, and cercariae. Chaohu basin is a schistosomiasis epidemic region with a snail area of 120 km^2 and schistosomiasis patients more than 40000 in history [49]. Therefore, it can be inferred that the HCB in the atmosphere may come from the use of sodium pentachlorophenate for the control of snails and schistosomiasis.

Aldrin, Dieldrin, Isodrin, and Endrin. Aldrin and dieldrin have only been experimentally synthesized, and no industrial syntheses have been performed. Isodrin and endrin were never produced in China [50]. The detection ratio and residual levels of Aldrin, dieldrin, isodrin, and endrin were low at Lake Chaohu, and they may come from the long-distance transport from other countries, such as Japan and Korea.

4. Conclusions

(1) Twenty types of OCPs were detected in the gas phase with a total concentration of 484.8 ± 550.4 pg/m^3. Endosulfan, DDTs, and chlordane were the primary OCPs in the gas phase, accounting for 50.7%, 22.4%, and 12.5%, respectively. Seventeen types of OCPs were detected in the particle phase with a total concentration of 18.3 ± 26.1 pg/m^3. DDTs were the primary OCPs in the particle phase, accounting for 63.4%.

(2) In the gas phase, HCHs and HCB were the dominant OCPs in the winter, whereas endosulfan and DDTs were the dominant types in the other three seasons. In the particle phase, HCHs and DDTs were the dominant OCPs in autumn, whereas DDTs were the dominant types in the other three seasons. The mean concentration of OCPs in the gas phase was significantly higher in the summer than in the winter. The concentration of OCPs in the particle phase decreased at first and then increased during the same period. The residual level of OCPs in the gas phase was higher in the central lake, whereas the concentration of OCPs in the particle phase was higher in the lakeside.

(3) In the gas phase, o, p′-DDE was the primary metabolite of DDT, which accounted for 64.9% of the DDTs. The proportions of α-HCH, γ-HCH, and β-HCH in the gas phase were 44.9%, 28.0%, and 20.3%, respectively. In the particle phase, DDT was the primary DDTs, which occupied 64.7%. The HCHs were composed of 51.2% α-HCH, 40.0% γ-HCH, and 8.8% δ-HCH, and β-HCH was not detected.

(4) The potential source of the HCHs in ambient air of Lake Chaohu might come from recent lindane usage. DDTs mainly came from historical dicofol usage, and an input of DDT was found in the spring, which may result from the present use of marine paint that contains technical DDT. Endosulfan and chlordane in the air may be due to the present use of technical endosulfan and chlordane.

Acknowledgments

References

[1] G. Carrera, P. Fernández, R. M. Vilanova, and J. O. Grimalt, "Persistent organic pollutants in snow from European high mountain areas," *Atmospheric Environment*, vol. 35, no. 2, pp. 245–254, 2001.

[2] A. T. Fisk, G. A. Stern, K. A. Hobson, W. J. Strachan, M. D. Loewen, and R. J. Norstrom, "Persistent Organic Pollutants (POPs) in a small, herbivorous, Arctic marine zooplankton (*Calanus hyperboreus*): trends from April to July and the Influence of lipids and trophic transfer," *Marine Pollution Bulletin*, vol. 43, no. 1–6, pp. 93–101, 2001.

[3] B. Van Wendel De Joode, C. Wesseling, H. Kromhout, P. Monge, M. García, and D. Mergler, "Chronic nervous-system effects of long-term occupational exposure to DDT," *The Lancet*, vol. 357, no. 9261, pp. 1014–1016, 2001.

[4] Y. Yang, D. Li, and D. Mu, "Levels, seasonal variations and sources of organochlorine pesticides in ambient air of Guangzhou, China," *Atmospheric Environment*, vol. 42, no. 4, pp. 677–687, 2008.

[5] C. Turgut, "The contamination with organochlorine pesticides and heavy metals in surface water in Küçük Menderes River in Turkey, 2000–2002," *Environment International*, vol. 29, no. 1, pp. 29–32, 2003.

[6] X. T. Wang, S. G. Chu, and X. B. Xu, "Organochlorine pesticide residues in water from Guanting reservoir and Yongding River, China," *Bulletin of Environmental Contamination and Toxicology*, vol. 70, no. 2, pp. 351–358, 2003.

[7] C. K. C. Wong, K. M. Leung, B. H. T. Poon, C. Y. Lan, and M. H. Wong, "Organochlorine hydrocarbons in human breast milk collected in Hong Kong and Guangzhou," *Archives of Environmental Contamination and Toxicology*, vol. 43, no. 3, pp. 364–372, 2002.

[8] F. Wania and D. Mackay, "Tracking the distribution of persistent organic pollutants," *Environmental Science and Technology*, vol. 30, no. 9, pp. 390A–396A, 1996.

[9] R. Bailey, L. A. Barrie, C. J. Halsall, P. Fellin, and D. C. G. Muir, "Atmospheric organochlorine pesticides in the western Canadian Arctic: evidence of transpacific transport," *Journal of Geophysical Research D*, vol. 105, no. 9, pp. 11805–11811, 2000.

[10] E. Lie, A. Bernhoft, F. Riget et al., "Geographical distribution of organochlorine pesticides (OCPs) in polar bears (Ursus maritimus) in the Norwegian and Russian Arctic," *Science of the Total Environment*, vol. 306, no. 1–3, pp. 159–170, 2003.

[11] W. E. Cotham and T. F. Bidleman, "Estimating the atmospheric deposition of organochlorine contaminants to the Arctic," *Chemosphere*, vol. 22, no. 1-2, pp. 165–188, 1991.

[12] X. Wu, J. C. W. Lam, C. Xia, H. Kang, Z. Xie, and P. K. S. Lam, "Atmospheric concentrations of DDTs and chlordanes measured from Shanghai, China to the Arctic Ocean during the Third China Arctic Research Expedition in 2008," *Atmospheric Environment*, vol. 45, no. 22, pp. 3750–3757, 2011.

[13] L. Shen, F. Wania, Y. D. Lei, C. Teixeira, D. C. G. Muir, and T. F. Bidleman, "Hexachlorocyclohexanes in the North American Atmosphere," *Environmental Science and Technology*, vol. 38, no. 4, pp. 965–975, 2004.

[14] F. L. Xu, S. Tao, and Z. R. Xu, "The restoration of riparian wetlands and macrophytes in Lake Chao, an eutrophic Chinese lake: possibilities and effects," *Hydrobiologia*, vol. 405, pp. 169–178, 1999.

[15] F. L. Xu, S. Tao, R. W. Dawson, P. G. Li, and J. Cao, "Lake ecosystem health assessment: indicators and methods," *Water Research*, vol. 35, no. 13, pp. 3157–3167, 2001.

[16] W. He, N. Qin, Q. S. He, Y. Wang, X. Z. Kong, and F. L Xu, "Characterization, ecological and health risks of DDTs and HCHs in water from a large shallow Chinese lake," *Ecological Informatics*, vol. 12, pp. 77–84, 2012.

[17] Y. Wang, W. He, N. Qin et al., "Residual levels and ecological risks of organochlorine pesticides in surface sediments from Lake Chaohu," *Acta Scientiae Circumstantiae*, vol. 32, no. 2, pp. 308–316, 2012.

[18] USEPA: Compendium Method TO-13A, "Determination of Polycyclic Aromatic Hydrocarbons (PAHs) in Ambient Air Using Gas Chromatography/Mass Spectrometry (GC/MS)," 1999.

[19] K. Pozo, T. Harner, F. Wania, D. C. G. Muir, K. C. Jones, and L. A. Barrie, "Toward a global network for persistent organic pollutants in air: results from the GAPS study," *Environmental Science and Technology*, vol. 40, no. 16, pp. 4867–4873, 2006.

[20] Y. M. Liu, C. Z. Zhang, W. H. Li et al., "Pollution characterization and source apportionment of organochlorine pesticides in air in Xi'an City," *Research of Environmental Sciences*, vol. 23, no. 3, pp. 266–271, 2010.

[21] G. Zhang, J. Li, H. Cheng, X. Li, W. Xu, and K. C. Jones, "Distribution of organochlorine pesticides in the northern South China Sea: implications for land outflow and air-sea exchange," *Environmental Science and Technology*, vol. 41, no. 11, pp. 3884–3890, 2007.

[22] J. Li, G. Zhang, L. Guo et al., "Organochlorine pesticides in the atmosphere of Guangzhou and Hong Kong: regional sources and long-range atmospheric transport," *Atmospheric Environment*, vol. 41, no. 18, pp. 3889–3903, 2007.

[23] H. Murayama, Y. Takase, H. Mitobe et al., "Seasonal change of persistent organic pollutant concentrations in air at Niigata area, Japan," *Chemosphere*, vol. 52, no. 4, pp. 683–694, 2003.

[24] G. Lammel, Y. S. Ghim, A. Grados, H. Gao, H. Hühnerfuss, and R. Lohmann, "Levels of persistent organic pollutants in air in China and over the Yellow Sea," *Atmospheric Environment*, vol. 41, no. 3, pp. 452–464, 2007.

[25] H. G. Yeo, M. Choi, M. Y. Chun, T. W. Kim, K. C. Cho, and Y. Sunwoo, "Concentration characteristics of atmospheric PCBs for urban and rural area, Korea," *Science of the Total Environment*, vol. 324, no. 1–3, pp. 261–270, 2004.

[26] D. D. Shao, S. T. Shi, L. Zhou, and Y. R. Huang, "A survey of atmosphere organochlorine pesticides residual levels in four provinces along the Yangtze River," *Environmental Protection*, vol. 386, no. 12B, pp. 68–69, 2007.

[27] L. M. M. Jantunen, T. F. Bidleman, T. Harner, and W. J. Parkhurst, "Toxaphene, chlordane, and other organochlorine pesticides in Alabama air," *Environmental Science and Technology*, vol. 34, no. 24, pp. 5097–5105, 2000.

[28] H. Alegria, T. F. Bidleman, and M. S. Figueroa, "Organochlorine pesticides in the ambient air of Chiapas, Mexico," *Environmental Pollution*, vol. 140, no. 3, pp. 483–491, 2006.

[29] H. A. Alegria, T. F. Bidleman, and T. J. Shaw, "Organochlorine pesticides in ambient air of Belize, Central America," *Environmental Science and Technology*, vol. 34, no. 10, pp. 1953–1958, 2000.

[30] X. Wang, X. Li, H. Cheng, X. Xu, G. Zhuang, and C. Zhao, "Organochlorine pesticides in particulate matter of Beijing, China," *Journal of Hazardous Materials*, vol. 155, no. 1-2, pp. 350–357, 2008.

[31] S. P. Wu, S. Tao, Z. H. Zhang, T. Lan, and Q. Zuo, "Distribution of particle-phase hydrocarbons, PAHs and OCPs in Tianjin, China," *Atmospheric Environment*, vol. 39, no. 38, pp. 7420–7432, 2005.

[32] Q. Tong, S. Y. Feng, Y. Y. Ruan, T. J. Zhao, and F. Tang, "Distribution of organochlorine pesticides on the different diametral atmospheric particulate," *Environmental Chemistry*, vol. 19, no. 4, pp. 306–312, 2000.

[33] C. S. Giam, E. Atlas, H. S. Chan, and G. S. Neff, "Phthalate esters, PCB and DDT residues in the gulf of Mexico atmosphere," *Atmospheric Environment A*, vol. 14, no. 1, pp. 65–69, 1980.

[34] T. F. Bidleman, U. Wideqvist, B. Jansson, and R. Soderlund, "Organochlorine pesticides and polychlorinated biphenyls in the atmosphere of southern Sweden," *Atmospheric Environment A*, vol. 21, no. 3, pp. 641–654, 1987.

[35] X. Qiu, T. Zhu, J. Li et al., "Organochlorine Pesticides in the Air around the Taihu Lake, China," *Environmental Science and Technology*, vol. 38, no. 5, pp. 1368–1374, 2004.

[36] H. Iwata, S. Tanabe, and R. Tatsukawa, "A new view on the divergence of HCH isomer compositions in oceanic air," *Marine Pollution Bulletin*, vol. 26, no. 6, pp. 302–305, 1993.

[37] H. Iwata, S. Tanabe, K. Ueda, and R. Tatsukawa, "Persistent organochlorine residues in air, water, sediments, and soils from the Lake Baikal Region, Russia," *Environmental Science and Technology*, vol. 29, no. 3, pp. 792–801, 1995.

[38] K. Walker, D. A. Vallero, and R. G. Lewis, "Factors influencing the distribution of lindane and other hexachlorocyclohexanes in the environment," *Environmental Science and Technology*, vol. 33, no. 24, pp. 4373–4378, 1999.

[39] K. L. Willett, E. M. Ulrich, and R. A. Hites, "Differential toxicity and environmental fates of hexachlorocyclohexane isomers," *Environmental Science and Technology*, vol. 32, no. 15, pp. 2197–2207, 1998.

[40] W. X. Liu, Y. Li, Q. Zuo et al., "Residual characteristics of HCHs and DDTs in surface soils from the western zone of Bohai Bay," *Acta Scientiae Circumstantiae*, vol. 28, no. 1, pp. 142–149, 2008.

[41] X. Qiu, T. Zhu, B. Yao, J. Hu, and S. Hu, "Contribution of dicofol to the current DDT pollution in China," *Environmental Science and Technology*, vol. 39, no. 12, pp. 4385–4390, 2005.

[42] G. G. Pandit, S. K. Sahu, S. Sharma, and V. D. Puranik, "Distribution and fate of persistent organochlorine pesticides in coastal marine environment of Mumbai," *Environment International*, vol. 32, no. 2, pp. 240–243, 2006.

[43] H. Jia, Y. Sun, Y. F. Li et al., "Endosulfan in China 2—emissions and residues," *Environmental Science and Pollution Research*, vol. 16, no. 3, pp. 302–311, 2009.

[44] Y. F. Jiang, X. T. Wang, Y. Jia et al., "Occurrence, distribution and possible sources of organochlorine pesticides in agricultural soil of Shanghai, China," *Journal of Hazardous Materials*, vol. 170, no. 2-3, pp. 989–997, 2009.

[45] H. L. Jia and Y. Li, Endosulfan in China: Usage, http://www.6weidu.com/huaxuenongyao/gaoweinongyao/2012/0321/1161.html.

[46] T. F. Bidleman, L. M. M. Jantunen, P. A. Helm, E. Brorström-Lundén, and S. Juntto, "Chlordane enantiomers and temporal trends of chlordane isomers in arctic air," *Environmental Science and Technology*, vol. 36, no. 4, pp. 539–544, 2002.

[47] G. Wayne, R. G. Lewis, R. L. Harless, N. K. Wilson, and R. D. Zehr, "Analysis of technical chlordane by gas chromatography/mass spectrometry," *Analytical Chemistry*, vol. 49, no. 6, pp. 734–740, 1977.

[48] J. C. Yan, X. Li, and J. L. Hu, "Termite control of Lake Chaohu Dam," *Anhui Water Resources Technology*, vol. 2, pp. 19–22, 2004.

[49] POPs Office of National Environmental Protection Bureau, "China Strategies for abating and controlling insecticide class of persistent organic pollutants," UNEP Project CPR/01/R51/A/CC/31, 2004.

[50] M. H. Wong, A. O. W. Leung, J. K. Y. Chan, and M. P. K. Choi, "A review on the usage of POP pesticides in China, with emphasis on DDT loadings in human milk," *Chemosphere*, vol. 60, no. 6, pp. 740–752, 2005.

The *S*cientificWorldJOURNAL

Research Article

Distributions, Sources, and Backward Trajectories of Atmospheric Polycyclic Aromatic Hydrocarbons at Lake Small Baiyangdian, Northern China

Ning Qin, Xiang-Zhen Kong, Ying Zhu, Wei He, Qi-Shuang He, Bin Yang, Hui-Ling Ou-Yang, Wen-Xiu Liu, Qing-Mei Wang, and Fu-Liu Xu

MOE Laboratory for Earth Surface Processes, College of Urban and Environmental Sciences, Peking University, Beijing 100871, China

Correspondence should be addressed to Fu-Liu Xu, xufl@urban.pku.edu.cn

Air samples were collected seasonally at Lake Small Baiyangdian, a shallow lake in northern China, between October 2007 and September 2008. Gas phase, particulate phase and dust fall concentrations of polycyclic aromatic hydrocarbons (PAHs) were measured using a gas chromatograph-mass spectrometer (GC-MS). The distribution and partitioning of atmospheric PAHs were studied, and the major sources were identified; the backward trajectories of air masses starting from the center of Lake Small Baiyangdian were calculated for the entire year. The following results were obtained: (1) The total concentration of 16 priority controlled PAHs (PAH16) in the gas phase was 417.2 ± 299.8 ng·m^{-3}, in the particulate phase was 150.9 ± 99.2 ng·m^{-3}, and in dust fall was 6930.2 ± 3206.5 ng·g^{-1}. (2) Vehicle emission, coal combustion, and biomass combustion were the major sources in the Small Baiyangdian atmosphere and accounted for 28.9%, 45.1% and 26.0% of the total PAHs, respectively. (3) Winter was dominated by relatively greater PAHs polluted northwesterly air mass pathways. Summer showed a dominant relatively clean southern pathway, whereas the trajectories in autumn and spring might be associated with high pollution from Shanxi or Henan province.

1. Introduction

Polycyclic aromatic hydrocarbons (PAHs) are a group of compounds composed of two or more fused aromatic rings [1]. They have been of concern because of their potentially toxic, mutagenic, and carcinogenic properties [2–4]; therefore, 16 PAHs are included on the priority pollutants list of the US EPA [5]. Coal combustion, vehicle emission, the coking industry, and biomass burning are the main sources of PAHs [6]. They occur in the environment as complex mixtures of many components [7]. As one of the fastest growing countries in the world, China is suffering from severe contamination of PAHs from various sources that pose serious threats to ecosystems and human health [8].

The aquatic ecosystem is one of the major sinks of PAHs contamination [9], and the atmosphere plays an important role in the PAHs contamination of aquatic systems [10, 11].

PAHs exist in the ambient air as gases or adsorb to airborne particulate matter [12]. Therefore, the atmosphere is an important pathway for the transport of PAHs. Atmospheric deposition and diffusive exchange across the air-water interface are the major input routes for PAHs to the aquatic system [13]. It is necessary to study the pollution characteristics of atmospheric PAHs and identify the major emission sources to access the atmospheric influence of aquatic system.

Lake Baiyangdian ($38°43' \sim 9°02'$N/$115°38' \sim 116°7'$E), with an area of 366 km^2, is located in the triangular region defined by three large cities, Beijing, Tianjin, and Baoding (Figure 1). It is the largest freshwater lake in north China and is regarded as the "Pearl of North China." Lake Baiyangdian plays an important role in maintaining the ecological balance of north China and in providing domestic, agricultural, and industrial water sources for the lake catchment [8]. The Lake
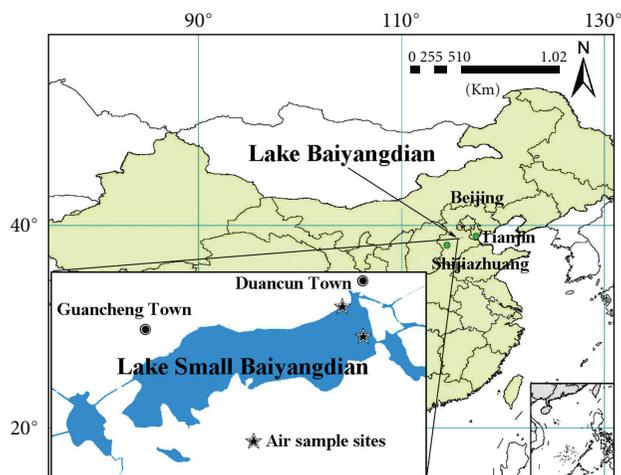
Figure 1: Location of Lake Small Baiyangdian and the sampling sites.

Baiyangdian area is one of the areas most polluted by PAHs in China [8]. Understanding the distributions and sources of atmospheric PAHs in Lake Baiyangdian could be useful for the mitigation of PAHs pollution. Lake Baiyangdian is composed of 143 small lakes and ponds, among which Lake Small Baiyangdian is the largest, with a total area of 13.3 km^2. This study of atmospheric PAHs at Lake Small Baiyangdian had four primary objectives: (1) to investigate the residual levels and spatial-temporal distributions of PAHs in gaseous and particulate phases and dust fall, (2) to elucidate the partitioning of PAHs in gaseous and particulate phases, (3) to identify major sources of PAHs, and (4) to analyze the backward trajectories of air masses starting from the center of Lake Small Baiyangdian.

2. Methodology

2.1. Measurement of PAHs in Gaseous and Particulate Phases and Dust Fall

2.1.1. Sample Collection. The passive sampler designed by our laboratory [14] was used to collect gaseous and particulate PAHs samples from two sites located at the lakeside near the village and above the lake (Figure 1). A polyurethane foam (PUF) disk (110 mm diameter × 15 mm thick, density 0.024 g·cm^{-3}) and a glass fiber filter (GFF, 110 mm diameter) were used as sampling media for gaseous and particulate phase PAHs, respectively. The PUF disks were previously extracted by Soxhlet with dichloromethane, acetone, and n-hexane sequentially for 12 h each reagent. The GFFs were preconditioned by heating in a furnace at 450°C for 4 h. After sampling, the PUF disks were wrapped with aluminum foil and kept in sealed bags sealed until measurement. The GFFs were wrapped with aluminum foil and saved in a desiccator without lights. The dust-fall samples were collected passively using stainless steel drums with a bottom area of 0.08 m^2 that were placed next to the passive sampler. Before sampling, the drum bottom was covered with a mixed solution of

200 mL glycol and deionized water (V : V, 1 : 1) to prevent the decomposition of organochlorine pesticides. The dust fall in the drum was washed into a 1 L brown jar. Jars were dried at 400°C for 6 h prior to use. The gaseous, particulate, and dust-fall samples were collected during four periods: (a) October 7–November 14, 2007 (autumn); (b) November 15, 2007–March 15, 2008 (winter); (c) March 16–June 20, 2008 (spring); (d) June 21–September 5, 2008 (summer). The second period corresponded to the heating period in northern China.

2.1.2. Extraction and Cleanup. The PUF, GFFs, and particle samples were extracted by Soxhlet with methylene chloride for 24 h, 12 h, and 24 h, respectively. The extract was concentrated to 1 mL, and the solvent exchanged with n-hexane and purified on a silica packed column. From the bottom to top, the column was filled with neutral silica gel (10 g, 3% deactivated) and anhydrous sodium sulfate (1 cm). The silica gel and anhydrous sodium sulfate were baked at 450°C for 4 h prior to use. The column was eluted with 50 mL of dichloromethane/hexane (2 : 3) at a rate of 2 mL·min^{-1} to yield the PAHs fraction. The elute was concentrated on a rotary evaporator at a temperature below 38°C to approximate 1 mL, and internal standards (2-fluoro-1,1′-biphenyl and p-terphenyl-d14, 2.0 μg·mL^{-1}, J&K Chemical, USA) were added before samples were measured.

All sampling media were extracted immediately after harvesting. PUF chips and plugs were Soxhlet extracted in a 1:1 mixture of *n*-hexane and cyclohexane for 10 h. GFFs were extracted using the same procedure for 10 h. The extracts were concentrated by rotary evaporation to approximately 1 mL. Quantification was performed using the internal standard method using 2-fluoro-1,1′-biphenyl and *p*-terphenyl-d_{14} (2.0 μg·mL^{-1}; J&K Chemical, USA).

2.1.3. Sample Analysis and Quality Control. All samples were analyzed on a gas chromatograph (Agilent GC6890/5973 MSD) connected to an HP-5MS capillary column and a mass

Table 1: Recoveries and instrumental detection limits.

PAHs	Recoveries			Instrumental detection limits (ng·mL^{-1})
	Gas	Particle	Dust fall	
NAP	46%	47%	56%	1.02
ACE	51%	48%	71%	0.76
ACY	67%	50%	77%	0.79
FLO	75%	57%	85%	0.87
PHE	83%	69%	83%	1.8
ANT	77%	71%	87%	0.64
FLA	98%	87%	98%	0.85
PYR	124%	88%	104%	0.8
BaA	99%	97%	99%	0.9
CHR	92%	102%	92%	1.2
BbF	121%	103%	121%	1.85
BkF	90%	111%	90%	1.1
BaP	108%	103%	108%	0.85
DahA	102%	119%	102%	1.52
IcdP	127%	118%	120%	1.8
BghiP	65%	115%	75%	1.38

selective detector (MSD, Agilent 5973). The column was programmed to warm from 60°C to 300°C over 5°C/min and then held isothermal for 20 min. The MSD was operated in electron impact mode at 70 eV, and the ion source temperature was 230°C. The mass spectra were recorded using selected ion monitoring mode.

Laboratory blanks and sample blanks were run with samples. Field blanks were sampling media (PUF and GFFs) taken with the samples. Both field blanks and laboratory blanks were extracted in the same way as the samples. All measurements were field-blank corrected. The mixed standard sample of 16 PAHs (PAH-Mixture, 610/525/550) produced by Chem Service Company was used to get the standard curve with the concentration series of 1 ppb, 10 ppb, 100 ppb, 1000 ppb. The blank experiment carried out using the glass beads to replace the gaseous and particular samples with the same extraction and purification procedures. Two procedure blanks were performed for about every eight samples, and the standard curve was calibrated using standard sample for about every 20 samples. The quantification was performed by the internal standard method using Nap-d8, Ace-d10, Ant-d10, Chr-d12, and Perylene-d12 (J&K Chemical, Beijing, China). The detection limits and method recoveries of the target PAHs are listed in Table 1.

2.1.4. Calibration of the Passive Sampler. The following equation (1) was used for the calibration of the gaseous and particulate phase PAHs in the air from the passive sampler to obtain the volume concentration, respectively. The equations were deduced by our colleagues based on the relationships between the gaseous and particulate PAHs from active and

passive samplers in Hebei—the Beijing region where Lake Small Baiyangdian is located [15]:

$$
\begin{aligned}
\log \text{PAH}_g(A) &= 0.7676 \ \log \text{PAH}_g(P) \\
&\quad - 2.167 \times 10^{-9} \text{MWt}^{3.776} \\
&\quad + 1.6202, \quad (r^2 = 0.878),
\end{aligned}
$$

$$
\frac{\text{PAH}_p(A) = \text{PAH}_p(P)}{(e^{3.701 - 0.0314 \text{MWt}})}, \quad (r^2 = 0.877),
$$

(1)

where $\text{PAH}_s(A)$ and $\text{PAH}_p(A)$ represent the gaseous and particulate phase PAHs in air (ng·m^{-3}) from the active sampler, respectively, $\text{PAH}_s(P)$ and $\text{PAH}_p(P)$ represent the gaseous and particulate phase PAHs in air (ng·d^{-1}) from the passive sampler, respectively, and MWt represents the molecular weight of the PAH compound.

It should be pointed that there were some uncertainties associated with using the equations to estimate atmospheric concentrations and the implication for the analysis of ratios and PCA for source identification, although the sampling in the present study was performed within the area of the above equations produced, and the gas-phase sampling was similar particle size distributions.

2.2. Source Apportionment. The PAH isomer ratios method and the combined method of principal component analysis (PCA) and multiregression analysis (MLA) (PCA-MLA) were employed to identify the source of atmospheric PAHs at Lake Small Baiyangdian. The former method could provide only qualitative to semiquantitative results; however, the PCA-MLA method could present quantitative results.

2.2.1. PAH Isomer Ratios. Isomer PAH ratios have been widely used to analyze atmospheric PAH sources [11, 16, 17]. Ratios of specific particulate phase PAHs are characteristic of different sources. Common ratios used include Fla/Pyr (mass 202), Baa/Chr (mass 228), and IcdP/BghiP (mass 276) [18].

For mass 202, fluoranthene to fluoranthene plus pyrene (Fla/Fla + Pyr), a ratio of 0.50 is usually defined as the petroleum/combustion transition point. For Fla/(Fla + Pyr), ratios between 0.40 and 0.50 are more characteristic of liquid fossil fuel (vehicle and crude oil) combustion, whereas ratios >0.50 are characteristic of grass, wood, or coal combustion; for mass 228, Baa/(Baa +Chr) ratios <0.20 indicate petroleum sources, from 0.20 to 0.35 indicate either petroleum or combustion, and >0.35 imply combustion; for IcdP/(IcdP + BghiP) ratios, <0.20 likely indicates petroleum, between 0.20 and 0.50 implies liquid fossil fuel (vehicle and crude oil) combustion, and ratios >0.50 imply grass, wood, and coal combustion [18].

2.2.2. PCA-MLR Method. For quantitative investigations of possible sources of PAH contamination, principal component analysis (PCA) and multiregression analysis (MLR) were employed. PCA and MLR are common types of receptor models and have been successfully used for PAH apportionment [19]. PCA is a data reduction technique that

aims to explain most of the variance in the data, while transforming a set of correlated measured variables into a set of a few uncorrelated components [20]. MLR is used to quantify the contribution of various source identified by PCA [4]. As a result of the PCA, normalized factor scores having a mean and standard deviation of 0 and 1 were obtained by PCA, then the factor scores from the PCA were used as independent variables, and the total PAH concentrations were used as dependent variable for a MLR.

The number of samples should be considered for PCA, a mathematical method widely used in principal component extraction in environmental statistics. The Kaiser-Meyer-Olkin (KMO) and Bartlett's test should be applied to analyze whether the samples were suitable for the PCA before it was used. When KMO >0.6, the data is suitable for PCA. When the number of samples is less than the number of variables, the KMO value cannot be calculated. However, this does not mean that the samples are not suitable for PCA. Some case studies showed that PCA could still be used to extract principal components, for instance, the atmosphere PAHs apportionment in Maryland [4], Lake Michigan [21], Prato [22], the sediment PAHs apportionment in the Pearl River Delta [23], and the soil PAHs apportionment in Delhi [24]. In the present study, the number of samples was eight, which is less than the number of variables; however, the PCA results showed that the samples were suitable for PCA (please see Section 3.2 for details), as indicated by previous case studies with the similar situation.

2.3. Backward Trajectory Analysis. The HYSPLIT (Hybrid Single-Particle Lagrangian Integrated Trajectory, Version 4.9) model [25] with NCEP/NCAR (National Centers for Environmental Prediction/National Center for Atmospheric Research) global reanalysis meteorological data was utilized to calculate 72 hours of backward trajectories starting from the center of Lake Small Baiyangdian (38.833°N, 115.937°E) at 00:00, 06:00, 12:00 and 18:00 UTC each day. The receptor height was set at 200 m as the lower level of the atmospheric boundary layer.

It has been demonstrated that clusters of trajectories arriving at a receptor location can serve as surrogates for different synoptic circulation patterns [26]. The nonhierarchical clustering algorithm (k-means) on the basis of the Euclidean distance is a common method of classifying air trajectories into subsets [26–28]. The optimum number of clusters was determined by comparing and analyzing the R^2 statistics [29] with the number of clusters included in the analysis. R^2 is defined as the proportion of the variance explained by the current number of clusters. A significantly large change in R^2 indicates that two highly dissimilar clusters are aggregated. Borge et al. [30] proposed a two-stage clustering procedure to further investigate "short" trajectory clusters with unclear directionalities. This method has been applied by Zhu et al. [31] to study the transport pathways and potential sources of PM_{10} in Beijing. In this study, the two-stage method was applied during the spring period because it was found that many short trajectories were grouped together in the spring, although they came from heterogeneous regions.

3. Results and Discussion

3.1. Residue Levels and Seasonal-Spatial Distributions of Atmospheric PAHs

3.1.1. Residue Levels of Atmospheric PAHs. The residue levels of PAHs in the gas-phase, particle-phase, and dust fall in the air were presented in Table 2. The PAH16 concentrations in the gaseous phase varied from 84.4 to 982.6 ng·m^{-3}, and the average concentration was 417.2 ± 299.8 ng·m^{-3}. PAH16 in particulates varied from 84.4 to 982.6 ng·m^{-3}, with a mean value of 150.9 ± 99.2 ng·m^{-3}. PAH16 in the Baiyangdian atmosphere (gas+particle) ranged from 104.2 to 1250. 2 ng·m^{-3}, with a mean value of 548.6 ± 392.4 ng·m^{-3}. The dust PAH16 concentration in this study ranged from 2916.9 to 12387.2 ng·g^{-1}, and the mean value was 6930.2 ± 3206.5 ng·g^{-1}.

From Table 2, we can see that the PAHs compositions were quite different in the gas, particulate, and dust fall samples. The PAHs in the gaseous phase were dominated by LMW-PAHs (93.5%); MMW-PAHs and HMW-PAHs accounted for 6.2% and 0.5% of the total PAHs, respectively. However, in the particulate samples, the proportion of LMW, MMW, and HMW PAHs were more balanced, accounting for 37.8%, 38.2%, and 33.7%, respectively. In the dust fall samples, the percentages of LMW, MMW, and HMW PAHs were 50.2%, 38.2%, and 11.6%, respectively.

3.1.2. Seasonal-Spatial Distributions of Atmospheric PAHs. The seasonal-spatial distributions of the PAHs in the gas-phase, particle-phase, and dust fall are shown in Figures 2, 3, and 4, respectively. The PAHs in the gaseous phase and particulate phase followed similar seasonal trends. The residual levels of PAH16 in the seasonal gas-phase contents exhibited the following order from high to low values: winter (757.94 ng·m^{-3}) > autumn (575.33 ng·m^{-3}) > spring (225.11 ng·m^{-3}) > summer (110.48 ng·m^{-3}). The seasonal particulate samples were ranked in the same order: winter (260.89 ng·m^{-3}) > autumn (177.38 ng·m^{-3}) > spring (145.79 ng·m^{-3}) > summer (19.55 ng·m^{-3}). In the dust fall, the seasonal average concentrations from high to low were winter (9.83 μg·g^{-1}) > autumn (9.69 μg·g^{-1}) > summer(5.07 μg·g^{-1}) > spring (4.58 μg·g^{-1}).

The average annual gaseous PAH16 content at the lake site was 370.0 ± 294.7 ng·m^{-3} and at the village site was 464.39 ± 341.9 ng·m^{-3}; the particulate phase content was 128.8 ± 80.0 ng·m^{-3} at the lake site and 173.0 ± 123.5 ng·m^{-3} at the village site. A one-way ANOVA was employed to compare the spatial differences. The results showed no significant differences between the gaseous ($P = 0.62$) and particle phases ($P = 0.19$); however, a difference at a significant level of 0.01 was found between the lake and village sites for the dust samples. The dust fall PAHs concentration at the lake site was 4980.1 ± 2038.8 ng·g^{-1}, which was much lower than the content at the village site (8392.7 ± 3337.3 ng·g^{-1}). This suggests that human activities (e.g., cooking) have a significant effect on the PAHs contents of dust fall.

TABLE 2: PAHs contents in the gaseous phase, particulate phase, and dust fall at Lake Small Baiyangdian.

	Gaseous phase (ng·m^{-3})				Particulate phase (ng·m^{-3})				Dust fall (ng·g^{-1})			
	Mean	SD	Min	Max	Mean	SD	Min	Max	Mean	SD	Min	Max
Nap	123.4	157.2	7.7	478.1	7.7	4.7	2.4	16.7	151.7	74.1	33.4	254.8
Ace	7.6	6.1	1.3	16.7	0.3	0.2	0.1	0.8	16.1	16.4	5.8	52.5
Acy	3.1	3.7	0.2	9.4	0.8	0.8	0.0	2.2	31.8	22.0	7.6	64.4
Flo	66.9	49.9	16.1	161.4	3.5	2.5	1.4	8.2	132.5	79.4	58.8	297.7
Phe	142.6	130.0	42.4	428.0	21.1	21.5	4.0	71.2	1553.5	1167.0	412.1	3738.6
Ant	6.5	5.9	1.6	19.1	2.1	1.7	0.9	5.0	121.6	105.8	36.7	350.1
Fla	39.9	36.7	6.6	120.2	22.3	20.1	4.2	64.9	1471.1	1149.9	391.8	3676.1
Pyr	19.5	18.4	3.9	60.5	12.6	10.3	3.5	34.7	796.9	579.4	232.9	1934.6
Baa	1.2	1.1	0.3	3.7	9.2	2.1	5.4	11.1	210.8	69.3	116.3	324.2
Chr	3.1	2.3	0.8	7.9	17.1	4.6	9.4	21.9	661.1	274.2	334.5	1140.4
Bbf	1.8	2.0	0.3	5.6	19.5	2.5	15.0	21.9	756.2	273.2	411.9	1162.2
Bkf	0.6	0.6	0.2	1.4	14.4	3.0	9.4	17.3	225.2	69.1	129.2	323.3
Bap	0.4	0.3	0.1	0.8	13.9	1.0	12.6	15.6	230.8	120.0	122.6	452.2
DahA	0.1	0.0	0.1	0.1	ND	ND	ND	ND	53.9	45.7	18.7	150.7
IcdP	1.0	0.5	0.2	1.4	20.7	0.5	20.0	21.1	302.9	186.1	29.8	556.4
BghiP	0.7	0.5	0.2	1.5	20.7	0.9	19.4	22.0	214.1	99.7	108.4	372.0
LMW	390.0	284.8	76.9	851.6	57.0	47.9	15.8	163.2	3478.3	2278.0	1156.9	6643.5
MMW	26.0	23.0	6.7	74.5	57.7	37.1	3.5	101.2	2650.2	1136.3	1277.5	4884.7
HMW	2.0	1.3	0.6	3.5	50.8	10.0	35.9	57.3	801.7	374.4	429.1	1446.7
PAH16	417.2	299.8	84.4	928.6	150.9	99.2	19.3	321.6	6930.2	3206.5	2916.9	12387.2

Nap: naphthalene; Ace: acenaphthene; Acy: acenaphthylene; Flo: fluorene; Phe: phenanthrene; Ant: anthracene; Fla: fluoranthene; Pyr: pyrene; Baa: benzo[a]anthracene; Chr: chrysene; Bbf: benzo[b]fluoranthene; Bkf: benzo[k]fluoranthene; Bap: benzo[a]pyrene; IcdP: indeno[1,2,3-cd]pyrene; DahA: dibenz[a,h]anthracene; BghiP: benzo[ghi]perylene; PAH16: the sum of 16 PAH components; LMW-PAH: low molecular weight PAHs including 2-3 ring PAHs (Nap, Ace, Acy, Flo, Phe, Ant, Fla); MMW-PAH: moderate molecular weight PAHs including 4 ring PAHs (Pyr, Baa, Chr, Bbf, Bkf); HMW-PAH: high molecular weight PAHs including 5-6 ring PAHs (Bap, Icdp, Daha, Bghip).
ND: not detected.

PAHs atmospheric residual levels in this study were compared with other research within and outside of China. Generally, PAH content in this study was at the same level or lower than most research in China but much higher than most reports from other countries. PAH content at Lake Small Baiyangdian was somewhat greater than found in Guangzhou (313 ng·m^{-3}+23.7 ng·m^{-3}) in southern China [32] and only slightly less than found in Tianjin in eastern China (485 ng·m^{-3}+267 ng·m^{-3}) [33]. The concentrations at Lake Small Baiyangdian were much greater than reported in Izmir, Turkey (PAH15 average 25.2 ng·m^{-3} in summer and 44.1 ng·m^{-3}in winter)[34], Southern Chesapeake Bay (total 5.31–71.6 ng·m^{-3}) [35], or Athens, Greece (4.8-76 ng·m^{-3}) [36]. The concentrations at Lake Small Baiyangdian were also greater than found in lake samples in Chicago (PAH14, 92.3–244.9 ng·m^{-3}) [12], which were considered to be highly contaminated.

3.1.3. Relationships of PAH Distributions in the Gaseous and Particulate Phase. Equation (2) was used to calculate the particle-gas (P/G) ratios of 16 PAHs between the particulate and gaseous phases:

$$\frac{G}{p} = \frac{C_{\text{particles}}}{C_{\text{gas}}}, \tag{2}$$

where C_{particle} (ng·m^{-3}) was the PAH concentration in the particle phase and C_{gas} (ng·m^{-3}) was the concentration in the gas phase. The partition was shown in Figure 5. Only data points with concentrations above the detection limit for both phases were included in the calculations. The particulate-gas partition ratios varied from 0.48 (Ace, autumn lake) to 3738.65 (Phe, winter village). From the figure, it appears that low molecular weight PAHs were largely contained in the gaseous phase, whereas high molecular weight PAHs were distributed in particulates.

Much work has been done to investigate the factors influencing the G/P ratios, the subcooled liquid vapor pressure (log P_L^O), and the octanol-air partition coefficient K_{oa} [37, 38]. Correlation analysis and linear regression were used to detect the relationship between K_{oa}, P_L^O and G/P ratios of PAHs, as shown in Figure 6. Significant correlations ($P < 0.01$) were found between G/P ratios and K_{oa} ($P < 0.01$), P_L^O ($P < 0.01$). In this study, the following relationship were found:

$$\log\left(\frac{P}{G}\right) = 2.941 \log K_{Oa} - 36.97,$$
$$\log\left(\frac{P}{G}\right) = 3.341 \log P_L^O - 3.24. \tag{3}$$

This result suggested that K_{oa}, P_L^O values have a significant influence on the partition of PAHs between the gas and
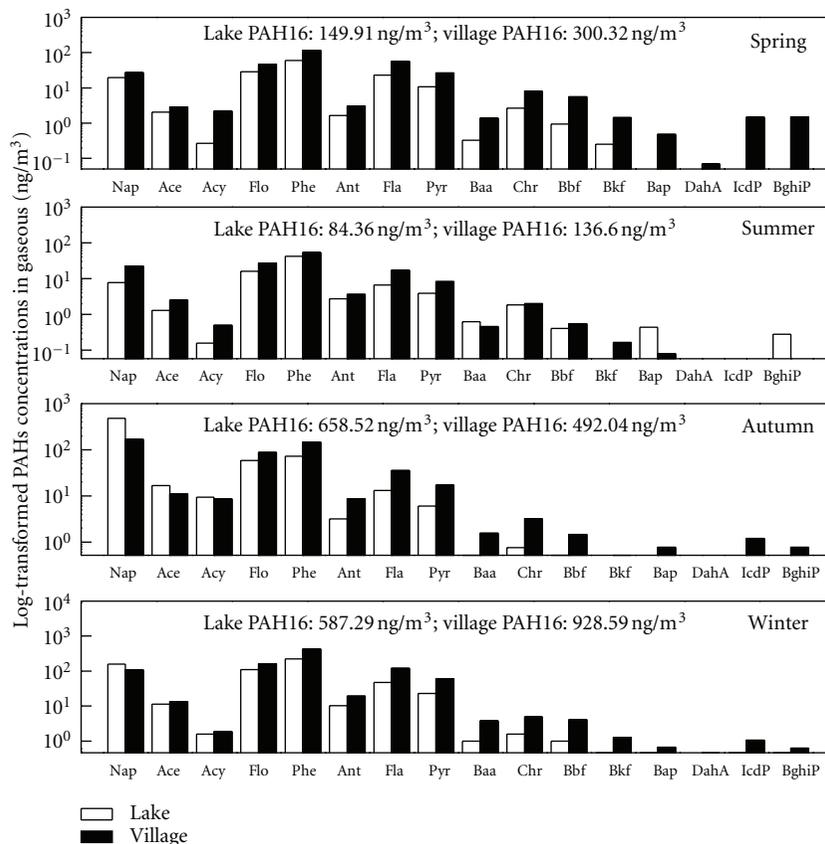
FIGURE 2: Seasonal-spatial variation in PAHs in the gaseous phase at Lake Small Baiyangdian.

particle phases, such that PAHs with higher K_{oa} but lower P_L^O values are more easily absorbed onto particles.

3.2. Source Apportionment of Atmospheric PAHs. The ratios of Fla/(Fla + Pyr) and IcdP/(IcdP + BghiP) are presented in Figure 7. From the figure, we can see that most of the ratios of Fla/(Fla + Pyr) were greater than 0.5. The values of IcdP/(IcdP + BghiP) were near the transition line of 0.5, with five points above the line, two points near the line, and another point between 0.2 and 0.5. Most of the Baa/(Baa + Chr) values were between 0.2 and 0.35. The results of Fla/(Fla + Pyr) and IcdP/(IcdP + BghiP) indicated that the sources of PAHs were primarily grass, wood, or coal combustion. However, the results of IcdP/(IcdP+BghiP) also implied that liquid fossil fuel combustion was also very important; therefore, the ratio points were near the 0.5 line. In contrast, the values of Baa/(Baa + Chr) implied that the PAHs at Lake Small Baiyangdian came from either petroleum or combustion or even a mixture of them. The high values of Fla/(Fla + Pyr) correspond with the results of IcdP/(IcdP + BghiP) and support the conclusion that combustion was the most important source of PAHs at Lake Small Baiyangdian, although the results of IcdP/(IcdP + BghiP) and Baa/(Baa+Chr) implied that liquid fossil fuel combustion might also exist in the area.

Using PCA, three components were extracted that represented more than 90 percent of the total variance. The rotated component matrix of the gas and particulate phase PAHs at Lake Small Baiyangdian is shown in Table 3. The primary sources of vehicle emission, coal combustion, and biomass combustion were identified. Factor 1 accounted for 38.86% of the total variance and was heavily weighted by Baa, Chr, Bbf, Bkf, Bap, IcdP, and BghiP. BghiP has been identified as tracers of autoemissions [39, 40]. Elevated levels of Bkf relative to other PAHs have been suggested to indicate diesel vehicles. IcdP was also found in both diesel and gas engine emissions [4], and this source appeared to be vehicle emission. The second factor accounted for 36.67% of the total variance. Factor 2 was predominately weighted by Ant Phe Flo Fla, Pyr [11, 41]. According to the literature, Flo, Pyr, Phe, and Ant were considered to be predominantly coal combustion profiles [4], and factor 2 suggests a coal combustion source. Factor 3 was heavily weighed by LMW PAHs, such as Nap, Ace, and Acy, and accounted for 21.42% of the total variance. PAHs produced by wood combustion are predominantly low molecule weight PAHs [42, 43]. Acy and Phe are mentioned as markers for wood combustion [2]. Therefore, Factor 3 indicates a biomass combustion source.

The factor scores from the PCA and the total PAH concentrations were used as independent and dependent
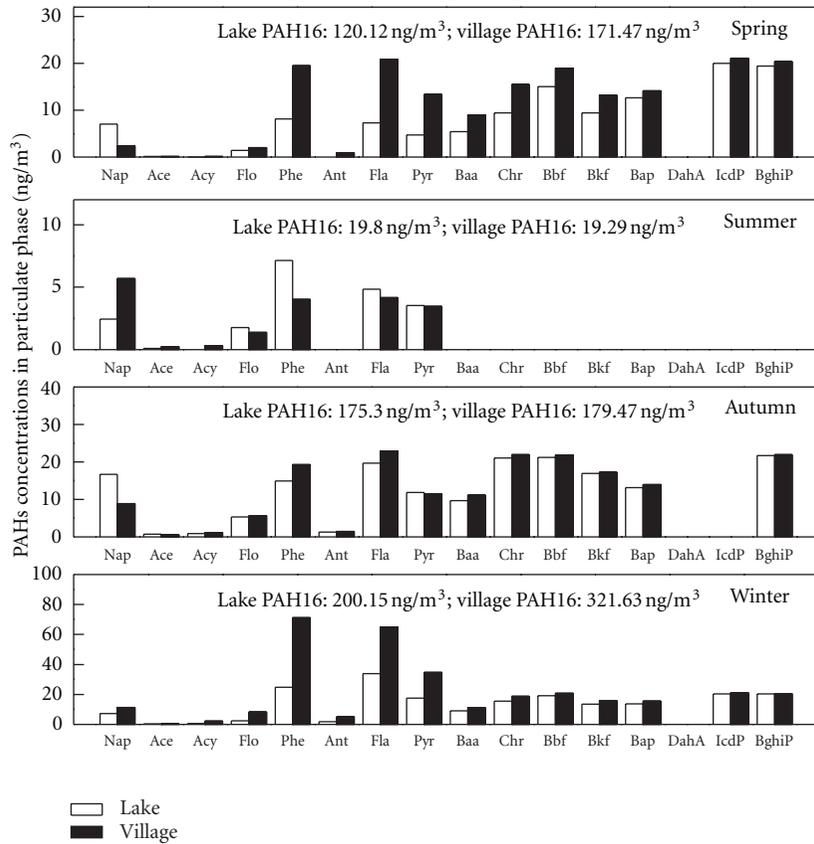
FIGURE 3: Seasonal-spatial variation in PAHs in the particulate phase at Lake Small Baiyangdian.

variable, respectively, for an MLR, and the following equation was obtained:

$$\sum(\text{gas} + \text{particles PAHs}) = 0.480\sigma_{\text{PAH}}\text{FS}_1$$
$$+ 0.749\sigma_{\text{PAH}}\text{FS}_2 \quad (4)$$
$$+ 0.432\sigma_{\text{PAH}}\text{FS}_3.$$

The percentages of the sources from vehicle emission, coal combustion, and biomass combustion could be calculated (8). The results showed that the sources from vehicle emission and coal and biomass combustions accounted for 28.9%, 45.1%, and 26.0% of the total PAHs, respectively. Coal was widely used in northern China to produce energy. In 2007, 695000 tons of coals were burned in China, accounting for 69.5% of the proportion of total energy consumption; therefore, coal combustion made the largest contribution to the atmospheric PAHs. Although biomass was used to a lesser extent than coal for energy production, biomass still represented a much greater contribution to the PAHs in the village, especially in cooking and heating. We also found that wood or coal combustion accounted for more than 70% of the total PAHs contribution, which is much greater than the vehicle emission contribution. These results are in accordance with the interpretation of the PAHs isomer ratios.

Compared with the method of PAH isomer ratios, the PCA-MLR method can give quantitative judgment of PAHs

TABLE 3: Rotated component matrix of PAHs in the gaseous and particulate phases at Lake Small Baiyangdian.

Principal components	1	2	3
Nap	0.275	−0.038	0.896
Acy	0.345	0.443	0.796
Ace	0.379	0.028	0.896
Flo	0.348	0.892	0.242
Phe	0.265	0.963	0.012
Ant	0.165	0.971	0.14
Fla	0.369	0.917	−0.069
Pyr	0.354	0.919	−0.069
Baa	0.77	0.54	0.317
Chr	0.852	0.332	0.352
Bbf	0.915	0.331	0.226
Bkf	0.853	0.338	0.397
Bap	0.923	0.336	0.159
Icdp	0.616	0.411	−0.615
BghiP	0.948	0.205	0.221
Estimated sources	Vehicle	Coal	Wood
Variance (%)	38.86	36.67	21.42

sources. However, there may be some limitations for the PCA-MLR method applied to PAHs source apportionment.
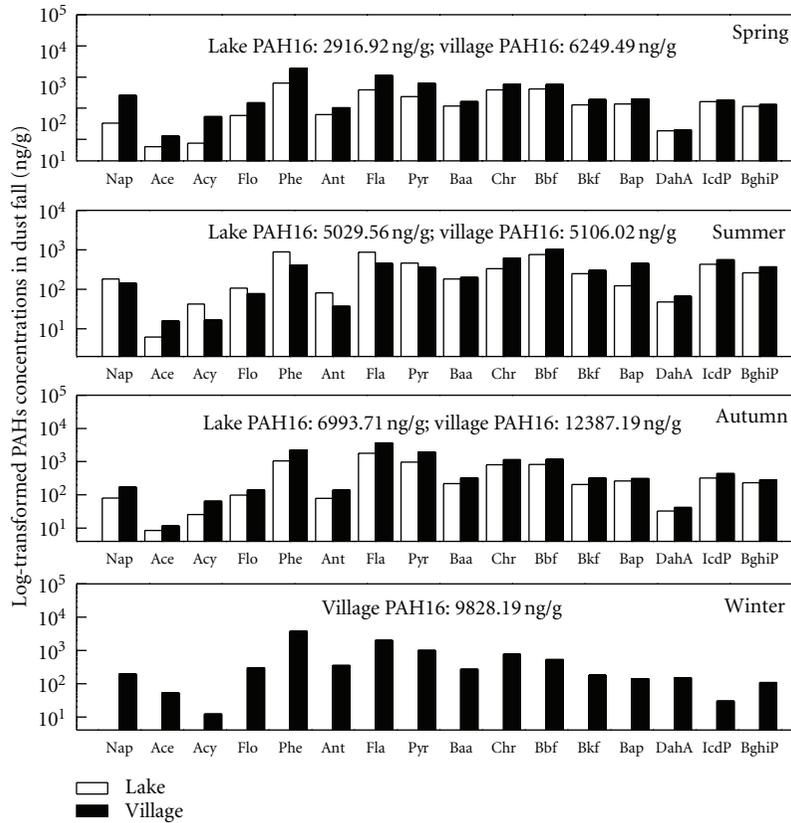
FIGURE 4: Seasonal-spatial variation in PAHs in the dust fall at Lake Small Baiyangdian.
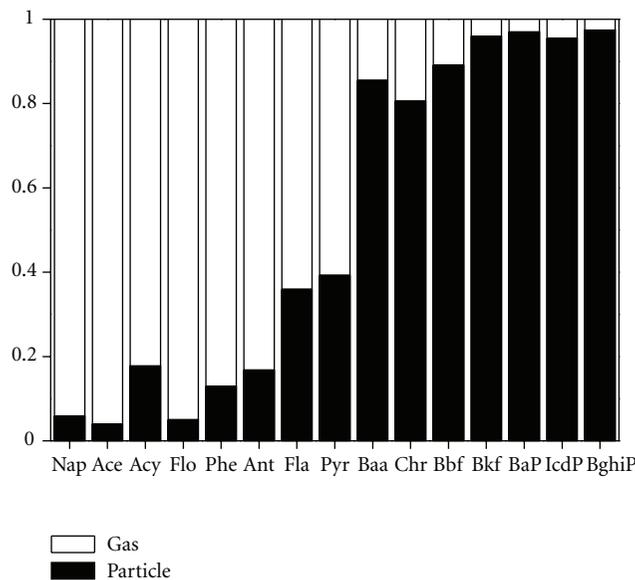
FIGURE 5: Ratio of particulate and gaseous PAHs (P/G) at Lake Small Baiyangdian.

First, the PCA-MLR method focuses the combination of compound characteristics with higher loads, and based on the monitoring of atmospheric gaseous and particulate PAHs nearby a single emission source, and it requires that the composition characteristics of the desired compound from

the emission source to the environmental receptors did not change [44, 45]. However, the composition characteristics of the PAHs compound may change due to some complex environmental processes from the emission source into the atmosphere. Second, the use of PCA for the main component
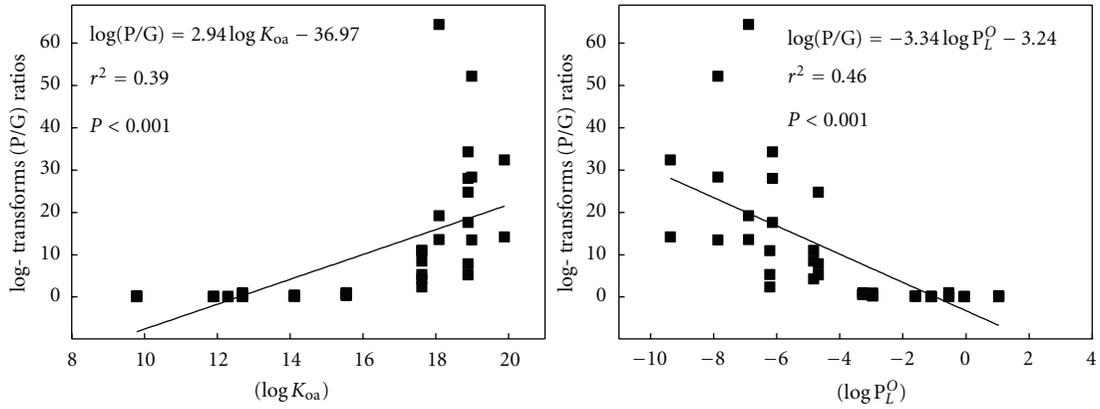
FIGURE 6: Relationships between log (P/G) and log K_{Oa} as well as log P_L^O at Lake Small Baiyangdian.
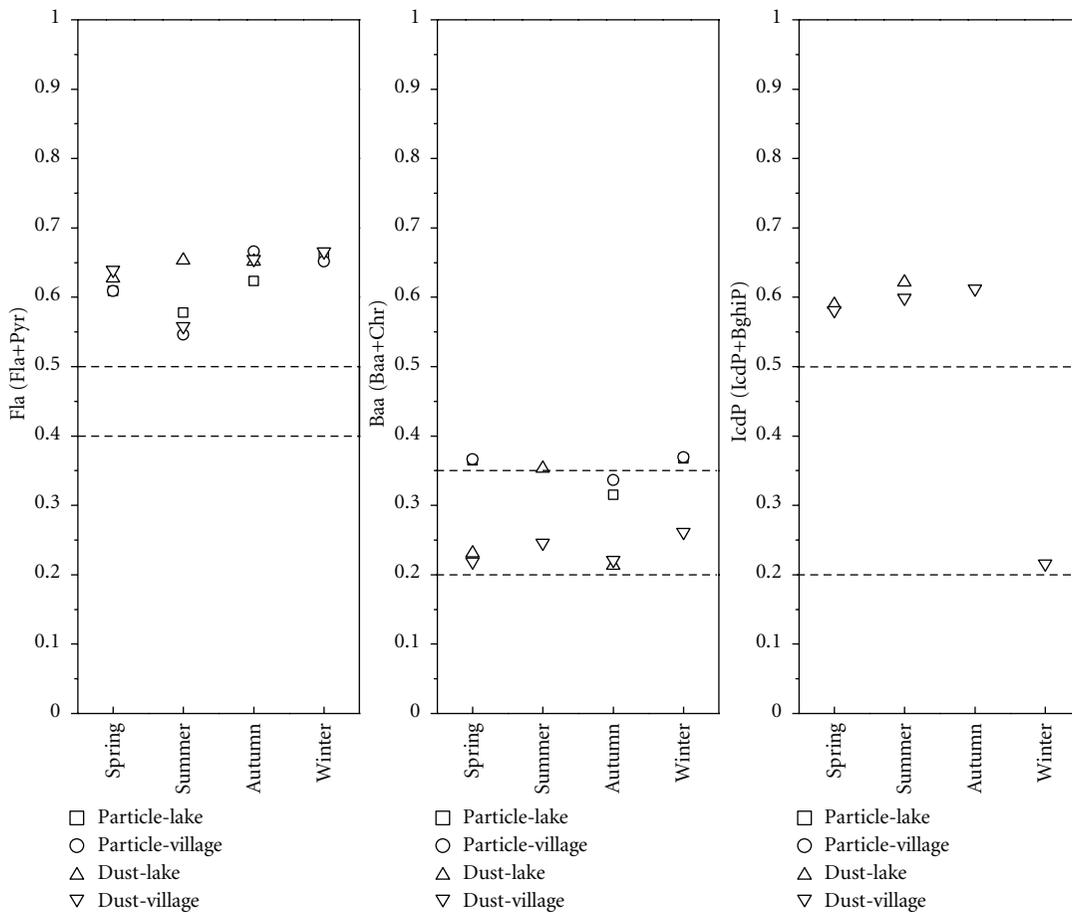

FIGURE 7: Isomer ratios of (Fla/Fla + Pyr), Baa/(Baa + Chr), and IcdP/(IcdP + BghiP).

extraction may not be able to distinguish effectively these sources, thus reducing the resolution and accuracy of the PCA-MLR method, since the PAHs compositions in the atmosphere are often a mixture of various emission sources. Third, The PCA-MLR method uses the findings from the source emission characteristics in different regions for PAHs source apportionment, which will bring some uncertainty in the results, since some differences in the PAHs composition in different regions with the same emission sources may exist [4].

3.3. Backward Trajectories and Possible Source Regions. The backward trajectories and possible source regions of air mass are illustrated in Figures 8 and 9, respectively. To further investigate the compositions of the trajectories, cluster analysis was applied, and the results are presented

(a)

(b)

(c)

(d)
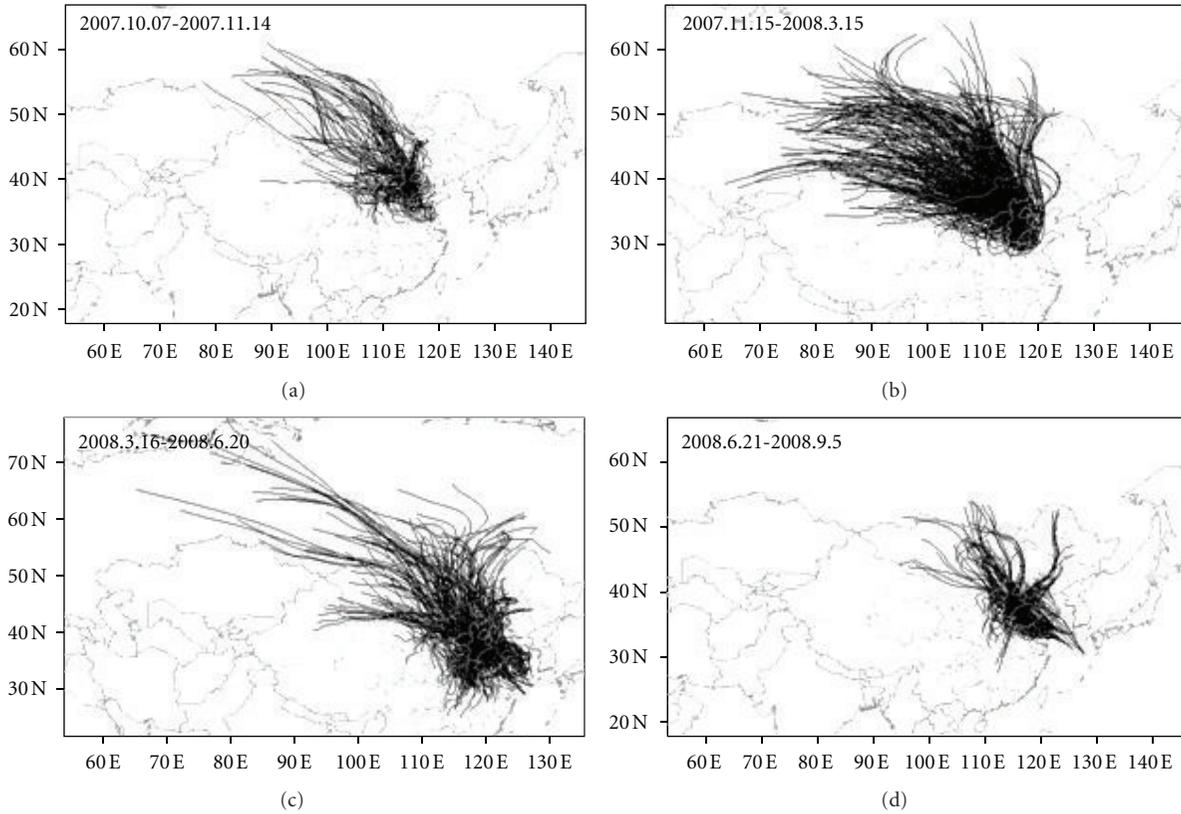
Figure 8: Backward trajectories to Lake Small Baiyangdian in four time.
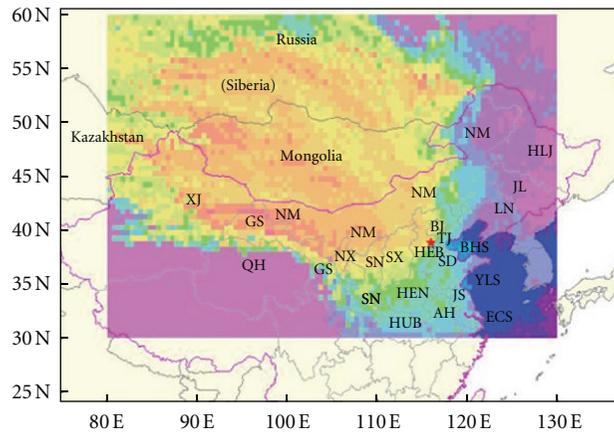
Figure 9: Distribution of possible source regions passed by backward trajectories to Lake Small Baiyangdian in four seasons. HEB : Hebei, HEN : Henan, HUB : Hubei, BJ : Beijing, TJ : Tianjin, SD : Shandong, JS : Jiangsu, AH : Anhui, SX : Shanxi, SN : Shaanxi, NX : Ningxia, GS : Gansu, QH : Qinghai, XJ : Xinjiang, NM : Neimeng, HLJ : Heilongjiang, JL : Jilin, Ln : Liaoning, BHS : Bohai Sea, YLS : Yellow Sea, ECS : East China Sea.

in Figure S1–S6 in the Supplementary Materials available online at doi:10.1100/2012/416321. The process of the cluster number determination and the monthly distribution of each cluster are shown in Figures S1 and S2, respectively. The trajectories in each cluster and the corresponding percentage in the four seasons, autumn, winter, spring, and summer are illustrated in Figures S3–S4, respectively.

In the autumn, the northwest (NNW-NWW) trajectories originated from Siberia and Mongolia (50–60N, 80–110E) were predominant with the percentage of about 31%, followed by the western (NWW-SWW) trajectories from Shanxi, Shaanxi, southwestern Neimeng and Gansu (25%), and by southern (SW-SE) trajectories from Shanxi, Shandong, Tianjin, the northern part of Anhui and Henan (21%).

The percentages for the northern trajectories (NNW-NNE) from the middle Neimeng, and for the trajectories from the local and surrounding area, Hebei, Beijing, Tianjing, and southern Neimeng were 10% and 13%, respectively (see Figure 8(a) and Figure S3 for details).

In the winter, the northwest (NNW-NWW) trajectories were predominant with the percentage of about 62%, in which the trajectories originated mainly from Xinjiang and western Mongolia (29%), followed by the trajectories from Siberia and Kazakhstan (18%) and by the trajectories from Shanxi, Shaanxi, Gansu, western Neimeng (15%). The percentages for the northern trajectories (NNW-NE) from Siberia and from the local and surrounding area, Hebei, Beijing, middle Neimeng, and eastern Mongolia were 20% and 18%, respectively (see Figure 8(b) and Figure S4 for details).

In the spring, the northwest (NNW-NWW) trajectories were predominant with the percentage of about 31%, in which the trajectories originated mainly from Siberia (19%), followed by the trajectories from Mongolia, Xinjiang, Neimeng, Gansu, Shanxi, and Shaanxi (12%). The percentage for the northern (NWW-NE) trajectories from Jinlin and the eastern part of Siberia, Mongolia, and Neimeng was 18%. The total percentage for the southern (SWW-SEE) trajectories was about 34%, in which the southwestern and southern (SWW-SSE) trajectories from Henan and the southern part of Shanxi and Shaanxi were predominant (22%), followed by the southeastern (SSE-SEE) trajectories from Shandong, Jiangsu, Anhui, and Yellow Sea (12%). The percentage for the trajectories from the local and surrounding area, Hebei, Beijing, and Tianjing was only about 7% (see Figure 8(c) and Figure S5 for details).

In the summer, the southeastern (SSE-SEE) trajectories from Shandong, Jiangsu, Anhui, Yellow Sea, and East Chinese Sea were predominant with the percentage of about 40%. The percentage for the southwestern (SSW-SWW) trajectories from Henan, Hubei, Hunan, and the southern part of Shanxi and Shaanxi was about 15%. The total percentage for the southern (SEE-SWW) trajectories including the southeastern (SSE-SEE) and southwestern (SSW-SWW) ones was 55%. However, the total percentage for the northern (NEE-NWW) trajectories was only about 32%, in which 17% was for the northern-northwestern (NNE-NWW) trajectories from Mongolia, Neimeng, and the adjacent area of Mongolia and Siberia and 15% for the northeastern (NNW-NEE) trajectories from Liaoning, Beijing, and the adjacent area of Mongolian with Heilongjiang, Jilin, and Liaoning. The percentage for the trajectories from the local and surrounding area, Hebei, Beijing and Tianjing was about 13% (see Figure 8(d) and Figure S6 for details).

It can be found through previous analysis that the directions and percentages of the trajectories and the regions passed by backward trajectories to Lake Small Baiyangdian in four seasons were different (Figure 8 and Figure S3–S6). From autumn to winter, the percentages for the northwestern (NNW-NWW) and northern (NNW-NNE) trajectories were increased from 31% and 10% to 62% and 38%, respectively; however, these for the southern (SW-SE) and western (SWW-NWW) trajectories were decreased from

21% and 25% to nearly zero. Such changes in the directions and percentages of the trajectories from autumn to winter were caused by the conversion of the summer monsoon with higher percentage of southern air mass to the winter monsoon with higher percentage of northern air mass in the Eastern Asia [46]. From winter to spring and to summer, the percentages for the northwestern (NNW-NWW) and northern (NNW-NNE) trajectories were decreased from 62% and 38% in winter to 31% and 18% in spring and to 17% and 15% in summer. However, the percentages for the southern (SWW-SEE) trajectories were increased from nearly zero in winter to 34% in spring and to 55% in summer. Such changes in the directions and percentages of the trajectories winter to spring and to summer were caused by the gradual conversion of the winter monsoon with higher percentage of northern air mass to the summer monsoon with higher percentage of southern air mass to the Eastern Asia [46].

The source regions of the backward trajectories and the distances from the source regions to Lake Small Baiyangdian in four seasons were also different (Figures 8 and 9 and Figures S3–S6). For northwestern trajectories caused by winter monsoon, the yearly dominant air mass, their effected distances in winter and spring are much longer than these in autumn and summer. However, for southeastern trajectories caused by summer monsoon, their effected distances in summer are longer than these in autumn, spring, and winter. The long-distance northwestern source regions of Siberia, Kazakhstan, Mongolia, and Xinjiang were caused by the strong northwestern air mass in winter and spring. The relative short-distance southwestern and southeastern source regions of Henan, Hunan, Anhui, Shandong, Jiangsu, Yellow Sea, and Eastern Chinese Sea were caused by the weak southwestern and southeastern air mass in summer.

4. Conclusion

The residual levels, distribution, and partition of PAHs in the gas phase, particulate phase, and in dust fall were studied; the major sources were identified, and the backward trajectories of the air masses for the entire year were calculated. It could be concluded that the PAH16 residual levels in the seasonal gas-phase and particle-phase contents exhibited the following order from high to low values: winter > autumn > spring > summer. The seasonal average concentrations in the dust fall from high to low were winter > autumn > summer > spring. Vehicle emission, coal combustion, and biomass combustion were the major sources of PAHs for the Lake Small Baiyangdian atmosphere. The backward trajectories air masses starting from the center of Lake Small Baiyangdian were dominated by the northwesterly air mass pathways. The long-distance northwestern source regions of Siberia, Kazakhstan, Mongolia, and Xinjiang were caused by the strong northwestern air mass in winter and spring. The relative short-distance southwestern and southeastern source regions of Henan, Hunan, Anhui, Shandong, Jiangsu, Yellow Sea, and Eastern Chinese Sea were caused by the weak southwestern and southeastern air mass in summer.

Acknowledgments

References

[1] C. A. Menzie, B. B. Potocki, and J. Santodonato, "Ambient concentrations and exposure to carcinogenic PAHs in the environment," *Environmental Science and Technology*, vol. 26, no. 7, pp. 1278–1284, 1992.

[2] N. R. Khalili, P. A. Scheff, and T. M. Holsen, "PAH source fingerprints for coke ovens, diesel and gasoline engines, highway tunnels, and wood combustion emissions," *Atmospheric Environment*, vol. 29, no. 4, pp. 533–542, 1995.

[3] M. B. Fernandes, M. A. Sicre, A. Boireau, and J. Tronczynski, "Polyaromatic hydrocarbon (PAH) distributions in the Seine River and its estuary," *Marine Pollution Bulletin*, vol. 34, no. 11, pp. 857–867, 1997.

[4] R. K. Larsen and J. E. Baker, "Source apportionment of polycyclic aromatic hydrocarbons in the urban atmosphere: a comparison of three methods," *Environmental Science and Technology*, vol. 37, no. 9, pp. 1873–1881, 2003.

[5] USEPA, "EPA appendix a to 40 CFR, Part 423-126 priority pollutants," 2003, http://www.epa.gov/region01/npdes/permits/generic/prioritypollutants.pdf.

[6] I. G. Kavouras, P. Koutrakis, M. Tsapakis et al., "Source apportionment of urban particulate aliphatic and polynuclear aromatic hydrocarbons (PAHs) using multivariate methods," *Environmental Science and Technology*, vol. 35, no. 11, pp. 2288–2294, 2001.

[7] T. Petry, P. Schmid, and C. Schlatter, "The use of toxic equivalency factors in assessing occupational and environmental health risk associated with exposure to airborne mixtures of polycyclic aromatic hydrocarbons (PAHs)," *Chemosphere*, vol. 32, no. 4, pp. 639–648, 1996.

[8] F. L. Xu, N. Qina, Y. Zhu et al., "Multimedia fate modeling of polycyclic aromatic hydrocarbons (PAHs) in Lake Small Baiyangdian," *Ecological Modelling*, 2012.

[9] S. Tao, H. Cao, W. Liu et al., "Fate modeling of phenanthrene with regional variation in Tianjin, China," *Environmental Science and Technology*, vol. 37, no. 11, pp. 2453–2459, 2003.

[10] S. L. Simonich and R. A. Hites, "Organic pollutant accumulation in vegetation," *Environmental Science and Technology*, vol. 29, no. 12, pp. 2905–2914, 1995.

[11] M. F. Simcik, S. J. Eisenreich, and P. J. Lioy, "Source apportionment and source/sink relationships of PAHs in the coastal atmosphere of Chicago and Lake Michigan," *Atmospheric Environment*, vol. 33, no. 30, pp. 5071–5079, 1999.

[12] N. Vardar, Y. Tasdemir, M. Odabasi, and K. E. Noll, "Characterization of atmospheric concentrations and partitioning of PAHs in the Chicago atmosphere," *Science of the Total Environment*, vol. 327, no. 1–3, pp. 163–174, 2004.

[13] F. Wania, J. Axelman, and D. Broman, "A review of processes involved in the exchange of persistent organic pollutants across the air-sea interface," *Environmental Pollution*, vol. 102, no. 1, pp. 3–23, 1998.

[14] S. Tao, J. Cao, W. Wang et al., "A passive sampler with improved performance for collecting gaseous and particulate phase polycyclic aromatic hydrocarbons in air," *Environmental Science and Technology*, vol. 43, no. 11, pp. 4124–4129, 2009.

[15] S. Tao, Y. N. Liu, C. Lang et al., "A directional passive air sampler for monitoring polycyclic aromatic hydrocarbons (PAHs) in air mass," *Environmental Pollution*, vol. 156, no. 2, pp. 435–441, 2008.

[16] R. M. Dickhut, E. A. Canuel, K. E. Gustafson et al., "Automotive sources of carcinogenic polycyclic aromatic hydrocarbons associated with particulate matter in the Chesapeake Bay region," *Environmental Science and Technology*, vol. 34, no. 21, pp. 4635–4640, 2000.

[17] A. Katsoyiannis, A. J. Sweetman, and K. C. Jones, "PAH molecular diagnostic ratios applied to atmospheric sources:a critical evaluation using two decades of source inventory and air concentration data from the UK," *Environmental Science & Technology*, vol. 45, no. 20, pp. 8897–8906, 2011.

[18] M. B. Yunker, R. W. Macdonald, R. Vingarzan, R. H. Mitchell, D. Goyette, and S. Sylvestre, "PAHs in the Fraser River basin: a critical appraisal of PAH ratios as indicators of PAH source and composition," *Organic Geochemistry*, vol. 33, no. 4, pp. 489–515, 2002.

[19] Q. Zuo, Y. H. Duan, Y. Yang, X. J. Wang, and S. Tao, "Source apportionment of polycyclic aromatic hydrocarbons in surface soil in Tianjin, China," *Environmental Pollution*, vol. 147, no. 2, pp. 303–310, 2007.

[20] A. Navarro-Ortega, R. Tauler, S. Lacorte, and D. Barceló, "Occurrence and transport of PAHs, pesticides and alkylphenols in sediment samples along the Ebro River Basin," *Journal of Hydrology*, vol. 383, no. 1-2, pp. 5–17, 2010.

[21] M. F. Simcik, S. J. Eisenreich, and P. J. Lioy, "Source apportionment and source/sink relationships of PAHs in the coastal atmosphere of Chicago and Lake Michigan," *Atmospheric Environment*, vol. 33, no. 30, pp. 5071–5079, 1999.

[22] A. Cincinelli, M. D. Bubba, T. Martellini, A. Gambaro, and L. Lepri, "Gas-particle concentration and distribution of n-alkanes and polycyclic aromatic hydrocarbons in the atmosphere of Prato (Italy)," *Chemosphere*, vol. 68, no. 3, pp. 472–478, 2007.

[23] X. J. Luo, S. J. Chen, B. X. Mai, G. Y. Sheng, J. M. Fu, and E. Y. Zeng, "Distribution, source apportionment, and transport of PAHs in sediments from the pearl river delta and the northern South China Sea," *Archives of Environmental Contamination and Toxicology*, vol. 55, no. 1, pp. 11–20, 2008.

[24] T. Agarwal, P. S. Khillare, V. Shridhar, and S. Ray, "Pattern, sources and toxic potential of PAHs in the agricultural soils of Delhi, India," *Journal of Hazardous Materials*, vol. 163, no. 2-3, pp. 1033–1039, 2009.

[25] R. R. Draxler and G. D. Hess, "Description of the Hysplit4 modeling system," NOAA Technical Memorandum ERL ARL-224, 1997.

[26] S. R. Dorling, T. D. Davies, and C. E. Pierce, "Cluster analysis: a technique for estimating the synoptic meteorological controls on air and precipitation chemistry—method and applications," *Atmospheric Environment A*, vol. 26, no. 14, pp. 2575–2581, 1992.

[27] A. Riccio, G. Giunta, and E. Chianese, "The application of a trajectory classification procedure to interpret air pollution measurements in the urban area of Naples (Southern Italy)," *Science of the Total Environment*, vol. 376, no. 1–3, pp. 198–214, 2007.

[28] J. Baker, "A cluster analysis of long range air transport pathways and associated pollutant concentrations within the UK," *Atmospheric Environment*, vol. 44, no. 4, pp. 563–571, 2010.

[29] L. S. Kalkstein, G. Tan, and J. A. Skindlov, "An evaluation of three clustering procedures for use in synoptic climatological classification," *Journal of Climate & Applied Meteorology*, vol. 26, no. 6, pp. 717–730, 1987.

[30] R. Borge, J. Lumbreras, S. Vardoulakis, P. Kassomenos, and E. Rodríguez, "Analysis of long-range transport influences on urban PM10 using two-stage atmospheric trajectory clusters," *Atmospheric Environment*, vol. 41, no. 21, pp. 4434–4450, 2007.

[31] L. Zhu, X. Huang, H. Shi, X. Cai, and Y. Song, "Transport pathways and potential sources of PM10 in Beijing," *Atmospheric Environment*, vol. 45, no. 3, pp. 594–604, 2011.

[32] J. Li, G. Zhang, X. D. Li, S. H. Qi, G. Q. Liu, and X. Z. Peng, "Source seasonality of polycyclic aromatic hydrocarbons (PAHs) in a subtropical city, Guangzhou, South China," *Science of the Total Environment*, vol. 355, no. 1–3, pp. 145–155, 2006.

[33] S. Liu, S. Tao, W. Liu et al., "Seasonal and spatial occurrence and distribution of atmospheric polycyclic aromatic hydrocarbons (PAHs) in rural and urban areas of the North Chinese Plain," *Environmental Pollution*, vol. 156, no. 3, pp. 651–656, 2008.

[34] A. Bozlaker, A. Muezzinoglu, and M. Odabasi, "Atmospheric concentrations, dry deposition and air-soil exchange of polycyclic aromatic hydrocarbons (PAHs) in an industrial region in Turkey," *Journal of Hazardous Materials*, vol. 153, no. 3, pp. 1093–1102, 2008.

[35] K. E. Gustafson and R. M. Dickhut, "Particle/gas concentrations and distributions of PAHs in the atmosphere of southern Chesapeake Bay," *Environmental Science and Technology*, vol. 31, no. 1, pp. 140–147, 1997.

[36] M. Mandalakis, M. Tsapakis, A. Tsoga, and E. G. Stephanou, "Gas-particle concentrations and distribution of aliphatic hydrocarbons, PAHs, PCBs and PCDD/Fs in the atmosphere of Athens (Greece)," *Atmospheric Environment*, vol. 36, no. 25, pp. 4023–4035, 2002.

[37] M. Odabasi, E. Cetin, and A. Sofuoglu, "Determination of octanol-air partition coefficients and supercooled liquid vapor pressures of PAHs as a function of temperature: application to gas-particle partitioning in an urban atmosphere," *Atmospheric Environment*, vol. 40, no. 34, pp. 6615–6625, 2006.

[38] W. L. Ma, D. Z. Sun, W. G. Shen et al., "Atmospheric concentrations, sources and gas-particle partitioning of PAHs in Beijing after the 29th Olympic Games," *Environmental Pollution*, vol. 159, no. 7, pp. 1794–1801, 2011.

[39] J. M. Daisey, J. L. Cheney, and P. J. Lioy, "Profiles of organic particulate emissions from air pollution sources: status and needs for receptor source apportionment modeling," *Journal of the Air Pollution Control Association*, vol. 36, no. 1, pp. 17–33, 1986.

[40] S. O. Baek, R. A. Field, M. E. Goldstone, P. W. Kirk, J. N. Lester, and R. Perry, "A review of atmospheric polycyclic aromatic hydrocarbons: sources, fate and behavior," *Water, Air, and Soil Pollution*, vol. 60, no. 3-4, pp. 279–300, 1991.

[41] R. M. Harrison, D. I. T. Smith, and L. Luhana, "Source apportionment of atmospheric polycyclic aromatic hydrocarbons collected from an urban location in Birmingham, U.K.," *Environmental Science and Technology*, vol. 30, no. 3, pp. 825–832, 1996.

[42] R. E. Laflamme and R. A. Hites, "The global distribution of polycyclic aromatic hydrocarbons in recent sediments," *Geochimica et Cosmochimica Acta*, vol. 42, no. 3, pp. 289–303, 1978.

[43] J. L. Lake, C. Norwood, C. Dimock, and R. Bowen, "Origins of polycyclic aromatic hydrocarbons in estuarine sediments," *Geochimica et Cosmochimica Acta*, vol. 43, no. 11, pp. 1847–1854, 1979.

[44] M. M. Duval and S. K. Friedlander, "Source resolution of polycyclic aromatic hydrocarbons in the Los Angeles atmospheres application of a CMB with first order decay," U.S. EPA Report EPA-600/2-81-161, U.S. Government Printing Office, Washington, DC, USA, 1981.

[45] H. Budzinski, I. Jones, J. Bellocq, C. Piérard, and P. Garrigues, "Evaluation of sediment contamination by polycyclic aromatic hydrocarbons in the Gironde estuary," *Marine Chemistry*, vol. 58, no. 1-2, pp. 85–97, 1997.

[46] T. M. Gu, *Climate in North China Plain*, China Meteorological Press, 1991.